

**ANTI-MARKOVNIKOV ADDITION REACTIONS OF OXY-ACIDS TO ALKENES  
ENABLED BY PHOTOREDOX CATALYSIS**

David S. Hamilton

A dissertation submitted to the faculty at the University of North Carolina at Chapel Hill in partial fulfillment of the requirements for the Degree of Doctor of Philosophy in the Department of Chemistry.

Chapel Hill  
2014

Approved by:

David A. Nicewicz

Erik J. Alexanian

Joseph L. Templeton

Maurice S. Brookhart

Malcolm D. E. Forbes

© 2014  
David S. Hamilton  
ALL RIGHTS RESERVED

## ABSTRACT

David S. Hamilton: Development of a Catalytic Platform for the Direct, Anti-Markovnikov Addition of Oxy-Acids to Alkenes *via* Cation-Radical Intermediates  
(Under the direction of David A. Nicewicz)

The addition of nucleophiles to alkenes with complete anti-Markovnikov selectivity employing reagents in catalytic quantities has been a major challenge for the field of organic synthesis, and Past efforts employing primarily transition-metal catalysis have only partially solved this long-standing problem. This work describes the development of a novel two-component catalytic system comprised of a photoredox catalyst and a catalytic hydrogen-atom donor, which we have demonstrated to be capable of carrying out the addition of oxy-acids to alkenes with complete regioselectivity. Some rudimentary mechanistic experiments are included to highlight the importance of both catalytic species used in the system, and applications to the synthesis of cyclic ethers and lactones are detailed. Other noteworthy applications of this system are discussed, as are preliminary results for future applications of the detailed catalytic platform.

## ACKNOWLEDGEMENTS

Arguably the most incredible thing about the prospect of publishing something is the opportunity to write some genuine and long overdue thank-yous, and to have them be a part of record for eternity.

Graduate school has been the ultimate humbling experience. If I have learned anything during my time here, it is this: though there is only one name on any dissertation, the amount of support from others that it takes to get anyone to the finish line is enormous. It certainly would take a stronger person than I to do this alone. I have been blessed with the most supportive family imaginable. Mom (Paula Raney-Hamilton), Dad (Scott Hamilton), Lauren: The patience you've shown me when I've hit my wits end on so many occasions has been incredible. To my many incredible friends, be they the old that I've known since I was a toddler, or the new that I've met in my time in the incredible town that is Chapel Hill: the many chats and trips to the bar (to both celebrate victory and commiserate in defeat) have made the good days memorable, and the truly awful days bearable.

To my labmates in the Nicewicz group: I will be extraordinarily lucky if I ever have the opportunity to work with such an eclectic, intelligent, and overall fantastic group of people ever again. It has been an honor to work, learn, and celebrate side-by-side with each and every one of you for the last five years as our lab has grown from nothing to something really awesome. I was told once that everyone is tired of their labmates by the time they leave graduate school. That couldn't be further from the truth. In fact, the thing I will miss the most about this experience is all of you. In particular, I need to acknowledge the four other members of my graduating class: Andrew Perkowski, Tien Nguyen, Michelle Riener, and Jean-Marc Grandjean. I can't imagine a better group to take this journey with, and I'm looking forward to seeing what paths you wind up taking in the future. I'm sure it holds nothing but good things for you all.



To my boss, Dave Nicewicz: I owe you the ultimate thanks for taking a flyer on me to help start your lab, for giving me such an interesting project to work on, and for giving me the latitude and space to come up with some really useful ideas (amongst all the truly terrible ones as well). You've been incredibly supportive and patient every step of the way, and couldn't have asked for a better advisor. I can leave here and honestly say that I worked for one of the good people in Chemistry today. It has been an honor and privilege to say the least, and I look forward to seeing where your career goes from here.

With respect to the work that appears in these pages, contributions were made by two very bright undergraduates (David Dong and Colin Price), who aided in the preparation of some of the compounds tested. Additionally, the computational results were obtained by Nathan Romero, as were some thermodynamic parameters for the acridinium salt. Beyond these specific contributions, thanks must be extended to members of the Alexanian, Meek, Johnson, Gagné, Waters, and Crimmins labs, for your intellectual input in a myriad of conversations, as well as for your generosity in sharing materials and instrumentation.

This work was funded by the University of North Carolina at Chapel Hill, and the National Institutes of Health, and I would be amiss if I did not acknowledge the contributions of these two fine institutions.

## **PREFACE**

The results and supporting information disclosed regarding the intramolecular hydroetherification were published in the Journal of the American Chemical Society in 2012, and was subsequently patented (PCT/US2013/039707). The rationale behind organic photoredox catalyst selection was disclosed in Synlett in 2014.

## TABLE OF CONTENTS

CHAPTER 1: ALKENE HETEROFUNCTIONALIZATION AND CHALLENGES ASSOCIATED WITH OBTAINING ANTI-MARKOVNIKOV REGIOSELECTIVITY .....	1
1.1 Introduction .....	1
1.2. Markovnikov's Rule.....	2
1.3. Circumvention of Markovnikov's Rule.....	5
1.4. Anti-Markovnikov Products from Reagent-Controlled Approaches .....	6
1.5 Transition Metal-Catalyzed Approaches to Direct Anti-Markovnikov Heterofunctionalization Reactions: Hydroamination .....	7
1.6. Transition Metal-Catalyzed Approaches to Direct Anti-Markovnikov Heterofunctionalization Reactions: Hydroetherification and Hydration.....	11
1.7. Summary.....	13
REFERENCES .....	15
CHAPTER 2: THE CATION-RADICAL APPROACH TO THE HETEROFUNCTIONALIZATION OF OLEFINS .....	17
2.1. Introduction .....	17
2.2. Anti-Markovnikov Heterofunctionalization: a Computational Analysis .....	17
2.3. Anti-Markovnikov Heterofunctionalization: Electrochemical Approaches.....	19
2.4. Anti-Markovnikov Heterofunctionalization: Photoredox Approaches .....	20
2.5. Attempted Hydroetherification of a Model Substrate Utilizing Prior Art.....	25
2.6. Consideration of Organic Photo-oxidants .....	26
2.7. Initial Results – Alkenol Cyclization Utilizing 9-Mesityl,10-Methylacridinium Perchlorate as Photocatalyst .....	29

2.8. Reaction Byproduct Analysis .....	30
2.9. Summary .....	33
REFERENCES .....	34
CHAPTER 3: THE USE OF HYDROGEN ATOM DONOR ADDITIVES TO EFFECT THE DIRECT, ANTI-MARKOVNIKOV HYDROETHERIFICATION OF ALKENOLS .....	37
3.1. Introduction .....	37
3.2. Catalytic Strategy Incorporating a Hydrogen-Atom Donor Additive .....	39
3.3. Rationale for the Unique Utility of 2-Phenylmalononitrile .....	42
3.4. Control Experiments to Validate the Catalytic Method .....	42
3.5. Evaluation of Reaction Scope .....	44
3.6. Complementarity to Brønsted-Acid Catalysis .....	47
3.7. The Use of Other Nucleophiles .....	48
3.8. Further Discussion of Selectivity .....	49
3.9. Summary .....	50
REFERENCES .....	52
CHAPTER 4 – IMPROVEMENTS TO THE ANTI-MARKOVNIKOV HYDROETHERIFICATION REACTION, AND EXTENSION TO HYDROLACTONIZATION .....	54
4.1. Introduction .....	54
4.2. Establishing the Role of the Additive as a Hydrogen Atom Donor .....	54
4.3. Re-visitation of Hydrogen Atom Sources .....	58
4.4. Re-optimization of the Hydroetherification Reaction with Thiophenol Employed as Hydrogen-Atom Donor .....	61
4.5. Comparison of Thiophenol System to First-Generation System .....	63
4.6. Thiophenol Evaluated in the H-Atom Redox Cycle .....	64

4.7. Expansion of the New System to Hydrolactonization.....	65
4.8. Applications to Total Synthesis and Medicinal Chemistry – Catechin Metabolites .....	69
4.9. Applications to Total Synthesis – Access to the Dihydroisocoumarin Motif .....	73
4.10. Summary.....	74
REFERENCES .....	76
CHAPTER 5 – OTHER APPLICATIONS OF THE IDENTIFIED CATALYTIC SYSTEM AND FUTURE DIRECTIONS .....	78
5.1. Introduction. ....	78
5.2 Other Anti-Markovnikov Transformations Developed in the Nicewicz Laboratory Based on the Previously Described Dual-Catalyst System. ....	78
5.3. Regioselective Polar Radical Crossover Cycloadditions. ....	81
5.4. Other Possible Future Directions for the Cation-Radical Intermediates. ....	82
5.5. Conclusions .....	83
REFERENCES .....	85
APPENDIX 1: SELECTED METHODS .....	86
A1.1. General Methods.....	86
A1.2. Synthesis of Alkenol Substrates .....	87
A1.3. Anti-Markovnikov Hydroetherification Reactions Using 2-Phenylmalononitrile .....	99
A1.4. Other Anti-Markovnikov Hydrofunctionalizations Using 2-Phenylmalononitrile .....	106
A1.5. Markovnikov-Selective Hydroetherification Reaction Catalyzed by Triflic Acid.....	107
A1.6. Method for Kinetic Trials .....	108
A1.7. Synthesis of Alkenoic Acids.....	109
A1.8. Anti-Markovnikov Hydrolactonization Reactions. ....	116

A1.9. Deprotection Conditions for Catechin Metabolite Products.....	126
A1.10. Regioselective Oxy-chlorination of an Alkenol. ....	128
REFERENCES .....	129
APPENDIX 2: SELECTED SPECTRA AND VOLTAMMOGRAMS .....	131

## LIST OF TABLES

Table 3.1. Results of Hydrogen Atom Donor Screen.....	41
Table 3.2. Control Experiments Confirming the Necessity of All Species to Promote Efficient Reactions.....	43
Table 3.3. 2-Phenylmalononitrile Loading Screen.....	43
Table 3.4. Electronic Diversity in Alkenol Cyclizations.....	44
Table 3.5. Variation in Alkenol Backbone Structure .....	45
Table 3.6. Demonstration of Cyclization Modes and Substrate Complexity with a Number of 2-Methyl-2-Butene-Derived Alkenols .....	46
Table 4.1. Screen of Second-Generation H-Atom Donors.....	61
Table 4.2. Control Experiments and Other Optimization of Second Generation System .....	62
Table 4.3. Solvent Effect on the Hydroetherification Reaction. ....	63
Table 4.4. Comparison of Thiophenol System to First-Generation System with 2-PMN.....	64
Table 4.5. Observation of Decarboxylation of Alkenoic Acid Upon Inclusion of Base.....	66
Table 4.6. Scope of Hydrolactonization Reactions to form $\gamma$ -Butyrolactones from Styrenyl-Alkenoic Acids.....	67
Table 4.7. Hydrolactonization Reactions of Exotic Substrate Motifs .....	69
Table 4.8. Results for Key Lactonization Step to Form Catechin Metabolite Precursors and Derivatives. ....	72

## LIST OF FIGURES

Figure 1.1. A Sampling of Alkenes Available from Petroleum Cracking or Natural Sources.....	2
Figure 1.2. Addition Reaction to an Asymmetric Alkene.....	2
Figure 1.3. Justification for Markovnikov Regioselectivity Upon Electrophilic Activation of Alkenes.....	4
Figure 1.4. Representative Industrial-Scale Transformations Demonstrating the Utility of Markovnikov-type Reactivity.....	4
Figure 1.5. Polarity Effects in Addition Reactions of Nucleophiles to Alkenes.....	5
Figure 1.6. Anti-Markovnikov Selectivity of Hydroboration Reactions.....	6
Figure 1.7. Some Reactions Allowing for Functional Group Interconversion of Organoboron Adducts, Giving Rise to Formal Anti-Markovnikov Heterofunctionalizations of Alkenes.....	7
Figure 1.8. Hartwig's First-Generation Anti-Markovnikov Hydroamination System (Intermolecular Variant).....	9
Figure 1.9. Modified System for Intramolecular Hydroamination of 1,1-Disubstituted Styrenes.....	9
Figure 1.10. Ruthenium-Catalyzed Hydroamination of Styrene and Derivatives.....	10
Figure 1.11. Buchwald's Anti-Markovnikov Hydroamination of Unactivated Alkenes.....	11
Figure 1.12. Anti-Markovnikov Hydroetherification Promoted by a Rhodium-TPP Hydride Promoter.....	12
Figure 1.13. The Grubbs System for "Triple-Relay Catalysis", Giving Rise to Products of Anti-Markovnikov Hydration.....	13
Figure 2.1. Comparison of Intermediates and Selectivities of Reactive Intermediates Proceeding to Produce Heterofunctionalized Products.....	18
Figure 2.2. Resonance Depiction of a Generic Alkene Cation-Radical.....	18
Figure 2.3. Computational Results for Addition of Methanol to 2-Methyl-2-Butene Cation-Radical.....	19
Figure 2.4. Regioselective Difunctionalization of Alkenols by Anodic Oxidation.....	20
Figure 2.5. Frontier Molecular Orbital Depiction of Photoinduced Electron Transfer.....	21



Figure 2.6. Reduction Potentials of a Variety of Oxidants and Photo-oxidants, and Oxidation Potentials of Some Representative Alkenes (vs. SCE, MeCN).....	22
Figure 2.7. Additions to Alkene Cation-Radicals Affected by 1-Cyanonaphthalene and Irradiation.....	23
Figure 2.8. Example of Photo-NOCAS Type Reactivity .....	24
Figure 2.9. Mizuno’s Hydroetherification of Alkenols. ....	24
Figure 2.9. Cyclization of a Generic Alkenol Substrate Upon Exposure to Cyanoarene Photooxidant Conditions .....	26
Figure 2.11. Oxidizing States of 9-Mesityl,10-Methyl Acridinium Ion and Exhibited Redox Reversibility .....	27
Figure 2.12. Hypothetical Mechanism for Anti-Markovnikov Heterofunctionalization of Alkenes with Mesityl Acridinium Ion as a Photocatalyst.....	29
Figure 2.13. Anti-Markovnikov Hydrofunctionalization of Alkenol B11 Under Irradiation in the Presence of 9-Mesityl,10-Methylacridinium Perchlorate.....	30
Figure 2.14. Highlights of Spectroscopic Evidence for the Structural Assignment of Byproduct B18 .....	32
Figure 2.15. Possible Mechanisms for the Formation of Compound B18 .....	33
Figure 3.1. Summary of Deuterium Labeling Experiments for Photoinduced Lactonization Promoted by 1-Cyanonaphthalene.....	38
Figure 3.2. Possible Mechanisms for Gassman’s Photoinduced Lactonization .....	38
Figure 3.3. Anti-Markovnikov Hydroamination through Stoichiometric Generation of an Alkene-Cation Radical, Promoted by Tributyltin Hydride. ....	39
Figure 3.4. Outline of Mechanism Incorporating a Radical Relay Strategy .....	40
Figure 3.5. Properties of the 2-Phenylmalononitrile Additive in All States of the Proposed Catalytic Cycle.....	42
Figure 3.6. Anti-Markovnikov Cyclization of a Styrene Derivative through a 6- <i>endo</i> Cyclization Mode with Complete Selectivity.....	47
Figure 3.7. Complementarity of New Method for Direct, Catalytic anti-Markovnikov Hydroetherification to Existing Bronsted Acid Catalytic Methods.....	48

Figure 3.8. Anti-Markovnikov Hydrofunctionalizations Demonstrated with Alternative Nucleophiles. ....	49
Figure 3.9. Relative Energies of Substituted Radicals .....	50
Figure 4.1. Mechanism with Postulated Turnover-Limiting Step .....	55
Figure 4.2. Incorporation of Label from 9-Cyanofluorene Into Product Material. ....	56
Figure 4.3. Observation of a Kinetic Isotope Effect for the Hydroetherification of an Alkenol Using 9-Cyanofluorene as H-Atom Donor. ....	57
Figure 4.4. Demonstration that Continuous Illumination is Necessary for Reaction Progression .....	57
Figure 4.5. Polarity Reversal Catalysis: Theory and Application .....	58
Figure 4.6. Partial Depiction of One Global Electrophilicity Scale for Radicals.....	59
Figure 4.7. The Thiol-Ene Reaction Promoted by Photoredox Catalysis, with Selected Scope .....	60
Figure 4.9. Thiophenol as Catalytic Redox-Active Hydrogen Atom Donor .....	65
Figure 4.10. Mechanism for Observed Decarboxylation. ....	66
Figure 4.11. Catechin and Metabolite M4.....	70
Figure 4.12. Lambert's Synthesis of Catechin Metabolite M4.....	70
Figure 4.13. Chang's Synthesis of Catechin Metabolite M4.....	71
Figure 4.14. Deprotection of Catechin Metabolite Precursors to Form Natural Products. ....	72
Figure 4.15. Natural Products Incorporating the Dihydroisocoumarin Motif.....	74
Figure 4.16. Synthesis of an Dihydroisocoumarin <i>via</i> anti-Markovnikov Hydrocyclization .....	74
Figure 5.1. Dual Reaction Vectors of Alkene Cation-Radicals.....	78
Figure 5.2. Anti-Markovnikov Hydrocarboxylation of Alkenes.....	79
Figure 5.3. Anti-Markovnikov Hydroamination of Alkenes.....	80
Figure 5.4. Anti-Markovnikov Hydrohalogenation of Styrene Derivatives.....	81

Figure 5.5. Polar-Radical Crossover Cycloaddition to form Tetrahydrofuran Products.....	82
Figure 5.6. Regioselective Oxychlorination of an Alkenol. ....	83

## LIST OF EQUATIONS

Equation 2.1. Equation for Gibbs Free Energy of Photoinduced Electron Transfer .....	21
Equation 2.2. Simplified Inequality for Prediction of Spontaneous Electron Transfer.....	21

## LIST OF ABBREVIATIONS

(4-NO <sub>2</sub> )-thiophenol	4-Nitrothiophenol
(4-OMe)-thiophenol	4-Methoxythiophenol
1-CN-Np	1-Cyanonaphthalene
2-PMN	2-Phenylmalononitrile
9-CN-FI	9-Cyanofluorene
9,10-DCA	9,10-Dicyanoanthracene
AcOH	Acetic Acid
AIBN	Azobisisobutyronitrile
Anethole	( <i>E</i> )-1-Methoxy-4-(1-propenyl)benzene
BDE	Bond Dissociation Energy
BHT	Butylated Hydroxy Toluene
BOC	Tert-butoxycarbonyl
bpy	2,2'-bipyridine
bpz	2,2'-bipyrazine
BQ	Benzoquinone
Bu	Butyl
Cod	1,5-cyclooctadiene
DCE	1,2-Dichloroethane
DCM	Dichloromethane
DDQ	2,3-Dichloro-5,6-dicyano-1,4-benzoquinone
DEMS	Diethylmethylsilane

DMSO	Dimethylsulfoxide
DPEPhos	(Oxydi-2,1-phenylene)bis(diphenylphosphine)
DPPB	1,4-Bis(diphenylphosphino)butane
DPPPent	1,4-Bis(diphenylphosphino)pentane
DTBP	Di-tert-butyl peroxide
HAT	Hydrogen Atom Transfer
HBr	Hydrobromic Acid
HCl	Hydrochloric Acid
HI	Hydroiodic Acid
HMBC	Heteronuclear multiple-bond correlation spectroscopy
HOMO	Highest Occupied Molecular Orbital
kcal	Kilocalorie
LE	Locally-Excited
LED	Light-Emitting Diode
LUMO	Lowest Occupied Molecular Orbital
MeCN	Acetonitrile
MeOH	Methanol
Mes-Acr	9-Mesityl, 10-Methylacridinium Ion
NADH	Nicotinamide adenine dinucleotide
NHC	N-Heterocyclic Carbene
nm	nanometer

NMR	Nuclear Magnetic Resonance
NOCAS	Nucleophile Olefin Combination, Aromatic Substitution
NOESY	Nuclear Overhauser effect spectroscopy
PET	Photoinduced Electron Transfer
PhH	Benzene
PhMe	Toluene
PhSH	Thiophenol
PRC	Polarity Reversal Catalysis
SCE	Saturated Calomel Electrode
SEGPPOS	4,4'-Bi-1,3-benzodioxole-5,5'-diylbis(diphenylphosphane)
SOMO	Singly Occupied Molecular Orbital
TPP	Tetraphenylporphyrin
Triflyl	Trifluoromethanesulfonyl
UV	Ultraviolet

## CHAPTER 1: ALKENE HETEROFUNCTIONALIZATION AND CHALLENGES ASSOCIATED WITH OBTAINING ANTI-MARKOVNIKOV REGIOSELECTIVITY

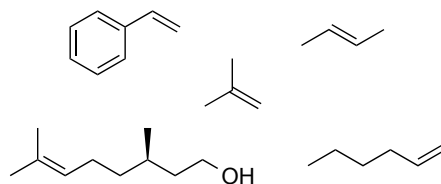
### 1.1 Introduction

The field of organic synthesis remains a vital area of chemical research, even with the tremendous strides made in the development of synthetic methodology over the last century and a half. While some would argue that we have entered an age where any desired chemical structure can be built using existing knowledge of chemical reactivity, the efficiency with which compounds can be prepared represents one major challenge facing modern synthetic chemists<sup>1</sup>. The ability to forge new chemical bonds with high yield and selectivity, from inexpensive and readily available feedstocks, and with the generation of minimal and benign waste products, represent a few of the cornerstones of the ideal synthetic transformation<sup>2</sup>. The development of new reactions that allow for the direct formation of new chemical bonds in a single step, rather than through a string of sequential reactions, represents one such approach to the improvement of synthetic efficiency, providing avenues to save the practicing synthetic chemist both time and resources, while also allowing for the minimization of waste products. New catalytic methods in particular, offer possible solutions to many of these challenges.

One functionality commonly used as a branching point for diversification in chemical synthesis is the alkene (also referred to as an olefin). Comprised of a simple carbon-carbon double bond, a number of olefinic building blocks are sourced from petrochemical cracking as well as from natural sources<sup>3</sup> (**Fig. 1.1**), and there is little doubt that these compounds represent one of the most prevalent classes of organic chemical feedstock. Additionally, there exist a vast array of protocols for the synthesis of complex alkenes, including (but certainly not restricted to) such vital transformations as the Wittig reaction, allylation/crotylation, metathesis reactions, and cross-coupling reactions<sup>4</sup>.



**Figure 1.1. A Sampling of Alkenes Available from Petroleum Cracking or Natural Sources.**

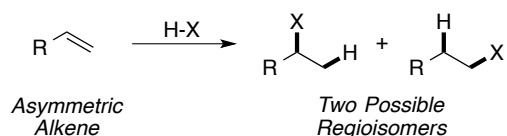


Equally as important as methods for the sourcing or construction of olefins is the broad reactivity profile that this simple element of unsaturation provides to the synthetic organic chemist, as the carbon-carbon double bond provides for an impressive assortment of avenues for scaffold diversification, allowing for structural elaboration to more complex molecular entities.

## 1.2. Markovnikov's Rule

Addition reactions of acids to alkenes are one class of reaction that possesses many of the characteristics of the previously described “ideal” chemical reaction. In this type of transformation, all atoms of the two requisite starting materials are incorporated into the end product. However, when the alkene is not symmetric, two potential products can form upon addition (**Fig. 1.2**), rendering control of the regioselectivity of this transformation vital to overall efficiency.

**Figure 1.2. Addition Reaction to an Asymmetric Alkene.**



“Markovnikov’s Rule” is one of the fundamental principles of alkene reactivity, and provides a general rule of thumb for the prediction of the regioselectivity for addition reactions. First coined by Russian chemist Vladimir Markovnikov in 1870, this illustrious rule arose from the observation that the addition of hydrochloric acid across an alkene proceeded to give chlorination on the more substituted of the carbon atoms<sup>5</sup>. Interestingly, this discovery was likely fortuitous<sup>6</sup>, as the requisite characterization methods for the products of addition were not available at the time of Markovnikov’s seminal disclosure, and it was not actually for several decades that Markovnikov’s rule would be confirmed by thorough

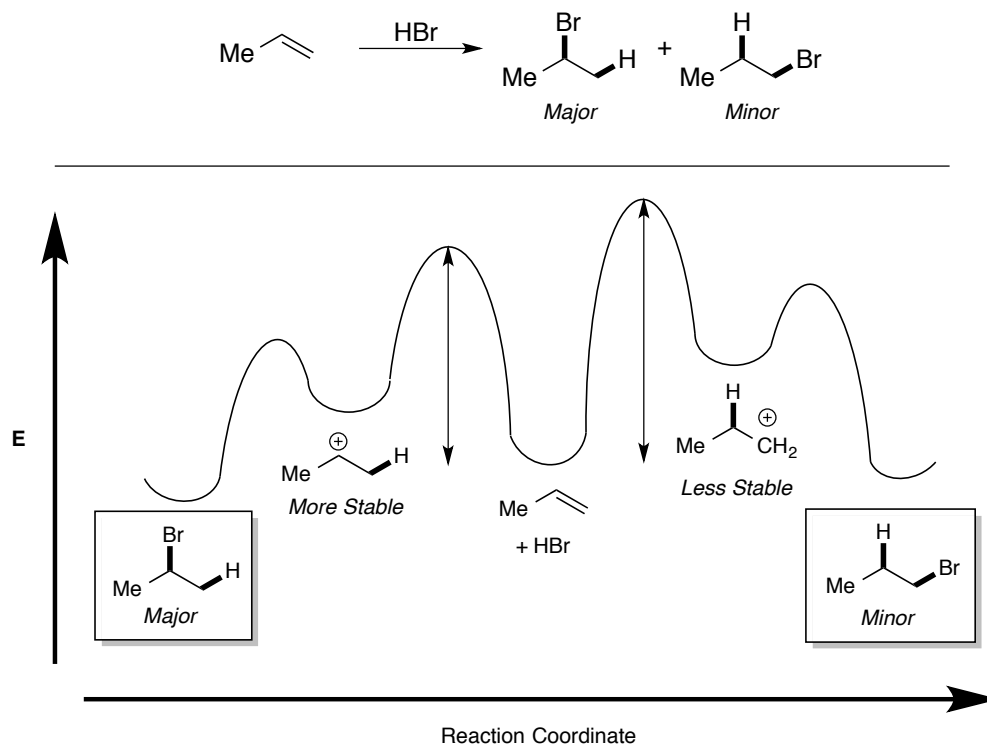
study<sup>7</sup>. Initially, Markovnikov's rule was meant only to describe the addition of mineral acids (e.g. HCl, HBr, HI) to alkenes, however, the use of the term has been broadened in modern times to encompass the pattern of regioselectivity observed for the addition of all classes of protic nucleophiles to alkenes and alkynes<sup>8</sup>.

While Markovnikov's rule is renowned partly due to its inherent simplicity as a mnemonic, the underlying mechanistic basis for the rule is fundamental, especially when considering the design of new, selective addition reactions. The regioselectivity profile of these transformations can be traced back to the innate electronic polarity of the alkene starting material that is undergoing addition<sup>9</sup>. In particular, the direct heterofunctionalization reaction is the result of an alkene with nucleophilic character being activated by a proton acting as an electrophile. This can give rise to two possible carbocation intermediates. The lower energy intermediate formed by protonation is the more substituted of the two carbocations, due to the higher degree of stabilization as the result of donation of electron density into the vacant p-orbital from neighboring  $\sigma_{C-H}$  bonds. The barrier to formation for this intermediate is also lower than protonation to form a carbocation at the alternative, less-substituted site, giving rise to an overall kinetic preference for the more substituted carbocation. This intermediate is very electrophilic and readily combines with even weak nucleophiles (water, alcohols, etc.) to furnish the overall product of addition. For the sake of simplicity, an energy diagram depicting such an addition reaction, that of hydrobromic acid to propene, is seen in **Fig. 1.3**.

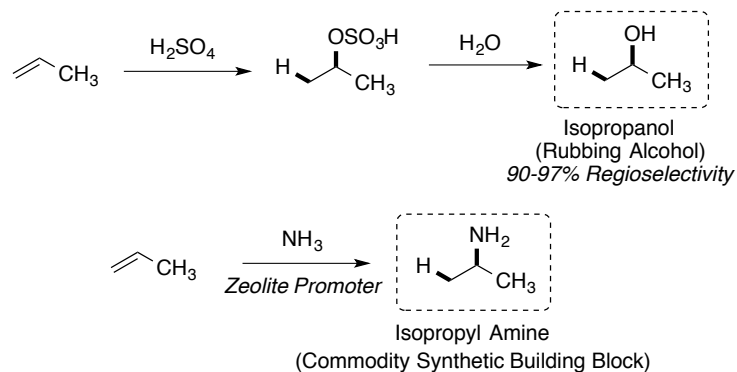
Given the strong effect of the electronic polarization of alkenes on the stability of the resulting carbocations, and therefore on the observed regioselectivity for the transformation, Markovnikov-type addition reactions are prevalent in organic synthesis. Considering that these transformations adhere to a number of desirable principles (in particular, their high atom-economy and reliable selectivity profiles), these addition reactions are used in laboratory-scale and industrial-scale reactions alike. For instance, isopropanol is manufactured by the addition of sulfuric acid to propene, and *tert*-butyl amine is manufactured on commodity scale by the addition of ammonia to 1,1-dimethylbutene using a Lewis-

acidic zeolite promoter<sup>3</sup> (**Fig. 1.4**). Both of these compounds are commercialized and used on the multi-ton scale every year, highlighting the broad applicability and importance of these transformations.

**Figure 1.3. Justification for Markovnikov Regioselectivity Upon Electrophilic Activation of Alkenes.**



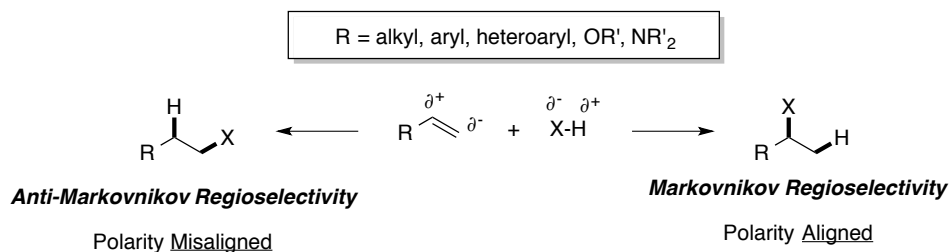
**Figure 1.4. Representative Industrial-Scale Transformations Demonstrating the Utility of Markovnikov-type Reactivity.**



### 1.3. Circumvention of Markovnikov's Rule

The remarkable utility of this predictable regioselectivity pattern, however, presents the practicing synthetic chemist with something of a conundrum. The innate nucleophilic nature of an alkene, and the manner in which it is polarized, provides efficient access to only half of the potential products that could arise from additions of acids to alkenes (**Fig. 1.5**). While Brønsted acid, Lewis acid, and transition metal protocols have all been developed for Markovnikov-type addition reactions<sup>10</sup>, reversal of the regioselectivity of addition reactions to furnish the so-called “anti-Markovnikov” products remains a major challenge in organic synthesis, and is one which chemists have been seeking solutions to for decades. In fact, one well-known perspective penned in the 1990's described catalytic methods for anti-Markovnikov heterofunctionalization of alkenes with water or ammonia as one of the top “Ten Challenges for Catalysis”<sup>11</sup> It is clear from underlying electronic principles that circumvention of Markovnikov's rule to give rise to the Anti-Markovnikov products is indeed a major challenge that requires unique and creative approaches. Given the importance of access to such products, an array of methods to circumvent the issues presented by polarization of alkenes have been developed.

**Figure 1.5. Polarity Effects in Addition Reactions of Nucleophiles to Alkenes.**

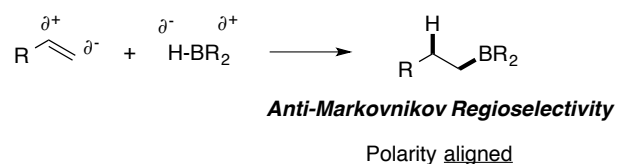


#### 1.4. Anti-Markovnikov Products from Reagent-Controlled Approaches

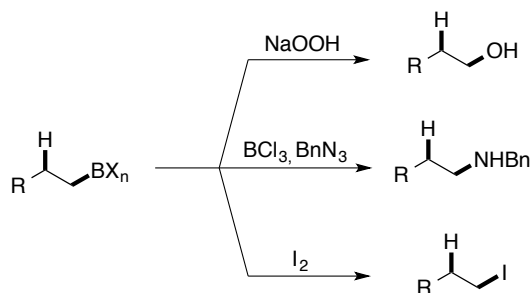
The best-known manner of circumventing the innate electronic preference for Markovnikov-type products is through the use of reagent control, which provides two ways in which selectivity can be altered. The first, and likely more intuitive of these methods of control, involves disfavoring the formation of the Markovnikov product by addition of steric bulk to the activating reagent interacting with the alkene: driving the more bulky group towards the less substituted carbon by nature of through-space interactions. The second, and perhaps less-obvious approach, is to invert of polarity of the activating agent, rendering the hydrogen atom on the activating reagent nucleophilic. This aligns the polarities of the reagent and the alkene to favor the anti-Markovnikov adduct.

Both strategies were combined some time ago in the form of the classic and well-known “Brown hydroboration reaction”, for which half of the Nobel Prize was awarded in 1979. Developed in the laboratory of the reaction’s namesake, H.C. Brown, hydroboration reactions were found to provide convenient access to primarily anti-Markovnikov substituted products<sup>12</sup>, based both on the inverted polarity of the B-H bond, and the additional steric bulk that can be incorporated around the Boron atom through the use of large ligands (**Fig. 1.6**). A remarkable amount of chemistry has been developed around this paradigm, including the development of reagents that give near exclusive Anti-Markovnikov selectivity for hydroborated products, and chiral boron reagents that give rise to high levels of observed enantioselectivity.<sup>13</sup> The borylated products that result from the addition of boranes and derivatives to alkenes are versatile, in the sense that a number of secondary transformations can be carried out to give access to heterofunctionalized products<sup>14–16</sup> (**Fig. 1.7**).

**Figure 1.6. Anti-Markovnikov Selectivity of Hydroboration Reactions**



**Figure 1.7. Some Reactions Allowing for Functional Group Interconversion of Organoboron Adducts, Giving Rise to Formal Anti-Markovnikov Heterofunctionalizations of Alkenes**



This methodology does come with limitations. First and foremost, it must be noted that useful secondary functionalizations frequently require the use of highly reactive reagents or harsh oxidants that do not necessarily scale well to industrial synthesis. Also of importance is the waste created in these transformations: as these processes generate, at the very least, a third of an equivalent of boron waste in addition to the byproducts of any secondary transformations. Synthetically, one of the most important gaps left by this methodology is the lack of flexibility with regards to the formation of cyclic systems. The sum of these limitations have led a number of groups to develop alternative strategies to try and circumvent the use of methods based on stoichiometric boron reagents, particularly through the utilization of catalytic strategies.

### 1.5 Transition Metal-Catalyzed Approaches to Direct Anti-Markovnikov Heterofunctionalization Reactions: Hydroamination

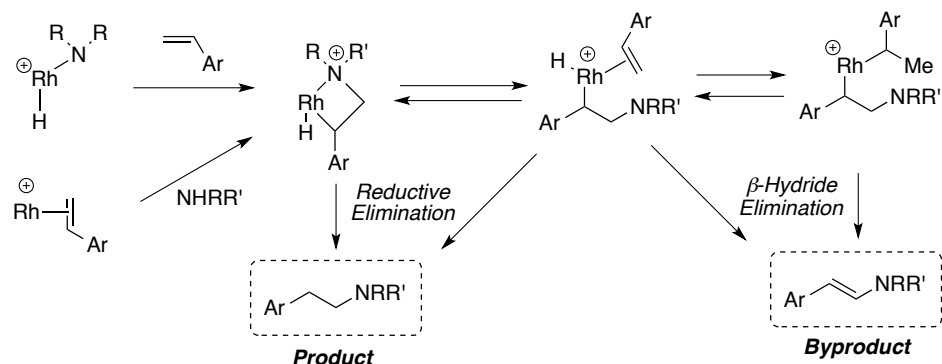
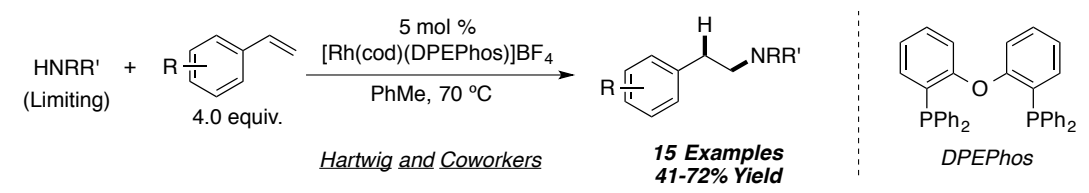
The past several decades have ushered in an era in synthetic chemistry marked by an explosion of methods using transition-metal catalysis for the formation of new chemical bonds. As such, new methods for alkene heterofunctionalization using transition metal activation have been sought, and a number of interesting transformations have been developed as a result. The majority of these efforts have been directed towards the production of products arising from Markovnikov selectivity, and have been reviewed in detail<sup>8,10</sup>. However, the field has also seen the development of a few useful alkene heterofunctionalization reactions that exhibit anti-Markovnikov selectivity, each of which warrants elaboration here.

The first system is a novel catalytic platform relying on rhodium catalysis to affect both inter-<sup>17</sup> and intramolecular<sup>18</sup> anti-Markovnikov hydroamination of styrenes, primarily using cyclic amines as the aminating reagent, and was developed by Hartwig and coworkers (**Fig. 1.8**). A key barrier that had to be overcome in the development of this chemistry was circumvention of  $\beta$ -hydride elimination to give undesired enamine side products. It was speculated in this communication that the ligand employed, DPEPhos, helps to favor the formation and reinforces the stability of a metallocyclic intermediate that disfavors an undesired pathway leading ultimately to enamine byproduct, and involves coordination with a second equivalent of styrene.

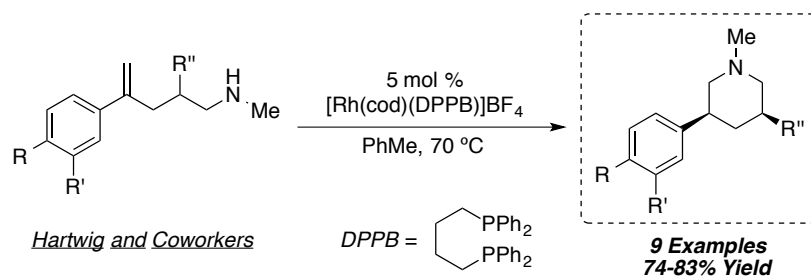
In a follow-up communication disclosing an intramolecular variant of this chemistry, the identity of not only the ligand set, but of the amine nucleophile as well, was found to be vital to the selectivity of the transformation for product over enamine, and by association, the overall yield of the reaction. A simple ligand switch from DPEphos to a more flexible DPPB ligand scaffold enabled smooth intramolecular reactions to form 2,4-disubstituted piperidine rings with high synthetic efficiency (**Fig. 1.9**). This reaction, however, was found to be ineffective with alternative substitution patterns, as the desired intramolecular, Anti-Markovnikov hydroamination did not occur when substitution was incorporated to neighbor either the styrene motif, or the amine nucleophile.

Additionally, the Hartwig lab has devised a third catalytic system for anti-Markovnikov hydroamination<sup>19</sup>. While the two previous systems were found to operate by a more traditional oxidative addition/reductive elimination-type of catalytic cycle, they discovered that particular ruthenium catalysts were capable of activating styrenes through complexation with  $\pi$ -systems of styrenes through an  $\eta^6$  coordination mode<sup>20</sup> (**Fig. 1.10**). This method of activation renders the terminus of the styrene very electrophilic, and as a result, makes it susceptible to attack from an amine nucleophile.

**Figure 1.8. Hartwig's First-Generation Anti-Markovnikov Hydroamination System (Intermolecular Variant)**



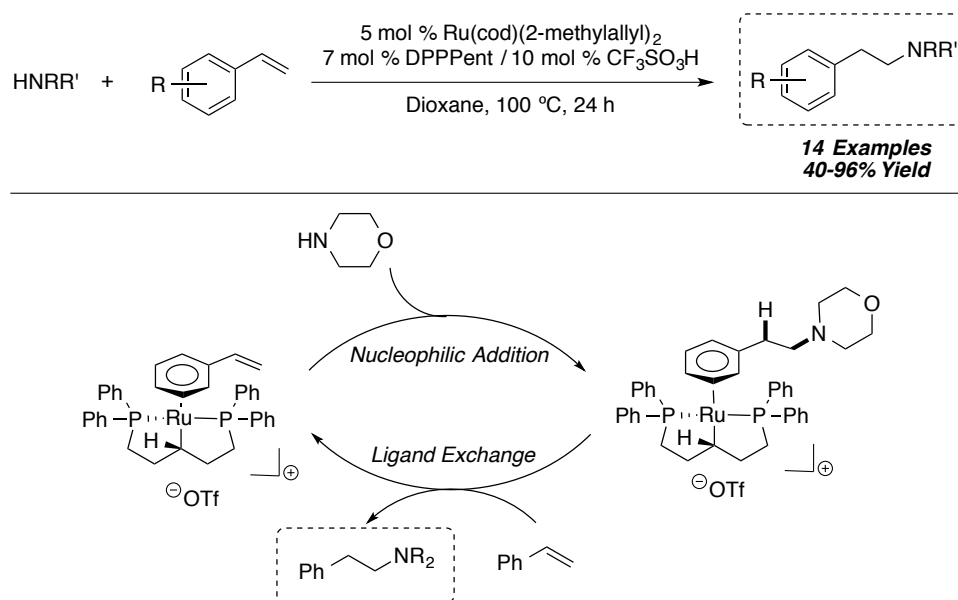
**Figure 1.9. Modified System for Intramolecular Hydroamination of 1,1-Disubstituted Styrenes**



Interestingly, this reaction was found to be affected not by a Ruthenium complex assembled from simple coordination of the added DPPent ligand to the metal center, but rather the active catalyst is the product of the Ruthenium center activating a C-H bond on the ligand, followed by protonolysis of the ensuing Ruthenium hydride to generate the active cationic Ruthenium catalyst. While it was found that an array of dialkylamines can be added to the styrene motif, it is once again important to point out that the alkene undergoing addition was required to be a styrene derivative possessing only substitution on the aryl ring.

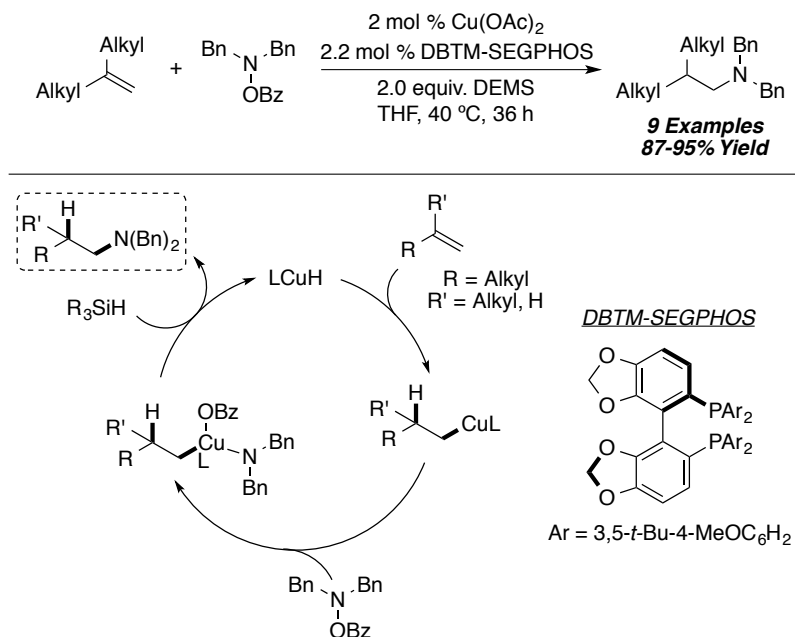


**Figure 1.10. Ruthenium-Catalyzed Hydroamination of Styrene and Derivatives**



One other transition metal-catalyzed approach of note was recently disseminated by the Buchwald lab<sup>21</sup>. The employment of a reactive copper hydride catalyst was found to affect Markovnikov-type hydrometallation of styrene derivatives, promptly followed by oxidative addition to an electrophilic hydroxylamine derivative. C-N bond-forming reductive elimination occurs, and high levels of enantioselectivity were observed when the appropriate SEGPHOS ligand was employed. Interestingly, a switch of substrate class to terminal aliphatic olefins led to a switch in selectivity to favor the formation of adducts arising from Anti-Markovnikov amination (**Fig. 1.11**). This was postulated to be due to the significantly diminished effect of electronic stabilization in the generated copper-alkyl intermediates for this class of substrate, which enabled steric interactions to become the dominant force driving selectivity. The copper catalyst was found in both cases to be efficiently turned over in the presence of excess silane acting as a hydride donor.

**Figure 1.11. Buchwald's Anti-Markovnikov Hydroamination of Unactivated Alkenes**



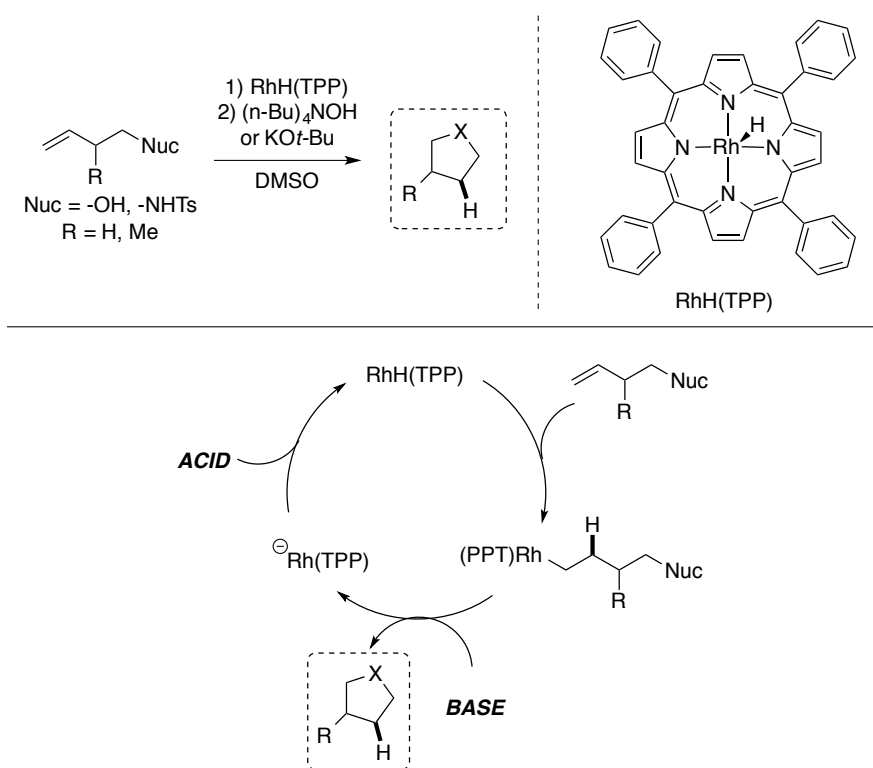
Additional chemistry has been recently developed for anti-Markovnikov hydroamination of alkenes based on the Grubbs “triple-relay” system, which will be discussed in more detail in the next section<sup>22</sup>.

### 1.6. Transition Metal-Catalyzed Approaches to Direct Anti-Markovnikov Heterofunctionalization Reactions: Hydroetherification and Hydration.

Direct, catalytic anti-Markovnikov additions of oxygen-centered nucleophiles to alkenes are even less prevalent than their amination counterparts. To date, there are only a pair of examples of such reactions to be found in the literature catalyzed by transition metals. The first example was disseminated by Sanford and Groves<sup>23</sup> in 2004, with their promoter of choice being a Rhodium tetraphenylporphyrin-hydride complex capable of carrying out the anti-Markovnikov hydrometallation of olefins (**Fig. 1.12**). When oxygen nucleophiles were tethered to the substrate, reductive elimination was found to be induced by the addition of an equivalent of strong base. It is thought that this process was the result of a “non-traditional” reductive elimination possessing character more typical of an  $\text{S}_{\text{N}}2$  reaction, with an anionic oxygen or nitrogen-centered nucleophile causing expulsion of an anionic Rhodium complex. The promoter can then be regenerated by subsequent acidification of the reaction mixture and re-isolation of

the hydride complex. It was reported that a number of cyclic ethers and amines could be formed by this protocol, but the conflicting necessity of both strongly basic and strongly acidic conditions at various points in the reaction does not allow for the operation of a closed catalytic cycle: thereby requiring the reaction to be carried out in stepwise fashion. In addition to this drawback, the authors observed diminished yields or no reactions with either additional substitution on the alkene precursor, or when the closure of cyclic systems with sizes other than five or six was attempted. In these instances, the authors noted the occurrence of a simple E2-type elimination reaction, reforming the alkene starting material rather than the desired cyclic products.

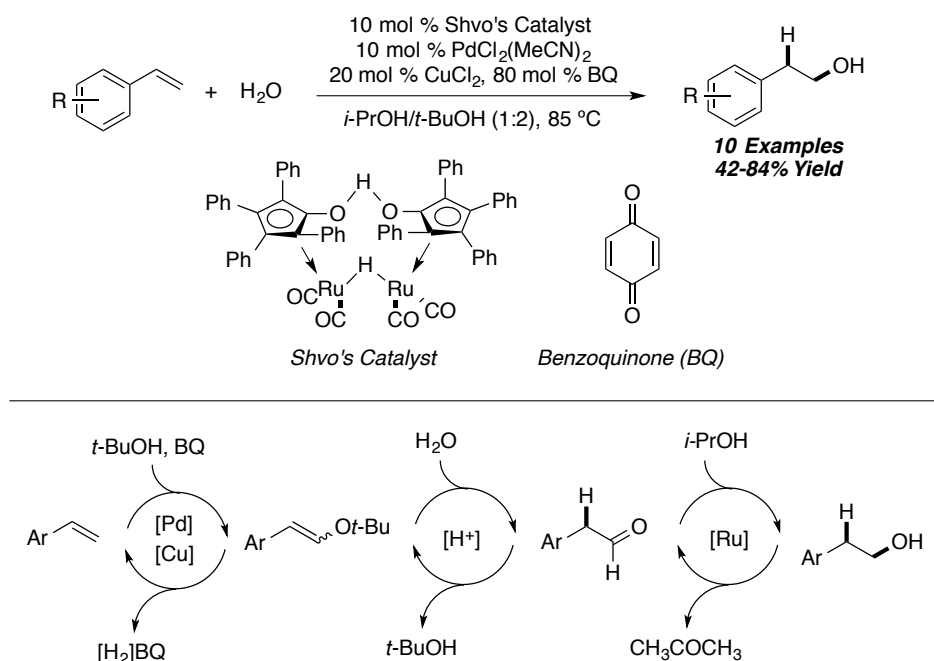
**Figure 1.12. Anti-Markovnikov Hydroetherification Promoted by a Rhodium-TPP Hydride Promoter.**



An indirect, yet one-pot protocol for anti-Markovnikov hydration has also been disclosed by the Grubbs laboratory<sup>24</sup> (**Fig. 1.13**). This approach was reliant on multiple catalytic cycles operating in tandem, and the authors titled the employed strategy “triple-relay catalysis”. The first stage of this

reaction involves the Palladium-catalyzed Wacker-type oxidation of a styrene to produce a *t*-butyl enol ether with anti-Markovnikov selectivity. Benzoquinone acts as the terminal oxidant for this first cycle, with an added copper catalyst and benzoquinone acting as an electron relay system to facilitate regeneration of the Palladium catalyst. The intermediate enol ether then undergoes hydrolysis by an equivalent of generated acid, affording the linear aldehyde. In turn, the aldehydes generated were efficiently hydrogenated by Shvo's catalyst, with an isopropanol co-solvent fulfilling the role of stoichiometric reductant. This transformation is remarkable for the oxidation/reduction cycles operating in tandem in the same reaction vessel, as well as for its superb levels of observed selectivity for the linear, anti-Markovnikov adducts, the basis of which is presumed to be the steric demand of the *t*-Butyl group in the Wacker step forming the enol ether. Importantly, however, was that selectivity was lost when moving from styrenyl-type substrates to aliphatic olefins, with slight preference for the Markovnikov adducts observed instead, thus limiting the scope of the transformation.

**Figure 1.13. The Grubbs System for “Triple-Relay Catalysis”, Giving Rise to Products of Anti-Markovnikov Hydration.**



## 1.7. Summary

Though some selective protocols have been developed for both inter- and intramolecular heterofunctionalization reactions of olefins with anti-Markovnikov selectivity, it is clear that in all instances, the scope of olefins that can undergo heterofunctionalization with high degrees of selectivity are limited. In addition, our assessment of precedent found in the literature led us to believe that, despite several unique and creative approaches to the problem of direct, catalytic addition of nucleophiles to alkenes with complete selectivity, the strategies that have been employed to furnish products of anti-Markovnikov heterofunctionalization have not been unified, and target only small parts of the overarching problem of anti-Markovnikov heterofunctionalization of unactivated alkenes. As such, we were inspired to develop a more general strategy for the addition of an array of nucleophiles to a broader subset of alkenes.

## REFERENCES

- (1) Newhouse, T.; Baran, P. S.; Hoffmann, R. W. The Economies of Synthesis. *Chem. Soc. Rev.* **2009**, 38, 3010–3021.
- (2) Trost, B. M. Atom Economy—A Challenge for Organic Synthesis: Homogeneous Catalysis Leads the Way. *Angew. Chem. Int. Ed. Engl.* **1995**, 34, 259–281.
- (3) Weissmehl, K.; Arpe, H.-J. Frontmatter. In *Industrial Organic Chemistry*; Wiley-VCH Verlag GmbH, 2008
- (4) Wang, J. *Stereoselective Alkene Synthesis*; Springer; Vol. 327.
- (5) Markownikoff, W. I. Ueber Die Abhängigkeit Der Verschiedenen Vertretbarkeit Des Radicalwasserstoffs in Den Isomeren Buttersäuren. *Justus Liebigs Ann. Chem.* **1870**, 153, 228–259.
- (6) Hughes, P. Was Markovnikov's Rule an Inspired Guess? *J. Chem. Educ.* **2006**, 83, 1152.
- (7) Maass, O.; Wright, C-H Molecular Attraction and Velocity of Reactions at Low Temperatures of Unsaturated Hydrocarbons. *J. Am. Chem. Soc.* **1924**, 46, 2664–2673.
- (8) Beller, M.; Seayad, J.; Tillack, A.; Jiao, H. Catalytic Markovnikov and Anti-Markovnikov Functionalization of Alkenes and Alkynes: Recent Developments and Trends. *Angew. Chem. Int. Ed.* **2004**, 43, 3368–3398.
- (9) Smith, M. B. *March's Advanced Organic Chemistry, 7th Edition*; 7th ed.; Wiley VCH, 2013.
- (10) Front Matter and Index. In *Catalytic Heterofunctionalization*; Togni, A.; Grützmacher, H., Eds.; Wiley-VCH Verlag GmbH, 2001
- (11) Haggin, J. Chemists Seek Greater Recognition for Catalysis. *Chem. Eng. News Arch.* **1993**, 71, 23–27.
- (12) Brown, H. C. Hydroboration—a Powerful Synthetic Tool. *Tetrahedron* **1961**, 12, 117–138.
- (13) Brown, H. C.; Singaram, B. The Development of a Simple General Procedure for Synthesis of Pure Enantiomers via Chiral Organoboranes. *Acc. Chem. Res.* **1988**, 21, 287–293.
- (14) Brown, H.; Rao, B. C. Communications - Selective Conversion of Olefins into Organoboranes Through Competitive Hydroboration, Isomerization and Displacement Reactions. *J. Org. Chem.* **1957**, 22, 1137–1138.
- (15) Brown, H. C.; Heydkamp, W. R.; Breuer, E.; Murphy, W. S. The Reaction of Organoboranes with Chloramine and with Hydroxylamine-O-Sulfonic Acid. A Convenient Synthesis of Amines from Olefins via Hydroboration. *J. Am. Chem. Soc.* **1964**, 86, 3565–3566.
- (16) Brown, H. C.; Rathke, M. W.; Rogic, M. M. A Fast Reaction of Organoboranes with Iodine under the Influence of Base. A Convenient Procedure for the Conversion of Terminal Olefins into Primary Iodides via Hydroboration-Iodination. *J. Am. Chem. Soc.* **1968**, 90, 5038–5040.

- (17) Utsunomiya, M.; Kuwano, R.; Kawatsura, M.; Hartwig, J. F. Rhodium-Catalyzed Anti-Markovnikov Hydroamination of Vinylarenes. *J. Am. Chem. Soc.* **2003**, *125*, 5608–5609.
- (18) Takemiya, A.; Hartwig, J. F. Rhodium-Catalyzed Intramolecular, Anti-Markovnikov Hydroamination. Synthesis of 3-Arylpiperidines. *J. Am. Chem. Soc.* **2006**, *128*, 6042–6043.
- (19) Utsunomiya, M.; Hartwig, J. F. Ruthenium-Catalyzed Anti-Markovnikov Hydroamination of Vinylarenes. *J. Am. Chem. Soc.* **2004**, *126*, 2702–2703.
- (20) Takaya, J.; Hartwig, J. F. Mechanistic Studies of Ruthenium-Catalyzed Anti-Markovnikov Hydroamination of Vinylarenes: Intermediates and Evidence for Catalysis through  $\pi$ -Arene Complexes. *J. Am. Chem. Soc.* **2005**, *127*, 5756–5757.
- (21) Zhu, S.; Niljianskul, N.; Buchwald, S. L. Enantio- and Regioselective CuH-Catalyzed Hydroamination of Alkenes. *J. Am. Chem. Soc.* **2013**, *135*, 15746–15749.
- (22) Bronner, S. M.; Grubbs, R. H. Formal Anti-Markovnikov Hydroamination of Terminal Olefins. *Chem. Sci.* **2013**, *5*, 101–106.
- (23) Sanford, M. S.; Groves, J. T. Anti-Markovnikov Hydrofunctionalization of Olefins Mediated by Rhodium–Porphyrin Complexes. *Angew. Chem. Int. Ed.* **2004**, *43*, 588–590.
- (24) Dong, G.; Teo, P.; Wickens, Z. K.; Grubbs, R. H. Primary Alcohols from Terminal Olefins: Formal Anti-Markovnikov Hydration via Triple Relay Catalysis. *Science* **2011**, *333*, 1609–1612.

## CHAPTER 2: THE CATION-RADICAL APPROACH TO THE HETEROFUNCTIONALIZATION OF OLEFINS

### 2.1. Introduction

As previously discussed, the basis on which the vast majority of alkene heterofunctionalization chemistry has been developed has been the activation of a nucleophilic alkene by an electrophile, with the intermediates proceeding to give products with Markovnikov selectivity upon addition of a nucleophile. Though transition-metal catalysis has provided some solutions to the problem of catalytic, anti-Markovnikov heterofunctionalization, we felt that reactions proceeding through alkene cation-radical intermediates could provide an alternative activation pathway that could provide access to products of anti-Markovnikov addition (**Fig. 2.1**).

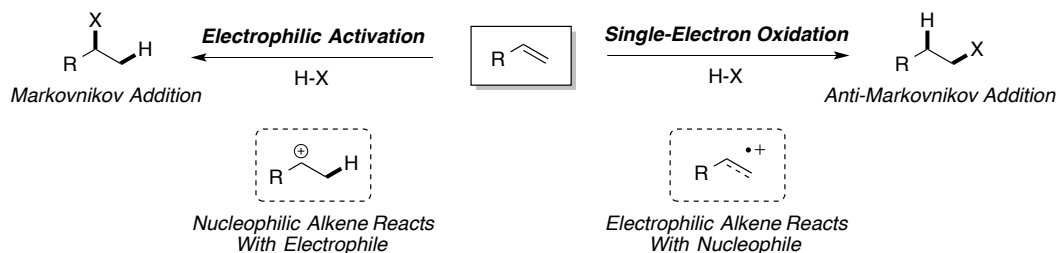
Alkene cation-radicals are, in their essence, alkenes with a single electron removed. This highly reactive species, as a result, possesses elements of both radical and cationic character, with the spin and charge elements shared between the atoms comprising the  $\pi$ -system: be it the two carbon centers comprising an isolated alkene, or distributed over a larger molecule with extended conjugation (**Fig. 2.2**). The element of charge renders the alkene cation-radical electrophilic, and susceptible to attack by an exogenous or tethered nucleophile<sup>1</sup>. The relevant literature in this field suggested to us that nucleophilic addition to alkene cation-radicals would proceed with high levels of selectivity for anti-Markovnikov products.

### 2.2. Anti-Markovnikov Heterofunctionalization: a Computational Analysis

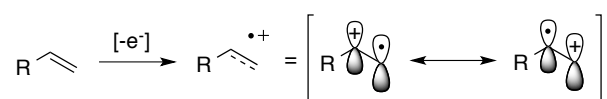
Though experimental evidence for the anti-Markovnikov regioselectivity of cation-radical mediated olefin heterofunctionalization had existed prior to publication, and will be discussed in due



**Figure 2.1. Comparison of Intermediates and Selectivities of Reactive Intermediates Proceeding to Produce Heterofunctionalized Products**

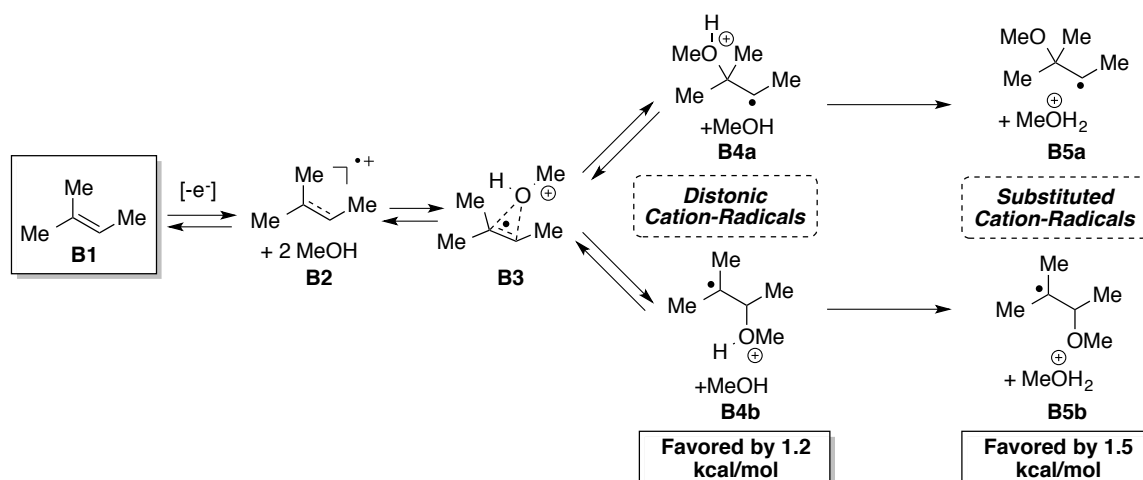


**Figure 2.2. Resonance Depiction of a Generic Alkene Cation-Radical**



course, computational justification for anti-Markovnikov selectivity of additions of nucleophiles to alkene cation-radicals was laid out in 1996 by Arnold and coworkers<sup>2</sup> (**Fig. 2.3**). In this study, the authors considered the nucleophilic addition of methanol to a set of alkenes, but for clarity only the addition of methanol to 2-methyl-2-butene (**B1**) will be illustrated here. Calculations revealed that, prior to addition, a methanol nucleophile complexed to the alkene cation-radical (**B2**), suggesting the formation of a three-membered, bridged intermediate (**3**). This species was found to collapse to either of two distonic cation-radical intermediates (**B4a**, **B4b**) in a process estimated (though not confirmed) to be reversible, and was followed by deprotonation of the intermediate by a second equivalent of methanol to form substituted radical species (**B5a**, **B5b**). Regardless of the rate-limiting step, the relative stabilities of the ensuing intermediates were believed to govern the selectivity of methanol addition, with a preference of 1.2 kcal/mol for distonic cation-radical **B4b**, and 1.5 kcal/mol for the deprotonated radical **B5b**, both the result of the anti-Markovnikov addition manifold.

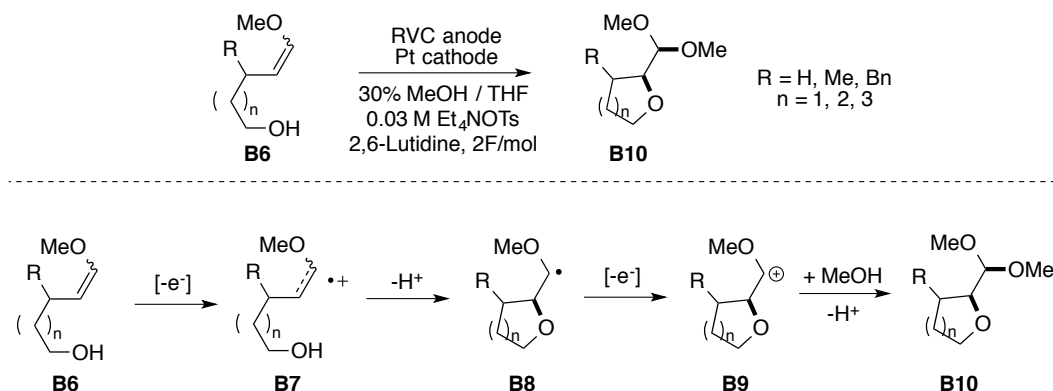
**Figure 2.3. Computational Results for Addition of Methanol to 2-Methyl-2-Butene Cation-Radical**



### 2.3. Anti-Markovnikov Heterofunctionalization: Electrochemical Approaches

Anti-Markovnikov selectivity for nucleophile addition to alkene cation-radicals is also well-precedented experimentally<sup>2</sup>. The most intuitive examples of methods designed to take advantage of the reactivity pattern of nucleophiles with alkene cation-radicals arose from the laboratory of Moeller and coworkers (**Fig. 2.4**). In their work, electrochemical oxidation was used to generate alkene cation-radicals (**B7**) from olefinic substrates with tethered nucleophiles (**B6**)<sup>3,4</sup>. Cyclization by the appended nucleophiles was found to proceed with anti-Markovnikov selectivity (**B8**). However, the strongly oxidizing conditions employed in these methods also affected a secondary oxidation event, and the substituted radical intermediate in all cases proceeded to form a carbocation (**B9**). This intermediate then recombined with a molecule of exogenous methanol to form product (**B10**). Despite the dioxygenation observed, the demonstrated regioselectivity indicated that the desired anti-Markovnikov regioselectivity could be obtained in the crucial addition step. It was also clear from this example that electrochemical methods for cation-radical generation would not be appropriate for the net redox-neutral alkene heterofunctionalization that we were hoping to affect. For the interested reader, an insightful and detailed mechanistic study of this transformation is available<sup>5</sup>.

**Figure 2.4. Regioselective Difunctionalization of Alkenols by Anodic Oxidation**



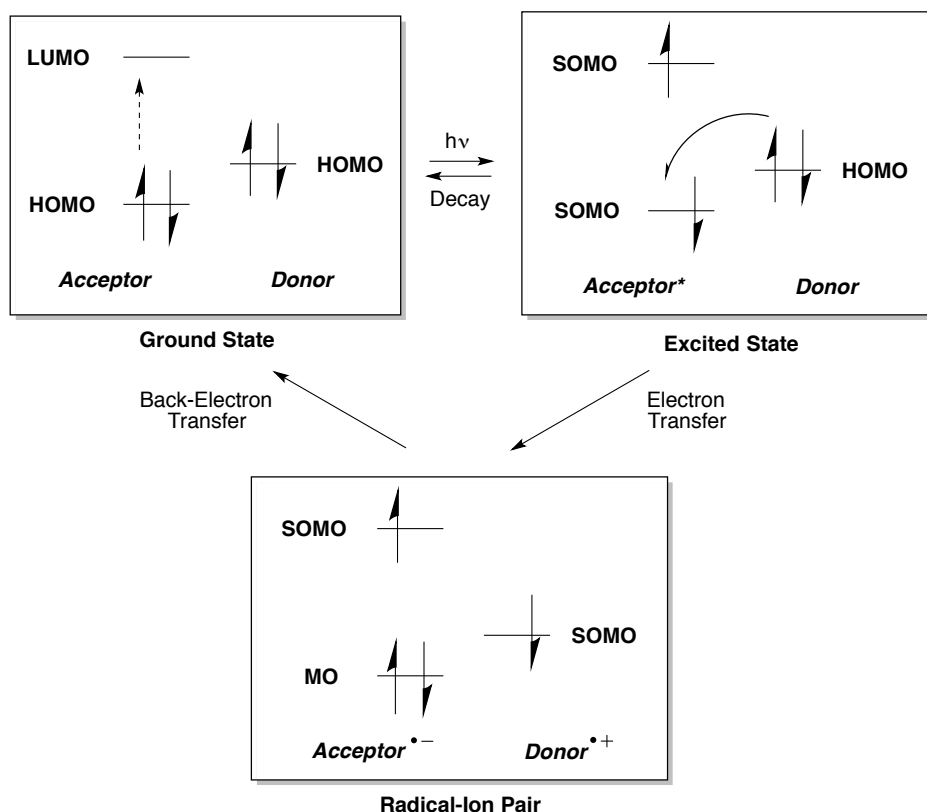
## 2.4. Anti-Markovnikov Heterofunctionalization: Photoredox Approaches

Given the tendency of electrochemical approaches to affect multi-electron oxidations of organic molecules, a more controlled method for alkene cation-radical generation is necessary to prevent over-oxidation of the generated cation-radical intermediates. The solution to this problem, in practice, has been the use of single-electron oxidants to generate alkene cation-radicals. While there are some examples of reactions proceeding through alkene cation-radicals that are generated by ground-state chemical oxidants, these oxidants are not strong enough to accept an electron from the majority of unactivated alkenes<sup>6</sup>.

As a result, the majority of successful transformations proceeding through alkene cation-radical intermediates have exploited a phenomenon known as photoinduced electron transfer (PET) to generate the reactive species (**Fig. 2.5**)<sup>7–10</sup>. In this process, a photon promotes a single electron from the HOMO to the LUMO of a molecule. This leaves an electron hole in the lower-energy of the two SOMOs formed by excitation. If the SOMO is low enough in energy, an electron can be transferred from the donor to the acceptor, forming a radical-ion pair (assuming that the interacting species are both neutral prior to transfer). The thermodynamics of PET processes can be calculated from the equation for the Gibbs energy of photoinduced electron transfer (**Eq. 1**)<sup>11</sup>, though in most cases a simplified relation (**Eq. 2**) is useful for predicting electron transfer between an excited acceptor and a donor. Boiled down to its essence, **Eq. 2** simply states that electron transfer is exergonic if the oxidation potential of the donor is

lower than the sum of the reduction potential of the acceptor plus the excited state energy ( $E_{0,0}$ ), a value calculated from the intersection of absorption and emission spectra of the photo-oxidant. For reference, a scale showing the reduction potentials of common ground-state (*italics*) and excited state (**bold**) oxidants is show in **Fig. 2.4.**, with the oxidation potentials of some common organic molecules shown in parallel to put the strengths of these oxidants in perspective.

**Figure 2.5. Frontier Molecular Orbital Depiction of Photoinduced Electron Transfer**



**Equation 1. Equation for Gibbs Free Energy of Photoinduced Electron Transfer**

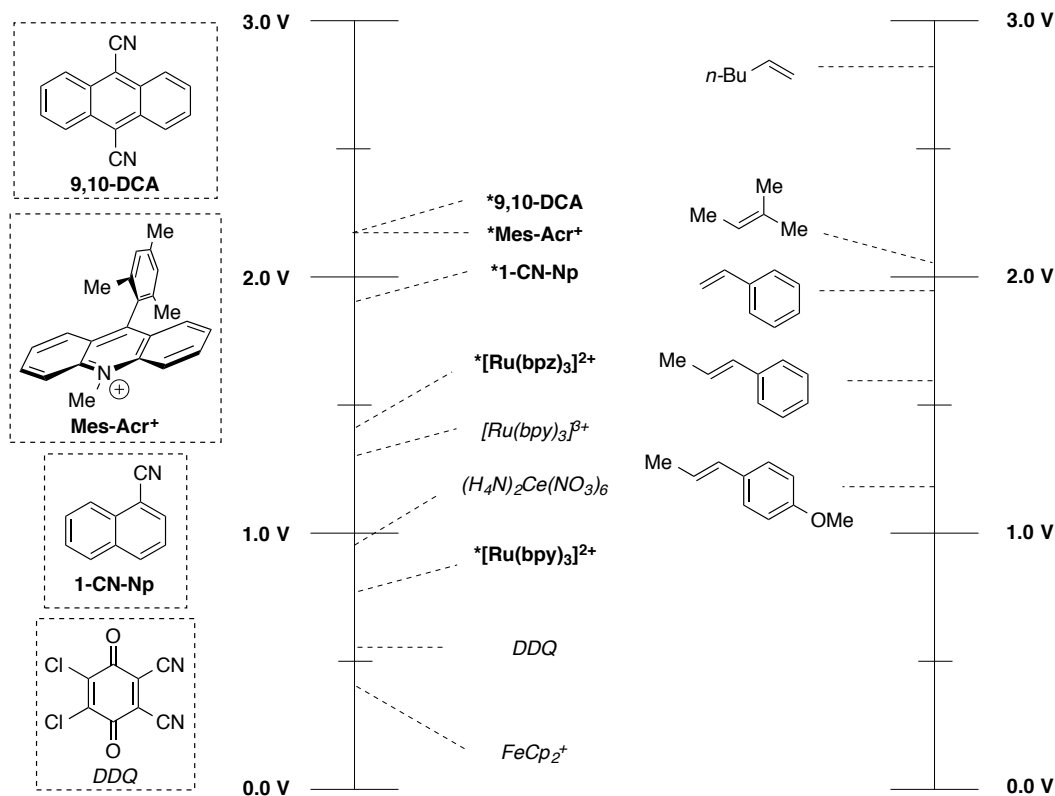
$$\Delta G^o = N_A \{ e [ E^o(D^{\bullet+}/D) - E^o(A/A^{\bullet-}) ] + w(D^{\bullet+}A^{\bullet-}) - w(DA) \} - E_{0,0}$$

**Equation 2. Simplified Inequality for Prediction of Spontaneous Electron Transfer**

*Electron transfer is exergonic if:*

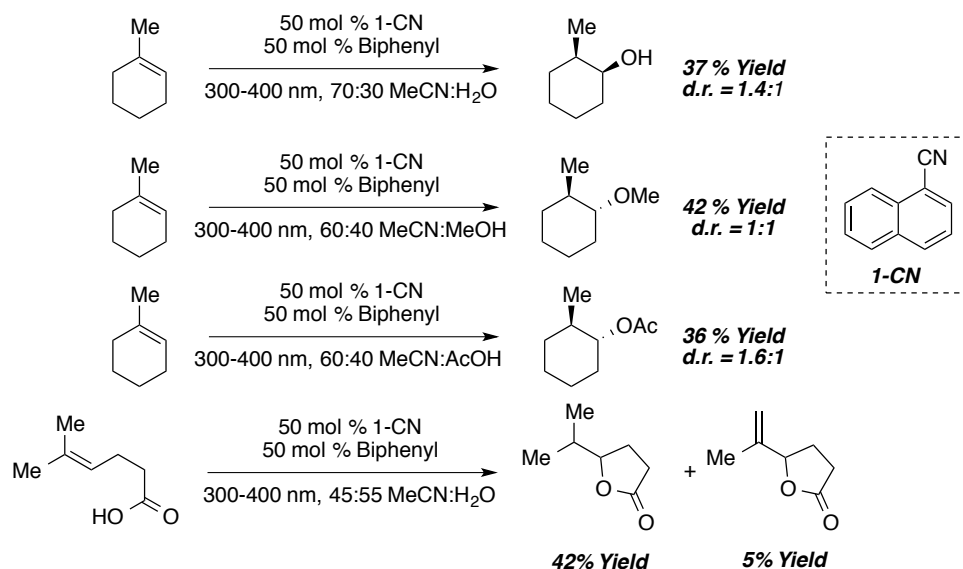
$$E_{red}^*(A/A^{\bullet-}) > E_{ox}(D^{\bullet+}/D)$$

**Figure 2.6. Reduction Potentials of a Variety of Oxidants and Photo-oxidants, and Oxidation Potentials of Some Representative Alkenes (vs. SCE)**



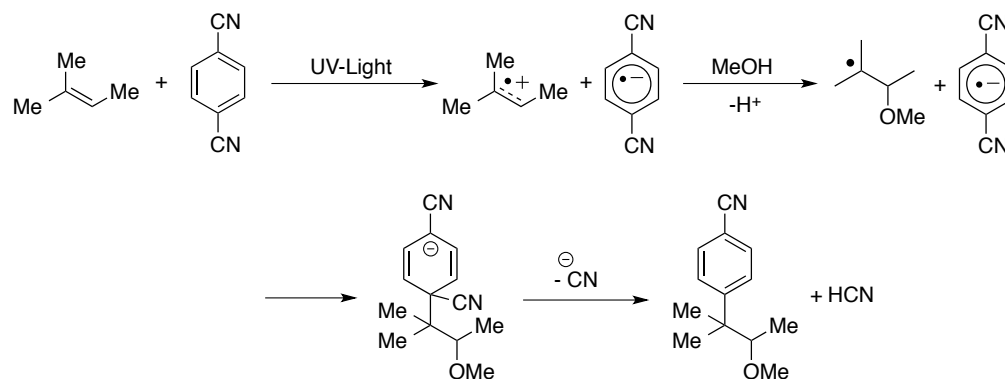
While seminal work on the addition of polar solvents to particular, privileged alkene cation-radicals generated by PET had carried out over a decade prior<sup>12,13</sup>, a pair of vital works on the use of PET to affect nucleophilic addition to unactivated alkene cation-radicals were published in 1987 by the Gassman lab. The first involved the addition of water, methanol, and acetic acid to 1-methylcyclohexene, promoted by the combination of an appropriate photo-oxidant (1-cyanonaphthalene) and biphenyl, which was hypothesized to act as a co-oxidant or electron relay<sup>14</sup>. Importantly, irradiation with ultraviolet light was necessary for productive reactions to occur. In the second work, Gassman also disclosed a photoinduced lactonization reaction, wherein an alkenoic acid was demonstrated to cyclize to a lactone with anti-Markovnikov selectivity<sup>15</sup>. In all cases demonstrated, 1-cyanonaphthalene was employed in a super-stoichiometric amount in comparison to product generated, and yields of all products were generally low. However, the regioselectivity obtained from these reactions serves as a vital benchmark for heterofunctionalization *via* the cation-radical (Fig. 2.7).

**Figure 2.7. Additions to Alkene Cation-Radicals Affected by 1-Cyanonaphthalene and Irradiation**



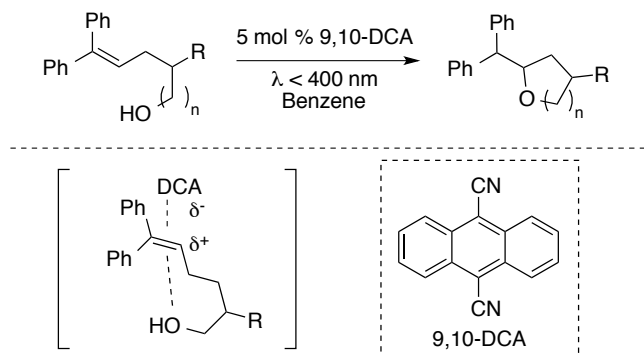
Further work in this vein has been also been carried out by Yamashita in the context of hydroamination of olefins *via* a PET mechanism<sup>16</sup>. In addition to the novelty of the studied transformation, this work included thorough study of the byproducts of reactions, and it was found that a frequent byproduct of these reactions was derived from oxidant incorporation into the final products. This type of reactivity pattern was later termed the “photo-NOCAS” (Photochemical Nucleophile-Olefin Combination, Aromatic Substitution) reaction by Arnold and coworkers, and its associated reactivity pattern has been well studied<sup>2,17,18</sup> (**Fig. 2.8**). While an interesting reaction in its own right, the arylation side-reaction serves to complicate the use of cyanoarene-derived photo-oxidants as catalysts for heterofunctionalization reactions.

**Figure 2.8. Example of Photo-NOCAS Type Reactivity**



Other work on nucleophilic additions to olefins by a photon-induced process has been carried out by Mizuno and coworkers. In an initial publication, the authors were able to demonstrate the efficient cyclization of alkenols derived from chain extension of 1,1-diphenylethylene<sup>19</sup> (**Fig. 2.8**). This work has been extended to include an enantioselective example from Inoue and coworkers, utilizing a chiral photosensitizer in concert with ultraviolet light to promote the transformation, but again the alkenes employed were restricted to 1,1-diphenylethylene derivatives<sup>20</sup>. The authors postulated that the reactivity observed is the result of a polarized exciplex, rather than the formation of discrete, solvent-separated cation-radicals (**Fig. 2.9**). Up to the point of our contributions, these transformations were the only known processes that employed catalytic amounts of a photosensitizer to promote heterofunctionalization reactions of olefins.

**Figure 2.9. Mizuno's Hydroetherification of Alkenols.**



This body of work demonstrated two things to us. First, there was precedent for the heterofunctionalization of olefins with a few different nucleophiles to unactivated alkenes, and extraordinary levels of regioselectivity favoring the anti-Markovnikov adduct could be achieved. However, it was also clear that these processes were either a) inefficient with respect the amounts of photo-oxidant that had to be employed, as well as the nature of the excitation that was required for reactions to occur, or b) restricted in terms of the demonstrated alkene scope. As such, we elected to further explore this reactivity pattern, to see if we could take an intriguing but restricted reactivity pattern out of the realm of obscurity, and develop a more synthetically applicable catalytic system for the anti-Markovnikov heterofunctionalization of olefins.

## 2.5. Attempted Hydroetherification of a Model Substrate Utilizing Prior Art

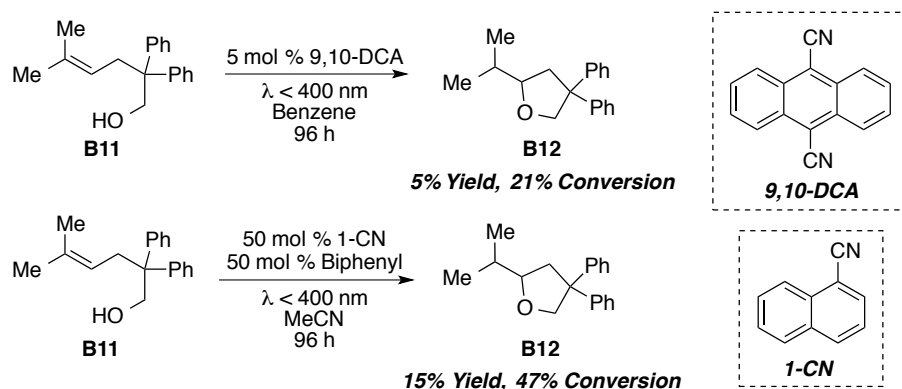
We elected to begin our studies on the development of such a platform with the hydroetherification of alkenols, as at the outset of our study, the only precedent that existed for this transformation were the aforementioned chemistry developed by Groves<sup>21</sup>, and the specialized hydroetherification chemistry developed by Mizuno<sup>19</sup>. We chose to start by optimizing this transformation on alkenol **B11** as our model substrate for several reasons. First was the fact that this substrate was found to possess a relatively high oxidation potential. At 1.95 V (MeCN, vs. SCE), we felt that the substrate was indicative of a typical, unactivated alkene that we could potentially target for cyclization. Secondly, the asymmetric substitution pattern of the alkene allows for unambiguous determination of the Markovnikov and anti-Markovnikov products, and the relative lack of strain in the developing rings (5 vs. 6) would give us a good probe for the regioselectivity of the reaction, without developing ring strain having a large effect on the consequent selectivity of the reaction.

Subjecting the alkenol substrate to both Gassman's conditions (0.5 equiv. 9-cyanonaphthalene, 0.5 equiv. biphenyl, MeCN as solvent, UV-irradiation) and Mizuno's conditions (0.2 equiv. 9,10-dicyanoanthracene, benzene as solvent, UV-irradiation) gave rise to markedly inefficient reactions (**Fig. 2.10**). Conversion was found to be incomplete even at extended reaction times, and we observed poor



mass balances and only small amounts of product tetrahydrofuran **B12** in crude reaction mixtures. Thus, we felt that we had identified a transformation with ample space for improvement and optimization.

**Figure 2.9. Cyclization of a Generic Alkenol Substrate Upon Exposure to Cyanoarene Photooxidant Conditions**



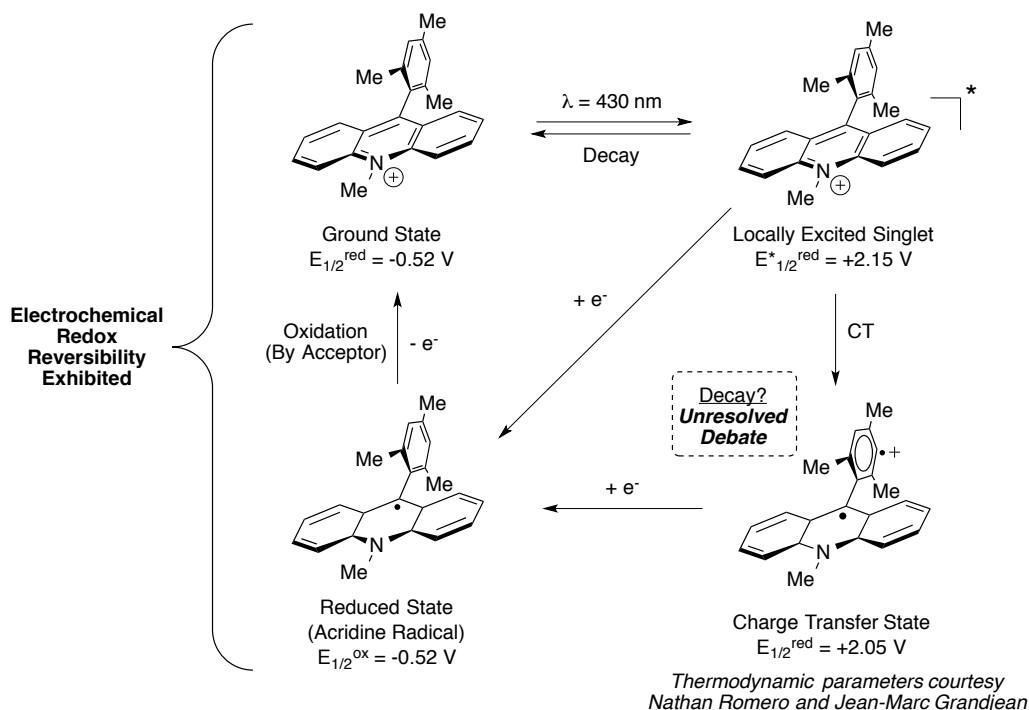
Our initial hypothesis was that this transformation was not limited by the oxidation of substrate, but rather by the photo-oxidants employed. That some conversion occurred was likely indicative of electron transfer leading to the desired, highly reactive cation-radical intermediates. The low yields observed were consistent with the low yields obtained in Gassman's original reactions, and we had correctly anticipated that Mizuno's conditions would not give rise to productive reactions given the lack of a 1,1-diphenylethylene unit for formation of the requisite exciplex.

## 2.6. Consideration of Organic Photo-oxidants

Our proposed remedy to the poor yields and the high oxidant loadings required for conversion was to approach the problem through the deployment of alternative photo-oxidants. Given the development of a vast array of reactions driven by electron transfer, and the associated development of a multitude of photo-oxidants, this seemed to us to be a viable strategy. In examining the literature for potential photo-oxidants to deploy for a catalytic, cation-radical mediated hydroetherification of alkenols, one stood out to us as a potentially applicable catalyst: 9-mesityl,10-methylacridinium perchlorate<sup>22</sup>. Pioneered by Fukuzumi, et al., the initial disclosure of this compound focused primarily on its posited long-lived (indefinite at cryogenic temperatures) and high-energy charge-transfer state, resulting from

intramolecular charge transfer from the mesityl moiety at the 9-position of the acridinium ring, to the excited acridinium chromophore<sup>23</sup> (**Fig. 2.11**). This was in contrast to most organic photo-oxidants, which tend to have lifetimes reported to be on the order of nanoseconds<sup>24</sup>. Fukuzumi's hypothesis for the existence of this state was that the methyl groups projected over the acridinium ring served to hold the mesityl group rigidly perpendicular to the acridinium ring, enabling charge transfer and separation but essentially prohibiting back electron transfer from the acridine radical back to the mesityl cation-radical. The existence of such a long-lived state, however, has been a contentious issue in the literature, and has been the subject of a vigorous and still ongoing debate<sup>25–31</sup>. In addition to the interesting photophysics of this molecule, Fukuzumi importantly demonstrated the electrochemical reversibility of single-electron transfer to the acridinium moiety, indicating that the ensuing radical was persistent, and by extension we postulated that the acridinium photocatalysts were more likely than the cyanoarene photo-oxidants to remain intact as a catalytic intermediate.

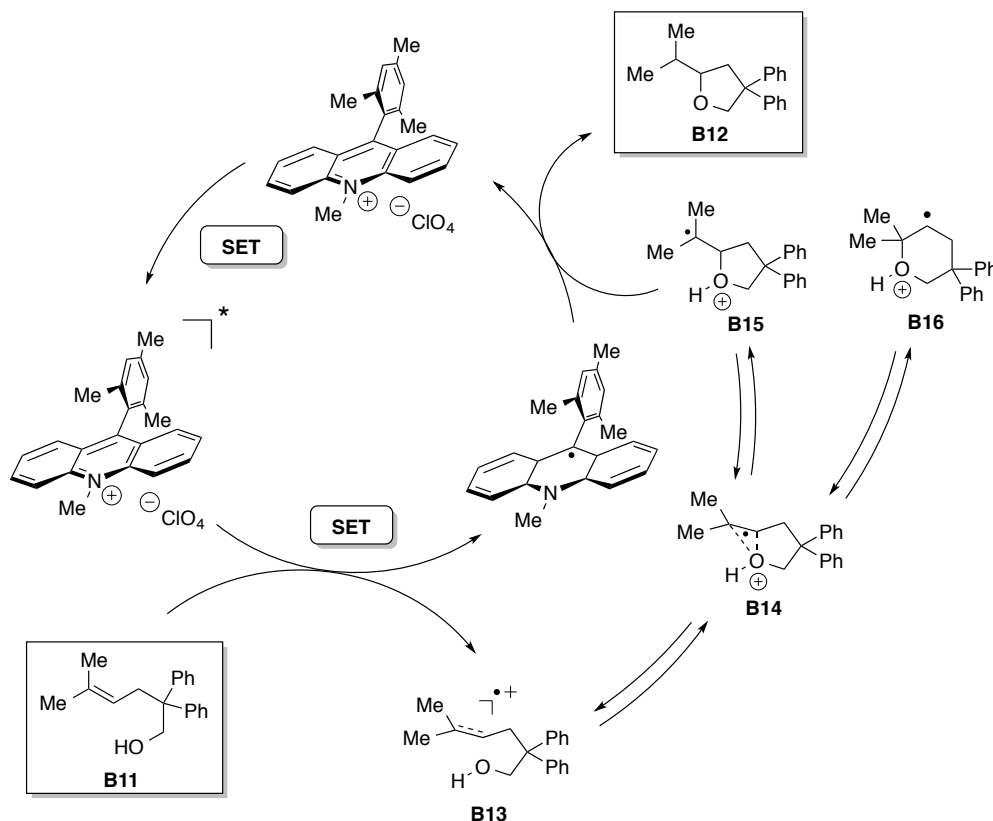
**Figure 2.11. Oxidizing States of 9-Mesityl,10-Methyl Acridinium Ion And Exhibited Redox Reversibility**



Acridinium-based photocatalysts had also been demonstrated to be robust catalysts in synthesis before we employed it in our chemistry. Fukuzumi and coworkers have disclosed a number of transformations utilizing this species, primarily employing it for its unique ability to affect oxidation of organic molecules and inorganic ions, and the ensuing acridine radical's ability to reduce oxygen to form superoxide radical-anion intermediates or hydrogen peroxide as an end product<sup>32-37</sup>. Besides this motif's ability to act as both a strong oxidant in the excited state, and as a moderate reductant as the ground state conjugate radical, the acridinium photocatalyst also possessed a number of other properties that we felt would be advantageous to the system we were seeking to develop. The cationic nature of the photo-oxidant would render the reduced species to be a neutral radical, minimizing coulombic attraction between the acridine radical and the cation-radical of the alkenol substrate. In turn, this would enable a more efficient formation of solvent-separated ion pairs and reduce effects of back-electron transfer. Additionally, the photocatalyst has as strong absorbance band in the visible light region ( $\lambda = 430$  nm). Given that a number of companies have developed convenient PAR38 LED bulbs that screw into simple light sockets that emit photons at wavelengths centered between 450-465 nm, the synthetic setup we would be able to employ would be far more simple than the high-pressure mercury lamps or ultraviolet lightboxes required for reactions with UV-active photo-oxidants.

Focusing on how we anticipated that this reaction could proceed in a catalytic fashion, the reader is directed to **Fig. 2.12**. Irradiation of the mesityl-acridinium photooxidant with blue light would generate the singlet excited state of the photo-oxidant, which could then act directly as a photooxidant for alkenol **B11**, or proceed to carry out oxidation through the ensuing charge-transfer state. Intramolecular nucleophilic addition of the pendant alcohol to the oxidized alkene (**B13**) would first produce the bridged intermediate (**B14**) first posited by Arnold, and then collapse to form either of two distonic cation-radicals in equilibration with one-another (**B15**, **B16**). We then proposed that the more energetically favorable tertiary radical species (**B15**) could be reduced by the acridine radical, and proton-transfer from the protonated oxygen center to the newly formed carbanion would furnish product (**B12**) selectively, with concurrent regeneration of the acridinium photocatalyst.

**Figure 2.12. Hypothetical Mechanism for Anti-Markovnikov Heterofunctionalization of Alkenes with Mesityl Acridinium Ion as a Photocatalyst**

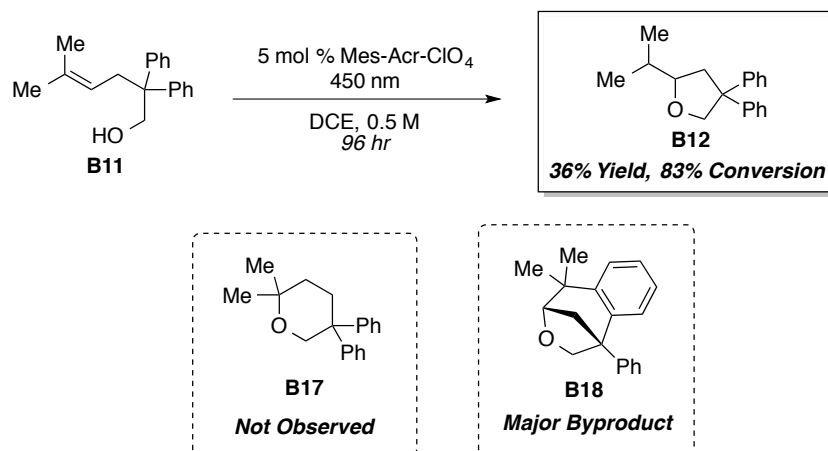


## 2.7. Initial Results – Alkenol Cyclization Utilizing 9-Mesityl,10-Methylacridinium Perchlorate as Photocatalyst

With this proposed mechanism in mind, we exposed alkenol **B11** to irradiation with blue light, using 5 mol % 9-mesityl,10-methyl acridinium perchlorate (5 mol %) as the photocatalyst. Care was taken to rigorously degas the solution to prevent oxygen from interfering with the reaction, which could occur by oxidizing the acridinium photocatalyst (thus preventing reduction of the intermediate radicals), or by trapping intermediate radicals as peroxides. Additionally, the reaction was irradiated for an extended period (96 hours) to allow for maximal conversion in a reasonable period of time. The results obtained from this initial trial were promising (**Fig. 2.13**). The desired product of anti-Markovnikov hydroetherification (**B12**) was observed, and notably we did not observe the product of Markovnikov hydroetherification (**B17**). However, the low yield obtained was due to the formation of high molecular

weight byproducts, likely as a result of oligomerization. Additionally, we observed the evolution of an interesting major reaction byproduct (**B18**).

**Figure 2.13. Anti-Markovnikov Hydrofunctionalization of Alkenol **B11** Under Irradiation in the Presence of 9-Mesityl,10-Methylacridinium Perchlorate**



## 2.8. Reaction Byproduct Analysis

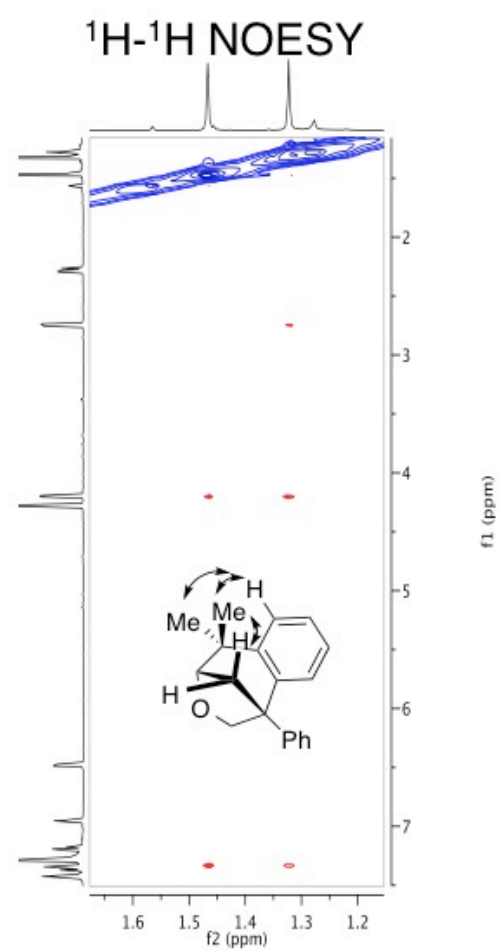
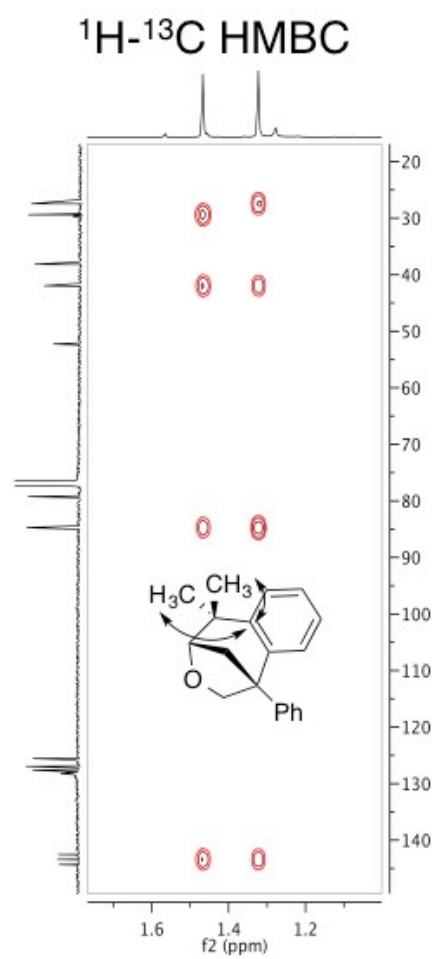
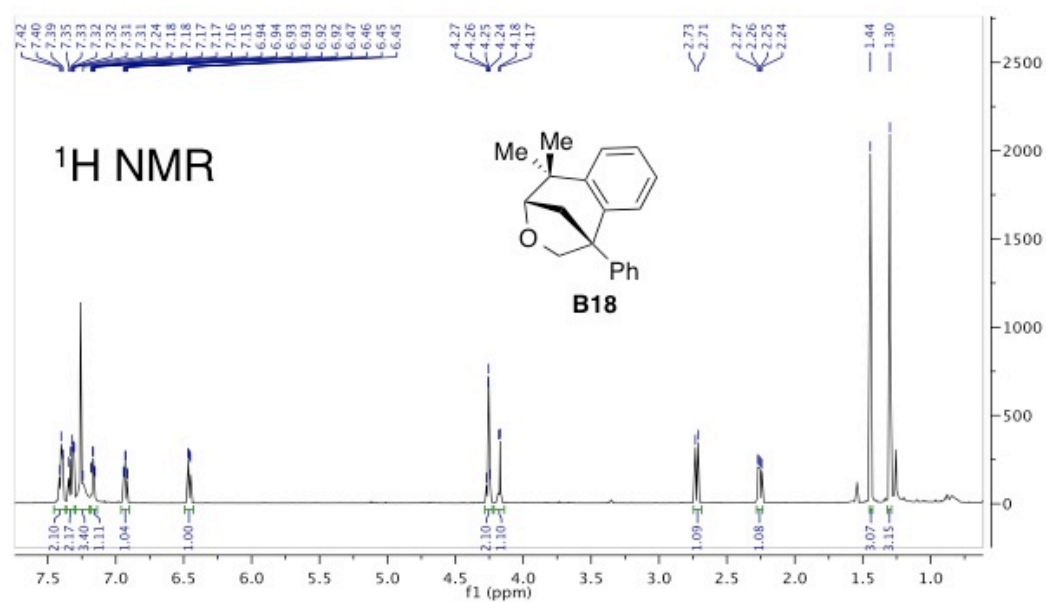
Careful analysis of characterization data for the isolated byproduct led to the assignment of this byproduct as polycyclic ether **B18** (Fig. 2.13), and this assignment was supported by several lines of evidence (Fig. 2.14). First, the mass spectrum obtained of the material indicated a molecular weight of 264 Da, indicative of a product that had been oxidized by two electrons and two protons. The <sup>1</sup>H NMR spectrum of the isolated material indicated significant upfield shifting of some of the aromatic resonances from one of the phenyl groups in the backbone, and the methyl groups on the substrate were observed as singlet resonances. Additionally, the diastereotopic protons observed suggested that the desired ring had, in fact, been formed. This led us to believe that a bond had formed between the tertiary carbon radical intermediate and one of the aryl groups. This hypothesis was confirmed by a <sup>1</sup>H-<sup>13</sup>C HMBC crosspeak between the two singlet methyl groups and carbons belonging to one of the aromatic rings. Finally, a <sup>1</sup>H-<sup>1</sup>H NOESY experiment produced a spectrum demonstrating several through-space interactions, most distinctively between the signals corresponding to the methyl groups (importantly, presenting as singlets) and a single aryl proton, as well as only one methyl group showing a cross-peak with a proton resonance posited to be on the bridging methylene unit. Computational optimization of the molecular geometry of

the posited product suggests that each of these resonances are, in fact, close enough in space to one another to observe the NOESY crosspeaks. (See **Appendix 2** for full spectral details).

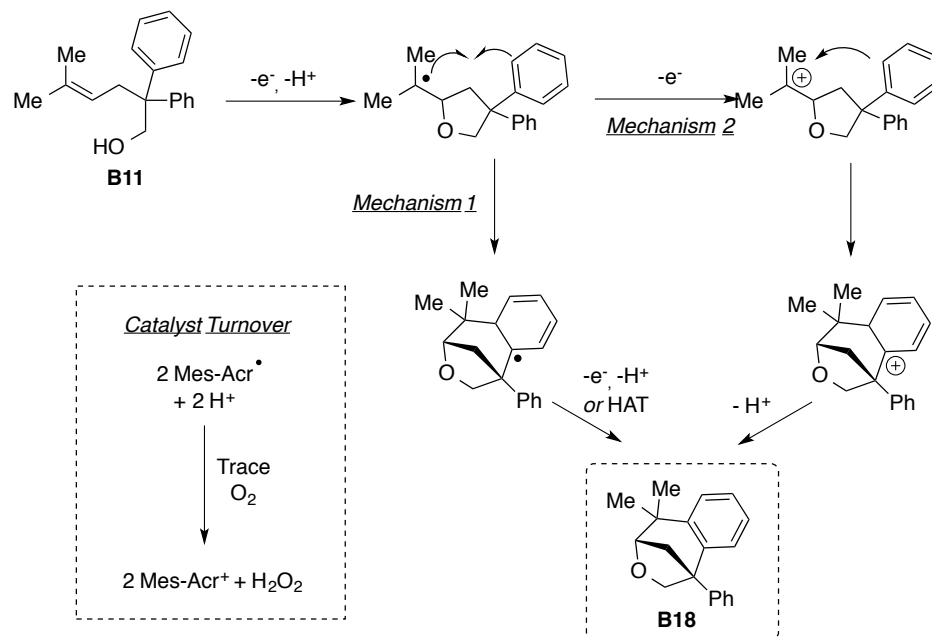
The implications of the observation of this product were profound. This structure, along with the associated oligomerization pathway, indicated to us that oxidation of substrate was likely occurring. However, the observed byproducts led us to believe that reduction of the tertiary radical by the acridine radical was not occurring at a sufficient rate to compete with the formation of byproducts, either through secondary oxidation followed by Friedel-Crafts type alkylation or by radical cyclization followed by secondary oxidation of the aryl radical and deprotonation (**Fig. 2.15**), and similar products have been shown to be accessible by the use of copper catalysis for hydroetherification in conjunction with an included oxidant<sup>38</sup>. The hypothesis of inefficient radical reduction is also supported by simple thermodynamic calculations: if the reduction potential of *t*-butyl radical (Estimated at -1.6 V vs. SCE)<sup>39</sup> is used as a reasonable estimate for the reduction potential of the tertiary radical on our substrate, the reduction event would be predicted to be unfavorable by approximately 1.0 V (23 kcal/mol).

As a result, we determined that attempting to affect anti-Markovnikov heterofunctionalization reactions through the use of *only* the Fukuzumi photooxidant was likely to be met with failure. However, given these promising initial results, we elected to pursue an alternative strategy to attempt to take advantage of, rather than battle, the radical intermediate left over after the key, anti-Markovnikov nucleophilic addition event, in order to both furnish product and turn over the acridinium photocatalyst.

**Figure 2.14. Highlights of Spectroscopic Evidence for the Structural Assignment of Byproduct B18**



**Figure 2.15. Possible Mechanisms for the Formation of Compound B18**



## 2.9. Summary

In this chapter, the justification for perusing alkene cation-radicals as reaction intermediates for anti-Markovnikov heterofunctionalization was presented, and it was shown that both experiment and theory had demonstrated a reliable reactivity pattern to build on. Previously developed systems, dependent on photoredox catalysis, were described, and it was demonstrated that application of these systems to a standard alkenol substrate led to minimal reaction efficiency. Our initial hypothesis, that the major issue preventing effective catalysis of the hydroetherification reaction was the choice of photo-oxidant, was presented, as well as details on our promising initial results with regards to the use the Fukuzumi photooxidant in a catalytic amount to affect a hydrotherification reaction enabled by visible-light photoredox catalysis.



## REFERENCES

- (1) Schmittel, M.; Burghart, A. Understanding Reactivity Patterns of Radical Cations. *Angew. Chem. Int. Ed. Engl.* **1997**, *36*, 2550–2589.
- (2) Arnold, D. R.; Chan, M. S. W.; McManus, K. A. Photochemical Nucleophile–olefin Combination, Aromatic Substitution (photo-NOCAS) Reaction, Part 12. Factors Controlling the Regiochemistry of the Reaction with Alcohol as the Nucleophile. *Can. J. Chem.* **1996**, *74*, 2143–2166.
- (3) Sutterer, A.; Moeller, K. D. Reversing the Polarity of Enol Ethers: An Anodic Route to Tetrahydrofuran and Tetrahydropyran Rings. *J. Am. Chem. Soc.* **2000**, *122*, 5636–5637.
- (4) Moeller, K. Intramolecular Anodic Olefin Coupling Reactions: Using Radical Cation Intermediates to Trigger New Umpolung Reactions. *Synlett* **2009**, *2009*, 1208–1218.
- (5) Campbell, J. M.; Xu, H.-C.; Moeller, K. D. Investigating the Reactivity of Radical Cations: Experimental and Computational Insights into the Reactions of Radical Cations with Alcohol and P-Toluene Sulfonamide Nucleophiles. *J. Am. Chem. Soc.* **2012**, *134*, 18338–18344.
- (6) Connelly, N. G.; Geiger, W. E. Chemical Redox Agents for Organometallic Chemistry. *Chem. Rev.* **1996**, *96*, 877–910.
- (7) Prier, C. K.; Rankic, D. A.; MacMillan, D. W. C. Visible Light Photoredox Catalysis with Transition Metal Complexes: Applications in Organic Synthesis. *Chem. Rev.* **2013**, *113*, 5322–5363.
- (8) Narayanam, J. M. R.; Stephenson, C. R. J. Visible Light Photoredox Catalysis: Applications in Organic Synthesis. *Chem. Soc. Rev.* **2010**, *40*, 102–113.
- (9) Nicewicz, D. A.; Nguyen, T. M. Recent Applications of Organic Dyes as Photoredox Catalysts in Organic Synthesis. *ACS Catal.* **2014**, *4*, 355–360.
- (10) Yoon, T. P.; Ischay, M. A.; Du, J. Visible Light Photocatalysis as a Greener Approach to Photochemical Synthesis. *Nat. Chem.* **2010**, *2*, 527–532.
- (11) Braslavsky, S. E. Glossary of Terms Used in Photochemistry, 3rd Edition (IUPAC Recommendations 2006). *Pure Appl. Chem.* **2007**, *79*.
- (12) Neunteufel, R. A.; Arnold, D. R. Radical Ions in Photochemistry. I. 1,1-Diphenylethylene Cation Radical. *J. Am. Chem. Soc.* **1973**, *95*, 4080–4081.
- (13) Shigemitsu, Y.; Arnold, D. R. Radical Ions in Photochemistry. Sensitised (electron-Transfer) Photochemical Reactions of Some 1-Phenylcycloalkenes in Polar, Nucleophilic Solvents. *J. Chem. Soc. Chem. Commun.* **1975**, 407–408.
- (14) Gassman, P. G.; Bottorff, K. J. Anti-Markovnikov Addition of Nucleophiles to a Non-Conjugated Olefin via Single Electron Transfer Photochemistry. *Tetrahedron Lett.* **1987**, *28*, 5449–5452.
- (15) Gassman, P. G.; Bottorff, K. J. Photoinduced Lactonization. A Useful but Mechanistically Complex Single Electron Transfer Process. *J. Am. Chem. Soc.* **1987**, *109*, 7547–7548.

- (16) Yamashita, T.; Yasuda, M.; Isami, T.; Tanabe, K.; Shima, K. Photoinduced Nucleophilic Addition of Ammonia and Alkylamines to Methoxy-Substituted Styrene Derivatives. *Tetrahedron* **1994**, *50*, 9275–9286.
- (17) McManus, K. A.; Arnold, D. R. The Photochemical Nucleophile–olefin Combination, Aromatic Substitution (photo-NOCAS) Reaction. Part 10: Intramolecular Reactions Involving Alk-4-Enols and 1,4-Dicyanobenzene. *Can. J. Chem.* **1995**, *73*, 2158–2169.
- (18) Mangion, D.; Arnold, D. R. Photochemical Nucleophile–Olefin Combination, Aromatic Substitution Reaction. Its Synthetic Development and Mechanistic Exploration. *Acc. Chem. Res.* **2002**, *35*, 297–304.
- (19) Mizuno, K.; Tamai, T.; Nishiyama, T.; Tani, K.; Sawasaki, M.; Otsuji, Y. Intramolecular Photocyclization of  $\Omega$ ,  $\Omega$ -Diphenyl-( $\omega$ -1)-Alken-1-Ols by an Exciplex Quenching Mechanism. *Angew. Chem. Int. Ed. Engl.* **1994**, *33*, 2113–2115.
- (20) Asaoka, S.; Kitazawa, T.; Wada, T.; Inoue, Y. Enantiodifferentiating Anti-Markovnikov Photoaddition of Alcohols to 1,1-Diphenylalkenes Sensitized by Chiral Naphthalenecarboxylates. *J. Am. Chem. Soc.* **1999**, *121*, 8486–8498.
- (21) Sanford, M. S.; Groves, J. T. Anti-Markovnikov Hydrofunctionalization of Olefins Mediated by Rhodium–Porphyrin Complexes. *Angew. Chem. Int. Ed.* **2004**, *43*, 588–590.
- (22) Nicewicz, D.; Hamilton, D. Organic Photoredox Catalysis as a General Strategy for Anti-Markovnikov Alkene Hydrofunctionalization. *Synlett* **2014**.
- (23) Fukuzumi, S.; Kotani, H.; Ohkubo, K.; Ogo, S.; Tkachenko, N. V.; Lemmetyinen, H. Electron-Transfer State of 9-Mesityl-10-Methylacridinium Ion with a Much Longer Lifetime and Higher Energy Than That of the Natural Photosynthetic Reaction Center. *J. Am. Chem. Soc.* **2004**, *126*, 1600–1601.
- (24) Ohkubo, K.; Suga, K.; Morikawa, K.; Fukuzumi, S. Selective Oxygenation of Ring-Substituted Toluenes with Electron-Donating and -Withdrawing Substituents by Molecular Oxygen via Photoinduced Electron Transfer. *J. Am. Chem. Soc.* **2003**, *125*, 12850–12859.
- (25) Benniston, A. C.; Harriman, A.; Li, P.; Rostron, J. P.; van Ramesdonk, H. J.; Groeneveld, M. M.; Zhang, H.; Verhoeven, J. W. Charge Shift and Triplet State Formation in the 9-Mesityl-10-Methylacridinium Cation. *J. Am. Chem. Soc.* **2005**, *127*, 16054–16064.
- (26) Ohkubo, K.; Kotani, H.; Fukuzumi, S. Misleading Effects of Impurities Derived from the Extremely Long-Lived Electron-Transfer State of 9-Mesityl-10-Methylacridinium Ion. *Chem. Commun.* **2005**, 4520–4522.
- (27) Benniston, A. C.; Harriman, A.; Li, P.; Rostron, J. P.; Verhoeven, J. W. Illumination of the 9-Mesityl-10-Methylacridinium Ion Does Not Give a Long-Lived Photoredox State. *Chem. Commun.* **2005**, 2701–2703.

- (28) Benniston, A. C.; Harriman, A.; Verhoeven, J. W. Comment: Electron-Transfer Reactions in the 9-Mesityl-10-Methylacridinium Ion: Impurities, Triplet States and Infinitely Long-Lived Charge-Shift States? *Phys. Chem. Chem. Phys.* **2008**, *10*, 5156–5158.
- (29) Fukuzumi, S.; Kotani, H.; Ohkubo, K. Response: Why Had Long-Lived Electron-Transfer States of Donor-Substituted 10-Methylacridinium Ions Been Overlooked? Formation of the Dimer Radical Cations Detected in the near-IR Region. *Phys. Chem. Chem. Phys.* **2008**, *10*, 5159–5162.
- (30) Benniston, A. C.; Elliott, K. J.; Harrington, R. W.; Clegg, W. On the Photochemical Stability of the 9-Mesityl-10-Methylacridinium Cation. *Eur. J. Org. Chem.* **2009**, *2009*, 253–258.
- (31) Hoshino, M.; Uekusa, H.; Tomita, A.; Koshihara, S.; Sato, T.; Nozawa, S.; Adachi, S.; Ohkubo, K.; Kotani, H.; Fukuzumi, S. Determination of the Structural Features of a Long-Lived Electron-Transfer State of 9-Mesityl-10-Methylacridinium Ion. *J. Am. Chem. Soc.* **2012**, *134*, 4569–4572.
- (32) Kotani, H.; Ohkubo, K.; Fukuzumi, S. Photocatalytic Oxygenation of Anthracenes and Olefins with Dioxygen via Selective Radical Coupling Using 9-Mesityl-10-Methylacridinium Ion as an Effective Electron-Transfer Photocatalyst. *J. Am. Chem. Soc.* **2004**, *126*, 15999–16006.
- (33) Ohkubo, K.; Nanjo, T.; Fukuzumi, S. Photocatalytic Electron-Transfer Oxidation of Triphenylphosphine and Benzylamine with Molecular Oxygen via Formation of Radical Cations and Superoxide Ion. *Bull. Chem. Soc. Jpn.* **2006**, *79*, 1489–1500.
- (34) Ohkubo, K.; Mizushima, K.; Iwata, R.; Souma, K.; Suzuki, N.; Fukuzumi, S. Simultaneous Production of P-Tolualdehyde and Hydrogen Peroxide in Photocatalytic Oxygenation of P-Xylene and Reduction of Oxygen with 9-Mesityl-10-Methylacridinium Ion Derivatives. *Chem. Commun.* **2010**, *46*, 601–603.
- (35) Ohkubo, K.; Fujimoto, A.; Fukuzumi, S. Metal-Free Oxygenation of Cyclohexane with Oxygen Catalyzed by 9-Mesityl-10-Methylacridinium and Hydrogen Chloride under Visible Light Irradiation. *Chem. Commun.* **2011**, *47*, 8515–8517.
- (36) Ohkubo, K.; Mizushima, K.; Iwata, R.; Fukuzumi, S. Selective Photocatalytic Aerobic Bromination with Hydrogen Bromide via an Electron-Transfer State of 9-Mesityl-10-Methylacridinium Ion. *Chem. Sci.* **2011**, *2*, 715–722.
- (37) Fukuzumi, S.; Ohkubo, K. Selective Photocatalytic Reactions with Organic Photocatalysts. *Chem. Sci.* **2013**, *4*, 561–574.
- (38) Miller, Y.; Miao, L.; Hosseini, A. S.; Chemler, S. R. Copper-Catalyzed Intramolecular Alkene Carboetherification: Synthesis of Fused-Ring and Bridged-Ring Tetrahydrofurans. *J. Am. Chem. Soc.* **2012**, *134*, 12149–12156.
- (39) Andrieux, C. P.; Gallardo, I.; Saveant, J. M. Outer-Sphere Electron-Transfer Reduction of Alkyl Halides. A Source of Alkyl Radicals or of Carbanions? Reduction of Alkyl Radicals. *J. Am. Chem. Soc.* **1989**, *111*, 1620–1626.

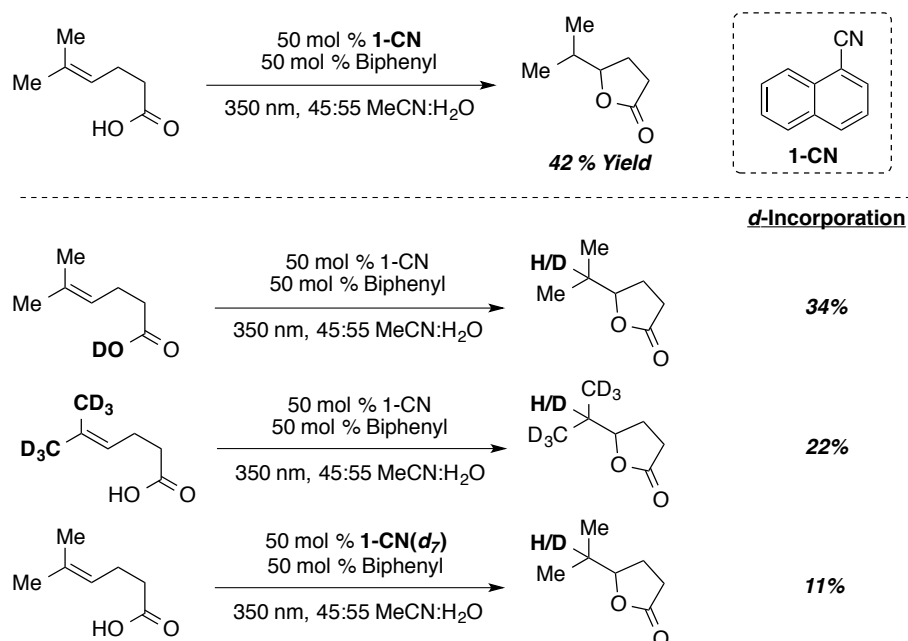
## CHAPTER 3: THE USE OF HYDROGEN ATOM DONOR ADDITIVES TO EFFECT THE DIRECT, ANTI-MARKOVNIKOV HYDROETHERIFICATION OF ALKENOLS

### 3.1. Introduction

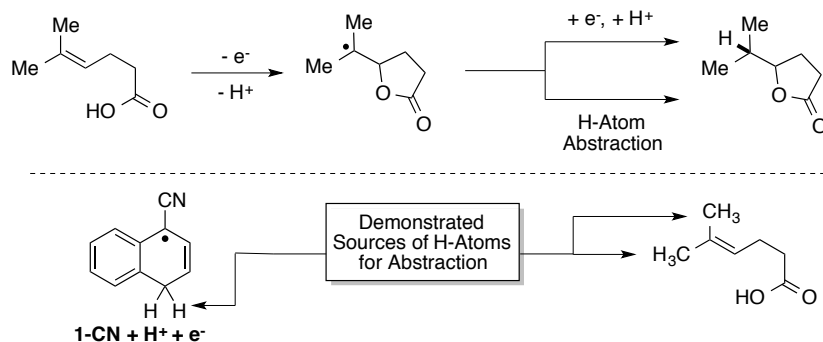
In Chapter 2, it was presented that an alkenol can be cyclized to form the anti-Markovnikov adduct with high regioselectivity with irradiation in the presence of the Fukuzumi catalyst, but with relatively low efficiency. This was in part due to the formation of an accompanying polycyclic byproduct. Our hypothesis for the formation of this undesired byproduct was that the reduction of a substituted radical likely to be produced over the course of the reactions was thermodynamically unfavorable, and therefore unlikely to occur. Thus, we had to reconsider the manner in which we could utilize the reactivity the radical intermediates. In devising such a strategy, we derived inspiration from a pair of key reports found in the literature.

The first of these communications was Gassman's report on photoinduced lactonization promoted by 1-cyanonaphthalene (1-CN)<sup>1</sup>. In this account, detailed deuterium-labeling studies suggested that the mechanism at play was exceedingly complex (**Fig. 3.1**). It was demonstrated the highlighted proton found on the isopropyl group in the final product was derived from a variety of sources. These included the acid (34% *d*- incorporation when labeled), the methyl groups on the substrate itself (22% *d*- incorporation, when labeled), and the photo-oxidant itself (11% *d*- incorporation, when completely labeled). This indicated to the authors that multiple, convergent mechanistic pathways were possible manners in which the observed major product was formed. Additionally, they determined that it was likely that both reduction of the radical by the photocatalyst, as well as Hydrogen-atom abstraction from a second molecule of substrate, were mechanistic steps by which the desired product was formed from the radical intermediate (**Fig. 3.2**).

**Figure 3.1. Summary of Deuterium Labeling Experiments for Photoinduced Lactonization Promoted by 1-Cyanonaphthalene**



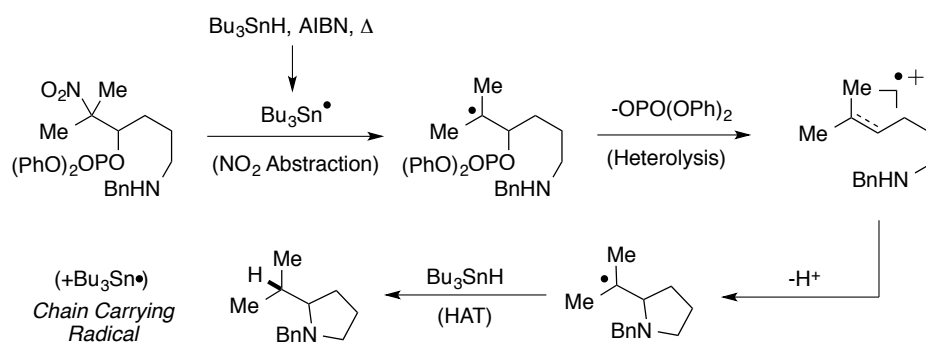
**Figure 3.2. Possible Mechanisms for Gassman's Photoinduced Lactonization**



A second inspiration came from a report by Crich and coworkers (**Fig. 3.3**). Though their work was primarily focused on the use of cation-radical intermediates generated by the heterolysis of  $\alpha$ -substituted radicals to affect a series of cascade reactions known as polar-radical crossover cyclizations<sup>2</sup>, the manner in which they were able to furnish product gave us a hint as to an appropriate strategy for handling the radical intermediate. The cation-radical intermediates in these examples were generated by generation of tributyltin radical in an initial initiation step, which is followed by departure of a leaving

group at the  $\alpha$ -position (commonly a diarylphosphate). The cation-radical intermediates then underwent reaction with tethered nucleophiles, affording cyclized products. Importantly, the concomitant radical was then trapped with a stoichiometric amount of tributyltin hydride as a hydrogen atom donor, regenerating the chain-carrying tin radical.

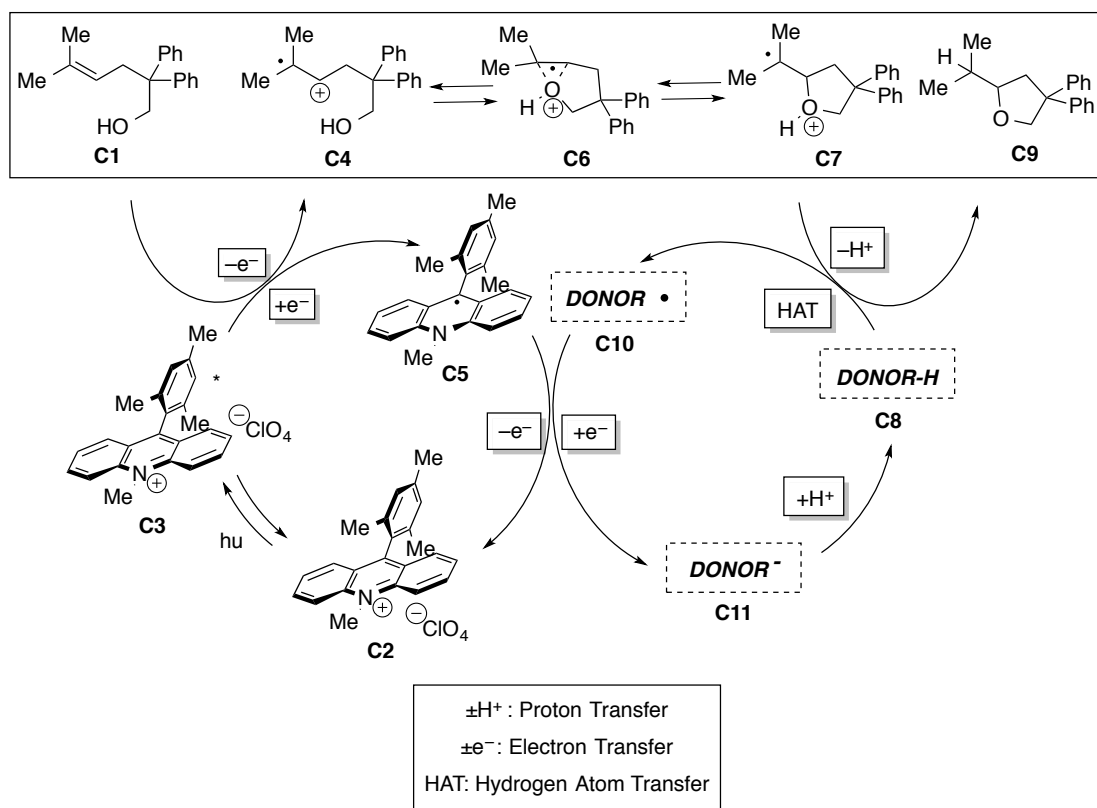
**Figure 3.3. Anti-Markovnikov Hydroamination through Stoichiometric Generation of an Alkene-Cation Radical, Promoted by Tributyltin Hydride.**



### 3.2. Catalytic Strategy Incorporating a Hydrogen-Atom Donor Additive.

These reports, taken in tandem, inspired us to consider the addition of a hydrogen atom donor to our reactions to promote efficient formation of the desired alkenol products over the observed polycyclic and oligomeric byproducts<sup>3</sup>. However, in devising such a strategy, we had to consider the entire mechanism that we were hoping could be operable. Such a cycle (**Fig. 3.4**) started with our representative alkenol substrate (**C1**), and the Fukuzumi photocatalyst (**C2**). Upon excitation of the catalyst with 450 nm light, the excited state of the photooxidant (**C3**) would oxidize the alkenol to the respective cation-radical intermediate (**C4**), and form acridine radical **C5**. The cation-radical could proceed through bridged intermediate (**C6**) to form the more favorable distonic cation-radical (**C7**), then deprotonate and abstract a hydrogen atom from donor **C8**. This would form the final tetrahydrofuran product **C9**, and also produce the conjugate radical of the donor (**C10**). Regeneration of the ground-state acridinium catalyst **C2** would have to occur through single-electron oxidation of radical **C5** by radical **C11**, producing anion **C12** in the process. Donor **C9** would then have to be regenerated by protonation of **C12** by the previously formed equivalent of acid.

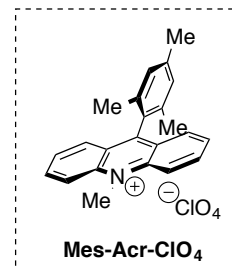
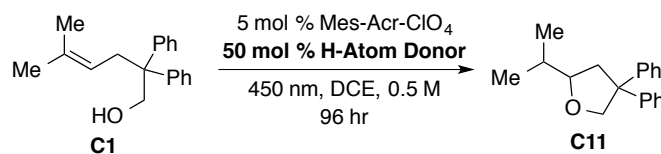
**Figure 3.4. Outline of Mechanism Incorporating a Radical Relay Strategy**



As we hoped to render this transformation catalytic in all components, we subjected our reaction to the same standard conditions that were outlined in Chapter 2, except in this case, half an equivalent of potential hydrogen atom donors were included in the reactions. The results of this screen, again carried out for a prolonged period of time (96 hours), can be seen in **Fig. 3.4**. Perhaps unsurprisingly, the two potential donors screened with the lowest known BDEs<sup>4-10</sup> were found to be the most effective for promoting the transformation (**Fig. 3.4, Entries 2-3**). In particular, 2-phenylmalononitrile (2-PMN) was found to be particularly effective, furnishing the product with complete anti-Markovnikov selectivity in 73% yield. It was initially surprising that more of the employed hydrogen atom donors did not improve the reaction efficiency and yield, especially considering the high bond strength of the new 3° C-H bond being formed (~90-95 kcal/mol)<sup>11</sup>. Given the high thermodynamic driving force for H-atom transfer from most of these donors, we hypothesized that the unique ability of 2-phenylmalonitrile to promote the

reaction was due to the combination of all of its properties: not just its extraordinarily low C-H bond dissociation energy.

**Table 3.1. Results of Hydrogen Atom Donor Screen**



Entry	H-Atom Donor	BDE (kcal/mol)	Yield <sup>a</sup>
1	None	N/A	36%
2	2- Phenylmalononitrile	77	73%
3	9-Phenylfluorene	74	51%
4	N-Hydroxyphthalimide	88	41%
5	Hydroxybenzotriazole	Not Available	37%
6	Ethylcyanoacetate	91	36%
7	Ascorbic Acid Acetonide	Not Available	33%
8	N-Hydroxysuccinimide	Not Available	33%
9	Phenylethylcyanoacetate	80	33%
10	Diethylphenylmalonate	Not Available	30%
11	Triphenylsilane	85	29%
12	Triphenylmethane	81	24%
13	Phthalimide	Not Available	24%
14	Succinimide	Not Available	22%
15	Benzyl Cyanide	82	16%
16	BHT	82	10%
17	Hantzsch Ester	69	<5%
18	Borane-triazole Complex	Not Available	<5%

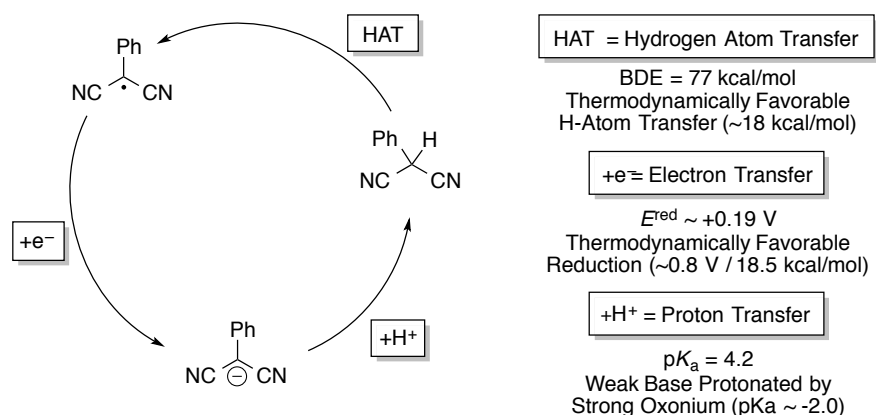
<sup>a</sup>Yields estimated by <sup>1</sup>H NMR vs. hexamethyldisiloxane internal standard



### 3.3. Rationale for the Unique Utility of 2-Phenylmalononitrile.

Reports in the literature suggest that 2-phenylmalononitrile, in addition to its low BDE, also has an extremely low radical reduction potential (+0.19 V, as estimated by the oxidation potential of the anion)<sup>12</sup>. This would allow for facile oxidation of the acridine radical to its respective anion, producing both the regenerated acridinium photocatalyst and the 2-phenylmalononitrile conjugate base with a thermodynamic driving force of ~0.8 V. The anion itself can also act as a weak base, considering its  $pK_a$  of 4.2<sup>4</sup>. This is in contrast to many of the other donors employed, as many radicals have a tendency to be oxidized to their respective cations, rather than reduced to the anions necessary to furnish product and turn over the acridinium catalyst. A depiction of the 2-PMN promoter in all stages the cycle we believed to be operable is depicted in **Fig. 3.5**.

**Figure 3.5. Properties of the 2-Phenylmalononitrile Additive in All States of the Proposed Catalytic Cycle**



### 3.4. Control Experiments to Validate the Catalytic Method

The appropriate control experiments were carried out in order to ensure the necessity of all components of the reaction (**Table 3.2**). In particular, no conversion or product was observed without the inclusion of the Fukuzumi catalyst (**Table 3.2, Entry 3**), and the reaction also did not proceed when the reaction was run in the dark (**Table 3.2, Entry 4**). Additionally, the reaction did not proceed when Ru(bpy)<sub>3</sub>Cl<sub>2</sub> was employed as the photooxidant, even in the presence of methyl viologen as a co-oxidant (**Table 3.2, Entry 5**). Other controls using AIBN or benzoyl peroxide to try to initiate cyclization either

through UV photolysis or thermal initiation also failed to furnish product (**Table 3.2, Entry 6**). This indicated to us the reaction was likely proceeding through the hypothesized photoredox mechanism. Additionally, a screen varying the equivalents of 2-PMN employed in the reaction revealed a clear trend: that reactions proceeded significantly faster (and with better mass balance) with higher loadings of the 2-PMN Hydrogen-atom donor (**Table 3.3**). The 2-PMN donor was typically observed in the crude reaction mixtures in near quantitative amounts and had to be separated from products, indicating that the compound was likely acting as a catalyst, but that high concentrations of the donor species was necessary in order to promote clean and efficient reactions.

**Table 3.2. Control Experiments Confirming the Necessity of All Species to Promote Efficient Reactions.**

Entry	Conditions	Conversion <sup>a</sup>	Yield <sup>a</sup>	Selectivity
1	Standard Conditions	83%	36%	>20:1
2	<b>With 0.5 equiv PhCH(CN)<sub>2</sub> (3)</b>	<b>89%</b>	<b>73%</b>	<b>&gt;20:1</b>
3	No Photooxidant	< 5%	< 5%	—
4	No Light	< 5%	< 5%	—
5	Ru(bpy) <sub>3</sub> Cl <sub>2</sub> instead of 2	< 5%	< 5%	—
6	AIBN or (BzO) <sub>2</sub> as Initiator	< 5%	< 5%	—

<sup>a</sup>Measured by <sup>1</sup>H NMR vs. Hexamethyldisiloxane Internal Standard

**Table 3.3. 2-Phenylmalononitrile Loading Screen**

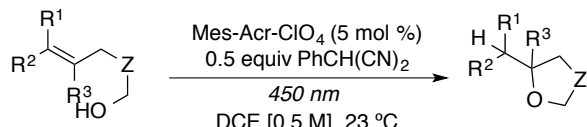
Entry	Conditions	Yield <sup>a</sup>	Reaction Time
1	0.25 equiv.	73%	96 hr.
2	<b>0.5 equiv.</b>	<b>76%</b>	<b>96 hr.</b>
3	1.0 equiv.	81%	72 hr.
4	2.0 equiv.	89%	60 hr
5	4.0 equiv.	90%	36 hr.

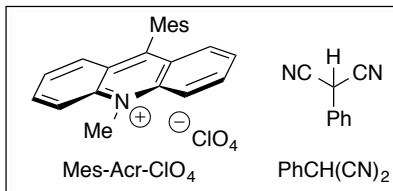
<sup>a</sup>Measured by <sup>1</sup>H NMR vs. Hexamethyldisiloxane Internal Standard

### 3.5. Evaluation of Reaction Scope

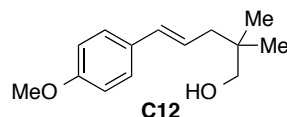
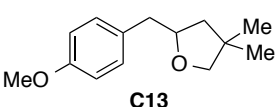
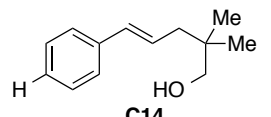
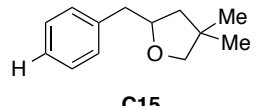
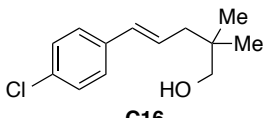
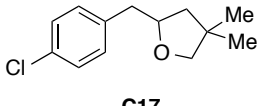
We then set out to evaluate our catalytic system with respect to the alkenol substrates that could be effectively cyclized to the desired products of hydroetherification. First, we elected to examine the breadth of electronically diverse alkenes that could be oxidized by the Fukuzumi catalyst. Given that the reaction was initiated by a single-electron oxidation event, it was necessary to evaluate how much electron density in the alkene was necessary for productive reactions to occur. A range of electronically diverse styrenes were used as such a probe, and each underwent anti-Markovnikov hydroetherification to afford the desired tetrahydrofurans in 60-80% yield (**Table 3.4**). Both yield and reaction time seemed to trend with the relative amount of electron density in the alkene. The oxidation potentials of these styrene-derived substrates ranged from 1.26 V vs. SCE on the low end (4-MeO) (**Table 3.4, Entry 1**) up to 1.69 V on the upper bound (4-Cl) (**Table 3.4, Entry 3**).

**Table 3.4. Electronic Diversity in Alkenol Cyclizations**





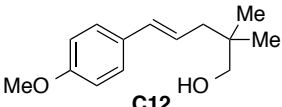
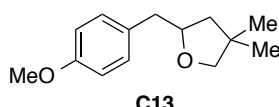
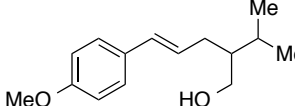
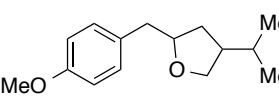
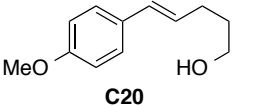
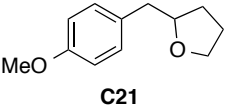
Mes-Acr-ClO<sub>4</sub>      PhCH(CN)<sub>2</sub>

Entry	Alkenol	E <sub>p/2</sub>	Product	Yield	Time
1	 <b>C12</b>	+1.26 V	 <b>C13</b>	<b>80%</b>	48 hr.
2	 <b>C14</b>	+1.62 V	 <b>C15</b>	<b>63%</b>	72 hr.
3	 <b>C16</b>	+1.69 V	 <b>C17</b>	<b>60%</b>	120 hr.

As a probe for the cyclization event, we also built and tested a substrate without any kind of substitution in the backbone of the developing tetrahydrofuran, which upon exposure to our developed

conditions furnished the anti-Markovnikov product in a nearly identical yield to the product with geminal dimethyl substitution in the backbone (**Table 3.5, Entries 1 and 3**). In this series of (4-MeO) substituted styrenes, we also included a substrate with an isopropyl substituent in the backbone to probe for diastereoselectivity (**Table 3.5, Entry 2**). While the observed yield was still quite good (77%), the diastereoselectivity observed was quite low (1.8:1) (**Table 3.5, Entry 2**).

**Table 3.5. Variation in Alkenol Backbone Structure**

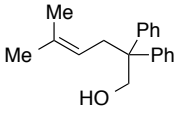
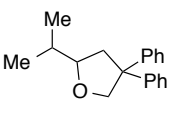
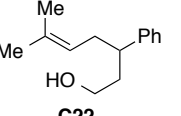
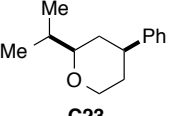
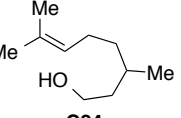
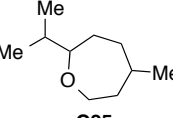
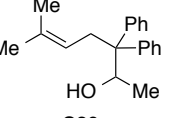
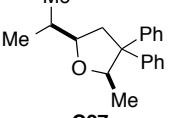
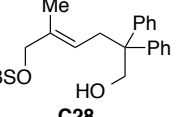
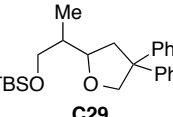
Entry	Alkenol	$E_{p/2}$	Product	Yield (d.r.)	Time
1	 C12	+1.26 V	 C13	80%	48 hr.
2	 C18	+1.30 V	 C19	77% (1.8:1)	72 hr.
3	 C20	+1.41 V	 C21	82%	36 hr.

We were also able to carry out cyclizations of alkenols to afford products by 6-*exo* and 7-*exo* cyclization modes on isoprene-derived substrates, but these transformations required additional 2-PMN included in the reaction mixtures in order to achieve reasonable reaction times. Yields with the 6-*exo* substrate were moderate, with slightly better diastereoselectivity being observed (2.5:1, *cis*-isomer favored) (**Table 3.6, Entry 2**). The yield for the product of 7-*exo* cyclization, using  $\beta$ -citronellol as a substrate was diminished, providing only a 42% yield with almost no diastereoselectivity observed (**Table 3.6 Entry 3**). This result is notable, however, for the fact that 7-*exo* cyclizations are generally slower and more difficult to affect than their 5 and 6-*exo* counterparts.

Relatively high levels of diastereoselectivity were demonstrated to be possible to obtain in a 5-*exo* cyclization mode, with stereocontrol being observed using a secondary alcohol as a nucleophile (**Table 3.6, Entry 4**). However, the added congestion around the nucleophilic site did cause a precipitous

drop in yield (41%) even with elevated loadings of 2-PMN (2.0 equivalents). As a probe for how this method would stand up in a more complex synthetic setting, we also built and tested a substrate that incorporated an allylic silyl ether. In this case, we were once again able to effect 5-*exo* cyclization, with the silyl ether intact, to afford the desired tetrahydrofuran product (**Table 3.6, Entry 5**).

**Table 3.6. Demonstration of Cyclization Modes and Substrate Complexity with a Number of 2-Methyl-2-Butene-Derived Alkenols**

Entry	Alkenol	E <sub>p/2</sub>	Product	Yield (d.r.) <sup>b</sup>	Time
1	 <b>C1</b>	+1.95 V	 <b>C11</b>	77%	192 hr. (gram scale)
2	 <b>C22</b>	+1.88 V	 <b>C23</b>	68% <sup>a</sup> (2.5:1) <sup>b</sup>	72 hr.
3	 <b>C24</b>	+1.92 V	 <b>C25</b>	46% <sup>a</sup> (1.2:1)	84 hr.
4	 <b>C26</b>	+1.98 V	 <b>C27</b>	41% <sup>a</sup> (5:1) <sup>b</sup>	168 hr.
5	 <b>C28</b>	+2.10 V	 <b>C29</b>	41% <sup>a</sup> (1.1:1) <sup>b</sup>	144 hr.

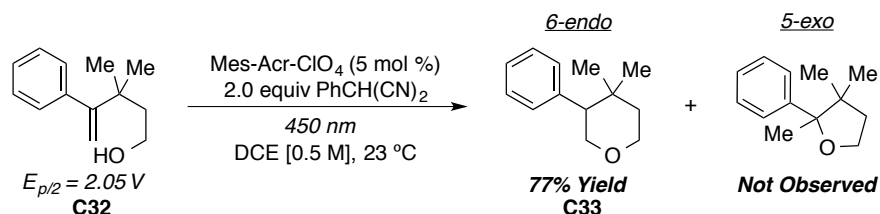
<sup>a</sup>2.0 Equivalents of 2-PMN employed as H-Atom Donor to Improve Reaction Rates

<sup>b</sup>Estimated by crude <sup>1</sup>H NMR

Arguably the most interesting substrate built and tested was a substrate containing an  $\alpha$ -substituted styrene unit, rather than the previously tested styrenes possessing  $\beta$ -substitution. This particular motif was interesting to us given the kinetic preference for 5-*exo* cyclizations over 6-*endo* modes in traditional polar reactions (though both are favorable modes of ring closure)<sup>13,14</sup>. Thus, this substrate served as an important probe to see if the selectivity we were obtaining was actually a kinetic effect masquerading as a thermodynamic phenomenon, given the intramolecular nature of our reactions. Surely enough, when exposed to our conditions, exclusively the anti-Markovnikov cyclization product

was formed, furnishing the tetrahydropyran with no observation of the undesired tetrahydrofuran (**Fig. 3.6**).

**Figure 3.6. Anti-Markovnikov Cyclization of a Styrene Derivative through a 6-*endo* Cyclization Mode with Complete Selectivity.**

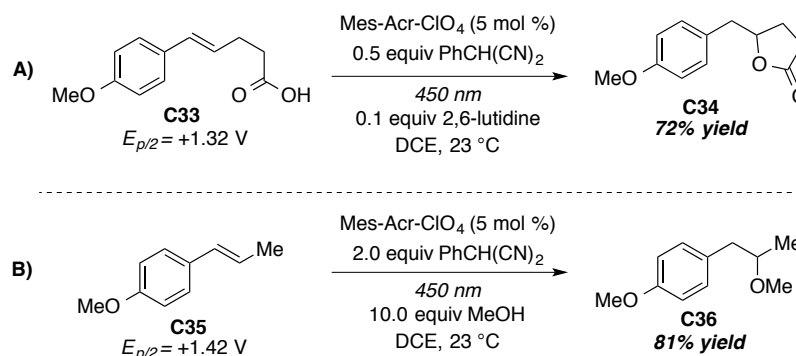


### 3.6. Complementarity to Brønsted-Acid Catalysis

It has been discussed that this method was developed to provide complementarity to the Markovnikov selectivity obtained upon activating alkenes with most electrophilic reagents. To further demonstrate the unique nature of our system to procure products that cannot be accessed directly by traditional polar chemistry, we exposed this same substrate to acid catalysis. A single drop of trifluoromethanesulfonic acid added to the aforementioned 6-*endo* substrate dissolved in DCM rapidly evolved exclusively the Markovnikov product and in 84% yield (**Fig. 3.7**). This demonstrates not only the orthogonality of our method to those in the literature, but also suggests the selectivity is not the result of steric bias. In addition, another of our substrates has been shown in a previous literature report to undergo acid-catalyzed cyclizations in the presence of an acidic ionic liquid to afford product with exclusive Markovnikov selectivity<sup>15</sup>.



**Figure 3.8. Anti-Markovnikov Hydrofunctionalizations Demonstrated With Alternative Nucleophiles.**

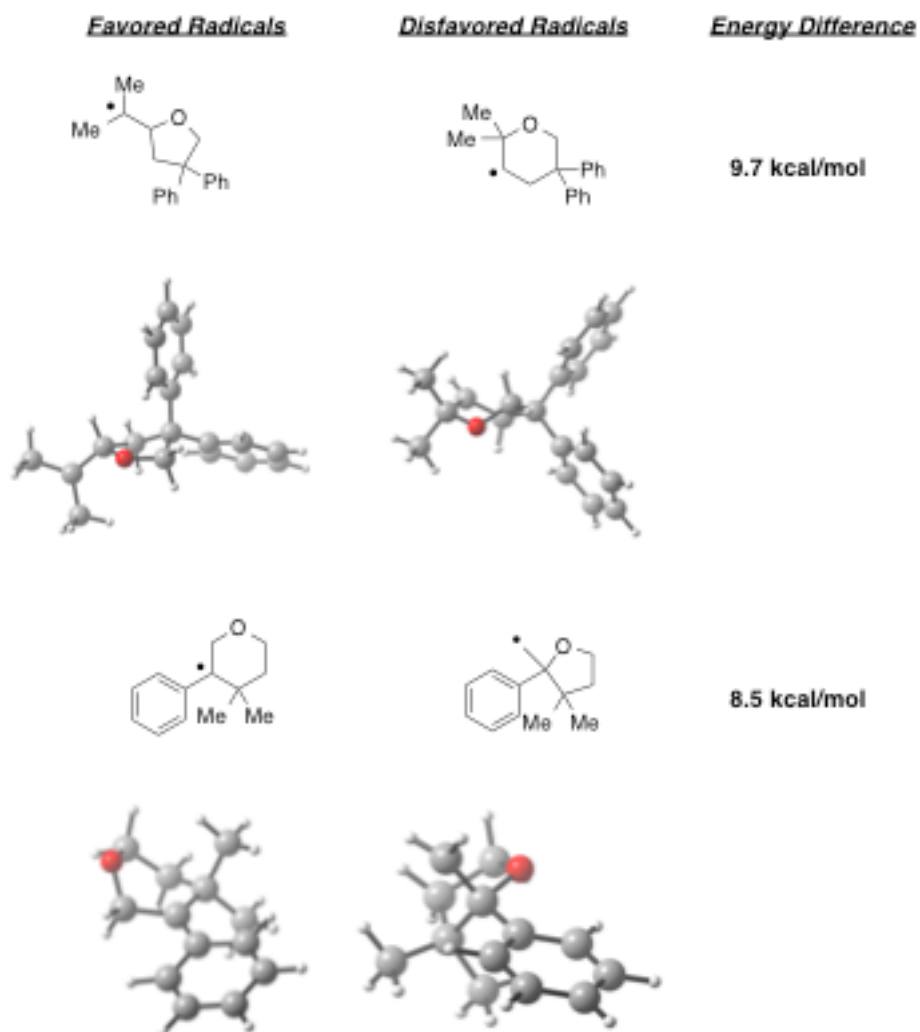


### 3.8. Further Discussion of Selectivity

While our experimentation has shown that these reactions proceed with complete selectivity, we also hoped to demonstrate computationally that the selectivity obtained is the result of thermodynamic phenomena, and not just kinetic preference. As part of a much larger study of the mechanism of this transformation currently being undertaken in our laboratory, we were able to calculate the relative energy differences for the radicals produced from anti-Markovnikov and Markovnikov nucleophilic additions to the cation-radicals derived from a selection of our alkenol substrates (**Fig. 3.9**). The results obtained for each of the substrates were striking. The radicals obtained from anti-Markovnikov addition were in each case much lower in energy than those formed from Markovnikov addition. This held true regardless of whether the resulting radical was stabilized at a benzylic position, or simply stabilized by localization on a tertiary center. These results reinforce that the exquisite selectivity that we have observed with this system is the result of a thermodynamic phenomenon and not simply an artifact of ring closure kinetics.



**Figure 3.9. Relative Energies of Substituted Radicals**



*Courtesy Nathan Romero*

### 3.9. Summary

In this chapter, the rationale for including a hydrogen atom donor as a promoter for our photocatalytic reactions was presented. It was shown that selectivity for desired products was improved drastically by the inclusion of 2-phenylmalononitrile as an additive, being employed in loadings of 0.5-2.0 equivalents. Yields were observed to be moderate to good, and reactivity was demonstrated across a broad scope of unactivated, yet oxidizable alkenes. We were also able to demonstrate the addition of a pendant carboxylic acid nucleophile to alkene cation-radical, as well as a single example of an

intermolecular addition of methanol to a styrene derivative. Hypotheses for the unique effect exhibited by 2-PMN on this transformation were presented, as was evidence for the selectivity exhibited being a result of thermodynamic factors.

## REFERENCES

- (1) Gassman, P. G.; Bottorff, K. J. Photoinduced Lactonization. A Useful but Mechanistically Complex Single Electron Transfer Process. *J. Am. Chem. Soc.* **1987**, *109*, 7547–7548.
- (2) Crich, D.; Shirai, M.; Brebion, F.; Rumthao, S. Enantioselective Alkene Radical Cations Reactions. *Tetrahedron* **2006**, *62*, 6501–6518.
- (3) Hamilton, D. S.; Nicewicz, D. A. Direct Catalytic Anti-Markovnikov Hydroetherification of Alkenols. *J. Am. Chem. Soc.* **2012**, *134*, 18577–18580.
- (4) Bordwell, F. G.; Cheng, J.; Ji, G. Z.; Satish, A. V.; Zhang, X. Bond Dissociation Energies in DMSO Related to the Gas Phase Values. *J. Am. Chem. Soc.* **1991**, *113*, 9790–9795.
- (5) Bordwell, F. G.; Branca, J. C.; Hughes, D. L.; Olmstead, W. N. Equilibriums Involving Organic Anions in Dimethyl Sulfoxide and N-Methylpyrrolidin-2-One: Acidities, Ion Pairing, and Hydrogen Bonding. *J. Org. Chem.* **1980**, *45*, 3305–3313.
- (6) Bordwell, F. G.; Harrelson, J. A.; Satish, A. V. Oxidation Potentials of Carbanions and Homolytic Bond Dissociation Energies of Their Conjugate Acids. *J. Org. Chem.* **1989**, *54*, 3101–3105.
- (7) Bordwell, F. G.; Cheng, J. Substituent Effects on the Stabilities of Phenoxyl Radicals and the Acidities of Phenoxyl Radical Cations. *J. Am. Chem. Soc.* **1991**, *113*, 1736–1743.
- (8) Amorati, R.; Lucarini, M.; Mugnaini, V.; Pedulli, G. F.; Minisci, F.; Recupero, F.; Fontana, F.; Astolfi, P.; Greci, L. Hydroxylamines as Oxidation Catalysts: Thermochemical and Kinetic Studies. *J. Org. Chem.* **2003**, *68*, 1747–1754.
- (9) Cheng, J.-P.; Liu, B.; Zhao, Y.; Wen, Z.; Sun, Y. Homolytic Cleavage Energies of R–H Bonds Centered on Carbon Atoms of High Electronegativity: First General Observations of O-Type Variation on C–H BDEs and the Implication for the Governing Factors Leading to the Distinct O/S Patterns of Radical Substituent Effects. *J. Am. Chem. Soc.* **2000**, *122*, 9987–9992.
- (10) Zhu, X.-Q.; Li, H.-R.; Li, Q.; Ai, T.; Lu, J.-Y.; Yang, Y.; Cheng, J.-P. Determination of the C4<sup>+</sup>H Bond Dissociation Energies of NADH Models and Their Radical Cations in Acetonitrile. *Chem. Eur. J.* **2003**, *9*, 871–880.
- (11) Luo, Y.-R. *Handbook of Bond Dissociation Energies in Organic Compounds*; CRC Press: Boca Raton, Fla., 2003.
- (12) Suzuki, T.; Yamada, M.; Ohkita, M.; Tsuji, T. Generation and Amphoteric Redox Properties of Novel Neutral Radicals with the TTF-TCNQ Hybrid Structure. *Heterocycles* **2001**, *54*, 387.
- (13) Baldwin, J. E. Rules for Ring Closure. *J. Chem. Soc. Chem. Commun.* **1976**, 734–736.
- (14) Gilmore, K.; Alabugin, I. V. Cyclizations of Alkynes: Revisiting Baldwin’s Rules for Ring Closure. *Chem. Rev.* **2011**, *111*, 6513–6556.

- (15) Jeong, Y.; Kim, D.-Y.; Choi, Y.; Ryu, J.-S. Intramolecular Hydroalkoxylation in Brønsted Acidic Ionic Liquids and Its Application to the Synthesis of (±)-Centrolobine. *Org. Biomol. Chem.* **2010**, *9*, 374–378.

## CHAPTER 4 – IMPROVEMENTS TO THE ANTI-MARKOVNIKOV HYDROETHERIFICATION REACTION, AND EXTENSION TO HYDROLACTONIZATION

### 4.1. Introduction

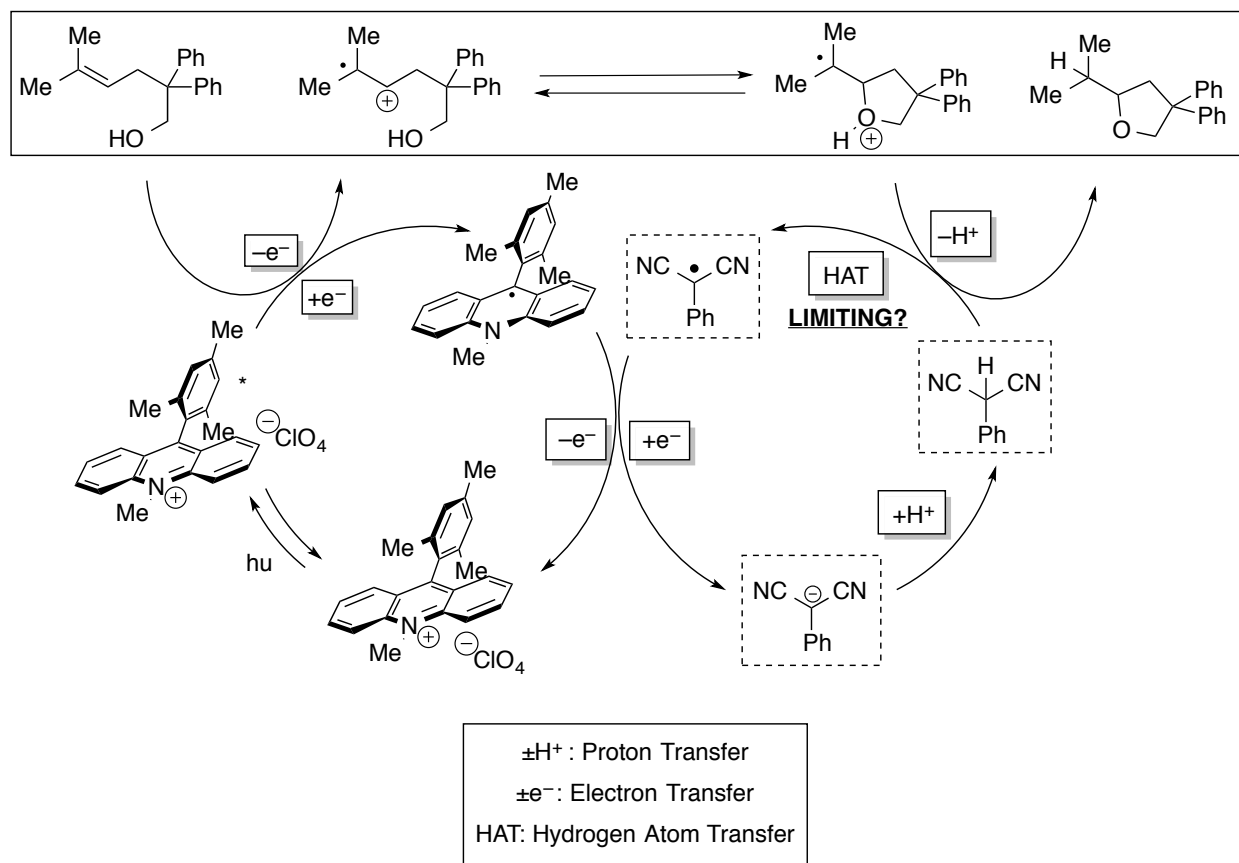
In Chapter 3, our successful strategy for the anti-Markovnikov hydroetherification of alkenes was presented. This system relied on the inclusion of an appropriate photo-oxidant (Mes-Acr-ClO<sub>4</sub>) employed in a catalytic quantity, as well as a hydrogen-atom donor (2-PMN) employed in sub-to-superstoichiometric amounts<sup>1</sup>. Importantly, we postulated that the 2-PMN donor was acting as a catalyst for the transformation (**Fig. 4.1**), despite the fact that elevated loadings of the donor were necessary to promote the transformation in a reasonable period of time.

However, we remained unsatisfied by a number of shortcomings of our protocol. First, these reactions required extremely prolonged irradiation times, and frequently did not proceed to completion. Secondly, we recognized that the amount of Hydrogen-atom donor necessary to efficiently promote the reaction was not ideal, especially considering the role we believed it was fulfilling should not require high loadings of material. As such, we sought to first try and better understand the mechanism of the transformation, to first ensure that the additive was actually fulfilling the role of a Hydrogen-atom donor, and also to gain some evidence that the Hydrogen-atom transfer step was limiting overall reaction rates.

### 4.2. Establishing the Role of the Additive as a Hydrogen Atom Donor

Another project ongoing in our laboratory at the time, seeking to affect the intermolecular, anti-Markovnikov hydroacetoxylation of alkenes, identified a new hydrogen atom donor capable of effecting

**Figure 4.1. Mechanism with Postulated Turnover-Limiting Step**

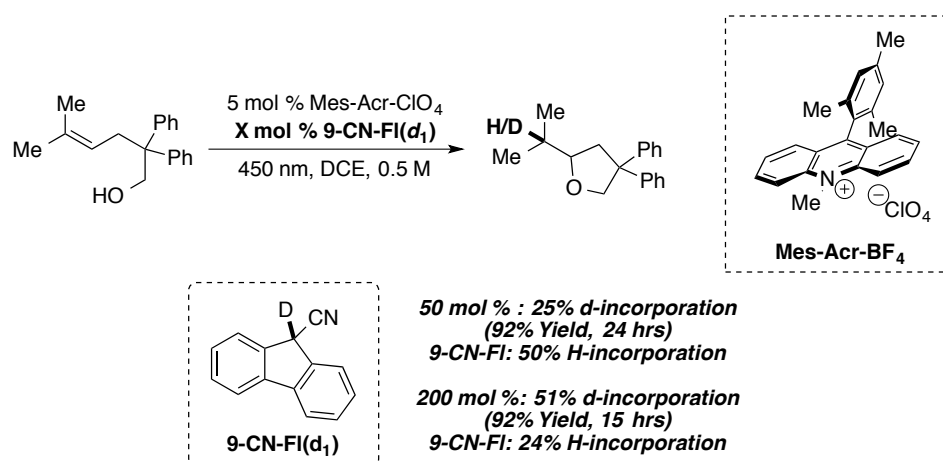


anti-Markovnikov transformations - 9-cyanofluorene (9-CN-FI)<sup>2</sup>. This molecule, like 2-phenylmalononitrile as employed in our initial system, is known to have a low bond dissociation energy (75 kcal/mol)<sup>3</sup>, possesses a conjugate radical that is capable of acting as an oxidant for the acridine radical ( $E_{\text{red}} = -0.45 \text{ V}$ )<sup>4</sup>, and has a high enough  $\text{pK}_a$  to anticipate facile protonation of the conjugate base by a generated oxonium ion intermediate (8.3, DMSO)<sup>5</sup>. The 9-cyanofluorene donor proved a useful probe for our hypothesis of limitation by slow H-atom transfer, as unlike 2-phenylmalononitrile, the active hydrogen atom on the donor proved to be non-exchangeable with the hydroxylic proton on the substrate when irradiated in DCE with the substrate for 24 hours.

We first looked at the extent of deuterium incorporation into product from the 9-cyanofluorene donor using both 0.5 and 2.0 equivalents of the H-atom donor (**Fig. 4.2**). We were able to observe significant amounts of deuterium incorporation at the position where the substituted radical was formed.

When half an equivalent of the hydrogen atom donor was used, we observed 25% *d*-incorporation, and when two equivalents were employed, we saw 51% incorporation of the label. We had anticipated incomplete incorporation of deuterium, given the fact that the protons on the alcohol nucleophiles would be transferred to 9-cyanofluorene anions over the course of the transformation. This was observed in final reaction mixtures, with proton incorporation at the 9-position of 9-CN-FI correlating to the amount of deuterium incorporation into the tetrahydrofuran product.

**Figure 4.2. Incorporation of Label from 9-Cyanofluorene Into Product Material.**

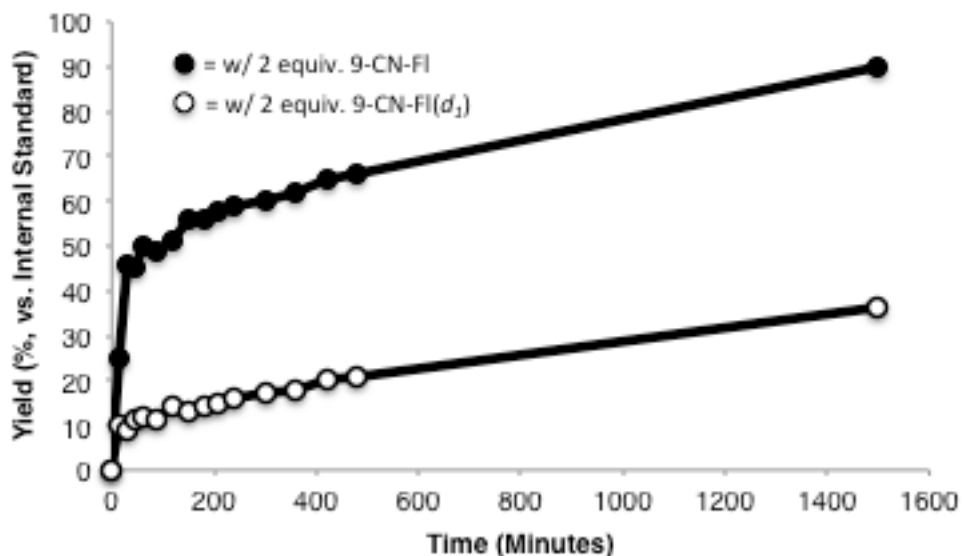


We also used the deuterated 9-CN-FI to obtain a rough sense of a kinetic isotope effect for this transformation through monitoring the rate of product evolution with both deuterated and non-deuterated 9-cyanofluorene. A trace of apparent product over time can be seen in **Fig. 4.3**. A  $k_H/k_D$  kinetic isotope effect ( $\sim 2.5$ ) is observed over the initial phase of the reaction, however, given that the proposed mechanism would enable exchange of the active deuterium with hydroxyl protons on the substrate as the reaction progresses (by protonation of the conjugate base of 9-CN-FI by intermediate distonic cation-radical), the effect seems to fade over time. The results obtained from this study suggested to us that, reaction velocity was likely still being limited by the nature of the Hydrogen-atom donor.

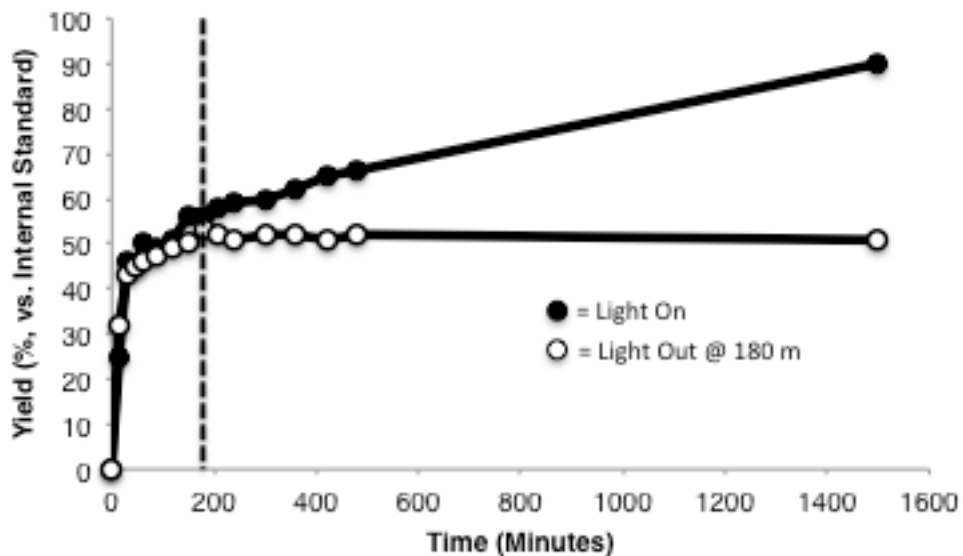
We also wanted to demonstrate that continuous illumination was necessary for the reaction to occur. We did this through the use of a simple “light-out” experiment, in which we turned off the light source at a particular time point of a kinetic trial. As seen in **Fig. 4.4**., conversion of starting material to

product halts at 180 m, the time when illumination was ceased, suggesting that the transformation is not occurring by a radical-chain mechanism.

**Figure 4.3. Observation of a Kinetic Isotope Effect for the Hydroetherification of an Alkenol Using 9-Cyanofluorene as H-Atom Donor.**



**Figure 4.4. Demonstration that Continuous Illumination is Necessary for Reaction Progression**

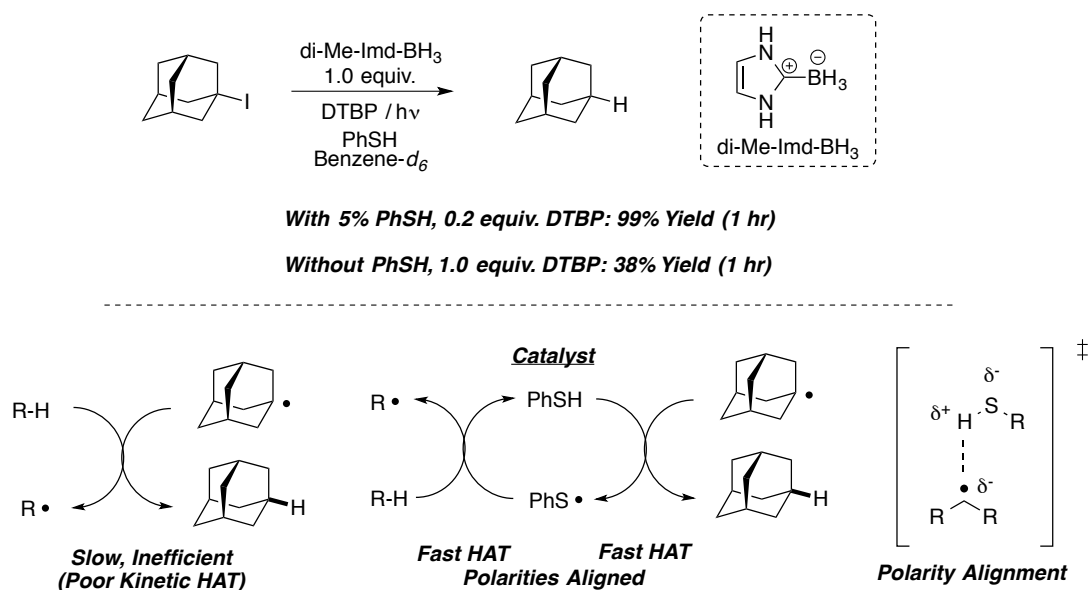




### 4.3. Re-visitation of Hydrogen Atom Sources


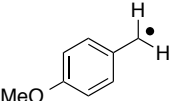
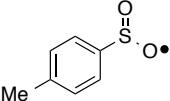
While we had previously attempted to optimize the identity of the hydrogen atom donor using bond dissociation energy as the vital benchmark, in this effort we looked to try and find donors capable of fast hydrogen atom transfer to the nucleophilic, carbon-centered radicals that we proposed to be generated over the course of the reaction. The effect of radical polarity matching on hydrogen-atom transfer rates has been well studied by a number of synthetic research groups, particularly in the context of polarity reversal catalysis, (PRC)<sup>6,7</sup>. In particular, researchers from the Curran lab has been particularly successful in their efforts to develop new reagents to transfer hydrogen atoms to alkyl radicals, employing thiol-based catalysts to transfer hydrogen atoms to alkyl radicals, with the thiyl radical then proceeding to abstract a hydrogen atom from a terminal Hydrogen-atom donor (**Fig. 4.5**)<sup>8</sup>. This application relies on the theory that the polarities of both the radical being reduced and the radical being formed must be aligned for fast Hydrogen-atom transfer to occur. For example, a nucleophilic radical (such as an alkyl radical) must partner with an electrophilic Hydrogen-atom source to allow for rapid transfer. The electrophilic thiyl radical can then proceed to abstract a Hydrogen atom from a more nucleophilic hydrogen atom source, such as the NHC-borane complex depicted below.

**Figure 4.5. Polarity Reversal Catalysis: Theory and Application**



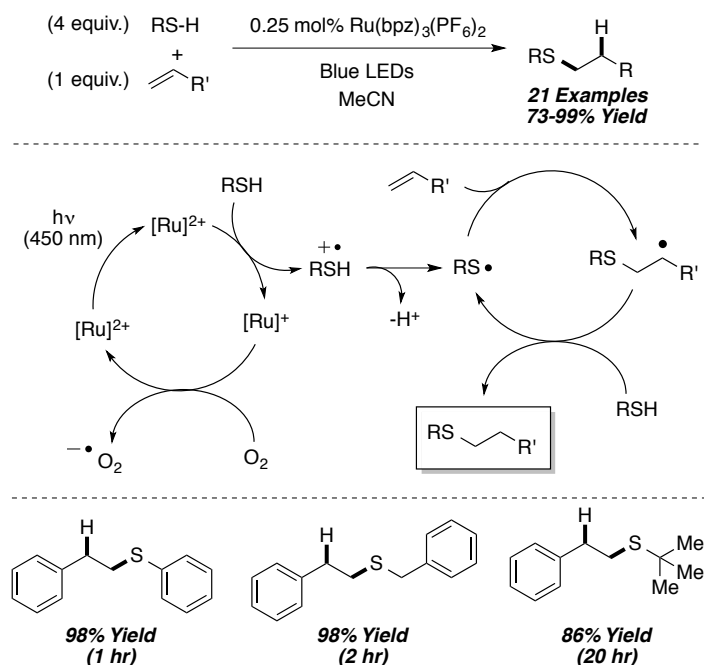
Given this active area of research, efforts have also been made by a number of groups to quantify the nucleophilicity and electrophilicity of radicals computationally, and one such scale is partially presented in **Fig. 4.6**<sup>9</sup>. This reveals one seemingly obvious class of potential donors that we had not screened in our first round of optimization: those containing a thiol group, which had also been successful in the previously presented Curran example. The rationale for our initial hesitation to screen such donors was the propensity of thiols themselves to be oxidized under photoredox conditions. This effect has been exploited by Yoon and coworkers in the development of a thiol-ene reaction promoted by photoredox catalysis (**Fig. 4.7**)<sup>10</sup>. Given that our transformation relied on alkene starting materials, and the employment of thiols as Hydrogen-atom transfer reagents would generate thiyl radicals over the course of the transformation, we were not initially optimistic about the outcome of such a strategy.

**Figure 4.6. Partial Depiction of One Global Electrophilicity Scale for Radicals**

<i>Nucleophilic Radicals</i>		<i>Electrophilic Radicals</i>	
Radical	$\omega$	Radical	$\omega$
	0.581	NCCH <sub>2</sub> •	2.003
H <sub>2</sub> COH•	0.717	H <sub>3</sub> CCH <sub>2</sub> S•	2.214
	1.138		2.283
H <sub>3</sub> C•	1.209	HS•	2.520

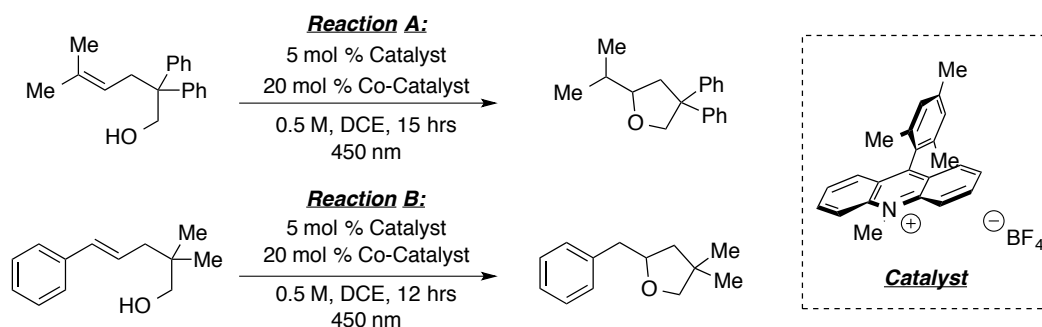
To our surprise, the use of sulfur-centered hydrogen-atom sources led to a remarkable enhancement of reactivity, in alignment with the greater electrophilicity of the developing thiyl radical. A scope of selected hydrogen-atom donors that were screened can be seen in **Fig. 4.8**. It is notable that in this screen, all donors were deployed in a catalytic amount (20 mol %), compared with the elevated loadings employed in our first-generation system. Also of note is the variability of yields observed in optimization of hydrogen atom donor with two different substrates, likely due to the varying

**Figure 4.7. The Thiol-Ene Reaction Promoted by Photoredox Catalysis, with Selected Scope**



nucleophilicity of the substrate-derived radical intermediates. Despite the variability in yield demonstrated across both types of substrate with some of the Hydrogen-atom sources tested, we were able to demonstrate that thiophenol was capable of serving as an excellent co-catalyst for the transformation with both types of substrate (**Table 4.1, Entry 5**). The thiol-ene pathway appears to be suppressed in this reaction, presumably due to favorable reduction of the thiyl-radical by the intermediate acridine radical outcompeting addition of thiyl radical to alkenes, or perhaps due to reversible dimerization of intermediate thiyl radicals. On top of these possible effects, a recent follow-up publication from the Yoon lab has identified that a key to improving the reaction efficiency of the thiol-ene process was the inclusion of an aniline derivative to act as a redox mediator, perhaps suggesting that oxidation of thiol is kinetically unfavorable<sup>11</sup>. Also of potential importance is the high degree of reversibility for the addition of thiyl-radicals to alkenes<sup>12</sup>. Given this surprising result, a detailed mechanistic study of the reaction is an active area of research being pursued by other members of our laboratory. At this point, however, we hypothesize that a combination of all of these effects is likely to contribute to the suppression of the potentially unproductive thiol-ene pathway.

**Table 4.1. Screen of Second-Generation H-Atom Donors**



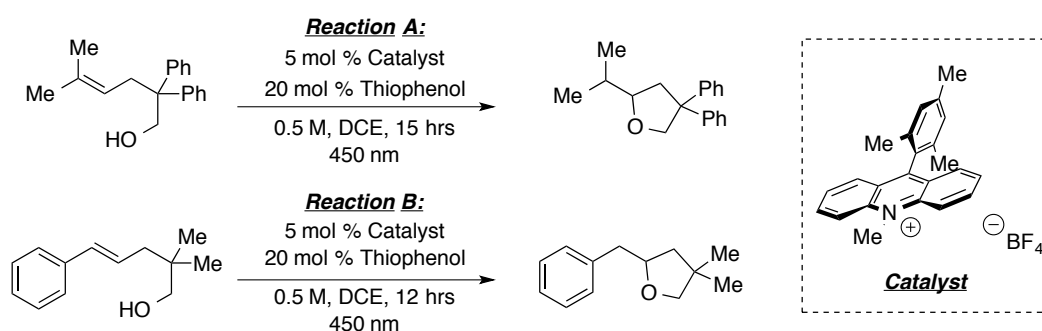
Entry	Cocatalyst	REACTION A		REACTION B	
		Yield	Conversion	Yield	Conversion
1	None	13%	25%	<5%	53%
2	2-Phenylmalononitrile	30%	34%	20%	37%
3	9-Cyanofluorene	77%	100%	14%	54%
4	Phenylsulfonic Acid	75%	95%	43%	92%
5	<b>Thiophenol</b>	<b>90%</b>	<b>96%</b>	<b>95%</b>	<b>100%</b>
6	Phenyldisulfide	80%	100%	91%	100%
7	(4-OMe)thiophenol	56%	63%	72%	100%
8	(4-NO <sub>2</sub> )thiophenol	61%	100%	77%	100%
9	<i>t</i> -Dodecanethiol	51%	55%	24%	65%

#### 4.4. Re-optimization of the Hydroetherification Reaction with Thiophenol Employed as Hydrogen-Atom Donor

Further optimization experiments were run in an effort to revalidate and improve the transformation. As in our previous efforts, control experiments highlight the necessity of both the acridinium photocatalyst and light to promote a productive reaction (**Table 4.2, Entries 1-4**). Additionally, a minor concentration effect was observed (**Table 4.2, Entries 5-6**). The addition of base (2,6-lutidine) to the reaction only served to impede reaction rate in both instances (**Table 4.2, Entry 7**), which we speculate could be due to deprotonation of thiol to form elevated amounts of potentially promiscuous thiolate intermediate, or deprotonation of intermediate cation-radicals to form byproducts and therefore take the reaction off-cycle. Running the reaction under an atmosphere of air led to

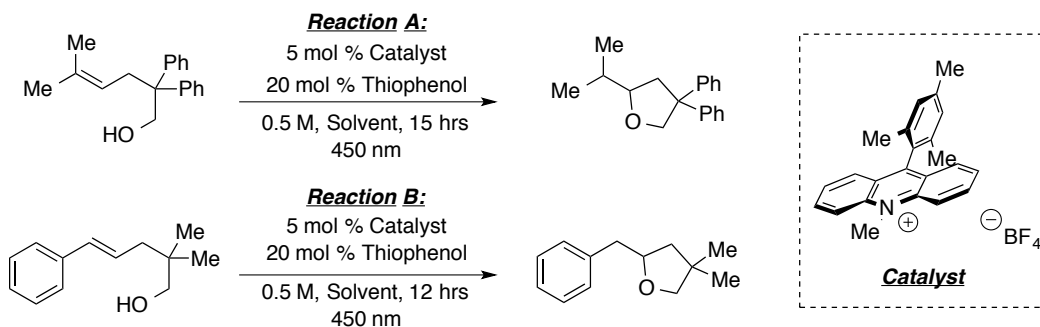
significant degradation of material in both reactions: likely due to both the instability of radical intermediates in the presence of oxygen and/or the ability of the acridine radical to reduce oxygen (**Table 4.2, Entry 8**). In particular, the styrene derivatives tend to oxidatively cleave to form benzaldehyde products along with other complex products as a result of either a peroxide or superoxide mediated pathway. The most profound effects observed was that of solvent choice: Running the reaction in more solvents more polar than DCE only diminished the observed rates of reaction while having minimal effect on the formation of byproducts (**Table 4.3**).

**Table 4.2. Control Experiments and Other Optimization of Second Generation System**



Entry	Conditions	REACTION A		REACTION B	
		Yield	Conversion	Yield	Conversion
1	Standard Conditions	90%	96%	90%	96%
2	No Thiophenol	13%	25%	<5%	53%
3	No Catalyst	<5%	<5%	<5%	<5%
4	No Light	<5%	<5%	<5%	<5%
5	0.2 M Substrate	77%	90%	82%	100%
6	0.05 M Substrate	76%	91%	83%	100%
7	Air Atmosphere	40%	75%	61%	100%
8	With 10 mol % 2,6-Lutidine	18%	22%	55%	85%

**Table 4.3. Solvent Effect on the Hydroetherification Reaction.**



Entry	Solvent	REACTION A		REACTION B	
		Yield	Conversion	Yield	Conversion
1	1,2-Dichloroethane	90%	96%	95%	100%
2	Acetonitrile	71%	74%	92%	100%
3	Acetone	66%	68%	84%	87%
4	2,2,2-Trifluoroethanol	61%	62%	58%	79%
5	Dimethylformamide	17%	18%	19%	32%

#### 4.5. Comparison of Thiophenol System to First-Generation System

While our re-optimization demonstrated the improvement of our developed reaction for two substrates, we wished to highlight the utility of the new, second-generation system. As a demonstration of the enhancement of reactivity obtained by simply switching to this new hydrogen atom donor, we carried out a direct comparison of our new system to the first generation system for alkenol cyclization. Results obtained for a selected part of our prior substrate scope can be seen in **Table 4.4**. Notably, reaction yields are significantly improved in all cases tested, and perhaps more importantly, the observed reaction times necessary for completion are significantly shorter. In all cases tested, the alkenol cyclizations were complete in less than a day: certainly better than the 36-96 hour timeframe observed applying the 2-phenylmalononitrile system to this set of substrates. At this point we felt that we had created a synthetically efficient, rather than simply intriguing, transformation.

**Table 4.4. Comparison of Thiophenol System to First-Generation System with 2-PMN**

Substrate	Product	Cocatalyst		
		w/ 0.5 equiv 2-PMN	w/ 0.2 equiv. PhSH <sup>b</sup>	
		80% Yield 36 hr.	98% Yield 8 hr.	
		63 % Yield 72 hr.	93% Yield 12 hr.	
		60% Yield 72 hr.	95% Yield 12 hr.	
		77% Yield <sup>a</sup> 96 hr.	91% Yield 12 hr.	
		77% Yield 96 hr.	93 % Yield 15 hr.	

<sup>a</sup>Reaction run with 2.0 equiv. 2-Phenylmalononitrile

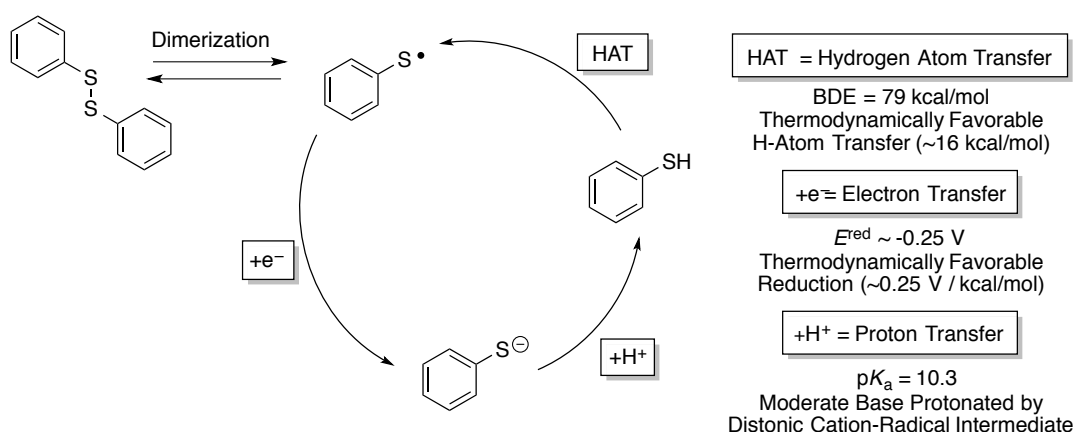
<sup>b</sup>Yield vs. hexamethyldisiloxane internal standard

#### 4.6. Thiophenol Evaluated in the H-Atom Redox Cycle

Much like 2-PMN in the first generation catalytic system, thiophenol possesses favorable thermodynamic properties to participate in every step of the proposed catalytic cycle (**Fig. 4.9**). Its bond dissociation energy (79 kcal/mol)<sup>12</sup> is sufficiently low to transfer a hydrogen atom to a variety of substrate-derived radicals<sup>13</sup>, the reduction potential of the radical is sufficient to predict exergonic reduction by the acridine radical<sup>14</sup>, and the *pKa* of the acid should again be sufficient for protonation by

the intermediate distonic cation-radical<sup>15</sup>. One observation that was made in these transformations was the production of small amounts of phenyldisulfide in most of our reactions. This species was shown to be a viable catalyst for this transformation (albeit proceeding to give slightly suppressed yields, see **Table 4.2, Entry 6**), likely entering the catalytic cycle *via* homolysis to form the thiyl radical. Thus, we believe the presence of phenyldisulfide to be the result of reversible dimerization of thiyl radicals generated over the course of the reaction.

**Figure 4.9. Thiophenol as Catalytic Redox-Active Hydrogen Atom Donor**



#### 4.7. Expansion of the New System to Hydrolactonization

Equipped with our new Hydrogen-Atom donor, we set out to briefly optimize conditions for the hydrolactonization of carboxylic acids with distant unsaturation. We first attempted this optimization by screening various bases under our photoredox conditions. Surprisingly, we found this transformation to operate ideally in the absence of base additive. This was in contrast to a parallel method developed in our laboratory for the intermolecular hydroacetoxylation of alkenes<sup>2</sup>, in which base was found to assist in addition of carboxylic acid additions to alkene cation-radical intermediates. The basis of this effect was found to be a competing reaction pathway in which decarboxylation of the substrate occurred, ultimately leading to the formation of an undesired side product with the alkene still intact (**Fig. 4.10**).

Decarboxylation by single-electron oxidation of carboxylates has been observed previously by other groups<sup>16–19</sup>. While this pathway is not advantageous in our chemistry, new methods for decarboxylation



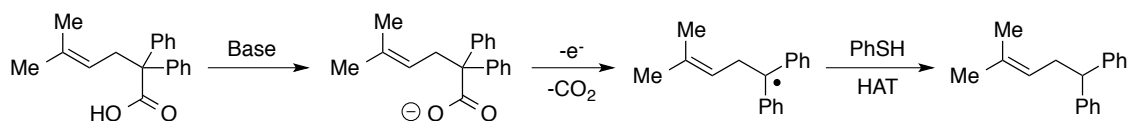
are still desirable, and this result is being developed into a useful synthetic protocol by another member of our laboratory.

**Table 4.5. Observation of Decarboxylation of Alkenoic Acid Upon Inclusion of Base.**

Base	Yield A	Yield B
None	85%	8%
2,6-Lutidine	34%	50%
Pyridine	57%	26%
Triethylamine	29%	59%
Cesium Carbonate	Trace	84%

<sup>a</sup>Yield estimated by <sup>1</sup>H NMR vs. Hexamethyldisiloxane internal standard

**Figure 4.10. Mechanism for Observed Decarboxylation.**



The variety of olefin structures that we were able to cyclize with complete selectivity once again demonstrates the capability of the strongly oxidizing Fukuzumi acridinium photooxidant as our catalyst of choice. We examined a range of hydrocyclizations, and much like the hydroetherification chemistry, a wide range of substitution patterns on the aromatic ring were well tolerated. Electron-donating groups are once again well-tolerated (**Table 4.6, Entries 1-3**), with substitution in the backbone being unnecessary for cyclization to occur (**Table 4.6, Entries 1,3,4, and 5**). We again observed only modest diastereoselectivity when substrates contained a resident chiral center (**Table 4.6, Entry 2**). Electron withdrawing groups, such as chlorides (**Table 4.6, Entries 6-7**), can be placed around the

aromatic ring of a styrenyl olefin. This was also shown to be appropriate even with the incorporation of an aryl fluoride (**Table 4.6, Entry 8**), a motif that is desirable for medicinal-chemistry applications.

**Table 4.6. Scope of Hydrolactonization Reactions to form  $\gamma$ -Butyrolactones from Styrenyl-Alkenoic Acids**

Entry	Alkenoic Acid	$E_{p/2}$	Product	Yield (d.r.)	Time
1		1.32 V		89%	15 hr
2		1.37 V		87% (d.r. = 2.4:1)	15 hr
3		1.37 V		81%	15 hr*
4		1.83 V		89%	24 hr
5		1.91 V		78%	36 hr
6		1.85 V		87%	36 hr
7		1.88 V		93%	72 hr
8		1.87 V		85%	36 hr

\*Indicates Heterogeneous Mixture at Initiation of Irradiation

In addition to these simple styrene motifs, trisubstituted aliphatic olefins (Table 4.9, Entry 1) are competent cyclization substrates, and the remarkably mild conditions can be highlighted by the ability of a malonic acid nucleophile (**Table 4.7, Entry 4**) to undergo efficient cyclization, as can an acid onto an alkene in conjugation with a heteroaromatic ring (**Table 4.87 Entry 5**), despite the relative benchtop instability of the cyclization precursor. A slight drop in yield was observed when moving to the formation of  $\delta$ -lactones by 6-*endo* ring closure modes (**Table 4.7, Entries 2-3**). However, the diminished yield was not found to be due to competing formation of the Markovnikov products, but rather due to formation of oligomeric and polymeric byproducts. It was unclear as to if these polymers were formed in the reaction or after workup, but samples of purified product allowed to stand on the benchtop for long periods of time were found to be almost completely degraded. Interestingly, the oxidation potentials of these two substrates lie above the excited-state reduction potential of the singlet excited state of the acridinium photooxidant ( $E_{1/2}^* = +2.15$  V vs. SCE), something that had not been observed in our laboratory's chemistry up to that point in time.

**Table 4.7. Hydrolactonization Reactions of Exotic Substrate Motifs**

**Mes-Acr-BF<sub>4</sub>**

Entry	Alkenoic Acid	E <sub>p/2</sub>	Product	Yield (d.r.)	Time
1	<p><b>D17</b></p>	2.12 V	<p><b>D18</b></p>	90%	24 hr
2	<p><b>D19</b></p>	2.22 V	<p><b>D20</b></p>	60%	36 hr
3	<p><b>D21</b></p>	2.09 V	<p><b>D22</b></p>	59%	36 hr
4	<p><b>D23</b></p>	1.77 V	<p><b>D24</b></p>	76% (d.r. = 1.3:1)	72 hr*
5	<p><b>D25</b></p>	1.47 V	<p><b>D26</b></p>	82%	36 hr

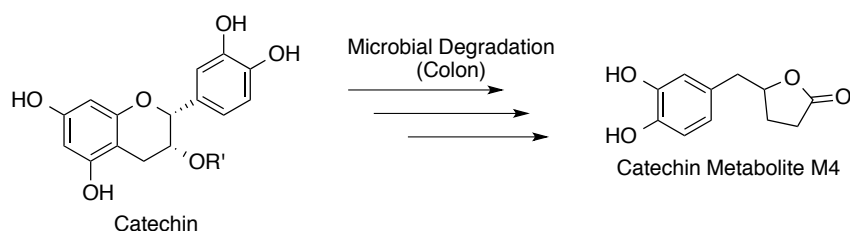
\*Indicates Heterogeneous Mixture at Initiation of Irradiation

#### 4.8. Applications to Total Synthesis and Medicinal Chemistry – Catechin Metabolites

While we had been able to demonstrate cyclization reactions to produce an array of  $\gamma$ - and  $\delta$ -lactone products, we wished to also demonstrate direct applications of our system to the total synthesis of biologically active natural products. As a first set of targets, we looked at an interesting class of bacterial secondary metabolites (**Fig. 4.11**), which have been demonstrated to inhibit the growth of multiple cancer cell lines, with some preliminary results suggesting that some selectivity for the inhibition of growth of pre-malignant cells is obtained<sup>20</sup>. In addition, it was shown in this report that these metabolites also possess anti-inflammatory activity through the inhibition of LPS-stimulated macrophage growth, as

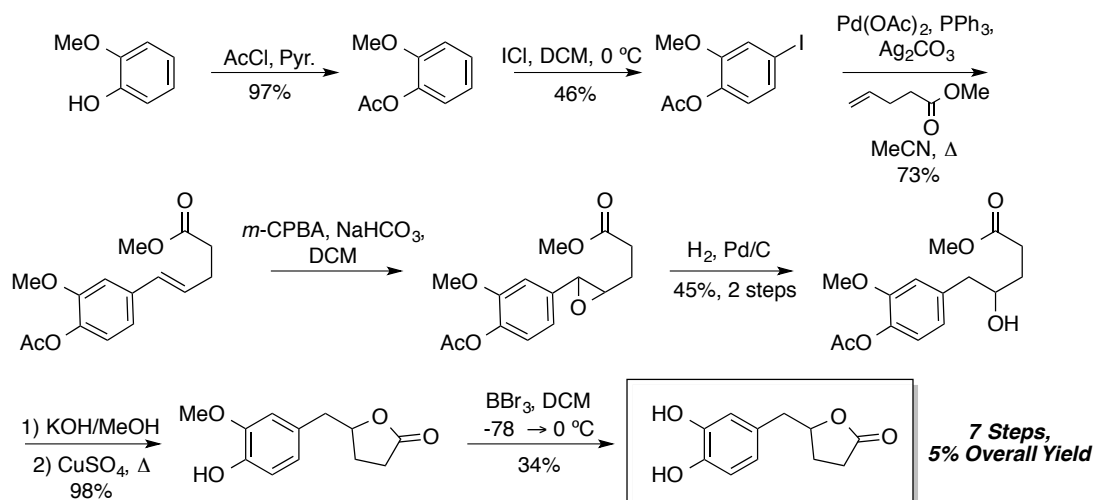
demonstrated by the suppression of arachidonic acid release and nitric oxide formation by some members of this class of natural product.

**Figure 4.11. Catechin and Metabolite M4**



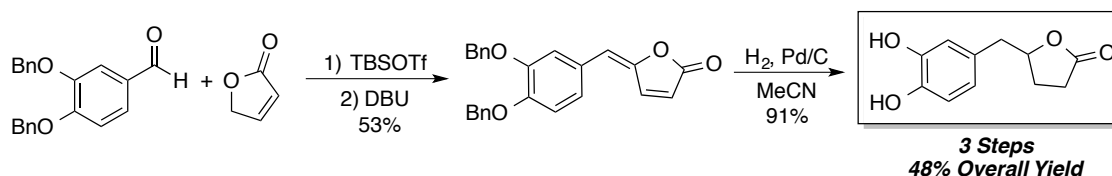
There have been two prior routes reported for the synthesis of this class of product. The first was reported by Lambert, et al. in 2005<sup>20</sup> (**Fig. 4.12**). Their route consisted of initial protection of a deoxygenated arene with acetyl chloride, followed by iodination and a Heck reaction to form an extended chain alkene with a pendant ester. This compound was then epoxidized, and the concomitant epoxide reduced to form a secondary alcohol. Saponification conditions liberated both the acid for lactonization and the acetyl protecting group, and was followed by treatment with copper sulfate in benzene to close the lactone, forming the desired 3-methoxylated form of the metabolite. The bis-phenolic derivative was formed by deprotection with boron tribromide, albeit in rather poor yield.

**Figure 4.12. Lambert's Synthesis of Catechin Metabolite M4**



A more concise protocol for the synthesis of catechin metabolites was developed by Chang, et al. in 2010<sup>21</sup> (**Fig. 4.13**). Their protocol was reliant on the addition of a siloxyfuran, generated *in situ*, to an aryl aldehyde. This was followed by dehydration, then global hydrogenation to both reduce the diene and deprotect the bisphenol moiety. The yield and convenience of this protocol marked a significant improvement over the previously disclosed method for the synthesis of this compound.

**Figure 4.13. Chang's Synthesis of Catechin Metabolite M4**



Our developed anti-Markovnikov hydrolactonization chemistry seemed to map well onto this scaffold, as unsaturated acids (readily synthesized by straightforward Wittig chemistry) could be considered retrons for these products. While the free phenols were ineffective due to their marked insolubility in organic solvents, we found that cyclization of protected precursors to be effective for the synthesis of the catechin metabolite M4, as well as two closely related structures. While the Wittig reactions were only modest yielding (See **Appendix 1**), the lactonization step was found to be exceedingly efficient (**Table 4.8**). It should be pointed out that the process was slightly modified from our standard conditions, given low solubility of our alkenoic acid starting materials in chlorinated solvents, with the reactions being diluted to 0.1 M with respect to substrate to solubilize more of the material. Even with this modification, some of the starting material remained insoluble, but this did not significantly preclude reaction efficiency other than to possibly extend reaction times. Interestingly, attempts to run these reactions in more polar solvents or solvent mixtures led to reactivity being shut down almost completely, possibly due to localization of cationic character in the oxygenated aromatic ring rather than the alkene terminus.

Each of the protecting groups could be successfully removed in straightforward fashion, with acidic hydrogenation conditions smoothly producing methoxylated M4 by selective removal of the benzyl

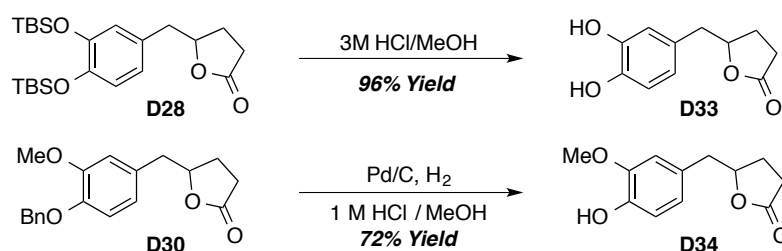
protecting group, and simple acidic hydrolysis allowing for the facile removal of both TBS groups to afford M4 (**Fig. 4.14**). As a final demonstration of the power of this chemistry to generate a library of modified metabolites in rapid fashion, we also built and tested a substrate incorporating an benzodioxane ring, and subjected it to lactonization conditions to afford yet another lactone from this class of product. Not only did these reactions highlight the ability to rapidly generate natural product-like structures, but they also reinforced the mild nature of these reaction conditions employed. In each instance, a potentially labile protecting group (-OMe, -OBn, -OTBS, -O-CH<sub>2</sub>-O-) remained intact.

**Table 4.8. Results for Key Lactonization Step to Form Catechin Metabolite Precursors and Derivatives.**

Entry	Alkenoic Acid	E <sub>p/2</sub>	Product	Yield	Time
1	<p><b>D27</b></p>	1.26 V	<p><b>D28</b></p>	89%	24 hr*
2	<p><b>D29</b></p>	1.10 V	<p><b>D30</b></p>	89%	36 hr*
3	<p><b>D31</b></p>	1.17 V	<p><b>D32</b></p>	95%	36 hr*

\*Indicates Reaction was Heterogeneous at Initiation of Irradiation

**Figure 4.14. Deprotection of Catechin Metabolite Precursors to Form Natural Products.**



While the overall synthetic efficiency demonstrated is similar to the method developed by Chang, the ability to close the lactone without a requiring a subsequent hydrogenation step to reduce a diene makes our method potentially advantageous for the synthesis of more complex variants of these metabolite structures: particularly given that an array of methods are available for the synthesis of more complex unsaturated acids are available. For example, one can envision products including substitution in the acid chain or on the alkene itself to allow for investigation of lactone structures that include more complex branching patterns and functionality.

#### 4.9. Applications to Total Synthesis – Access to the Dihydroisocoumarin Motif

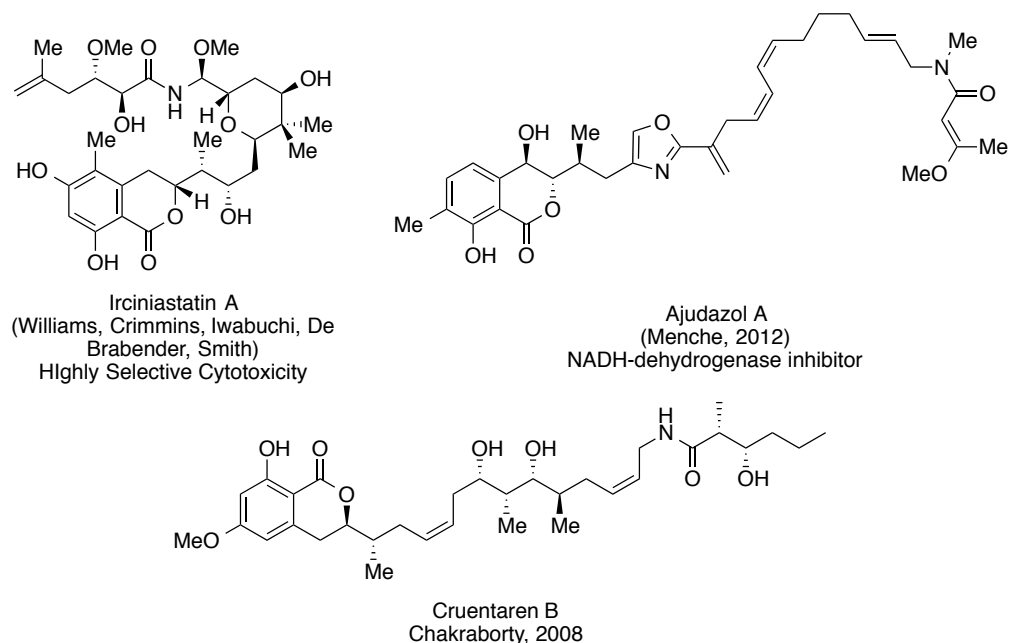
Several biologically relevant natural products contain the dihydroisocoumarin motif. A trio of such examples can be seen in **Fig. 4.15**. Psymberin is a molecule of particular importance and interest, given its selective cytotoxicity against human cancer cell lines, and as a result several syntheses of this compound have been reported<sup>22–26</sup>. In addition, the natural product Ajudazol A has been shown to be a potent inhibitor of NADH-dehydrogenase, a key protein in mitochondrial respiration. Thus, this natural product has been identified as potentially useful in studying neurodegenerative disease mechanisms, such as those associated with Parkinsons’ disease and Alzheimer’s disease, and has also been the target of synthetic efforts.<sup>27</sup>

While we were not interested in designing a total synthesis of any of these compounds at this point in time, we did want to investigate whether our chemistry could be applicable to the synthesis of the dihydroisocoumarin scaffold, which we thought to be accessible *via* a 6-*endo*, anti-Markovnikov hydrolactonization of an *ortho*-alkenyl benzoic acid. To this point, we had not investigated deactivated or congested carboxylic acids as substrates for our lactonization chemistry. Perhaps unsurprisingly, this substrate reacted very slowly under our standard reaction conditions, with only ~10% of the desired material formed after a 24 hr. period. However, the addition of 10 mol % 2,6-lutidine as a base to catalytically generate the more active carboxylate nucleophile did lead to much more efficient cyclization, furnishing the desired isochromanone in 78% yield after 72 hours of irradiation (**Fig. 4.16**).

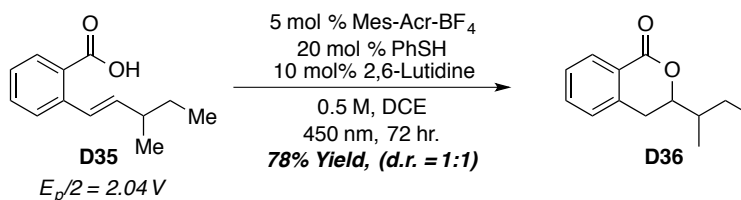


Unfortunately, the reaction was found to proceed with no observable diastereoselectivity. However, we remain excited about the prospect of this chemistry with regard to the synthesis of natural products as the direction of our laboratory's research begins to shift from simple development of bond-forming reactions to the development of diastereoselective and enantioselective variants of both the hydroetherification and hydrolactonization reactions.

**Figure 4.15. Natural Products Incorporating the Dihydroisocoumarin Motif**



**Figure 4.16. Synthesis of an Dihydroisocoumarin *via* anti-Markovnikov Hydrolactonization**



#### 4.10. Summary

In this chapter, some rudimentary mechanistic experiments that aided in the crystallization of our central hypothesis about the slow rates of conversion observed in our first generation system: that slow Hydrogen atom transfer was the key limitation that suppressing reaction rate, leading to the requirement

of elevated loadings of the Hydrogen-atom donor to affect anti-Markovnikov hydroetherification. Our justification for attempting Sulfur-centered Hydrogen-atom donors as co-catalysts was presented, as was the marked decrease of observed reaction times and increases in yield that we were able to obtain by employing thiophenol as a Hydrogen-atom donor, even when used in a catalytic, rather than sub- to superstoichiometric amount. Our successful efforts to expand this methodology beyond anti-Markovnikov hydroetherification to Anti-Markovnikov hydrolactonization were also presented, with the synthesis of an array of  $\gamma$ - and  $\delta$ -lactones being presented. The direct application of this hydrolactonization reaction to the synthesis of catechin metabolite natural products, as were preliminary results regarding the synthesis of the dihydroisocoumarin scaffold through the use of slight modifications of the developed methodology.

## REFERENCES

- (1) Hamilton, D. S.; Nicewicz, D. A. Direct Catalytic Anti-Markovnikov Hydroetherification of Alkenols. *J. Am. Chem. Soc.* **2012**, *134*, 18577–18580.
- (2) Perkowski, A. J.; Nicewicz, D. A. Direct Catalytic Anti-Markovnikov Addition of Carboxylic Acids to Alkenes. *J. Am. Chem. Soc.* **2013**, *135*, 10334–10337.
- (3) Bordwell, F. G.; Zhang, X.; Cheng, J. P. Comparisons of the Acidities and Homolytic Bond Dissociation Energies of the Acidic Nitrogen-Hydrogen and Carbon-Hydrogen Bonds in Diphenylmethanes and Carbazoles. *J. Org. Chem.* **1991**, *56*, 3216–3219.
- (4) Arnett, E. M.; Amarnath, K.; Harvey, N. G.; Cheng, J. Determination and Interrelation of Bond Heterolysis and Homolysis Energies in Solution. *J. Am. Chem. Soc.* **1990**, *112*, 344–355.
- (5) Bordwell, F. G.; Hughes, D. L. Rate-Equilibrium Relationships for Reactions of Families of Carbanion Nucleophiles with N-Benzyl-N,N-Dimethylanilinium Cations and with Alkyl Chlorides, Bromides, and Iodides. *J. Am. Chem. Soc.* **1986**, *108*, 7300–7309.
- (6) Roberts, B. P. Polarity-Reversal Catalysis of Hydrogen-Atom Abstraction Reactions: Concepts and Applications in Organic Chemistry. *Chem. Soc. Rev.* **1999**, *28*, 25–35.
- (7) Crich, D.; Grant, D.; Krishnamurthy, V.; Patel, M. Catalysis of Stannane-Mediated Radical Chain Reactions by Benzeneselenol. *Acc. Chem. Res.* **2007**, *40*, 453–463.
- (8) Pan, X.; Lacôte, E.; Lalevée, J.; Curran, D. P. Polarity Reversal Catalysis in Radical Reductions of Halides by N-Heterocyclic Carbene Boranes. *J. Am. Chem. Soc.* **2012**, *134*, 5669–5674.
- (9) De Vleeschouwer, F.; Van Speybroeck, V.; Waroquier, M.; Geerlings, P.; De Proft, F. Electrophilicity and Nucleophilicity Index for Radicals. *Org. Lett.* **2007**, *9*, 2721–2724.
- (10) Tyson, E. L.; Ament, M. S.; Yoon, T. P. Transition Metal Photoredox Catalysis of Radical Thiol-Ene Reactions. *J. Org. Chem.* **2013**, *78*, 2046–2050.
- (11) Tyson, E. L.; Niemeyer, Z. L.; Yoon, T. P. Redox Mediators in Visible Light Photocatalysis: Photocatalytic Radical Thiol–Ene Additions. *J. Org. Chem.* **2014**, *79*, 1427–1436.
- (12) Dénès, F.; Pichowicz, M.; Povie, G.; Renaud, P. Thiyl Radicals in Organic Synthesis. *Chem. Rev.* **2014**, *114*, 2587–2693.
- (13) Bordwell, F. G.; Cheng, J. P.; Harrelson, J. A. Homolytic Bond Dissociation Energies in Solution from Equilibrium Acidity and Electrochemical Data. *J. Am. Chem. Soc.* **1988**, *110*, 1229–1231.
- (14) Bordwell, F. G.; Harrelson, J. A. Role of Single Electron Transfer in SN2-Type Substitution Reactions of Anions with Alkyl Halides. *J. Org. Chem.* **1989**, *54*, 4893–4898.
- (15) Bordwell, F. G.; Cheng, J.; Ji, G. Z.; Satish, A. V.; Zhang, X. Bond Dissociation Energies in DMSO Related to the Gas Phase Values. *J. Am. Chem. Soc.* **1991**, *113*, 9790–9795.

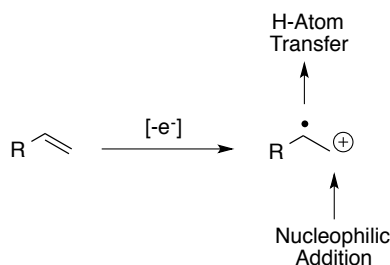
- (16) Zuo, Z.; MacMillan, D. W. C. Decarboxylative Arylation of  $\alpha$ -Amino Acids via Photoredox Catalysis: A One-Step Conversion of Biomass to Drug Pharmacophore. *J. Am. Chem. Soc.* **2014**, *136*, 5257–5260.
- (17) Liu, J.; Liu, Q.; Yi, H.; Qin, C.; Bai, R.; Qi, X.; Lan, Y.; Lei, A. Visible-Light-Mediated Decarboxylation/Oxidative Amidation of  $\alpha$ -Keto Acids with Amines under Mild Reaction Conditions Using O<sub>2</sub>. *Angew. Chem. Int. Ed.* **2014**, *53*, 502–506.
- (18) Miyake, Y.; Nakajima, K.; Nishibayashi, Y. Visible Light-Mediated Oxidative Decarboxylation of Arylacetic Acids into Benzyl Radicals: Addition to Electron-Deficient Alkenes by Using Photoredox Catalysts. *Chem. Commun.* **2013**, *49*, 7854–7856.
- (19) Budac, D.; Wan, P. Photodecarboxylation: Mechanism and Synthetic Utility. *J. Photochem. Photobiol. Chem.* **1992**, *67*, 135–166.
- (20) Lambert, J. D.; Rice, J. E.; Hong, J.; Hou, Z.; Yang, C. S. Synthesis and Biological Activity of the Tea Catechin Metabolites, M4 and M6 and Their Methoxy-Derivatives. *Bioorg. Med. Chem. Lett.* **2005**, *15*, 873–876.
- (21) Chang, X.; Peng, W.; Yao, Y.-F.; Koek, J. Concise Synthesis of Ring-Fission Metabolites of Epicatechin: 5-(3,4-Dihydroxybenzyl)dihydrofuran-2(3H)-One M6. *Synth. Commun.* **2010**, *40*, 3346–3352.
- (22) Shangguan, N.; Kiren, S.; Williams, L. J. A Formal Synthesis of Psymberin. *Org. Lett.* **2007**, *9*, 1093–1096.
- (23) Crimmins, M. T.; Stevens, J. M.; Schaaf, G. M. Total Synthesis of Irciniastatin A (Psymberin). *Org. Lett.* **2009**, *11*, 3990–3993.
- (24) Watanabe, T.; Imaizumi, T.; Chinen, T.; Nagumo, Y.; Shibuya, M.; Usui, T.; Kanoh, N.; Iwabuchi, Y. Syntheses and Biological Evaluation of Irciniastatin A and the C1–C2 Alkyne Analogue. *Org. Lett.* **2010**, *12*, 1040–1043.
- (25) Feng, Y.; Jiang, X.; De Brabander, J. K. Studies toward the Unique Pederin Family Member Psymberin: Full Structure Elucidation, Two Alternative Total Syntheses, and Analogs. *J. Am. Chem. Soc.* **2012**, *134*, 17083–17093.
- (26) An, C.; Jurica, J. A.; Walsh, S. P.; Hoye, A. T.; Smith, A. B. Total Synthesis of (+)-Irciniastatin A (a.k.a. Psymberin) and (–)-Irciniastatin B. *J. Org. Chem.* **2013**, *78*, 4278–4296.
- (27) Buntin, K.; Rachid, S.; Scharfe, M.; Blöcker, H.; Weissman, K. J.; Müller, R. Production of the Antifungal Isochromanone Ajudazols A and B in *Chondromyces Crocatus* Cm c5: Biosynthetic Machinery and Cytochrome P450 Modifications. *Angew. Chem. Int. Ed.* **2008**, *47*, 4595–4599.

## CHAPTER 5 – OTHER APPLICATIONS OF THE IDENTIFIED CATALYTIC SYSTEM AND FUTURE DIRECTIONS

### 5.1. Introduction.

The goal of this project was not simply to identify a catalytic system to allow for the intramolecular, anti-Markovnikov addition of oxygen-centered nucleophiles to alkenes. Rather, the purpose was to identify a general platform which would allow for the additions of a variety of nucleophiles to alkenes with complete anti-Markovnikov selectivity, and we had felt from the beginning that the insights that we could gain from developing one reaction to take advantage of the cation-radical intermediate could be expanded to other nucleophiles with ease. Once we identified the proper manner in which we could take advantage of the cation-radical intermediate – that is, accounting for both the charge and the spin of the cation-radical as reaction vectors that must be accounted for, the development of systems related to the ones presented here have come at a rapid pace (**Fig. 5.1**).

**Figure 5.1. Dual Reaction Vectors of Alkene Cation-Radicals.**

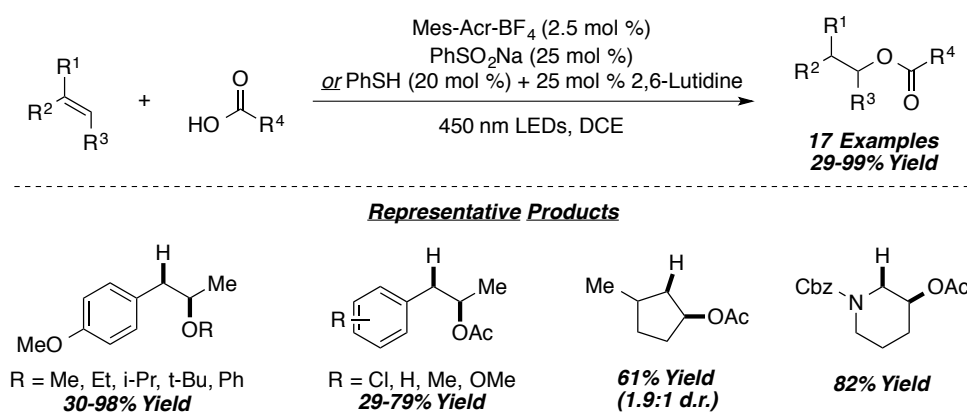


### 5.2 Other Anti-Markovnikov Transformations Developed in the Nicewicz Laboratory Based on the Previously Described Dual-Catalyst System.

The first transformation that the identified reactivity pattern enabled our lab to develop was an intermolecular variant of the nucleophilic addition pattern, utilizing carboxylic acids or carboxylates as nucleophiles (**Fig. 5.2**). In this work, Perkowski and Nicewicz were able to demonstrate the addition of

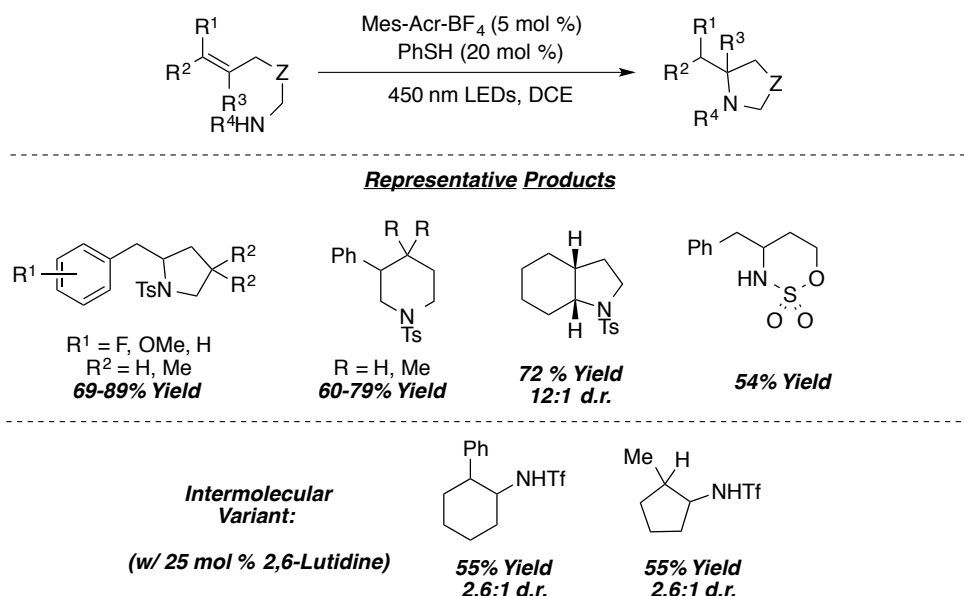
acetic acid to a variety of alkenes in moderate to good yield<sup>1</sup>. They were also able to demonstrate that a number of carboxylic acids could be delivered to alkenes allowing for a convergent synthesis of complex esters through a novel synthetic disconnection. Key to this transformation was the use of some of our developed second-generation hydrogen atom donors or donor-precursors, such as sodium benzenesulfinate and thiophenol, and the application of a catalytic amount of base to promote the transformation.

**Figure 5.2. Anti-Markovnikov Hydrocarboxylation of Alkenes.**



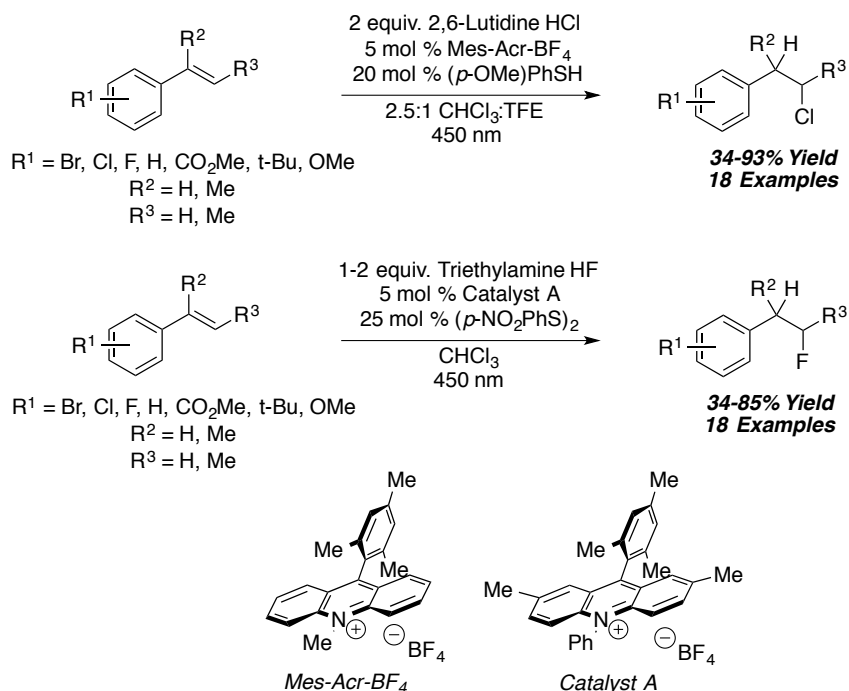
The second method was disclosed by Nguyen and Nicewicz in 2013. Their method enables the addition of pendant amine nucleophiles to alkenes with complete anti-Markovnikov selectivity<sup>2</sup>. This chemistry employed thiophenol as the hydrogen atom donor, and allows for the synthesis of cyclic amines protected with either a boc- or triflyl- protecting group. Once again, the addition of catalytic amounts of base proved to be vital to engineering a successful reaction. In a follow-up publication (not shown), Nguyen, Manohar, and Nicewicz were able to demonstrate an intermolecular variant, employing triflylamide as the nucleophile in the presence of 2,6-lutidine and phenyldisulfide<sup>3</sup>. On top of simple hydroamination products (**Fig. 5.3**), they were also able to demonstrate the addition of an array of nitrogen heterocycles to alkenes, providing access to structures that could find use in medicinal chemistry explorations.

**Figure 5.3. Anti-Markovnikov Hydroamination of Alkenes.**



Finally, Wilger, Grandjean, Lammert and Nicewicz have recently developed a method for the hydrochlorination and hydrofluorination of styrenyl motifs using acridinium photocatalysts and thiophenol derivatives (**Fig. 5.4**)<sup>4</sup>. For class of transformation, changes to the catalytic system were required to appropriately tune for the unique properties required by the nucleophile: be it the basicity of the thiolate (in the case of the hydrochlorination chemistry, (4-OMe)thiophenol was required, while (*p*-NO<sub>2</sub>)PhS)<sub>2</sub> was the optimal source of thiyl-radical in the hydrofluorination chemistry), or decoration of the acridinium scaffold with methyl and phenyl groups to render it more stable in the presence of strong nucleophiles. The authors were able to demonstrate that complete anti-Markovnikov selectivity was obtainable, offering complementarity to the traditional Markovnikov addition of mineral acids to alkenes. Select additions of sulfonic acids and phosphoric acids were also offered in this report (not shown).

**Figure 5.4. Anti-Markovnikov Hydrohalogenation of Styrene Derivatives.**

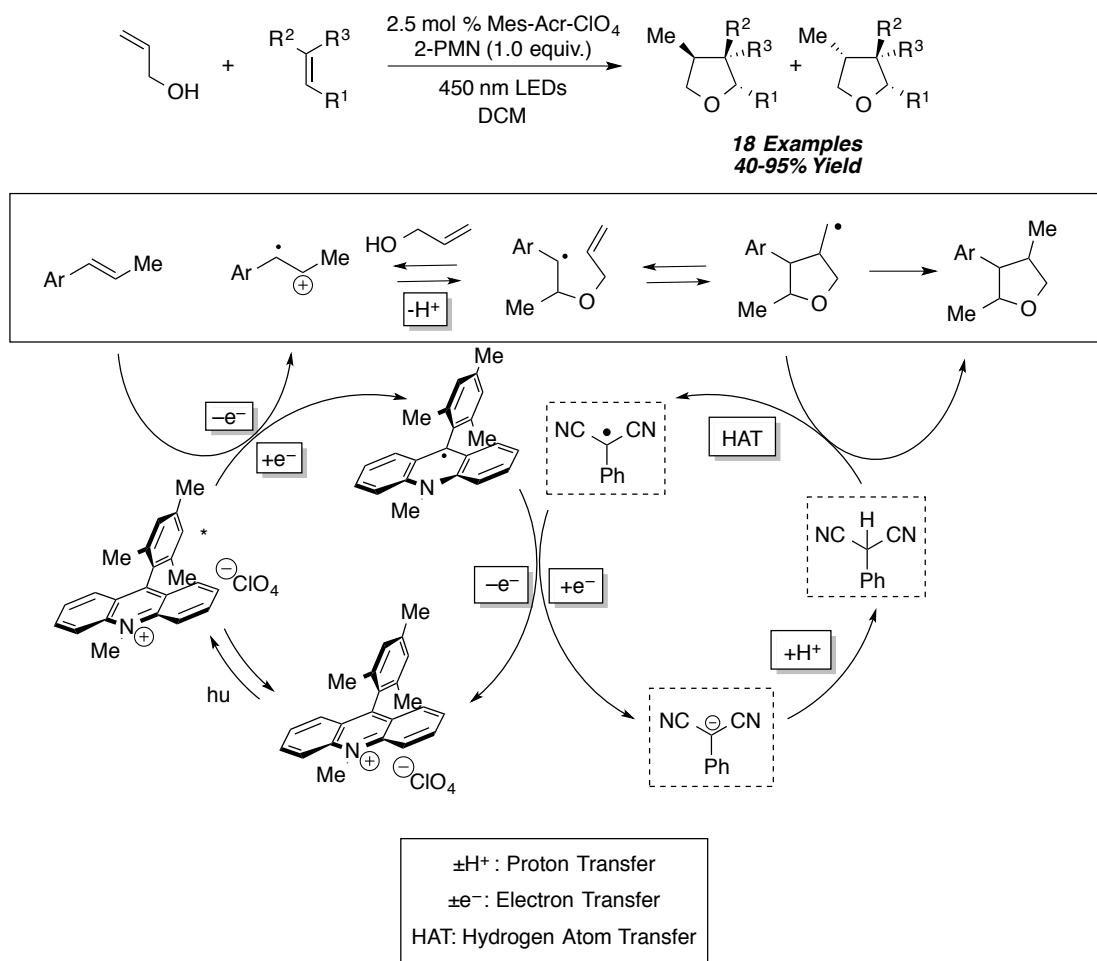


### 5.3. Regioselective Polar Radical Crossover Cycloadditions.

In 2013, Grandjean and Nicewicz reported the polar-radical crossover cycloaddition of allyl alcohols to alkenes, affording access to densely substituted tetrahydrofurans in a highly convergent manner<sup>5</sup>. This transformation relies on initial nucleophilic addition to an alkene cation-radical generated by single-electron oxidation of the alkene with the Fukuzumi catalyst. Addition of the allyl alcohol, as expected, proceeded with complete anti-Markovnikov selectivity. The resulting radical species then proceeds to initiate a 5-*exo* cyclization onto the pendant alkene to afford primary radicals. Finally, this radical then abstracts a hydrogen atom from the included hydrogen atom donor, 2-PMN, to afford the final tetrahydrofuran products. Importantly, cyclization was found to outcompete hydrogen atom transfer in all cases, as uncyclized products were not observed in this report.



**Figure 5.5. Polar-Radical Crossover Cycloaddition to form Tetrahydrofuran Products.**

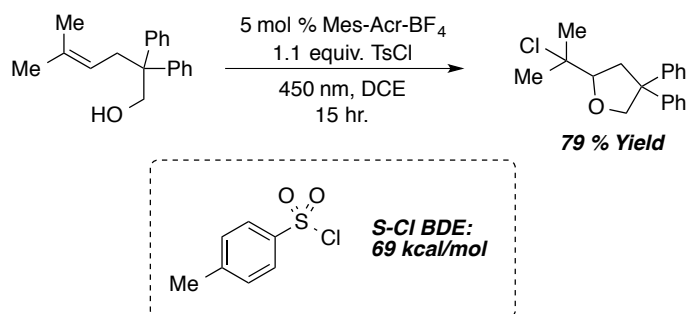


#### 5.4. Other Possible Future Directions for the Cation-Radical Intermediates.

It is also possible to consider alternate fates for the radical intermediate to affect difunctionalization reactions of alkenes. The research in our laboratory, as demonstrated above, has focused on only two possible fates for this radical: trapping with hydrogen atoms to give anti-Markovnikov hydrofunctionalization products, or initial cyclization of an alkene onto the radical to form a cyclic scaffold prior to trapping with a hydrogen atom. However, these transformations only take advantage of a limited amount of the plethora of reactivity patterns that are offered by radical intermediates. For example, we can consider trapping radical intermediates with heteroatom based spin traps, to afford products of difunctionalization.

We have obtained preliminary results along this avenue. Inclusion of a slight excess of tosyl chloride (BDE estimated at 69 kcal/mol, on the basis of data reported for benzenesulfonyl chloride)<sup>6</sup> in lieu of the hydrogen atom donor when carrying out the cyclization of our standard alkenol substrate proceeds to give complete selectivity for the product of anti-Markovnikov hydroetherification, with incorporation of chloride onto the more substituted center.

**Figure 5.6. Regioselective Oxychlorination of an Alkenol.**



## 5.5. Conclusions

It is hoped that this dissertation has illustrated the unique opportunity offered by alkene cation-radical intermediates for catalysis of the direct, catalytic additions of nucleophiles to alkenes. While this work has offered significant advances with regards to the scope, selectivity, efficiency, and ease of setup of these unique reactions, not to be lost in the shuffle are the tremendous contributions made by others in the field. Arnold, Gassman and Mizuno established a reactivity pattern and a theory for selectivity to build on, and Fukuzumi's catalyst catalyst offered us a tool to generate a plethora of cation-radicals from their respective olefins, without being incorporated into the final products. The work of Crich enabled us to recognize an alternative way to work with the radical intermediate, and the efforts of Bordwell and countless others gave us thermodynamic benchmarks with which to evaluate the catalytic cycle we believe to be operative.

Our work lay in piecing the puzzle together. Careful analysis of our initial reactions enabled us to recognize that we could effect reactivity, but that further developing the reaction would require rethinking

the way we approached our reactive intermediates. Recognizing that reduction of the intermediate radicals was unlikely to work, we elected instead to hand the radical off through hydrogen-atom transfer to furnish product. The lower reduction potential of the ensuing radical was what ultimately what we believe enabled efficient catalyst turnover, and as a result, we were able to develop and utilize an extraordinarily versatile reactivity pattern to develop a class of catalytic transformation that has been sought for decades.

This is not to say by any stretch of the imagination that the work is done: being able to obtain complete regioselectivity in good yield with a catalytic system is only the first step in what is certain to be a long journey. Further improvements to reaction efficiency will certainly be required to pull this chemistry off the benchtop and into industrial pilot plants, and methods allowing for control of diastereo- and enantioselectivity are needed in order to render the transformation more applicable in complex synthetic settings. There is also still a lot that we still do not understand about the unique reaction mechanism that we have proposed and believe to be operable, and this understanding will doubtlessly make our laboratory's task easier in the future. It appears that we have only begun to scratch the surface of a myriad of possibilities for this interesting system and its associated reactivity pattern, and future avenues for this chemistry appear bright.

“Learn the rules: So that you know how to break them properly”

*-Attributed to the Dalai Lama*

## REFERENCES

- (1) Perkowski, A. J.; Nicewicz, D. A. Direct Catalytic Anti-Markovnikov Addition of Carboxylic Acids to Alkenes. *J. Am. Chem. Soc.* **2013**, *135*, 10334–10337.
- (2) Nguyen, T. M.; Nicewicz, D. A. Anti-Markovnikov Hydroamination of Alkenes Catalyzed by an Organic Photoredox System. *J. Am. Chem. Soc.* **2013**, *135*, 9588–9591.
- (3) Nguyen, T. M.; Manohar, N.; Nicewicz, D. A. anti-Markovnikov Hydroamination of Alkenes Catalyzed by a Two-Component Organic Photoredox System: Direct Access to Phenethylamine Derivatives. *Angew. Chem. Int. Ed.* **2014**, *In Press*.
- (4) Wilger, D. J.; Grandjean, J.-M. M.; Lammert, T.; Nicewicz, D. A. The Direct Anti-Markovnikov Addition of Mineral Acids to Styrenes. *Unpubl. Results*.
- (5) Grandjean, J.-M. M.; Nicewicz, D. A. Synthesis of Highly Substituted Tetrahydrofurans by Catalytic Polar-Radical-Crossover Cycloadditions of Alkenes and Alkenols. *Angew. Chem. Int. Ed.* **2013**, *52*, 3967–3971.
- (6) Chatgililoglu, C.; Griller, D.; Kanabus-Kaminska, J. M.; Lossing, F. P. Sulfur–chlorine Bond Dissociation Enthalpies in Methane- and Benzene-sulfonyl Chlorides. *J. Chem. Soc. Perkin Trans. 2* **1994**, 357–360.

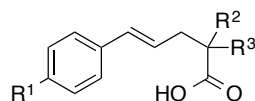
## APPENDIX 1: SELECTED METHODS

### A1.1. General Methods

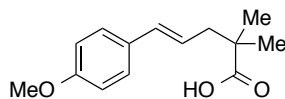
Infrared (IR) spectra were obtained using a Jasco 260 Plus Fourier transform infrared spectrometer. Proton and carbon magnetic resonance spectra ( $^1\text{H}$  NMR and  $^{13}\text{C}$  NMR) were recorded on a Bruker model DRX 400, DRX 500, or a Bruker AVANCE III 600 CryoProbe ( $^1\text{H}$  NMR at 400 MHz, 500 MHz or 600 MHz and  $^{13}\text{C}$  NMR at 101, 126, or 151 MHz) spectrometer with solvent resonance as the internal standard ( $^1\text{H}$  NMR:  $\text{CDCl}_3$  at 7.24 ppm;  $^{13}\text{C}$  NMR:  $\text{CDCl}_3$  at 77.0 ppm).  $^1\text{H}$  NMR data are reported as follows: chemical shift, multiplicity (s = singlet, d = doublet, t = triplet, dd = doublet of doublets, ddt = doublet of doublet of triplets, ddd = doublet of doublet of doublets, dddd = doublet of doublet of doublet of doublets m = multiplet, brs = broad singlet), coupling constants (Hz), and integration. Mass spectra were obtained using a Micromass (now Waters Corporation, 34 Maple Street, Milford, MA 01757) Quattro-II, Triple Quadrupole Mass Spectrometer, with a Z-spray nano-Electrospray source design, in combination with a NanoMate (Advion 19 Brown Road, Ithaca, NY 14850) chip based electrospray sample introduction system and nozzle. Cyclic voltammograms were obtained with a platinum disc working electrode, Ag/AgCl reference electrode, a platinum wire auxiliary, and CHI-760 or WaveNow potentiostat using 1-20 mM solutions of analyte in acetonitrile with 0.1 M tetrabutylammonium perchlorate or tetrabutylammonium hexafluorophosphate as supporting electrolyte. Thin layer chromatography (TLC) was performed on SiliaPlate 250  $\mu\text{m}$  thick silica gel plates provided by Silicycle. Visualization was accomplished with short wave UV light (254 nm), aqueous basic potassium permanganate solution, or cerium ammonium molybdate solution followed by heating. Flash chromatography was performed using SiliaFlash P60 silica gel (40-63  $\mu\text{m}$ ) purchased from Silicycle. Tetrahydrofuran, diethyl ether, dichloromethane, and toluene were dried by passage through a column of neutral alumina under nitrogen prior to use. Irradiation of photochemical reactions was carried out using one of two different models of 15W PAR38 blue LED floodlamps purchased from EagleLight (Carlsbad, CA), or a PAR38 blue LED floodlamp purchased from Ecoxotic equipped with CREE Royal Blue LEDs.

Reactions with visible irradiation were performed in borosilicate glass vials purchased from Fisher Scientific. In the case of UV irradiation, reactions were carried out in a Luzchem photobox equipped with 10 X 5W fluorescent UV bulbs with emission > 290 nm, with reactions being carried out in Pyrex screwcap tubes. All other reagents were obtained from commercial sources and used without further purification unless otherwise noted.

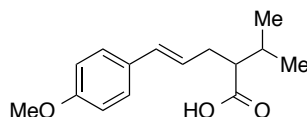
### A1.2. Synthesis of Alkenol Substrates



**General Procedure A:** A round-bottomed flask was charged with a solution of freshly distilled hexamethyldisilazane (3.0 equiv.), equipped with a stirbar and fitted with a septum. Toluene (80 mL) and freshly distilled triethylamine (20 mL) were added, and the reaction was cooled to 0 °C. A solution of n-BuLi in hexanes (2.5 M, 3.0 equiv.) was added carefully, and the solution was allowed to stir at 0 °C for 30 minutes. The reaction was then cooled to -78 °C, and the allylic ester was added to the reaction dropwise in toluene (10 mL). After 1 hour at -78 °C, trimethylsilyl chloride (1.1 equiv) was added at -78 °C, dropwise, the reaction was warmed to 25 °C, and stirred at room temperature for an additional 2 hours. The reaction was quenched with 1M HCl (50 mL), and transferred to an Erlenmeyer flask. The mixture was cooled to 0 °C, and acidified further to pH 1 with concentrated hydrochloric acid. Water was added to dissolve any precipitate, and the organics were separated. The aqueous layer was extracted with 3 X 50 mL portions of ether, and the combined organics were washed successively with water (75 mL) and brine (75 mL). The organics were dried over sodium sulfate and concentrated to give a crude oil. The material was recrystallized from ethyl acetate/hexanes to give the desired  $\gamma,\delta$  unsaturated acid.

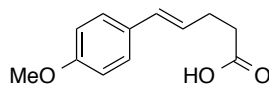


**(E)-5-(4-methoxyphenyl)-2,2-dimethylpent-4-enoic acid (D1).** The  $\gamma,\delta$  unsaturated acid was prepared according to General Procedure A, using 2.52 g (11.6 mmol) 1-(4-methoxyphenyl)allyl isobutyrate<sup>1</sup>, 7.3 mL (34.8 mmol) hexamethyldisilazane, 13.9 mL (34.8 mmol) *n*-BuLi in hexanes (2.5 M), and 1.6 mL (12.8 mmol) trimethylsilylchloride to furnish 1.74 g of product as colorless crystals (7.98 mmol, 69%). Analytical data for (E)-5-(4-methoxyphenyl)-2,2-dimethylpent-4-enoic acid: **<sup>1</sup>H NMR:** (400 MHz, CDCl<sub>3</sub>)  $\delta$  7.26 (d,  $J$  = 8.6 Hz, 2H), 6.81 (d,  $J$  = 8.6 Hz, 2H), 6.36 (d,  $J$  = 15.7 Hz, 1H), 6.01 (dt,  $J$  = 15.4, 7.5 Hz, 1H), 3.78 (s, 3H), 2.42 (d,  $J$  = 7.5 Hz, 2H), 1.23 (s, 6H). **<sup>13</sup>C NMR** (101 MHz, CDCl<sub>3</sub>)  $\delta$  182.22, 158.80, 132.60, 130.16, 127.19, 123.31, 113.81, 55.19, 43.43, 42.52, 24.61. **MS** (+ESI) Calculated  $m/z$  for  $[M+H]^+$  = 235.13, Found  $m/z$  for  $[M+H]^+$  = 235.06 **IR** (Thin Film, cm<sup>-1</sup>) 3032, 2972, 2836, 1698, 1607, 1577, 1511, 1473, 1265, 1250 **R<sub>f</sub>** (15% EtOAc / 85% Hexanes): 0.30

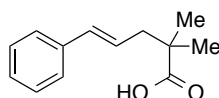


**(E)-2-isopropyl-5-(4-methoxyphenyl)pent-4-enoic acid (D3).** The  $\gamma,\delta$  unsaturated acid was prepared according to General Procedure A, using 4.78 g (19.2 mmol) 1-(4-methoxyphenyl)allyl 3-methylbutanoate<sup>1</sup>, 12.1 mL (57.6 mmol) hexamethyldisilazane, 23.0 mL (57.6 mmol) *n*-BuLi in hexanes (2.5 M), and 1.8 mL (63.4 mmol) trimethylsilylchloride to furnish 1.41 g of product as colorless crystals (5.57 mmol, 29%). Analytical data for (E)-2-isopropyl-5-(4-methoxyphenyl)pent-4-enoic acid: **<sup>1</sup>H NMR:**  $\delta$  7.23 (d,  $J$  = 7.2 Hz, 2H), 6.79 (d,  $J$  = 8.6 Hz, 2H), 6.36 (d,  $J$  = 15.9 Hz, 1H), 6.11 – 5.93 (m, 1H), 3.77 (s, 3H), 2.49 – 2.36 (m, 2H), 2.34 – 2.23 (m, 1H), 2.06 – 1.83 (m, 1H), 0.98 (d,  $J$  = 7.0 Hz, 3H), 0.96 (d,  $J$  = 7.3 Hz, 3H). **<sup>13</sup>C NMR** (101 MHz, CDCl<sub>3</sub>)  $\delta$  180.80, 158.73, 131.14, 130.16, 127.11, 125.00, 113.78, 55.18, 52.38, 32.63, 29.94, 20.07, 20.02. **MS** (+ESI) Calculated  $m/z$  for  $[M+H]^+$  = 249.14, Found  $m/z$  for

$[M+H]^+ = 249.15$  **IR** (Thin Film,  $\text{cm}^{-1}$ ) 3403, 2955, 2930, 1693, 1605, 1513, 1441, 1281, 1250, 1208 **R<sub>f</sub>** (15% EtOAc / 85% Hexanes): 0.20



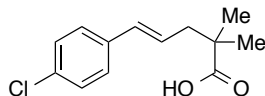
**(E)-5-(4-methoxyphenyl)pent-4-enoic acid (C33, D5).** The  $\gamma,\delta$  unsaturated acid was prepared according to General Procedure A, using 2.52 g (13.3 mmol) 1-(4-methoxyphenyl)allyl acetate<sup>1</sup>, 6.4 mL (39.9 mmol) hexamethyldisilazane, 16.0 mL (39.9 mmol) *n*-BuLi in hexanes (2.5 M), and 1.9 mL of trimethylsilylchloride (14.6 mmol) to furnish 1.74 g of product as colorless crystals (6.16 mmol, 46%). Analytical data for (E)-5-(4-methoxyphenyl)pent-4-enoic acid: **<sup>1</sup>H NMR** (400 MHz,  $\text{CDCl}_3$ )  $\delta$  7.25 (d,  $J = 9.3$  Hz, 2H), 6.82 (d,  $J = 8.7$  Hz, 2H), 6.37 (d,  $J = 15.8$  Hz, 1H), 6.14 – 5.96 (m, 1H), 3.78 (s, 3H), 2.51 (s, 4H). **<sup>13</sup>C NMR** (101 MHz,  $\text{CDCl}_3$ )  $\delta$  183.09, 135.54, 132.51, 131.85, 128.31, 127.05, 126.09, 43.16, 42.22, 24.47. **MS** (+ESI) Calculated  $m/z$  for  $[M+H]^+ = 207.09$ , Found  $m/z$  for  $[M+H]^+ = 207.07$  **IR** (Thin Film,  $\text{cm}^{-1}$ ) 3403, 2955, 2930, 1693, 1605, 1513, 1441, 1281, 1250, 1208 **R<sub>f</sub>** (15% EtOAc / 85% Hexanes): 0.10



**(E)-2,2-dimethyl-5-phenylpent-4-enoic acid (D7).** The  $\gamma,\delta$  unsaturated acid was prepared according to General Procedure A, using 2.67 g (13.1 mmol) 1-phenylallyl isobutyrate<sup>1</sup>, 8.2 mL (39.3 mL) hexamethyldisilazane, 15.7 mL (39.3 mmol) *n*-BuLi in hexanes (2.5 M), and 1.8 mL (14.4 mmol) trimethylsilylchloride to furnish 1.50 g of product as colorless crystals (7.35 mmol, 56%). Analytical data for (E)-2,2-dimethyl-5-phenylpent-4-enoic acid matches that found in the literature<sup>2</sup>: **<sup>1</sup>H NMR**: (400 MHz,  $\text{CDCl}_3$ )  $\delta$  7.33 (d,  $J = 7.6$  Hz, 2H), 7.28 (t,  $J = 7.5$  Hz, 2H), 7.19 (t,  $J = 7.1$  Hz, 1H), 6.42 (d,  $J = 15.7$  Hz, 1H), 6.25 – 6.08 (dt,  $J = 15.7$  Hz,  $J = 7.5$  Hz, 1H), 2.45 (d,  $J = 7.5$  Hz, 2H), 1.24 (s, 6H). **<sup>13</sup>C NMR** (101 MHz,  $\text{CDCl}_3$ )  $\delta$  184.48, 137.34, 133.31, 128.45, 127.16, 126.13, 125.60, 43.43, 42.55, 24.69. **MS** (+ESI)

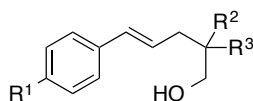


Calculated  $m/z$  for  $[M+H]^+ = 205.12$ , Found  $m/z$  for  $[M+H]^+ = 205.08$  **IR** (Thin Film,  $\text{cm}^{-1}$ ) 3403, 2955, 2930, 1693, 1605, 1513, 1441, 1281, 1250, 1208 **R<sub>f</sub>** (15% EtOAc / 85% Hexanes): 0.40



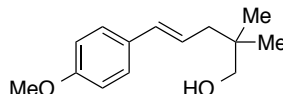
**(E)-5-(4-chlorophenyl)-2,2-dimethylpent-4-enoic acid (D11).** The  $\gamma,\delta$  unsaturated acid was prepared according to General Procedure A, using 3.51 g (14.7 mmol) 1-(4-chlorophenyl)allyl isobutyrate<sup>1</sup>, 9.2 mL (44.1 mmol) hexamethyldisilazane, 17.6 mL (44.1 mmol) *n*-BuLi in hexanes (2.5 M), and 2.05 mL (16.2 mmol) trimethylsilylchloride to furnish 1.28 g of product as off-white crystals (5.37 mmol, 36%).

Analytical data for (E)-5-(4-chlorophenyl)-2,2-dimethylpent-4-enoic acid: **<sup>1</sup>H NMR**: (400 MHz,  $\text{CDCl}_3$ )  $\delta$  7.24 (s, 4H), 6.37 (d,  $J = 15.7$  Hz, 1H), 6.14 (dt,  $J = 15.4, 7.5$  Hz, 1H), 2.43 (d,  $J = 7.5$  Hz, 2H), 1.23 (s, 6H). **<sup>13</sup>C NMR** (101 MHz,  $\text{CDCl}_3$ )  $\delta$  183.75, 153.53, 132.50, 131.86, 128.33, 127.08, 126.11, 43.16, 42.27, 24.49. **MS** (+ESI) Calculated  $m/z$  for  $[M+H]^+ = 239.08$ , Found  $m/z$  for  $[M+H]^+ = 239.13$  **IR** (Thin Film,  $\text{cm}^{-1}$ ) 2976, 1695, 1471, 1403, 1267, 1209. **R<sub>f</sub>** (15% EtOAc / 85% Hexanes): 0.30

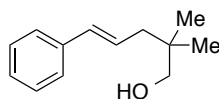


**General Procedure C:** A 50 mL round bottom flask was charged with lithium aluminum hydride (1.0 equiv.), was equipped with a stirbar, reflux condenser and septum, and was purged with a stream of nitrogen. Dry THF (15 mL) was added, and the solution was cooled to 0 °C. The unsaturated acid was then added as a solution in dry THF (5 mL). After hydrogen evolution ceased, the reaction was warmed to room temperature and heated to reflux overnight. The reaction was cooled to room temperature, then to 0 °C, and diluted with ether (15 mL). The reaction was quenched by slow successive dropwise addition of 0.2 mL water, 0.4 mL 1M NaOH, and 0.6 mL water, successively, affording an off white precipitate. The mixture was then vacuum-filtered through a pad of celite, and eluted with several portions of diethyl ether.

The filtrate was concentrated to give the crude alkenol, which was further purified by flash chromatography or recrystallization.

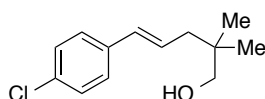


**(E)-5-(4-methoxyphenyl)-2,2-dimethylpent-4-en-1-ol (C12).** The alkenol was prepared according to General Procedure C, using 1.00 g of (*E*)-5-(4-methoxyphenyl)-2,2-dimethylpent-4-enoic acid<sup>1</sup> as the  $\gamma,\delta$  unsaturated acid, and 128 mg of lithium aluminum hydride. The crude oil was purified by flash chromatography (15% EtOAc / 85% Hexanes), affording the pure product as a colorless oil that gave 701 mg of a colorless solid upon prolonged standing (3.20 mmol, 75%). Analytical data for (*E*)-5-(4-methoxyphenyl)-2,2-dimethylpent-4-en-1-ol: <sup>1</sup>H NMR (400 MHz, CDCl<sub>3</sub>)  $\delta$  7.27 (d,  $J$  = 8.7 Hz, 2H), 6.83 (d,  $J$  = 8.7 Hz, 2H), 6.34 (d,  $J$  = 15.7 Hz, 1H), 6.09 (dt,  $J$  = 15.5, 7.6 Hz, 1H), 3.78 (s, 3H), 3.35 (s, 2H), 2.17 – 2.10 (m, 2H), 1.50 (s, 1H), 0.92 (s, 6H). <sup>13</sup>C NMR (101 MHz, CDCl<sub>3</sub>)  $\delta$  158.78, 131.69, 130.52, 127.09, 124.85, 113.93, 71.75, 55.28, 42.38, 36.14, 23.95. MS (+ESI) Calculated  $m/z$  for [M+H]<sup>+</sup>, Found  $m/z$  for [M+H]<sup>+</sup> = 221.16. IR (Thin Film, cm<sup>-1</sup>) 3419, 3062, 3025, 2962, 2951, 2916, 2869, 2841, 1646, 1608, 1577, 1511, 1467, 1444, 1419, 1380, 1363, 1299, 1250 R<sub>f</sub> (15% EtOAc / 85% Hexanes): 0.15

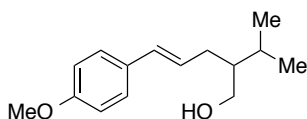


**(E)-2,2-dimethyl-5-phenylpent-4-en-1-ol (C14).** The alkenol was prepared according to General Procedure C, using 1.00 g of (*E*)-2,2-dimethyl-5-phenylpent-4-enoic acid as the  $\gamma,\delta$  unsaturated acid, and 186 mg of lithium aluminum hydride. The crude oil was purified by flash chromatography (15% EtOAc / 85% Hexanes), affording pure product as 757 mg of colorless oil (3.97 mmol, 81%). Analytical data for (*E*)-2,2-dimethyl-5-phenylpent-4-en-1-ol matches that previously reported in the literature<sup>3</sup>: <sup>1</sup>H NMR (400 MHz, CDCl<sub>3</sub>)  $\delta$  7.34 (d,  $J$  = 7.3 Hz, 2H), 7.32 – 7.26 (m, 2H), 7.19 (t,  $J$  = 7.2 Hz, 1H), 6.40 (d,  $J$  =

15.8 Hz, 1H), 6.31 – 6.19 (m, 1H), 3.36 (s, 2H), 2.17 (d,  $J = 7.5$  Hz, 2H), 1.52 (s, 1H), 0.93 (s, 6H).  $^{13}\text{C}$  NMR (101 MHz,  $\text{CDCl}_3$ )  $\delta$  137.51, 132.22, 128.34, 126.96, 126.83, 125.87, 71.60, 42.23, 36.02, 23.81. MS (+ESI)  $m/z$  for  $[\text{M}+\text{H}]^+ = 191.14$ , Found  $m/z$  for  $[\text{M}+\text{H}]^+ = 191.12$  IR (Thin Film,  $\text{cm}^{-1}$ ) 3401, 3081, 3059, 3026, 2957, 2869, 1651, 1599, 1495, 1471, 1449, 1389, 1364, 1291, 1267, 1200  $R_f$  (15% EtOAc / 85% Hexanes): 0.20.

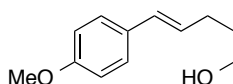


**(E)-5-(4-chlorophenyl)-2,2-dimethylpent-4-en-1-ol (C16).** The alkenol was prepared according to General Procedure C, using 800 mg of (*E*)-5-(4-chlorophenyl)-2,2-dimethylpent-4-enoic acid as the  $\gamma,\delta$  unsaturated acid, and 162 mg of lithium aluminum hydride. The crude oil was purified by flash chromatography (15% EtOAc/85% Hexanes), affording the pure product as an oil that crystallized to 558 mg of a colorless solid upon prolonged standing (2.49 mmol, 74%). Analytical data for (*E*)-5-(4-chlorophenyl)-2,2-dimethylpent-4-en-1-ol (Table 2, Entry 3):  $^1\text{H}$  NMR (400 MHz,  $\text{CDCl}_3$ )  $\delta$  7.24 (brs, 4H), 6.34 (d,  $J = 15.8$  Hz, 1H), 6.21 (dt,  $J = 15.8$  Hz, 7.5 Hz, 1H), 3.35 (s, 2H), 2.15 (d,  $J = 7.5$  Hz, 2H), 1.49 (brs, 1H), 0.91 (s, 6H).  $^{13}\text{C}$  NMR (101 MHz,  $\text{CDCl}_3$ )  $\delta$  136.45, 132.85, 131.47, 128.92, 128.23, 127.52, 72.01, 42.62, 36.48, 24.26. MS (+ESI) Calculated  $m/z$  for  $[\text{M}+\text{H}]^+ = 225.10$ , Found  $m/z$  for  $[\text{M}+\text{H}]^+ = 225.16$ . IR (Thin Film,  $\text{cm}^{-1}$ ) 3387, 3027, 2957, 2928, 2871, 1650, 1594, 1491, 1471, 1404, 1390, 1364, 1335, 1297, 1266  $R_f$  (15% EtOAc / 85% Hexanes): 0.20

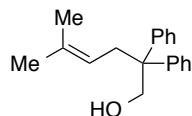


**(E)-2-isopropyl-5-(4-methoxyphenyl)pent-4-en-1-ol (C18).** The alken-ol was prepared according to General Procedure C, using 800 mg of (*E*)-2-isopropyl-5-(4-methoxyphenyl)pent-4-enoic acid as the  $\gamma,\delta$  unsaturated acid, and 130 mg of lithium aluminum hydride. The crude oil was purified by flash column

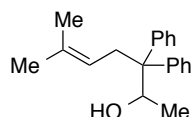
chromatography (15% EtOAc/Hexanes), affording the product as 605 mg of colorless oil. (2.57 mmol, 75%). Analytical data for (*E*)-2-isopropyl-5-(4-methoxyphenyl)pent-4-en-1-ol:  $^1\text{H NMR}$  (400 MHz,  $\text{CDCl}_3$ )  $\delta$  7.26 (d,  $J = 8.6$  Hz, 2H), 6.82 (d,  $J = 8.6$  Hz, 2H), 6.35 (d,  $J = 15.8$  Hz, 1H), 6.14 – 6.01 (m, 1H), 3.78 (s, 3H), 3.69 – 3.55 (m, 2H), 2.35 – 2.10 (m, 2H), 1.92 – 1.72 (m, 1H), 1.56 (brs, 1H), 1.53 – 1.44 (m, 1H), 0.93 (d,  $J = 6.9$  Hz, 6H).  $^{13}\text{C NMR}$  (101 MHz,  $\text{CDCl}_3$ )  $\delta$  158.35, 130.09, 127.15, 126.65, 113.56, 63.33, 54.90, 46.66, 31.63, 27.56, 19.48, 19.15. It is believed that here is one set of coincidental peaks in the aryl region. **MS** (+ESI) Calculated  $m/z$  for  $[\text{M}+\text{H}]^+ = 235.16$ , Found  $m/z$  for  $[\text{M}+\text{H}]^+ = 235.12$ . **IR** (Thin Film,  $\text{cm}^{-1}$ ) 3283, 2934, 2911, 2862, 2841, 1606, 1512, 1463, 1442, 1277, 1246 **R<sub>f</sub>** (15% EtOAc / 85% Hexanes): 0.15



**(*E*)-5-(4-methoxyphenyl)pent-4-en-1-ol (C20).** The alkenol was prepared according to General Procedure C, using 800 mg of (*E*)-5-(4-methoxyphenyl)pent-4-enoic acid as the  $\gamma,\delta$  unsaturated acid, and 148 mg of lithium aluminum hydride. Crude oil was recrystallized from hexanes, affording purified product as 560 mg of colorless needles (2.91 mmol, 75%). Analytical data for (*E*)-5-(4-chlorophenyl)-2,2-dimethylpent-4-en-1-ol matches that found in the literature<sup>S9</sup>:  $^1\text{H NMR}$  (400 MHz,  $\text{CDCl}_3$ )  $\delta$  7.25 (d,  $J = 8.9$  Hz, 2H), 6.82 (d,  $J = 8.9$  Hz, 2H), 6.35 (d,  $J = 15.8$  Hz, 1H), 6.06 (dt,  $J = 15.7, 7.0$  Hz, 1H), 3.78 (s, 3H), 3.69 (dd,  $J = 10.6, 6.1$  Hz, 2H), 2.27 (dt,  $J = 8.0, 1.1$  Hz, 2H), 1.78 – 1.66 (m, 2H), 1.30 (brs, 1H).  $^{13}\text{C NMR}$  (101 MHz,  $\text{CDCl}_3$ ) \ **MS** (+ESI) Calculated  $m/z$  for  $[\text{M}+\text{H}]^+ = 193.15$ , Found  $m/z$  for  $[\text{M}+\text{H}]^+ = 193.04$ . **IR** (Thin Film,  $\text{cm}^{-1}$ ) 3283, 2934, 2911, 2862, 2841, 1606, 1512, 1463, 1442, 1277, 1246 **R<sub>f</sub>** (15% EtOAc / 85% Hexanes): 0.10

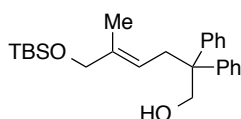


**5-methyl-2,2-diphenylhex-4-en-1-ol (C1).** A 50 mL round bottom flask was charged with lithium aluminum hydride (1.33 g, 35.0 mmol, 1.0 equiv.), equipped with a reflux condenser and septum, and purged with a stream of nitrogen. Dry THF (15 mL) was added, and the solution was cooled to 0 °C. 5-methyl-2,2-diphenylhex-4-enoic acid (9.4 g, 35.0 mmol, 1.0 equiv.) was then added dropwise as a solution in dry THF (5 mL). After hydrogen evolution ceased, the reaction was warmed to room temperature, then heated to reflux overnight. The reaction was cooled to 0 °C, and diluted with ether (15 mL). The reaction was quenched by slow successive dropwise addition of 1.3 mL water, 2.6 mL 1M NaOH, and 3.9 mL water, successively, affording an off white precipitate. The mixture was then vacuum-filtered through a pad of celite, and eluted with several portions of diethyl ether. The filtrate was concentrated to give crude oil, which was further purified by flash column chromatography (20% EtOAc/Hexanes). Product was afforded as a colorless oil that crystallized to a white solid (5.61 g, 60%) upon scratching of the glass surface. Analytical data for 5-methyl-2,2-diphenylhex-4-en-1-ol matches literature data<sup>3</sup>: **<sup>1</sup>H NMR** (400 MHz, CDCl<sub>3</sub>) δ 7.33 – 7.15 (m, 10H), 4.84 (m, 1H), 4.11 (d, *J* = 6.9 Hz, 2H), 2.87 (d, *J* = 7.2 Hz, 2H), 1.59 (s, 3H), 1.53 (s, 3H), 1.17 (t, *J* = 6.9 Hz, 1H). **<sup>13</sup>C NMR** (101 MHz, CDCl<sub>3</sub>) δ 145.21, 134.23, 127.95, 127.77, 125.90, 119.44, 67.92, 51.91, 34.65, 25.63, 17.54. **MS** (+ESI) Calculated *m/z* for [M+H]<sup>+</sup> = 267.17, Found [M+H]=267.14. **IR** (Thin Film, cm<sup>-1</sup>) 3435, 3087, 3057, 3030, 2968, 2917, 2857, 1639, 1600, 1541, 1496, 1444, 1377, 1265, 1233 **R<sub>f</sub>** (15% EtOAc / 85% Hexanes): 0.35



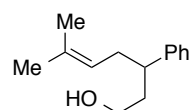
**6-methyl-3,3-diphenylhept-5-en-2-ol (C26).** A dry round bottom flask was charged with 5-methyl-2,2-diphenylhex-4-enal<sup>1</sup> (500 mg, 1.89 mmol, 1.0 equiv.), equipped with a stirbar, fitted with a septum, and

purged with a stream of nitrogen. The aldehyde was then dissolved in dry diethyl ether (10 mL), and methyl magnesium bromide (2.08 mmol, 1.1 equiv.) in diethyl ether was added as a 3.0 M solution in diethyl ether at 0 °C. The reaction was allowed to warm to room temperature, and stirred for thirty minutes. The reaction was quenched with saturated ammonium chloride, and the organics separated. The aqueous was extracted three times with diethyl ether, and the combined organics were washed with water and brine. The organics were dried over sodium sulfate, filtered, and concentrated to afford a crude oil. The material was further purified by flash column chromatography (15% EtOAc / 85% Hexanes), affording product as a colorless oil (475 mg, 90%). Analytical data for 6-methyl-3,3-diphenylhept-5-en-2-ol: **<sup>1</sup>H NMR** (400 MHz, CDCl<sub>3</sub>) δ 7.39 – 7.02 (m, 10H), 4.88 (t, *J* = 7.0 Hz, 1H), 4.69 – 4.59 (m, 1H), 3.12 – 2.57 (m, 2H), 1.57 (s, 3H), 1.46 (d, *J* = 8.0 Hz, 1H), 1.41 (s, 3H), 1.04 (d, *J* = 6.3 Hz, 3H). **<sup>13</sup>C NMR** (101 MHz, CDCl<sub>3</sub>) δ 144.16, 143.42, 133.82, 129.42, 129.27, 127.29, 127.15, 125.80, 125.73, 119.48, 69.73, 56.01, 36.19, 25.61, 18.74, 17.39. **MS** (+ESI) Calculated *m/z* for [2M+H]<sup>+</sup> = 560.36, Found *m/z* for [2M+H]<sup>+</sup> = 561.40. **IR** (Thin Film, cm<sup>-1</sup>): 3464, 3088, 3055, 2983, 2916, 2858, 1669, 1600, 1496, 1444, 1377, 1265. **R<sub>f</sub>** (15% EtOAc / 85% Hexanes): 0.40

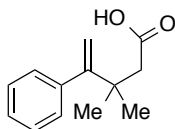


**(*E*)-6-((*tert*-butyldimethylsilyl)oxy)-5-methyl-2,2-diphenylhex-4-en-1-ol (C28).** A solution of (*E*)-5-((*tert*-butyldimethylsilyl)oxy)-2,2-diphenylhex-4-en-1-yl acetate<sup>1</sup> in methanol was stirred with potassium carbonate for four hours. The reaction mixture was concentrated, triturated with 10% Ethyl Acetate / 90% Hexanes, and purified by flash column chromatography (10% EtOAc / 90 % hexanes). Upon discovery of a co-eluting impurity, the material was further purified by flash column chromatography (5% Acetone / 95% Hexanes) to give product as a colorless oil. Impure fractions were retained for later purification. Yield, 89 mg (0.323 mmol, 32%). Analytical data for (*E*)-6-((*tert*-butyldimethylsilyl)oxy)-5-methyl-2,2-diphenylhex-4-en-1-ol: **<sup>1</sup>H NMR** (400 MHz, CDCl<sub>3</sub>) δ 7.38 – 7.16 (m, 10H), 5.17 (t, *J* = 7.1

Hz, 1H), 4.15 (d,  $J = 6.6$  Hz, 2H), 3.93 (s, 2H), 2.98 (d,  $J = 7.2$  Hz, 2H), 1.57 (s, 2H), 0.85 (s, 9H), -0.01 (s, 6H).  $^{13}\text{C}$  NMR (101 MHz,  $\text{CDCl}_3$ )  $\delta$  145.41, 137.20, 128.28, 128.20, 126.33, 119.28, 68.34, 68.10, 52.21, 34.43, 25.90, 18.31, 13.62, -5.40. **MS** (+ESI) Calculated  $m/z$  for  $[\text{M}+\text{H}]^+ = 397.25$ , Found  $m/z$  for  $[\text{M}+\text{H}]^+ = 397.30$ . **IR** (Thin Film,  $\text{cm}^{-1}$ ) 3446, 3088, 3058, 3030, 2954, 2928, 2884, 2856, 1642, 1601, 1496, 1471, 1462, 1444, 1361, 1304, 1253 **R<sub>f</sub>** (15% EtOAc / 85% Hexanes): 0.35

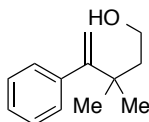


**6-methyl-3-phenylhept-5-en-1-ol (C22).** A dry roundbottom flask was equipped with a stirbar, charged with isopropyltriphenylphosphonium iodide (1.17 g, 2.70 mmol, 1.2 equiv.), fitted with a septum, and purged with a stream of nitrogen. The salt was dissolved in dry THF (10 mL), cooled to 0 °C, and a solution of 2.5 M *n*-Buli in hexanes (1.0 mL, 2.50 mmol, 1.1 equiv.) was added carefully. The reaction was stirred for 1 hour at 0 °C, then 4-phenyltetrahydro-2*H*-pyran-2-ol<sup>4</sup> (400 mg, 2.25 mmol) was added to the solution in 5 mL dry THF, and the reaction was allowed to warm to room temperature and was stirred overnight. The reaction was quenched with saturated ammonium chloride (10 mL), the organics were separated, and the aqueous was extracted with 3 X 10 mL portions of ether. The combined organics were washed with water (20 mL) and brine (20 mL), dried over sodium sulfate, and concentrated onto silica gel. The residue was dry loaded and purified by flash column chromatography (15% EtOAc/Hexanes) to afford 126 mg of product as a colorless oil (27%). Analytical data for 6-methyl-3-phenylhept-5-en-1-ol:  $^1\text{H}$  NMR (400 MHz,  $\text{CDCl}_3$ )  $\delta$  7.27 (t,  $J = 7.5$  Hz, 2H), 7.21 – 7.13 (m, 3H), 5.03 (t,  $J = 7.2$  Hz, 1H), 3.64 – 3.29 (m, 2H), 2.77 – 2.61 (m, 1H), 2.46 – 2.13 (m, 2H), 2.07 – 1.88 (m, 1H), 1.88 – 1.69 (m, 1H), 1.62 (s, 3H), 1.51 (s, 3H), 1.16 (brs, 1H).  $^{13}\text{C}$  NMR (101 MHz,  $\text{CDCl}_3$ )  $\delta$  144.92, 132.62, 128.21, 127.44, 125.99, 122.26, 61.13, 42.74, 38.28, 35.48, 25.59, 17.65. **MS** (+ESI) Calculated  $m/z$  for  $[\text{M}+\text{H}]^+ = 409.30$ , Found  $m/z$  for  $[\text{M}+\text{H}]^+ = 409.28$ . **IR** (Thin Film,  $\text{cm}^{-1}$ ) 3338, 3084, 3061, 3027, 2965, 2927, 2880, 1671, 1602, 1494, 1452, 1375, 1266. **R<sub>f</sub>** (15% EtOAc / 85% Hexanes): 0.25.



**3,3-dimethyl-4-phenylpent-4-enoic acid (D21).** A dry 500 mL round bottom flask equipped with a teflon coated stir bar was charged with 14.6 g (41 mmol, 1.2 equiv.) of methyltriphenylphosphonium bromide, 9.5 g (85 mmol, 2.5 equiv.) of potassium *tert*-butoxide, and 350 mL of anhydrous tetrahydrofuran followed by purging with nitrogen gas. Next, 7.0 g (34 mmol, 1.0 equiv.) of a mixture of 3,3-dimethyl-4-oxo-4-phenylbutanoic acid and its corresponding lactol were added to the solution in one portion. Upon the complete consumption of starting material (as indicated by thin-layer chromatography) the reaction was quenched with approximately 10 mL of deionized water. The solvent volume was reduced under vacuum to approximately 100 mL, and transferred into a 2 L separatory funnel, to which a further 300 mL of diethyl ether was added. The organic layer was washed with two 100 mL portions of deionized water and one 100 mL portion of brine. The organic layer was separated, dried over magnesium sulfate, and the solvent was removed under vacuum. The resulting oil was re-dissolved in 300 mL of dichloromethane, transferred to a 1 L separatory funnel, and treated with 400 mL of 3 M sodium hydroxide solution generating a white precipitate that aggregated at the interface of the aqueous and organic layers. The aqueous layer was removed with care, and the precipitate was collected over filter paper via Buchner funnel. The white precipitate was acidified, and extracted with diethyl ether, which after drying over magnesium sulfate, and removal of solvent under vacuum yielded 4.70 g (68%) of 3,3-dimethyl-4-phenylpent-4-enoic acid, which was carried on crude without further purification. **<sup>1</sup>H NMR** (600 MHz, Chloroform-*d*)  $\delta$  7.33 - 7.27 (m, 3H), 7.24 - 7.20 (m, 2H), 5.26 (s, 1H), 4.91 (s, 1H), 2.47 (s, 2H), 1.29 (s, 6H). **<sup>13</sup>C NMR** (151 MHz, CDCl<sub>3</sub>)  $\delta$  178.43, 156.54, 142.36, 129.14, 127.51, 126.63, 113.71, 45.40, 38.46, 27.69. . **MS** (+ESI) Calculated  $m/z$  for [M+H]<sup>+</sup> = 204.12, Found  $m/z$  for [M+H]<sup>+</sup> = 205.16. **IR** (Thin Film, cm<sup>-1</sup>) 3074, 2971, 2694, 2692, 1707, 1627, 1600, 1492, 1410 **R<sub>f</sub>** (30% EtOAc / 85% Hexanes): 0.35.

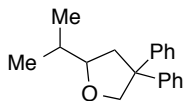




**3,3-dimethyl-4-phenylpent-4-en-1-ol (C32).** A clean, dry 100 mL round bottom flask equipped with a Teflon coated stir bar was charged with 280 mg (7.3 mmol, 1.0 equiv.) of lithium aluminum hydride, followed by 50 mL of anhydrous tetrahydrofuran, and purged with nitrogen gas. The flask was lowered into an ice bath, and stirring was begun. Then, a solution of 1.5 g (7.3 mmol, 1.0 equiv.) of 3,3-dimethyl-4-phenylpent-4-enoic acid in 5 mL anhydrous tetrahydrofuran was added to the mixture dropwise. The reaction was left to stir and come to room temperature. Upon complete consumption of 3,3-dimethyl-4-phenylpent-4-enoic acid (as indicated by thin-layer chromatography), the solution was cooled back down to 0° C, and 0.3 mL of deionized water was added dropwise to the solution. This was followed by dropwise addition of 0.6 mL of a 1 M sodium hydroxide solution, and then a further 1 mL of deionized water by dropwise addition. The mixture was left to stir for ten minutes. The reaction mixture was filtered through a pad of celite and rinsed with 150 mL of diethyl ether. The collected organics were dried over magnesium sulfate, filtered through filter paper, and the solvent was removed under vacuum to yield an oil. The oil was then purified by flash chromatography (hexanes:ethyl acetate 90:10), yielding 553 mg (40%). Analytical data for 3,3-dimethyl-4-phenylpent-4-en-1-ol:  $^1\text{H NMR}$  (400 MHz,  $\text{CDCl}_3$ )  $\delta$  7.29 – 7.20 (m, 3H), 7.16 – 7.09 (m, 2H), 5.16 (s, 1H), 4.86 (s, 1H), 3.71 (t,  $J = 7.5$  Hz, 2H), 1.68 (t,  $J = 7.5$  Hz, 2H), 1.57 (brs, 1H), 1.10 (s, 6H).  $^{13}\text{C NMR}$  (101 MHz,  $\text{CDCl}_3$ )  $\delta$  157.84, 142.90, 128.79, 127.45, 126.47, 113.57, 60.12, 43.13, 38.11, 27.99. **MS** (+ESI) Calculated  $m/z$  for  $[2\text{M}+\text{H}]^+ = 381.28$ , Found  $m/z$  for  $[\text{M}+\text{H}]^+ = 381.28$ . **IR** (Thin Film,  $\text{cm}^{-1}$ ) 3349, 3081, 3054, 3029, 2967, 1626, 1599, 1574, 1491, 1476, 1458, 1441, 1381, 1362, 1266, 1223 **R<sub>f</sub>** (15% EtOAc / 85% Hexanes): 0.20.

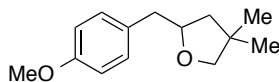
### A1.3. Anti-Markovnikov Hydroetherification Reactions Using 2-Phenylmalononitrile

**General Procedure B.** To a flame-dried vial equipped with a magnetic stir bar was added the alkene-ol (1.0 equiv.), 2-phenylmalononitrile (0.5 equiv.), and 9-mesityl-10-methylacridinium perchlorate<sup>1</sup> (0.05 equiv.). The mixture was diluted with anhydrous 1,2-dichloroethane to a concentration of 0.5 M with respect to substrate, then sealed with a septum screwcap and Teflon tape. The reaction was then degassed by the freeze pump thaw method using an inlet needle attached to a Schlenk manifold, and the needle removed. The reaction was irradiated with a 450 nm bulb and stirred the indicated time period, initially bleaching to form colorless solutions that evolved an amber color upon reaction progression. The reaction was monitored by TLC, with aliquots removed by a small gauge needle purged with nitrogen. Upon completion, the reaction was eluted through a short plug of silica with DCM (20 mL). The eluent was washed with 10 mL 0.1 M NaOH, and the aqueous back extracted with three portions of DCM. The combined organics were dried over sodium sulfate, concentrated, and further purified by flash column chromatography with 2.5 – 5% ether/pentane as eluent mixture.

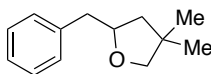


**2-isopropyl-4,4-diphenyltetrahydrofuran (C11).** The heterocycle was prepared according to General Procedure **B** Using 1.00 g of 5-methyl-2,2-diphenylhex-4-en-1-ol, 267 mg of 2-phenylmalononitrile, and 77.4 mg of 9-mesityl-10-methylacridinium perchlorate. A 25 mL-schlenk flask was used as the reaction vessel. Reaction time was 192 hours. Yield was 772 mg of viscous oil (77%). Reaction time was 192 hours. Analytical data for 2-isopropyl-4,4-diphenyltetrahydrofuran: <sup>1</sup>H NMR (400 MHz, CDCl<sub>3</sub>) δ 7.36 – 7.13 (m, 10H), 4.65 (d, J = 8.7 Hz, 1H), 4.06 (d, J = 8.7 Hz, 1H), 3.71 (ddd, J = 9.9, 7.3, 5.8 Hz, 1H), 2.53 (dd, J = 12.1, 5.7 Hz, 1H), 2.33 (dd, J = 12.1, 10.0 Hz, 1H), 1.98 – 1.66 (m, 1H), 0.98 (d, J = 6.6 Hz, 3H), 0.88 (d, J = 6.8 Hz, 3H). <sup>13</sup>C NMR (101 MHz, CDCl<sub>3</sub>) δ 146.10, 145.79, 128.04, 127.94, 126.83, 126.80, 126.03, 125.81, 83.81, 55.66, 42.12, 33.17, 18.92, 18.04. It is believed that one carbon signal is

coincidental with the residual solvent peak. **MS** (+ESI) Calculated  $m/z$  for  $[2M+H]^+ = 533.34$ , Found  $m/z$  for  $[M+H]^+ = 533.35$ . **IR** (Thin Film,  $\text{cm}^{-1}$ ): 3059, 3026, 2958, 2870, 1599, 1495, 1446, 1385, 1253 **R<sub>f</sub>** (15% EtOAc / 85% Hexanes): 0.55.

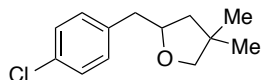


**2-(4-methoxybenzyl)-4,4-dimethyltetrahydrofuran (C13).** The heterocycle was prepared according to General Procedure **B** using 100 mg of (*E*)-5-(4-methoxyphenyl)-2,2-dimethylpent-4-en-1-ol, 32 mg of 2-phenylmalononitrile, and 9.3 mg of 9-mesityl-10-methylacridinium perchlorate. Reaction time was 48 hours. Yield was 83 mg of desired anti-Markovnikov adduct as a viscous oil. (83%). Analytical data for 2-(4-methoxybenzyl)-4,4-dimethyltetrahydrofuran: **<sup>1</sup>H NMR** (400 MHz,  $\text{CDCl}_3$ )  $\delta$  7.13 (d,  $J = 8.6$  Hz, 2H), 6.82 (d,  $J = 8.6$  Hz, 2H), 4.18 (dddd,  $J = 9.0, 6.5$  Hz, 1H), 3.76 (s, 3H), 3.52 (d,  $J = 8.1$  Hz, 1H), 3.44 (d,  $J = 8.1$  Hz, 1H), 2.88 (dd,  $J = 13.6, 6.6$  Hz, 1H), 2.68 (dd,  $J = 13.6, 6.4$  Hz, 1H), 1.70 (dd,  $J = 12.2, 6.4$  Hz, 1H), 1.41 (dddd,  $J = 12.2, 9.0$  Hz, 1H), 1.07 (s, 3H), 1.05 (s, 3H). **<sup>13</sup>C NMR** (101 MHz,  $\text{CDCl}_3$ )  $\delta$  157.71, 130.66, 129.74, 113.40, 79.95, 79.78, 54.84, 46.16, 41.25, 39.21, 26.54, 26.21. **MS** (+ESI) Calculated  $m/z$  for  $[M+H]^+ = 221.15$ , Found  $m/z$  for  $[M+H]^+ = 221.15$ . **IR** (Thin Film,  $\text{cm}^{-1}$ ): 2955, 2866, 1612, 1513, 1464, 1368, 1300, 1281, 1247, 1201 **R<sub>f</sub>** (15% EtOAc / 85% Hexanes): 0.40.

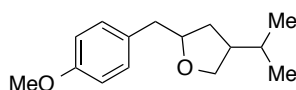


**2-benzyl-4,4-dimethyltetrahydrofuran (C15).** The heterocycle was prepared according to General Procedure **B** using 100 mg of (*E*)-2,2-dimethyl-5-phenylpent-4-en-1-ol, 37 mg of 2-phenylmalononitrile, and 11 mg of 9-mesityl-10-methylacridinium perchlorate. Reaction time was 72 hours. Yield was 64 mg of the desired anti-Markovnikov adduct as a viscous oil (64%). Analytical data for 2-benzyl-4,4-dimethyltetrahydrofuran: **<sup>1</sup>H NMR** (400 MHz,  $\text{CDCl}_3$ )  $\delta$  7.32-7.14 (m, 5H), 4.23 (dq,  $J = 9.0, 6.5$  Hz, 1H), 3.54 (d,  $J = 8.1$  Hz, 1H), 3.45 (d,  $J = 8.1$  Hz, 1H), 2.95 (dd,  $J = 13.5, 6.6$  Hz, 1H), 2.74 (dd,  $J = 13.5, 6.5$

Hz, 1H), 1.71 (dd,  $J = 12.3, 6.4$  Hz 1H), 1.43 (dd,  $J = 12.2, 9.0$  Hz, 1H), 1.08 (s, 3H), 1.05 (s, 3H).  $^{13}\text{C}$  NMR (101 MHz,  $\text{CDCl}_3$ )  $\delta$  138.58, 128.85, 127.95, 125.80, 79.81, 79.78, 46.25, 42.23, 39.24, 26.55, 26.22. MS (+ESI) Calculated  $m/z$  for  $[2\text{M}+\text{H}]^+ = 381.28$ , Found  $m/z$  for  $[2\text{M}+\text{H}]^+ = 381.28$ . IR (Thin Film,  $\text{cm}^{-1}$ ): 3089, 3062, 3028, 2956, 2867, 1604, 1496, 1454, 1307  $R_f$  (15% EtOAc / 85% Hexanes): 0.50.

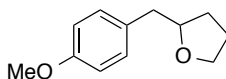


**2-(4-chlorobenzyl)-4,4-dimethyltetrahydrofuran (C17).** The heterocycle was prepared according to General Procedure B using 100 mg of (*E*)-5-(4-chlorophenyl)-2,2-dimethylpent-4-en-1-ol, 32 mg of 2-phenylmalononitrile, and 9.2 mg of 9-mesityl-10-methylacridinium perchlorate. Reaction time was 120 hours. Yield was 61 mg of the desired anti-Markovnikov adduct as a viscous oil. (61%). Analytical data for 2-(4-chlorobenzyl)-4,4-dimethyltetrahydrofuran:  $^1\text{H}$  NMR (400 MHz,  $\text{CDCl}_3$ )  $\delta$  7.20 (d,  $J = 8.5$  Hz, 2H), 7.11 (d,  $J = 8.4$  Hz, 2H), 4.15 (dddd,  $J = 9.0, 6.4$  Hz, 1H), 3.48 (d,  $J = 8.1$  Hz, 1H), 3.40 (d,  $J = 8.1$  Hz, 1H), 2.83 (dd,  $J = 13.7, 6.9$  Hz, 1H), 2.69 (dd,  $J = 13.7, 5.9$  Hz, 1H), 1.68 (dd,  $J = 12.2, 6.4$  Hz, 1H), 1.36 (dd,  $J = 12.3, 9.1$  Hz, 1H), 1.03 (s, 3H), 1.02 (s, 3H).  $^{13}\text{C}$  NMR  $\delta$  137.42, 131.98, 130.54, 128.38, 80.14, 79.79, 46.49, 41.77, 39.59, 26.80, 26.51. MS (+ESI) Calculated  $m/z$  for  $[\text{M}+\text{H}]^+ = 225.10$ , Found  $m/z$  for  $[\text{M}+\text{H}]^+ = 225.06$ . IR (Thin Film,  $\text{cm}^{-1}$ ): 2957, 2867, 1597, 1497, 1465, 1368, 1204  $R_f$  (15% EtOAc / 85% Hexanes): 0.50.

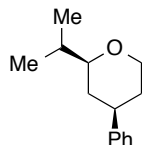


**4-isopropyl-2-(4-methoxybenzyl)tetrahydrofuran (C19).** The heterocycle was prepared according to General Procedure B using 100 mg of (*E*)-2-isopropyl-5-(4-methoxyphenyl)pent-4-en-1-ol, 30 mg of 2-phenylmalononitrile, and 8.8 mg of 9-mesityl-10-methylacridinium perchlorate. Reaction time was 72 hours. Yield was 81 mg of a mixture desired, inseparable diastereomeric anti-Markovnikov adducts as a viscous oil. (Yield: 81%). The identity of the major diastereomer could not be determined. Analytical

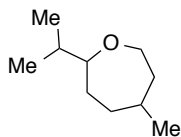
data for 4-isopropyl-2-(4-methoxybenzyl)tetrahydrofuran: **<sup>1</sup>H NMR (Major Diastereomer)** (400 MHz, CDCl<sub>3</sub>) δ 7.12 (d, *J* = 8.6 Hz, 2H), 6.82 (d, *J* = 8.5 Hz, 2H), 4.14 – 3.97 (m, 1H), 3.89 (t, *J* = 8.0 Hz, 1H), 3.77 (s, 3H), 3.49 (t, *J* = 8.3 Hz, 1H), 2.87 (dd, *J* = 13.6, 6.3 Hz, 1H), 2.68 (dd, *J* = 13.6, 6.6 Hz, 1H), 1.94 (m, 1H), 1.50 – 1.36 (m, 1H), 1.24 – 1.13 (m, 1H), 0.88 (d, *J* = 6.6 Hz, 3H), 0.84 (d, *J* = 6.6 Hz, 3H). **<sup>1</sup>H NMR (Minor Diastereomer)** (400 MHz, CDCl<sub>3</sub>) δ 7.12 (d, *J* = 8.6 Hz, 3H), 6.82 (d, *J* = 8.5 Hz, 3H), 4.14 – 3.97 (m, 2H), 3.77 (s, 3H), 3.33 (t, *J* = 8.7 Hz, 1H), 2.81 (dd, *J* = 13.7, 6.5 Hz, 1H), 2.63 (dd, *J* = 13.7, 6.7 Hz, 1H), 2.04 – 1.83 (m, 2H), 1.75 – 1.66 (m, 1H), 1.59 (m, 1H), 1.50 – 1.36 (m, 1H), 0.88 (d, *J* = 6.6 Hz, 3H), 0.84 (d, *J* = 6.6 Hz, 3H). **<sup>13</sup>C NMR (Mixture of Diastereomers)** δ 157.67, 130.69, 130.67, 129.76, 129.71, 113.40, 113.38, 80.79, 79.85, 72.14, 71.72, 54.85, 47.28, 45.94, 41.17, 40.84, 36.89, 35.07, 31.79, 31.36, 21.24, 21.12, 21.04. Multiple signals appear to be equivalent. **MS** (+ESI) Calculated *m/z* for [M+H]<sup>+</sup> = 235.16, Found *m/z* for [M+H]<sup>+</sup> = 235.12. **IR** (Thin Film, cm<sup>-1</sup>) 2957, 2869, 1612, 1513, 1465, 1368, 1300, 1247 **R<sub>f</sub>** (15% EtOAc / 85% Hexanes): 0.45.



**2-(4-methoxybenzyl)tetrahydrofuran (C21).** The heterocycle was prepared according to General Procedure **B** using 100 mg of (*E*)-5-(4-methoxyphenyl)pent-4-en-1-ol, 30 mg of 2-phenylmalononitrile, and 8.8 mg of 9-mesityl-10-methylacridinium perchlorate. Reaction time was 36 hours. Yield was 84 mg of the desired anti-Markovnikov adduct as a viscous oil. (84%). Analytical data for 2-(4-methoxybenzyl)tetrahydrofuran matches literature reports<sup>5</sup>: **<sup>1</sup>H NMR** (400 MHz, CDCl<sub>3</sub>) δ 7.13 (d, *J* = 8.6 Hz, 2H), 6.82 (d, *J* = 8.6 Hz, 2H), 4.07 – 3.95 (m, 1H), 3.90 – 3.84 (m, 1H), 3.76 (s, 3H), 3.75 – 3.66 (m, 1H), 2.84 (dd, *J* = 13.7, 6.4 Hz, 1H), 2.68 (dd, *J* = 13.7, 6.4 Hz, 1H), 1.95 – 1.75 (m, 3H), 1.59 – 1.47 (m, 1H). **<sup>13</sup>C NMR** (101 MHz, CDCl<sub>3</sub>) δ 157.92, 130.95, 129.97, 113.62, 80.07, 67.75, 55.06, 40.84, 30.76, 25.47. **MS** (+ESI) Calculated *m/z* for [2M+H]<sup>+</sup> = 385.30, Found *m/z* for [2M+H]<sup>+</sup> = 385.26. **IR** (Thin Film, cm<sup>-1</sup>): 2935, 2862, 1698, 1612, 1513, 1465, 1368, 1300, 1267 **R<sub>f</sub>** (15% EtOAc / 85% Hexanes): 0.30.

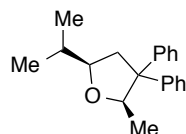


**cis-2-isopropyl-4-phenyltetrahydro-2H-pyran (C23).** The heterocycle was prepared according to a variation of General Procedure **B** using 25 mg of 3,3-dimethyl-4-phenylpent-4-en-1-ol, 35 mg of 2-phenylmalononitrile, and 2.5 mg of 9-mesityl,10-methylacridinium perchlorate. Reaction time was 72 hours. Yield was 18 mg of a 2.25:1 mixture of diastereomeric anti-Markovnikov adducts as a viscous oil (Yield: 72%). The diastereomers were found to be separable by flash column chromatography. Analytical data for 4,4-dimethyl-3-phenyltetrahydro-2H-pyran: **<sup>1</sup>H NMR (Major Diastereomer)** (400 MHz, CDCl<sub>3</sub>) δ 7.35 – 7.27 (m, 2H), 7.23 – 7.14 (m, 3H), 4.16 – 4.08 (m, 1H), 3.59 – 3.48 (m, 1H), 3.11 (ddd, J = 11.0, 6.2, 1.9 Hz, 1H), 2.83 – 2.62 (m, 1H), 1.86 – 1.79 (m, 1H), 1.78 – 1.65 (m, 3H), 1.47 – 1.35 (m, 1H), 0.95 (d, J = 6.8 Hz, 3H), 0.90 (d, J = 6.8 Hz, 3H). **<sup>13</sup>C NMR (Major Diastereomer)** (101 MHz, CDCl<sub>3</sub>) δ 146.17, 128.49, 126.79, 126.26, 82.93, 68.34, 41.99, 36.21, 33.60, 33.22, 18.67, 18.34. **MS (+ESI)** Calculated *m/z* for [M+H]<sup>+</sup> = 205.14, Found *m/z* for [M+H]<sup>+</sup> = 205.15 **IR** (Thin Film, cm<sup>-1</sup>) 2956, 2914, 2872, 2840, 1603, 1496, 1453, 1383, 1252. **R<sub>f</sub>**(15% EtOAc / 85% Hexanes): 0.45. **R<sub>f</sub>(Major Diastereomer)** (15% EtOAc / 85% Hexanes): 0.60 **R<sub>f</sub>(Minor Diastereomer)** (15% EtOAc / 85% Hexanes): 0.55 (diastereomeric spots overlap).



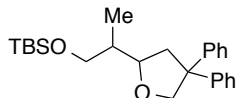
**2-isopropyl-5-methyloxepane (C25).** The heterocycle was prepared according to a variation of General Procedure **B** using 50 mg of β-citronellol, 91 mg of 2-phenylmalononitrile, and 6.6 mg of 9-mesityl-10-methylacridinium perchlorate, and DCM as solvent instead of DCE. Reaction time was 84 hours. No aqueous workup used. Due to volatility of product, the reaction was concentrated by careful distillation of solvent at atmospheric pressure, dissolved in minimal 5% ether / 95% pentane and chromatographed

with 5% ether / pentane. This compound does not visualize by TLC, thus all column fractions are pooled up to the point of elution of 2-phenylmalononitrile. The pooled fractions were concentrated by careful removal of solvent by distillation at ambient pressure to afford 22 mg of the desired product as an inseparable mixture of diastereomeric anti-Markovnikov adducts as a highly volatile oil. (Yield: 44%, *d.r.*: 1.2:1). Analytical data for 2-isopropyl-5-methyloxepane: **<sup>1</sup>H NMR (Major Diastereomer)** (400 MHz, CDCl<sub>3</sub>) δ 3.73-3.67 (m, 1H), 3.61-3.56 (m, 1H), 3.17-3.10 (m, 1H), 1.69-1.10 (m, 8H), 0.93-0.83 (m, 9H) **<sup>1</sup>H NMR (Minor Diastereomer)** (400 MHz, CDCl<sub>3</sub>) δ 3.98-3.93 (m, 1H), 3.37-3.30 (m, 1H), 3.17-3.10 (m, 1H), 1.69-1.10 (m, 8H), 0.93-0.83 (m, 9H) **<sup>13</sup>C NMR (Mixture of Diastereomers)** (400 MHz, CDCl<sub>3</sub>) δ 82.21, 81.13, 67.31, 62.58, 37.59, 35.95, 32.64, 31.08, 30.61, 30.44, 30.14, 30.12, 28.87, 26.86, 20.70, 20.33, 16.06, 15.89, 15.65, 15.59 **IR** (Thin Film, cm<sup>-1</sup>): 2954, 2926, 2870, 1456, 1379, 1272. **MS** (+ESI) Calculated *m/z* for [M+H]<sup>+</sup> = 157.15, found *m/z* 157.10. **R<sub>f</sub>**: Unknown (*R<sub>f</sub>* > 0.30).



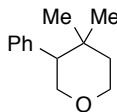
**5-isopropyl-2-methyl-3,3-diphenyltetrahydrofuran (C27).** The heterocycle was prepared according to a variation of General Procedure **B** using 100 mg of 6-methyl-3,3-diphenylhept-5-en-2-ol, 7.4 mg of 2-phenylmalononitrile, and 102 mg of 9-mesityl,10-methylacridinium perchlorate. Reaction time was 168 hours. Yield was 40 mg of the desired inseparable diastereomeric anti-Markovnikov adducts as a viscous oil (42% Yield, 5:1 *d.r.*, *cis*- product as major diastereomer as determined by NOESY analysis of the product). Analytical data for *cis*-5-isopropyl-2-methyl-3,3-diphenyltetrahydrofuran: **<sup>1</sup>H NMR** (400 MHz, CDCl<sub>3</sub>) δ 7.32 – 7.08 (m, 10H), 4.91 (q, *J* = 6.4 Hz, 1H), 3.50 (ddd, *J* = 10.5, 7.7, 5.5 Hz, 1H), 2.67 – 2.49 (m, 1H), 2.20 (dd, *J* = 12.0, 5.4 Hz, 1H), 1.77 (dq, *J* = 13.6, 6.8 Hz, 1H), 1.00 (d, *J* = 6.6 Hz, 3H), 0.88 (d, *J* = 6.8 Hz, 3H), 0.86 (d, *J* = 6.4 Hz, 3H). **<sup>13</sup>C NMR** δ 148.26, 145.51, 128.45, 128.07, 128.02, 127.81, 126.18, 125.95, 82.99, 80.11, 58.86, 40.73, 34.24, 21.12, 19.72, 18.71. **MS** (+ESI) Calculated *m/z* for

$[2M+H]^+ = 561.36$ , Found  $m/z$  for  $[2M+H]^+ = 561.40$ . **IR** (Thin Film,  $\text{cm}^{-1}$ ): 3058, 3025, 2959, 2931, 2870, 1599, 1494, 1445, 1384 **R<sub>f</sub>** (15% EtOAc / 85% Hexanes): 0.60.



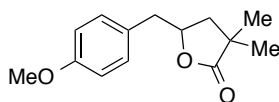
**tert-butyl(2-(4,4-diphenyltetrahydrofuran-2-yl)propoxy)dimethylsilane (C29).** The heterocycle was prepared according to a variation of General Procedure **B** using 75 mg of 6-methyl-3,3-diphenylhept-5-en-2-ol, 54 mg of 2-phenylmalononitrile, and 3.9 mg of 9-mesityl,10-methylacridinium perchlorate. Reaction time was 144 hours. No aqueous workup was used. Instead, the reaction was concentrated, triturated with minimal 2.5% ether / 97.5% pentane, then chromatographed. Yield was 31 mg of desired inseparable, diastereomeric anti-Markovnikov adducts as a viscous oil. (41%). Analytical data for *tert*-butyl(2-(4,4-diphenyltetrahydrofuran-2-yl)propoxy)dimethylsilane: **<sup>1</sup>H NMR (Major diastereomer)** (600 MHz,  $\text{CDCl}_3$ )  $\delta$  7.31 – 7.13 (m, 10H), 4.61 (d,  $J = 8.6$  Hz, 1H), 4.03 (d,  $J = 8.7$  Hz, 1H), 3.87 – 3.79 (m, 1H), 3.73 (dd,  $J = 9.8, 4.3$  Hz, 1H), 3.45 (dd,  $J = 9.7, 7.0$  Hz, 1H), 2.48 – 2.43 (m, 1H), 2.36 (dd,  $J = 11.8, 10.4$  Hz, 1H), 1.86 – 1.79 (m, 1H), 0.87 (d,  $J = 6.8$  Hz, 3H), 0.84 (s, 9H), -0.00 (s, 6H). **<sup>1</sup>H NMR (Minor diastereomer)** (600 MHz,  $\text{CDCl}_3$ )  $\delta$  7.31 – 7.13 (m, 10H), 4.62 (d,  $J = 8.6$  Hz, 1H), 4.00 (d,  $J = 8.6$  Hz, 1H), 3.94 – 3.89 (m, 1H), 3.53 (dd,  $J = 9.9, 6.1$  Hz, 1H), 3.48 (dd,  $J = 9.8, 6.2$  Hz, 1H), 2.51 (m, 2H), 1.79 – 1.73 (m, 1H), 0.95 (d,  $J = 6.7$  Hz, 3H), 0.84 (s, 9H), 0.01 – -0.02 (m, 6H). **<sup>13</sup>C NMR (Mixture of diastereomers)** (151 MHz,  $\text{CDCl}_3$ )  $\delta$  146.12, 145.88, 128.16, 128.03, 126.96, 126.91, 126.89, 126.16, 125.93, 125.90, 79.95, 79.88, 65.52, 65.24, 55.73, 55.59, 42.34, 41.10, 40.51, 25.70, 25.68, 18.07, 12.69, 12.53, -5.62, -5.64, -5.67. Several peaks appear coincidental. **IR** (Thin Film,  $\text{cm}^{-1}$ ): 3059, 2955, 2930, 1693, 1605, 1513, 1441, 1281, 1250, 1208 **MS** (+ESI) Calculated  $m/z$  for  $[M+H]^+ = 397.25$ , Found  $m/z$  for  $[M+H]^+ = 397.30$ . **R<sub>f</sub>** (15% EtOAc / 85% Hexanes): 0.55





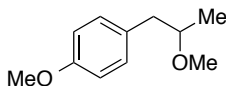
**4,4-dimethyl-3-phenyltetrahydro-2H-pyran (C31).** The heterocycle was prepared according to General Procedure **B** using 100 mg of 3,3-dimethyl-4-phenylpent-4-en-1-ol, 37 mg of 2-phenylmalononitrile, and 10.8 mg of 9-mesityl-10-methylacridinium perchlorate. Reaction time was 72 hours. Yield was 76 mg of the desired anti-Markovnikov adduct as a viscous oil. (Yield: 76%). Analytical data for 4,4-dimethyl-3-phenyltetrahydro-2H-pyran:  $^1\text{H}$  NMR (400 MHz,  $\text{CDCl}_3$ )  $\delta$  7.30 – 7.18 (m, 3H), 7.13 – 7.06 (m, 2H), 3.93 – 3.68 (m, 4H), 2.67 (dd,  $J$  = 11.3, 4.2 Hz, 1H), 1.72 – 1.62 (m, 1H), 1.39 (dt,  $J$  = 13.6, 2.3 Hz, 1H), 0.90 (s, 3H), 0.88 (s, 3H).  $^{13}\text{C}$  NMR (101 MHz,  $\text{CDCl}_3$ )  $\delta$  139.23, 129.03, 127.44, 126.18, 67.25, 64.32, 52.25, 40.20, 32.09, 30.13, 19.72. **MS** (+ESI) Calculated  $m/z$  for  $[\text{M}+\text{H}]^+ = 191.14$ , Found  $[\text{M}+\text{H}] = 191.11$ . **IR** (Thin Film,  $\text{cm}^{-1}$ ): 3027, 2958, 2855, 1601, 1494, 1452, 1389, 1365, 1221. **R<sub>f</sub>** (15% EtOAc / 85% Hexanes): 0.45.

#### A1.4. Other Anti-Markovnikov Hydrofunctionalizations Using 2-Phenylmalononitrile



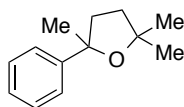
**5-(4-methoxybenzyl)dihydrofuran-2(3H)-one (C34).** The heterocycle was prepared according to a variation of General Procedure **B** using 100 mg of **10**, 30 mg of 2-phenylmalononitrile, 8.8 mg of 9-mesityl-10-methylacridinium perchlorate and 5.0  $\mu\text{L}$  of 2,6-lutidine (0.1 equiv). Initial reaction is heterogeneous, with substrate dissolving into solution with time. Reaction time was 96 hours. The reaction was concentrated, triturated with 30% EtOAc / hexanes and chromatographed with 30% EtOAc / hexanes, with no aqueous workup used. Yield was 72 mg of desired anti-Markovnikov adduct as a viscous oil. Analytical data for 2-isopropyl-5-methyloxepane matches previous literature reports<sup>6</sup>:  $^1\text{H}$  NMR (400 MHz,  $\text{CDCl}_3$ )  $\delta$  7.11 (d,  $J$  = 8.6 Hz, 2H), 6.81 (d,  $J$  = 8.7 Hz, 2H), 4.71 – 4.59 (m, 1H), 3.75 (s, 3H), 2.95 (dd,  $J$  = 14.1, 6.0 Hz, 1H), 2.84 (dd,  $J$  = 14.1, 6.1 Hz, 1H), 2.48 – 2.13 (m, 3H), 1.97 – 1.82 (m,

1H).  $^{13}\text{C}$  NMR (400 MHz,  $\text{CDCl}_3$ ):  $\delta$  176.70, 158.15, 130.03, 127.40, 113.58, 80.53, 54.79, 39.91, 28.20, 26.51. IR (Thin Film,  $\text{cm}^{-1}$ ): 2937, 2837, 1772, 1612, 1514, 1462, 1354, 1249. MS (+ESI) Calculated  $m/z$  for  $[\text{M}+\text{H}]^+ = 207.09$ , Found  $m/z$  for  $[\text{M}+\text{H}]^+ = 207.10$ .  $R_f$  (15% EtOAc / 85% Hexanes): 0.1.



**1-methoxy-4-(2-methoxypropyl)benzene (C36).** The ether was prepared according to a variation of General Procedure B. The reaction was assembled in a glovebox rather than with freeze-pump-thaw cycles, and was carried out using 50 mg of distilled *trans*-anethole, 96 mg of 2-phenylmalononitrile, and 7.0 mg of 9-mesityl-10-methylacridinium perchlorate, with 136 L of MeOH included along with the 0.7 mL of DCE solvent. Reaction time was 96 hours. The reaction was concentrated under a gentle stream of air, with no aqueous workup used. The crude product was purified by flash chromatography on silica gel, using 2.5% diethyl ether/ 97.5% pentane as eluent mixture. Yield was 51 mg of desired anti-Markovnikov adduct as a colorless oil (84%). Analytical data for 1-methoxy-4-(2-methoxypropyl)benzene:  $^1\text{H}$  NMR (400 MHz,  $\text{CDCl}_3$ )  $\delta$  7.11 (d,  $J = 8.7$  Hz, 2H), 6.82 (d,  $J = 8.7$  Hz, 2H), 3.78 (s, 3H), 3.49 – 3.43 (m, 1H), 3.33 (s, 3H), 2.84 (dd,  $J = 13.7, 5.9$  Hz, 1H), 2.53 (dd,  $J = 13.7, 6.8$  Hz, 1H), 1.10 (d,  $J = 6.1$  Hz, 3H).  $^{13}\text{C}$  NMR (400 MHz,  $\text{CDCl}_3$ ):  $\delta$  158.00, 131.06, 130.01, 113.67, 78.21, 56.26, 55.22, 41.77, 18.82. IR (Thin Film,  $\text{cm}^{-1}$ ): 2971, 2930, 2833, 1613, 1583, 1512, 1463, 1375, 1300, 1247. MS (+ESI) Calculated  $m/z$  for  $[\text{M}+\text{H}]^+ = 180.12$ , Found  $m/z$  for  $[\text{M}+\text{H}]^+ = 180.96$ .  $R_f$  (15% EtOAc / 85% Hexanes): 0.45.

#### A1.5. Markovnikov-Selective Hydroetherification Reaction Catalyzed by Triflic Acid



**2,3,3-trimethyl-2-phenyltetrahydrofuran (C32).** To a flame-dried vial equipped with a stirbar was added 50 mg 3,3-dimethyl-4-phenylpent-4-en-1-ol, covered with a septum cap and purged with nitrogen.

2 mL dry DCM was added, and a single drop of TfOH was added under a stream of nitrogen. The reaction was allowed to stir for 3 h, at which time the reaction was judged complete by TLC. The reaction was quenched with saturated sodium bicarbonate (1 mL), and the organics separated. The aqueous was extracted with two portions of 2 mL DCM, then the combined organics were diluted twofold with DCM, dried over sodium sulfate, filtered and concentrated to afford oil. Material was further purified by elution through a plug of silica gel eluting with DCM. Product was isolated as 42 mg of colorless oil (84%). Analytical data for 2,3,3-trimethyl-2-phenyltetrahydrofuran:  $^1\text{H}$  NMR (400 MHz,  $\text{CDCl}_3$ ):  $\delta$  7.37 (d,  $J = 7.2$  Hz, 2H), 7.28 (t,  $J = 7.2$  Hz, 2H), 7.19 (t,  $J = 7.2$  Hz, 1H), 4.16-3.91 (m, 2H), 2.11-1.90 (m, 1H) (dd,  $J = 14$  Hz,  $J = 6.8$  Hz, 1H), 1.85-1.68 (m, 1H), 1.44 (s, 3H), 1.17 (s, 3H), 0.59 (s, 3H)  $^{13}\text{C}$  NMR (400 MHz,  $\text{CDCl}_3$ ):  $\delta$  145.6, 127.6, 126.2, 125.3, 87.3, 64.3, 43.8, 40.6, 25.7, 24.3, 23.7. IR (Thin Film,  $\text{cm}^{-1}$ ): 3057, 3024, 2972, 2874, 1602, 1493, 1467, 1445, 1387, 1371, 1275. MS (+ESI) Calculated  $m/z$  for  $[\text{M}+\text{H}]^+ = 191.14$ , found  $m/z$  191.09;  $\text{R}_f$  (15% EtOAc / 85% Hexanes): 0.60.

#### A1.6. Method for Kinetic Trials

9-Cyanofluorene was deuterated by multiple recrystallizations from 3:1  $\text{D}_2\text{O}$ /Acetone (99.9%). The material was judged to be 96% deuterated by  $^1\text{H}$  NMR analysis.

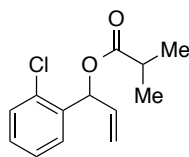
Kinetic trials were carried out in their entirety in a glovebox. Each reaction was assembled with alkenol **C1** (66 mg, 0.25 mmol), 9-cyanofluorene or its deuterated counterpart (96 mg for 9-CN-FI, 96.5 mg for 9-CN-FI( $d_1$ ), 0.50 mmol), and 1,4-cyclohexanedione (28.0 mg, 0.25 mmol) used as a  $^1\text{H}$  NMR standard. Each reaction was diluted with 0.5 mL 1,2-dichloroethane, and the vials were irradiated side-by-side, with stirring, with the light passing through the plexiglass pane of the box. At given timepoints, aliquots (10 microliters) were removed and added to 500 microliter HPLC vials, then diluted with 500 microliters of  $\text{CDCl}_3$ . Yields were determined by analysis of each sample by  $^1\text{H}$  NMR vs. the cyclohexanedione internal standard.

### A1.7. Synthesis of Alkenoic Acids.

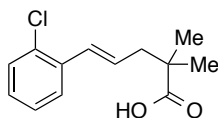
Alkenoic acids (**D1**, **D3**, **D5**, **D7**, **D11**, **D17**, **D19**) were prepared as detailed above.

Alkenoic acids (**D9**<sup>7</sup>, **D21**<sup>8</sup>) were prepared according to literature precedent, and characterization matches published data.

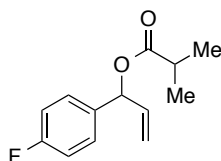
**General Procedure A.** A 250 mL round bottom flask equipped with a stirbar was charged with the aldehyde, fitted with a septum, and purged with nitrogen. Dry THF (100 mL) was added, and the solution was cooled to 0 °C. A solution of 1.0 M vinyl magnesium bromide (1.1 equiv.) was added to the reaction dropwise. The reaction was allowed to warm to room temperature, and was stirred for an additional hour. After confirming consumption of starting material by TLC, the appropriate electrophile (isobutyryl chloride, acetic anhydride, or isovaleryl chloride, 1.2-1.5 equiv.) was added to the reaction carefully. After 30 minutes, the reaction was quenched with saturated ammonium chloride (50 mL), and the organics separated. The aqueous was extracted with 3 X 50 mL portions of diethyl ether in a separatory funnel, then the combined organics were washed with brine, dried, filtered, and concentrated to afford crude oil, which was further purified by flash chromatography.



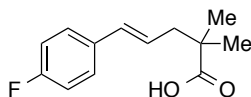
**1-(4-chlorophenyl)allyl isobutyrate.** The title compound was prepared according to General Procedure A, using 2.81 g *o*-chlorobenzaldehyde (20.0 mmol, 1.0 equiv.) dissolved in 50 mL THF, 22.0 mL 1.0 M vinylmagnesium bromide in THF (22.0 mmol, 1.1 equiv.), and 2.51 mL isobutyryl chloride (24.0 mmol, 1.2 equiv.) as electrophile. Intermediate was chromatographed with 5% EtOAc/Hexanes to product as an oil with minor impurities and carried forward without further purification. Yield was 9.11g (41 mmol, 90%).



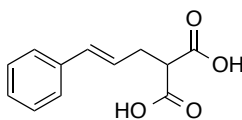
**(*E*)-5-(2-chlorophenyl)-2,2-dimethylpent-4-enoic acid (D7).** The  $\gamma,\delta$  unsaturated acid was prepared according to General Procedure **B** as described in **A1.2.**, using 4.07 g (17.0 mmol, 1.0 equiv.) 1-(4-chlorophenyl)allyl isobutyrate, 10.7 mL hexamethyldisilazane (3.3 equiv, 51.0 mmol), 20.4 mL 2.5 M *n*-BuLi (51.0 mmol, 3.0 equiv.), and 7.1 mL TMSCl (135.3 mmol, 3.3 equiv.). Reaction was stirred at room temperature overnight instead of the typical period. Product was isolated by recrystallization of oil from hexanes. Yield was 2.81 g (11.8 mmol, 69%). Analytical data for (*E*)-5-(2-chlorophenyl)-2,2-dimethylpent-4-enoic acid:  $^1\text{H NMR}$  (600 MHz, Chloroform-*d*)  $\delta$  7.49 (d,  $J = 7.7$  Hz, 1H), 7.32 (d,  $J = 7.9$  Hz, 1H), 7.20 (t,  $J = 7.5$  Hz, 1H), 7.15 (t,  $J = 7.6$  Hz, 1H), 6.81 (d,  $J = 15.6$  Hz, 1H), 6.22 - 6.11 (m, 1H), 2.51 (d,  $J = 7.5$  Hz, 2H), 1.27 (s, 6H).  $^{13}\text{C NMR}$  (151 MHz,  $\text{CDCl}_3$ )  $\delta$  183.65, 135.59, 132.68, 129.76, 129.53, 128.74, 128.22, 126.94, 126.75, 43.58, 42.61, 24.79. **MS** (+ESI) Calculated  $m/z$  for  $[\text{M}+\text{Na}]^+ = 499.15$ , found  $m/z = 499.19$ . **IR** (Thin Film,  $\text{cm}^{-1}$ ): 3060, 2981, 2657, 1700, 1471, 1441. **R<sub>f</sub>** (30% EtOAc / Hexanes) = 0.40



**1-(4-fluorophenyl)allyl isobutyrate.** The title compound was prepared according to General Procedure **A** found in **A1.2**, using 5.63 g *p*-Fluorobenzaldehyde (45.4 mmol, 1.0 equiv.) dissolved in 200 mL THF, 50 mL 1.0M vinylmagnesium bromide in THF (50.0 mmol, 1.1 equiv.), and 5.7 mL isobutyryl chloride (54.48 mmol, 1.2 equiv.) as electrophile. Intermediate was chromatographed with 5% EtOAc/Hexanes to product as an oil with minor impurities product as an oil with minor impurities and carried forward without further purification. Yield: 9.11g (41 mmol, 90%).



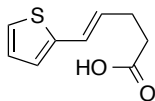
**(E)-5-(4-fluorophenyl)-2,2-dimethylpent-4-enoic acid (D9).** The  $\gamma,\delta$  unsaturated acid was prepared according to General Procedure **B** as described in **A1.2**, using 9.11 g (41.0 mmol, 1.0 equiv.) 1-(4-fluorophenyl)allyl isobutyrate, 28.36 mL hexamethyldisilazane (3.3 equiv, 135.3 mmol), 49.2 mL 2.5M *n*-BuLi (123 mmol, 3.0 equiv.), and 17.17 mL TMSCl (135.3 mmol, 3.3 equiv.). Product was isolated by recrystallization of oil from hexanes. Yield, 1.62 g (white solid, 18%). Analytical data for (E)-5-(4-fluorophenyl)-2,2-dimethylpent-4-enoic acid:  $^1\text{H NMR}$  (600 MHz, Chloroform-*d*)  $\delta$  7.30 (dd,  $J = 8.6, 5.5$  Hz, 2H), 6.98 (t,  $J = 8.7$  Hz, 2H), 6.39 (d,  $J = 15.7$  Hz, 1H), 6.09 (dt,  $J = 15.4, 7.5$  Hz, 1H), 2.45 (d,  $J = 8.5$  Hz, 2H), 1.25 (s, 6H).  $^{13}\text{C NMR}$  (151 MHz,  $\text{CDCl}_3$ )  $\delta$  183.95, 162.89, 161.26, 133.51, 133.49, 132.14, 127.62, 127.57, 125.36, 125.34, 115.40, 115.26, 43.44, 42.56, 24.75. **IR** (Thin Film,  $\text{cm}^{-1}$ ): 3060, 2976, 1698, 1652, 1636, 1602, 1508, 1473, 1416. **MS** (+ESI) Calculated  $m/z$  for  $[\text{M}+\text{Na}]^+ = 245.10$ , found  $m/z$  245.13. **R<sub>f</sub>** (30% EtOAc / 70% Hexanes): 0.30.



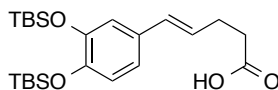
**2-cinnamylmalonic acid (D23).** A round-bottomed flask was charged with a 60% sodium hydride suspension in mineral oil (3.44 g, 86.0 mmol), and the base was washed with minimal hexanes three times. The material was suspended in 200 mL anhydrous THF, and cooled to 0 °C. Diethyl malonate was added dropwise, and the reaction was stirred at 0 °C for 15 minutes. Cinnamyl bromide (16.94 g, 86.0 mmol) dissolved in 50 mL anhydrous THF, was then added by cannula addition carefully at 0 °C over the course of 15 minutes. The reaction was warmed to room temperature, and stirred for an additional 2 hr. The reaction was then quenched with saturated ammonium chloride (100 mL), the organics were separated, and the aqueous layer was extracted with three portions of diethyl ether. The combined organics were washed with water and brine in succession, then the organics were dried, filtered and concentrated to

afford an oil. The oil was subjected to hydrolysis for 15 hours with 10 equivalents of KOH (4.38 g) in 1:1 MeOH/H<sub>2</sub>O (100 mL). The mixture was extracted with three portions of diethyl ether (50 mL), then acidified to pH=1 with concentrated HCl. The mixture was then extracted with EtOAc (3 x 50 mL), and the extracts were washed with 1M HCl and brine. The organics were dried over sodium sulfate, filtered, and concentrated to yield the title compound as a white powder (9.02 g, 52%) **<sup>1</sup>H NMR** (600 MHz, Chloroform-*d*)  $\delta$  7.34 (d, *J* = 7.0 Hz, 2H), 7.30 (t, *J* = 7.7 Hz, 2H), 7.23 (t, *J* = 7.2 Hz, 1H), 6.60 ? 6.47 (m, 1H), 6.16 (dt, *J* = 15.7, 7.2 Hz, 1H), 3.62 (t, *J* = 7.2 Hz, 1H), 2.87 (td, *J* = 7.2, 1.4 Hz, 2H). **<sup>13</sup>C NMR** (151 MHz, CDCl<sub>3</sub>)  $\delta$  172.32, 136.69, 133.66, 128.55, 127.63, 126.29, 124.26, 50.82, 32.24. **IR** (Thin Film, cm<sup>-1</sup>, MeCN as blank): 3214, 3151, 1758. **MS** (+ESI) Calculated *m/z* for [M+Na]<sup>+</sup> = 243.06, found *m/z* 243.14. **R<sub>f</sub>** (30% EtOAc / 70% Hexanes): 0.05.

**General Procedure D:** Alkenoic acids were prepared by suspension of (3-carboxypropyl)triphenylphosphonium chloride<sup>9</sup> (1.0 equiv.) in tetrahydrofuran (solvent to assume 0.25 M concentration of wittig salt), in a roundbottom flask equipped with a large magnetic stirbar. The reaction was cooled to 0 °C, and potassium *t*-butoxide (1.0 equiv.) was added in one portion, evolving a yellow solid and an orange solution. The reaction was warmed to room temperature, then to 45 °C to enable more efficient stirring of the very thick mixture. Aldehyde (1.1 equiv.) was added to the reaction either neat or dissolved in minimal THF), and stirred for 1 hr. The reaction was stirred at 45 °C for 2 hr, then cooled to 0 °C and quenched with 1M HCl (25 mL). The organics were separated, and the aqueous layer was extracted with 3X Et<sub>2</sub>O. The combined organics were washed with water and brine, then concentrated onto silica gel. The material was then chromatographed with 15-30% EtOAc/Hexanes to afford the desired alkenoic acid products. Purity of material could be upgraded by recrystallization of material from minimal EtOAc/Hexanes. Alkenes were isolated in >10:1 geometric purity, with *E*-selectivity being dominant.



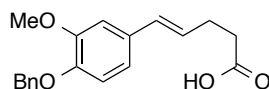
**(E)-4-(thiophen-2-yl)but-3-enoic acid (D25).** The  $\gamma,\delta$  unsaturated acid was prepared according to General Procedure **D**, using 10 g (3-carboxypropyl)triphenylphosphonium chloride (28.7 mmol, 1.0 equiv.) in 200 mL THF as solvent, 6.43 g of potassium *t*-butoxide (6.43 g, 57.3 mmol), and 5.36 mL thiophene 2-carboxaldehyde (57.3 mmol, 2.0 equiv.). Chromatography of material with 20% Acetone/Hexanes preceded recrystallization from acetone/hexanes. Yield was 2.32 g of transparent plates (12.7 mmol, 44%). \*Note: material was found to be prone to decomposition upon standing, but could be conveniently repurified by recrystallization from hexanes, with a hot filtration being performed to remove deeply colored impurities from the otherwise colorless, desired material. **<sup>1</sup>H NMR** (600 MHz, Chloroform-*d*)  $\delta$  7.13 - 7.09 (m, 1H), 6.94 (dd,  $J$  = 5.1, 3.5 Hz, 1H), 6.90 (dd,  $J$  = 3.6, 1.1 Hz, 1H), 6.58 (d,  $J$  = 15.5 Hz, 1H), 6.05 (dt,  $J$  = 15.7, 6.5 Hz, 1H), 2.53 (dt,  $J$  = 4.3, 2.3 Hz, 4H). **<sup>13</sup>C NMR** (151 MHz, CDCl<sub>3</sub>)  $\delta$  179.00, 178.99, 142.32, 127.78, 127.23, 124.88, 124.43, 123.61, 33.58, 27.68. **IR** (Thin Film, cm<sup>-1</sup>): 3054, 2987, 2684, 1711, 1422, 1265. **MS** (+ESI) Calculated  $m/z$  for [2M+K]<sup>+</sup> = 403.04, found  $m/z$  403.04. **R<sub>f</sub>** (30% EtOAc / 70% Hexanes): 0.30.



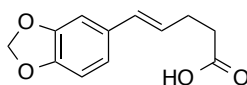
**(E)-5-(3,4-bis((*tert*-butyldimethylsilyl)oxy)phenyl)pent-4-enoic acid (D27).** The  $\gamma,\delta$  unsaturated acid was prepared according to a modification of General Procedure **D**. 4.21 g (11.5 mmol, 1.1 equiv.) of 3,4-bis((*tert*-butyldimethylsilyl)oxy)benzaldehyde<sup>10</sup>, 4.02 g Wittig reagent (10.45 mmol, 1.0 equiv.), and 2.35 g of potassium *t*-butoxide (20.90 mmol, 2.0 equiv.) were used, and 60 mL THF was employed as solvent. Yield was 1.83 g (4.19 mmol, 40%) of a white powder. Analytical data for (E)-5-(3,4-bis((*tert*-butyldimethylsilyl)oxy)phenyl)pent-4-enoic acid: **<sup>1</sup>H NMR** (600 MHz, Chloroform-*d*)  $\delta$  6.84 - 6.79 (m, 2H), 6.75 (d,  $J$  = 8.1 Hz, 1H), 6.31 (d,  $J$  = 15.6 Hz, 1H), 6.08 - 5.96 (m, 1H), 2.52 (s, 4H), 0.99 (s, 9H),



0.98 (s, 9H), 0.20 (s, 6H), 0.19 (s, 6H).  $^{13}\text{C}$  NMR (151 MHz,  $\text{CDCl}_3$ ):  $\delta$  178.42, 146.79, 146.39, 130.95, 130.73, 125.84, 121.02, 119.30, 118.78, 33.75, 27.86, 25.96, 25.94, 25.92, 18.47, 18.45, -4.10. **IR** (Thin Film,  $\text{cm}^{-1}$ ): **MS** (+ESI) Calculated  $m/z$  for  $[\text{M}+\text{H}]^+ = 437.25$ , found  $m/z$  437.28. **R<sub>f</sub>** (30% EtOAc / 70% Hexanes): 0.30.

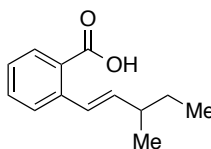


**(E)-5-(4-(benzyloxy)-3-methoxyphenyl)pent-4-enoic acid (D29).** The  $\gamma,\delta$  unsaturated acid was prepared according to General Procedure **D**. 2.42 g (10.0 mmol) of 4-Benzyloxy-3-methoxybenzaldehyde, 3.84 g Wittig reagent (10.0 mmol), and 2.24 g of potassium t-butoxide (20.0 mmol) were used, and 40 mL THF was employed as solvent. Yield was 1.21 g (39%) of a very pale-yellow crystalline solid. Analytical data for (E)-5-(4-(benzyloxy)-3-methoxyphenyl)pent-4-enoic acid:  $^1\text{H}$  NMR (600 MHz, Chloroform-*d*)  $\delta$  7.45 - 7.41 (m, 2H), 7.38 - 7.33 (m, 2H), 7.32 - 7.27 (m, 1H), 6.91 (s, 1H), 6.83 - 6.79 (m, 2H), 6.37 (d,  $J = 15.7$  Hz, 1H), 6.07 (d,  $J = 15.9$  Hz, 1H), 5.15 (s, 2H), 3.90 (s, 3H), 2.53 (s, 4H).  $^{13}\text{C}$  NMR (151 MHz,  $\text{CDCl}_3$ ):  $\delta$  178.48, 149.68, 147.64, 137.12, 130.92, 130.83, 128.53, 127.82, 127.24, 126.25, 118.98, 114.02, 109.23, 71.05, 55.98, 33.75, 27.88. **IR** (Thin Film,  $\text{cm}^{-1}$ ): 3026, 2910, 2867, 1705, 1584, 1509, 1466, 1455, 1417, 1381. **MS** (+ESI) Calculated  $m/z$  for  $[\text{M}+\text{H}]^+ = 313.14$ , found  $m/z$  313.13; **R<sub>f</sub>** (30% EtOAc / 70% Hexanes): 0.10.



**(E)-5-(benzo[d][1,3]dioxol-5-yl)pent-4-enoic acid (D31).** The  $\gamma,\delta$  unsaturated acid was prepared according to General Procedure **D**. The  $\gamma,\delta$  unsaturated acid was prepared according to General Procedure **D**. 1.41 g (10.0 mmol) of aldehyde, 3.84 g Wittig reagent (10.0 mmol), and 2.24 g of potassium t-butoxide (20.0 mmol) were used, and 40 mL THF was employed as solvent. Yield was 1.42 g (64%) of a very pale-yellow crystalline solid Analytical data for (E)-5-(benzo[d][1,3]dioxol-5-yl)pent-

4-enoic acid: **<sup>1</sup>H NMR** (600 MHz, Chloroform-*d*)  $\delta$  6.89 (d,  $J$  = 1.5 Hz, 1H), 6.80 - 6.71 (m, 2H), 6.36 (d,  $J$  = 15.7 Hz, 1H), 6.07 - 5.99 (m, 1H), 5.94 (s, 2H), 2.53 (s, 4H). **<sup>13</sup>C NMR** (151 MHz, CDCl<sub>3</sub>):  $\delta$  178.71, 147.94, 146.86, 131.75, 130.74, 126.21, 120.53, 108.22, 105.47, 100.97, 33.76, 27.81.. **IR** (Thin Film, cm<sup>-1</sup>): 3054, 2987, 2305, 1710, 1490, 1421. **MS** (+ESI) Calculated  $m/z$  for [M+H]<sup>+</sup> = 221.07, found  $m/z$  221.03; **R<sub>f</sub>** (30% EtOAc / 70% Hexanes): 0.15.

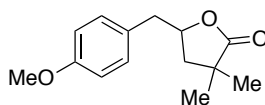


**2-(3-methylpent-1-en-1-yl)benzoic acid (Mixture of Geometric Isomers) (D35).** Methyl 2-(methyltriphenylphosphonium)benzoate bromide (5.00 g, 10.2 mmol, 1.0 equiv.) was suspended in 50 mL THF, and cooled to 0 °C. Potassium *t*-butoxide (1.14 g, 10.2 mmol, 1.0 equiv.) was added at this temperature, and the reaction stirred for 30 min. To the reaction mixture was added 2-methylbutanal (1.20 mL, 11.2 mmol, 1.1 equiv.), and the reaction was warmed to room temperature. After apparently slow progress, the reaction was heated to 60 °C for 15 hours. The reaction was quenched with saturated ammonium chloride (25 mL), and diluted with 50 mL diethyl ether and 25 mL water. The organics were separated, and the aqueous extracted with three portions of diethyl ether. The combined organics were washed with water, then saturated sodium chloride, then dried over sodium sulfate, filtered and concentrated to give product, which was partially purified by flash chromatography on silica gel. The resulting oil was then subjected to hydrolytic conditions (30 mL 3M NaOH/30mL Ethanol), and stirred at room temperature for 15 hours. The solution was diluted with 50 mL water and 50 mL diethyl ether, then the organics were separated and the aqueous layer extracted twice with diethyl ether. The aqueous layer was then acidified to pH 2 with concentrated HCl, and the aqueous was extracted again with 3 x 50mL diethyl ether. These extracts were washed with water and brine, then dried, filtered, and concentrated to give the title compound as an oil, in a mixture of geometric isomers (3.5:1 *E*:*Z*). Yield was 69% over both steps (1.43 g, 69%). Analytical data for (*E*)-2-(3-methylpent-1-en-1-yl)benzoic acid: **<sup>1</sup>H NMR**: (600

MHz, Chloroform-*d*)  $\delta$  8.03 (dd,  $J$  = 7.9, 1.4 Hz, 1H), 7.62 - 7.55 (m, 1H), 7.50 (td,  $J$  = 7.5, 1.4 Hz, 1H), 7.30 (td,  $J$  = 7.6, 1.3 Hz, 1H), 7.27 - 7.21 (m, 1H), 6.03 (dd,  $J$  = 15.8, 7.8 Hz, 1H), 2.34 - 2.26 (m, 1H), 1.45 (p,  $J$  = 7.3 Hz, 2H), 1.12 (d,  $J$  = 6.7 Hz, 3H), 0.95 (t,  $J$  = 7.4 Hz, 3H).  $^{13}\text{C}$  NMR (151 MHz, Chloroform-*d*)  $\delta$  173.51, 140.85, 139.96, 132.85, 131.24, 127.53, 127.14, 126.86, 126.52, 38.94, 29.72, 20.06, 11.78. **MS** (+ESI) Calculated  $m/z$  for  $[\text{M}+\text{K}]^+ = 243.12$ , Found 243.08 **IR** (Thin Film,  $\text{cm}^{-1}$ ): 3053, 2986, 2965, 1692, 1421. **R<sub>f</sub>** (30% EtOAc / Hexanes) = 0.40.

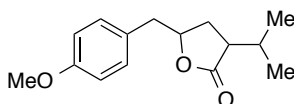
### A1.8. Anti-Markovnikov Hydrolactonization Reactions.

**General Procedure E.** To a flame-dried, 1-dram vial charged with a stirbar was added alkenoic acid (100 mg), and 9-mesityl-10-methylacridinium tetrafluoroborate. The reaction vial was sealed with a septum cap and pumped into a glovebox with a nitrogen atmosphere. Solvent (appropriate amount to dilute the reaction to 0.5 M with respect to substrate) was added, and the vial re-sealed and removed from the glovebox. Thiophenol (0.20 equiv., sparged with nitrogen gas in a fumehood in a separate vial, CAUTION! Stench/Toxicity hazard!) was added via a 10  $\mu\text{L}$  syringe. The reaction was then irradiated with a PAR38 blue LED lamp (With emission centered at 450 nm, purchased from Ecoxotic, Part # LED 5-455nm Blue 21W) for the given time period, with aluminum foil being used to shield light. The reaction was then concentrated onto silica gel and chromatographed to afford the desired lactone products.

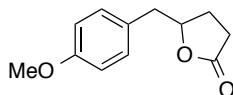


**5-(4-methoxybenzyl)-3,3-dimethyldihydrofuran-2(3H)-one (D2)** : The title compound was synthesized by general procedure **E**, employing 100 mg ((*E*)-5-(4-methoxyphenyl)-2,2-dimethylpent-4-enoic acid) (0.427 mmol, 1.0 equiv.), 8.4 mg 9-mesityl,10-methylacridinium tetrafluoroborate (.021 mmol, 0.05 equiv.), 8.7  $\mu\text{L}$  thiophenol (0.085 mmol, 0.2 equiv.), and 1,2-dichloroethane (0.9 mL) as solvent. Reaction time was 24 hr. Product was obtained as viscous oil (Average 89 mg, 89 % yield over two trials).  $^1\text{H}$  NMR: (600 MHz, Chloroform-*d*)  $\delta$  7.14 (d,  $J$  = 8.6 Hz, 2H), 6.84 (d,  $J$  = 8.6 Hz, 2H), 4.64 -

4.53 (m, 1H), 3.78 (s, 3H), 3.03 (dd,  $J = 14.1, 6.4$  Hz, 1H), 2.82 (dd,  $J = 14.1, 6.2$  Hz, 1H), 2.06 (dd,  $J = 12.7, 5.9$  Hz, 1H), 1.79 (dd,  $J = 12.8, 9.9$  Hz, 1H), 1.22 (s, 3H), 1.21 (s, 3H).  $^{13}\text{C}$  NMR (151 MHz, Chloroform- $d$ )  $\delta$  181.72, 158.49, 130.32, 128.09, 113.92, 77.42, 55.19, 42.72, 40.59, 40.35, 24.91, 24.35. **MS** (+ESI) Calculated  $m/z$  for  $[\text{M}+\text{H}]^+ = 235.13$ , Found 235.18 **IR** (Thin Film,  $\text{cm}^{-1}$ ) 2968, 2836, 1767, 1612, 1583, 1512, 1460. **R<sub>f</sub>** (25% EtOAc / Hexanes) = 0.35.

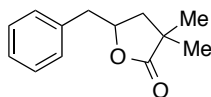


**3-isopropyl-5-(4-methoxybenzyl)dihydrofuran-2(3H)-one (D4)** : The title compound was synthesized by general procedure **E**, employing 100 mg ((*E*)-2-isopropyl-5-(4-methoxyphenyl)pent-4-enoic acid) (0.403 mmol, 1.0 equiv.), 8.0 mg 9-mesityl,10-methylacridinium tetrafluoroborate (.020 mmol, 0.05 equiv.), 8.2  $\mu\text{L}$  thiophenol (.081 mmol, 0.2 equiv.), and 1,2-dichloroethane (.08 mL) as solvent. Reaction time was 15 hr. Product was obtained as viscous oil (Average 87 mg, 87 % yield over two trials). Isolated as a mixture of inseparable diastereomers (2.4:1, Identity of Major is Unknown).  **$^1\text{H}$  NMR (Major)**: (600 MHz, Chloroform- $d$ )  $\delta$  7.16 (d,  $J = 8.6$  Hz, 2H), 6.86 (d,  $J = 8.7$  Hz, 2H), 4.55 - 4.47 (m, 1H), 3.80 (s, 3H), 3.04 (dd,  $J = 14.1, 6.2$  Hz, 1H), 2.87 (dd,  $J = 13.8, 6.2$  Hz, 1H), 2.60 - 2.51 (m, 1H), 2.20 - 2.13 (m, 2H), 1.73 - 1.65 (m, 1H), 1.00 (d,  $J = 6.9$  Hz, 3H), 0.86 (d,  $J = 6.8$  Hz, 3H).  **$^{13}\text{C}$  NMR (Major)** (151 MHz, Chloroform- $d$ )  $\delta$  177.80, 158.45, 130.32, 128.01, 113.87, 78.53, 55.16, 46.87, 40.29, 29.50, 27.30, 20.54, 18.00. **MS** (+ESI) Calculated  $m/z$  for  $[\text{M}+\text{H}]^+ = 249.14$ , Found 249.19 **IR** (Thin Film,  $\text{cm}^{-1}$ ) 2961, 2836, 1766, 1612, 1584, 1513, 1466. **R<sub>f</sub>** (25% EtOAc / Hexanes) = 0.45

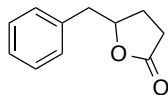


**5-(4-methoxybenzyl)dihydrofuran-2(3H)-one (D6)**: The title compound was synthesized by general procedure **E**, employing 100 mg (*E*)-5-(4-methoxyphenyl)pent-4-enoic acid (0.485 mmol, 1.0 equiv.), 9.7 mg 9-mesityl,10-methylacridinium tetrafluoroborate (0.024 mmol, 0.05 equiv.), 9.9  $\mu\text{L}$  thiophenol (0.097

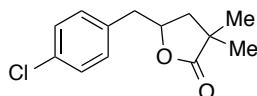
mmol, 0.2 equiv.), and 1,2-dichloroethane (1.0 mL) as solvent. Reaction is heterogeneous at beginning of reaction. Reaction time was 15 hr. Product was obtained as viscous oil (Average 89 mg, 89 % yield over two trials). Characterization matches literature data<sup>6</sup>. **<sup>1</sup>H NMR**: (600 MHz, Chloroform-*d*)  $\delta$  7.14 (d, *J* = 8.1 Hz, 2H), 6.84 (d, *J* = 8.5 Hz, 2H), 4.72 - 4.65 (m, 1H), 3.78 (s, 3H), 3.03 - 2.95 (m, 1H), 2.91 - 2.84 (m, 1H), 2.48 - 2.39 (m, 1H), 2.38 - 2.30 (m, 1H), 2.27 - 2.19 (m, 1H), 1.98 - 1.88 (m, 1H). **<sup>13</sup>C NMR** (151 MHz, Chloroform-*d*)  $\delta$  177.05, 158.53, 130.41, 127.74, 113.97, 80.90, 55.19, 40.31, 28.59, 26.90. **MS** (+ESI) Calculated *m/z* for [M+H]<sup>+</sup> = 207.09, Found 207.17 **IR** (Thin Film, cm<sup>-1</sup>) 2937, 2837, 1772, 1612, 1583, 1513. **R<sub>f</sub>** (25% EtOAc / Hexanes) = 0.2



**5-benzyl-3,3-dimethyldihydrofuran-2(3H)-one (D8)**: The title compound was synthesized by general procedure **E**, employing 100 mg (*E*)-2,2-dimethyl-5-phenylpent-4-enoic acid (0.490 mmol, 1.0 equiv.), 7.8 mg 9-mesityl,10-methylacridinium tetrafluoroborate (.098 mmol, 0.05 equiv.), 10  $\mu$ L thiophenol (.098 mmol, 0.2 equiv.), and 1,2-dichloroethane (1.0 mL) as solvent. Reaction time was 24 hr. Product was obtained as viscous oil (Average 85 mg, 85% yield over two trials). Characterization matches literature data<sup>11</sup>. **<sup>1</sup>H NMR**: (600 MHz, Chloroform-*d*)  $\delta$  7.34 - 7.29 (m, 2H), 7.27 - 7.21 (m, 3H), 4.68 - 4.58 (m, 1H), 3.10 (dd, *J* = 13.9, 6.5 Hz, 1H), 2.88 (dd, *J* = 13.9, 6.2 Hz, 1H), 2.08 (dd, *J* = 12.8, 5.9 Hz, 1H), 1.82 (dd, *J* = 12.8, 9.9 Hz, 1H), 1.23 (s, 3H), 1.22 (s, 3H). **<sup>13</sup>C NMR** (151 MHz, Chloroform-*d*)  $\delta$  181.67, 136.12, 129.31, 128.54, 126.85, 77.22, 42.84, 41.55, 40.34, 24.91, 24.33. **MS** (+ESI) Calculated *m/z* for [M+H]<sup>+</sup> = 205.27, Found 205.16 **IR** (Thin Film, cm<sup>-1</sup>) 2970, 2931, 2871, 1769, 1604, 1455. **R<sub>f</sub>** (25% EtOAc / Hexanes) = 0.5

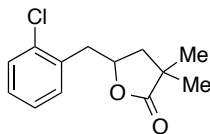


**5-benzyl-2,3-dihydrofuran-2(3H)-one (D10):** The title compound was synthesized by general procedure E, employing 100 mg (*E*)-5-phenylpent-4-enoic acid (0.567 mmol, 1.0 equiv.), 11.3 mg 9-mesityl,10-methylacridinium tetrafluoroborate (0.028 mmol, 0.05 equiv.), 11.6  $\mu$ L thiophenol (0.113 mmol, 0.2 equiv.), and 1,2-dichloroethane (1.2 mL) as solvent. Reaction time was 36 hr. Product was obtained as viscous oil (Average 78 mg, 78 % yield over two trials). Characterization matches literature values<sup>12</sup>. **<sup>1</sup>H NMR:** (600 MHz, Chloroform-*d*)  $\delta$  7.32 (dd, *J* = 8.1, 6.7 Hz, 2H), 7.28 - 7.17 (m, 3H), 4.79 - 4.69 (m, 1H), 3.07 (dd, *J* = 14.0, 6.1 Hz, 1H), 2.93 (dd, *J* = 14.0, 6.2 Hz, 1H), 2.54 - 2.41 (m, 1H), 2.41 - 2.32 (m, 1H), 2.30 - 2.19 (m, 1H), 2.03 - 1.89 (m, 1H). **<sup>13</sup>C NMR** (151 MHz, Chloroform-*d*)  $\delta$  176.96, 135.83, 129.39, 128.58, 126.91, 80.73, 41.26, 28.59, 27.07. **MS** (+ESI) Calculated *m/z* for [M+H]<sup>+</sup> = 177.08, Found 177.13 **IR** (Thin Film, cm<sup>-1</sup>) 3062, 3030, 2926, 1773, 1604, 1498, 1455, 1420, 1354. **R<sub>f</sub>** (25% EtOAc / Hexanes) = 0.55

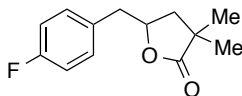


**5-(4-chlorobenzyl)-3,3-dimethyl-2,3-dihydrofuran-2(3H)-one (D12):** The title compound was synthesized by general procedure E, employing 100 mg (*E*)-5-(4-chlorophenyl)-2,2-dimethylpent-4-enoic acid (.420 mmol, 1.0 equiv.), 8.37 mg 9-mesityl,10-methylacridinium tetrafluoroborate (.021 mmol, 0.05 equiv.), 8.6  $\mu$ L thiophenol (.084 mmol, 0.2 equiv.), and 1,2-dichloroethane (0.9 mL) as solvent. Reaction time was 36 hr. Product was obtained as viscous oil (Average 87 mg, 87% yield over two trials). **<sup>1</sup>H NMR:** (600 MHz, Chloroform-*d*)  $\delta$  7.27 (d, *J* = 8.4 Hz, 2H), 7.16 (d, *J* = 8.4 Hz, 2H), 4.63 - 4.54 (m, 1H), 3.01 (dd, *J* = 14.2, 6.9 Hz, 1H), 2.86 (dd, *J* = 14.2, 5.7 Hz, 1H), 2.09 (dd, *J* = 12.7, 5.8 Hz, 1H), 1.78 (dd, *J* = 12.8, 10.0 Hz, 1H), 1.22 (s, 3H), 1.21 (s, 3H). **<sup>13</sup>C NMR:** (151 MHz, Chloroform-*d*)  $\delta$  181.47, 134.69, 132.73, 130.66, 128.64, 76.87, 42.76, 40.81, 40.31, 24.87, 24.29. **MS** (+ESI): Calculated *m/z* for [M+H]<sup>+</sup>

= 239.08, Found 239.14. **IR** (Thin Film,  $\text{cm}^{-1}$ ): 2968, 2931, 2871, 1770, 1596, 1493, 1456, 1409. **R<sub>f</sub>** (25% EtOAc / Hexanes) = 0.45.

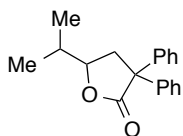


**5-(2-chlorobenzyl)-3,3-dimethyldihydrofuran-2(3H)-one (D14):** The title compound was synthesized by general procedure **E**, employing 100 mg (*E*)-5-(2-chlorophenyl)-2,2-dimethylpent-4-enoic acid (0.490 mmol, 1.0 equiv.), 9.6 mg 9-mesityl,10-methylacridinium tetrafluoroborate (0.024 mmol, 0.05 equiv.), 10.0  $\mu\text{L}$  thiophenol (0.097 mmol, 0.2 equiv.), and 1,2-dichloroethane (0.9 mL) as solvent. Reaction time was 72 hr. Product (x mg) was obtained as viscous oil (Average 93 mg, 93% yield over two trials). **<sup>1</sup>H NMR:** (600 MHz, Chloroform-*d*)  $\delta$  7.42 - 7.33 (m, 1H), 7.33 - 7.28 (m, 1H), 7.24 - 7.15 (m, 2H), 4.72 (ddt,  $J$  = 9.9, 7.2, 5.7 Hz, 1H), 3.15 (dd,  $J$  = 14.1, 7.2 Hz, 1H), 3.09 (dd,  $J$  = 14.1, 5.5 Hz, 1H), 2.13 (dd,  $J$  = 12.8, 5.9 Hz, 1H), 1.85 (dd,  $J$  = 12.8, 9.9 Hz, 1H), 1.26 (s, 3H), 1.23 (s, 3H). **<sup>13</sup>C NMR:** (151 MHz,  $\text{CDCl}_3$ )  $\delta$  181.53, 134.10, 133.97, 131.72, 129.49, 128.40, 126.94, 75.73, 42.88, 40.37, 39.01, 24.95, 24.28. **MS** (+ESI): Calculated  $m/z$  for  $[\text{M}+\text{H}]^+$  = 239.08, Found 239.09. **IR** (Thin Film,  $\text{cm}^{-1}$ ): 3057, 2973, 2934, 2872, 1771, 1475, 1456, 1388, 1351. **R<sub>f</sub>** (25% EtOAc / Hexanes) = 0.50.

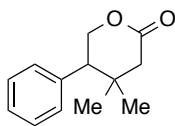


**5-(4-fluorobenzyl)-3,3-dimethyldihydrofuran-2(3H)-one (D16):** The title compound was synthesized by general procedure **E**, employing 100 mg (*E*)-5-(4-fluorophenyl)-2,2-dimethylpent-4-enoic acid (.450 mmol, 1.0 equiv.), 9.0 mg 9-mesityl,10-methylacridinium tetrafluoroborate (.023 mmol, 0.05 equiv.), 9.2  $\mu\text{L}$  thiophenol (.090 mmol, 0.2 equiv.), and 1,2-dichloroethane (0.9 mL) as solvent. Reaction time was 36 hr. Product was obtained as viscous oil (Average 85 mg, 85% yield over two trials). **<sup>1</sup>H NMR:** (600 MHz, Chloroform-*d*)  $\delta$  7.19 (dd,  $J$  = 8.5, 5.4 Hz, 2H), 6.99 (dd,  $J$  = 8.7 Hz, 2H), 4.65 - 4.54 (m, 1H), 3.02 (dd,  $J$

= 14.2, 6.8 Hz, 1H), 2.87 (dd,  $J$  = 14.2, 5.7 Hz, 1H), 2.08 (dd,  $J$  = 12.8, 5.9 Hz, 1H), 1.79 (dd,  $J$  = 12.8, 10.0 Hz, 1H), 1.22 (s, 3H), 1.22 (s, 3H).  **$^{13}\text{C}$  NMR**: (151 MHz, Chloroform- $d$ )  $\delta$  181.56, 161.82 (d,  $J$  = 245.0 Hz), 131.91 (d,  $J$  = 3.3 Hz), 130.81 (d,  $J$  = 8.1 Hz), 115.34 (d,  $J$  = 21.2 Hz), 77.08, 42.73, 40.66, 40.33, 24.88, 24.32. **MS** (+ESI): Calculated  $m/z$  for  $[\text{M}+\text{H}]^+ = 223.11$ , Found 223.19. **IR** (Thin Film,  $\text{cm}^{-1}$ ): 3057, 2970, 2933, 2872, 1769, 1603, 1511, 1456, 1418.  **$R_f$**  (25% EtOAc / Hexanes) = 0.5.



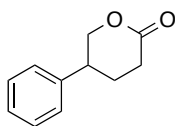
**5-isopropyl-3,3-diphenyldihydrofuran-2(3H)-one (D18)**: The title compound was synthesized by general procedure E, employing 100 mg 5-methyl-2,2-diphenylhex-4-enoic acid (0.36 mmol, 1.0 equiv.), 7.1 mg 9-mesityl,10-methylacridinium tetrafluoroborate (.018 mmol, 0.05 equiv.), 7.2  $\mu\text{L}$  thiophenol (.071 mmol, 0.2 equiv.), and 1,2-dichloroethane (0.7 mL) as solvent. Reaction time was 24 hr. Product was obtained as viscous oil (Average 90 mg, 90% yield over two trials).  **$^1\text{H}$  NMR**: (600 MHz, Chloroform- $d$ )  $\delta$  7.41 - 7.35 (m, 4H), 7.34 - 7.27 (m, 5H), 7.26 - 7.22 (m, 1H), 4.08 - 3.99 (m, 1H), 2.99 (dd,  $J$  = 12.9, 4.8 Hz, 1H), 2.62 (dd,  $J$  = 12.9, 10.8 Hz, 1H), 1.95 - 1.85 (m, 1H), 1.07 (d,  $J$  = 6.6 Hz, 3H), 0.96 (d,  $J$  = 6.8 Hz, 3H).  **$^{13}\text{C}$  NMR** (151 MHz, Chloroform- $d$ )  $\delta$  177.22, 142.28, 139.81, 128.89, 128.34, 127.69, 127.66, 127.38, 127.13, 82.04, 58.33, 41.56, 32.80, 18.80, 17.35. **MS** (+ESI) Calculated  $m/z$  for  $[\text{M}+\text{H}]^+ = 281.15$ , Found 281.18 **IR** (Thin Film,  $\text{cm}^{-1}$ ) 3060, 3026, 2962, 2930, 2874, 1766, 1600, 1496, 1469, 1447.  **$R_f$**  (25% EtOAc / Hexanes) = 0.65



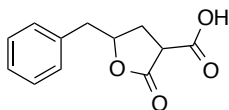
**4,4-dimethyl-5-phenyltetrahydro-2H-pyran-2-one (D20)**: The title compound was synthesized by general procedure E, employing 100 mg 3,3-dimethyl-4-phenylpent-4-enoic acid (0.490 mmol, 1.0 equiv.), 9.8 mg 9-mesityl,10-methylacridinium tetrafluoroborate (.098 mmol, 0.05 equiv.), 10.0  $\mu\text{L}$



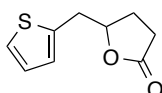
thiophenol (.098 mmol, 0.2 equiv.), and 1,2-dichloroethane (1.0 mL) as solvent. Reaction time was 36 hr. Product was obtained as viscous oil (Average 60 mg, 60% yield over two trials). \*Note, product material is prone to decomposition upon standing, likely by polymerization. **<sup>1</sup>H NMR:** (600 MHz, Chloroform-*d*)  $\delta$  7.40 - 7.27 (m, 3H), 7.20 - 7.13 (m, 2H), 4.67 (dd,  $J$  = 11.2 Hz, 1H), 4.50 (dd,  $J$  = 11.7, 5.4 Hz, 1H), 2.97 (dd,  $J$  = 10.6, 5.4 Hz, 1H), 2.51 (d,  $J$  = 17.1 Hz, 1H), 2.43 (d,  $J$  = 17.1 Hz, 1H), 0.97 (s, 3H), 0.96 (s, 3H). **<sup>13</sup>C NMR:** (151 MHz, Chloroform-*d*)  $\delta$  170.92 , 136.98 , 128.87 , 128.39 , 127.57 , 70.12 , 49.39 , 44.91 , 33.44 , 29.19 , 22.85. **MS** (+ESI): Calculated  $m/z$  for  $[M+H]^+$  = 205.12, Found 205.16. **IR** (Thin Film,  $\text{cm}^{-1}$ ): 3059, 2965, 1737, 1601, 1496, 1464, 1409. **R<sub>f</sub>** (25% EtOAc / Hexanes) = 0.30.



**5-phenyltetrahydro-2H-pyran-2-one (D22):** The title compound was synthesized by general procedure E, employing 100 mg (4-phenylpent-4-enoic acid) (0.568 mmol, 1.0 equiv.), 11.3 mg 9-mesityl, 10-methylacridinium tetrafluoroborate (.028 mmol, 0.05 equiv.), 11.6  $\mu\text{L}$  thiophenol (0.114 mmol, 0.2 equiv.), and 1,2-dichloroethane (1.1 mL) as solvent. Reaction time was 36 hr. Product was obtained as viscous oil (Average 59 mg, 59% yield over two trials). \*Note, material is prone to decomposition upon standing, likely by polymerization. **<sup>1</sup>H NMR:** (600 MHz, Chloroform-*d*)  $\delta$  7.36 (dd,  $J$  = 8.1, 6.8 Hz, 2H), 7.31 - 7.27 (m, 1H), 7.25 (dd,  $J$  = 8.2, 1.3 Hz, 2H), 4.48 (ddd,  $J$  = 11.3, 4.9, 2.1 Hz, 1H), 4.31 (t,  $J$  = 10.9 Hz, 1H), 3.25 - 3.15 (m, 1H), 2.79 (ddd,  $J$  = 18.0, 6.6, 4.2 Hz, 1H), 2.66 (ddd,  $J$  = 17.8, 10.1, 7.1 Hz, 1H), 2.27 - 2.19 (m, 1H), 2.19 - 2.11 (m, 1H). **<sup>13</sup>C NMR:** (151 MHz,  $\text{CDCl}_3$ )  $\delta$  170.54, 139.46, 128.93, 127.53, 127.14, 73.89, 39.28, 29.62, 26.51. **MS** (+ESI): Calculated  $m/z$  for  $[M+H]^+$  = 177.08, Found 177.07. **IR** (Thin Film,  $\text{cm}^{-1}$ ): 3030, 2954, 1735, 1603, 1558, 1496, 1473, 1456, 1402. **R<sub>f</sub>** (25% EtOAc / Hexanes) = 0.25.

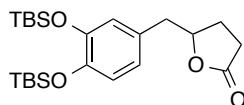


**5-benzyl-2-oxotetrahydrofuran-3-carboxylic acid (D24):** The title compound was synthesized by general procedure E, employing 100 mg 2-cinnamylmalonic acid (0.455 mmol, 1.0 equiv.), 9.2 mg 9-mesityl, 10-methylacridinium tetrafluoroborate (.023 mmol, 0.05 equiv.), 9.3  $\mu$ L thiophenol (.092 mmol, 0.2 equiv.), and 1,2-dichloroethane (0.9 mL) as solvent. Reaction is heterogeneous at outset of irradiation. Reaction time was 72 hr. Product was obtained as a viscous oil (Average 76 mg, 1.3:1 d.r. over two trials). Characterization for 5-benzyl-2-oxotetrahydrofuran-3-carboxylic acid (*inseparable mixture of diastereomers*):  $^1\text{H NMR}$  (600 MHz, Chloroform-*d*)  $\delta$  7.38 - 7.18 (m, 10H), 5.01 - 4.93 (m, 1H), 4.75 - 4.67 (m, 1H), 3.69 - 3.61 (m, 1H), 3.28 (dd,  $J$  = 9.8, 6.5 Hz, 1H), 3.19 (dd,  $J$  = 14.0, 6.6 Hz, 1H), 3.04 - 3.00 (m, 2H), 2.99 - 2.93 (m, 1H), 2.70 - 2.63 (m, 1H), 2.60 - 2.51 (m, 1H), 2.44 - 2.34 (m, 1H), 2.31 - 2.23 (m, 1H).  $^{13}\text{C NMR}$  (151 MHz,  $\text{CDCl}_3$ )  $\delta$  172.18, 172.03, 171.23, 170.72, 135.18, 134.84, 129.54, 129.31, 128.87, 128.78, 127.35, 127.23, 80.13, 79.95, 46.70, 46.11, 41.10, 40.91, 31.24, 30.22. **IR** (Thin Film,  $\text{cm}^{-1}$ ) 3054, 2929, 1775, 1712, 1455, 1357. **MS** (+ESI): Calculated  $m/z$  for  $[\text{M}+\text{H}]^+ = 221.07$ , Found 221.11. **R<sub>f</sub>** (25% EtOAc / Hexanes) = 0.05

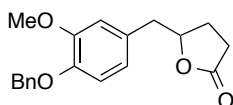


**5-(thiophen-2-ylmethyl)dihydrofuran-2(3H)-one (D26):** The title compound was synthesized by general procedure E, employing 100 mg (*E*)-4-(thiophen-2-yl)but-3-enoic acid (0.549 mmol, 1.0 equiv.), 11.0 mg 9-mesityl, 10-methylacridinium tetrafluoroborate (.027 mmol, 0.05 equiv.), 11.2  $\mu$ L thiophenol (0.110 mmol, 0.2 equiv.), and 1,2-dichloroethane (1.1 mL) as solvent. Reaction time was 36 hr. Product was obtained as viscous oil (Average 82 mg, 82% yield over two trials). \*Note, material is prone to decomposition upon standing.  $^1\text{H NMR}$ :  $^1\text{H NMR}$  (600 MHz, Chloroform-*d*)  $\delta$  7.19 (dd,  $J$  = 5.1, 1.2 Hz, 1H), 6.96 (dd,  $J$  = 5.1, 3.4 Hz, 1H), 6.90 (dd,  $J$  = 3.5, 1.0 Hz, 1H), 4.79 - 4.71 (m, 1H), 3.25 (dd,  $J$  = 15.3, 5.3 Hz, 1H), 3.18 (dd,  $J$  = 14.9, 6.0 Hz, 1H), 2.52 - 2.46 (m, 1H), 2.42 - 2.36 (m, 1H), 2.33 - 2.26 (m, 1H),

2.02 - 1.95 (m, 1H).  $^{13}\text{C}$  NMR: (151 MHz,  $\text{CDCl}_3$ )  $\delta$  176.82, 137.06, 127.09, 126.78, 124.73, 79.95, 35.22, 28.55, 26.73. MS (+ESI): Calculated  $m/z$  for  $[\text{M}+\text{H}]^+ = 183.04$ , Found 183.05. IR (Thin Film,  $\text{cm}^{-1}$ ): 3107, 2924, 1770, 1458, 1438, 1419.  $R_f$  (25% EtOAc / Hexanes) = 0.25.

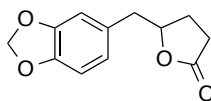


**5-(3,4-bis((*tert*-butyldimethylsilyl)oxy)benzyl)dihydrofuran-2(3*H*)-one (D28):** The title compound was synthesized by a variation of general procedure **E**, with the reaction being run at a more dilute concentration (0.1 M), employing 100 mg (*E*)-5-(3,4-bis((*tert*-butyldimethylsilyl)oxy)phenyl)pent-4-enoic acid (.0229 mmol, 1.0 equiv.), 4.6 mg 9-mesityl,10-methylacridinium tetrafluoroborate (.011 mmol, 0.05 equiv.), 4.7  $\mu\text{L}$  thiophenol (.045 mmol, 0.2 equiv.), and 1,2-dichloroethane (2.3 mL) as solvent. Reaction time was 24 hr. Reaction was heterogeneous at initiation. Product was obtained as viscous oil (Average 89 mg, 89% yield over two trials).  $^1\text{H}$  NMR: (600 MHz, Chloroform-*d*)  $\delta$  6.76 (d,  $J = 8.0$  Hz, 1H), 6.72 - 6.60 (m, 2H), 4.77 - 4.58 (m, 1H), 2.96 (dd,  $J = 14.0, 5.7$  Hz, 1H), 2.78 (dd,  $J = 14.0, 6.6$  Hz, 1H), 2.53 - 2.29 (m, 2H), 2.27 - 2.14 (m, 1H), 2.00 - 1.84 (m, 1H), 0.98 (s, 9H), 0.97 (s, 9H), 0.19 (s, 6H), 0.18 (s, 6H).  $^{13}\text{C}$  NMR: (101 MHz,  $\text{CDCl}_3$ )  $\delta$  177.00, 146.73, 145.86, 128.70, 122.36, 122.29, 121.06, 80.88, 40.51, 28.63, 26.93, 25.89, 18.41, -4.12, -4.14. MS (+ESI): Calculated  $m/z$  for  $[\text{M}+\text{H}]^+ = 437.25$ , Found 437.34. IR (Thin Film,  $\text{cm}^{-1}$ ): 2955, 2930, 2896, 2857, 1779, 1604, 1576, 1510.  $R_f$  (25% EtOAc / Hexanes) = 0.5.

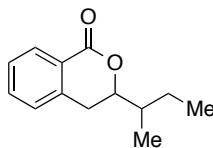


**5-(4-(benzyloxy)-3-methoxybenzyl)dihydrofuran-2(3*H*)-one (D30):** The title compound was synthesized by a variation of general procedure **E**, with the reaction being run at a more dilute concentration (0.1 M), employing 100 mg (*E*)-5-(4-(benzyloxy)-3-methoxyphenyl)pent-4-enoic acid (.320

mmol, 1.0 equiv.), 6.4 mg 9-mesityl,10-methylacridinium tetrafluoroborate (.016 mmol, 0.05 equiv.), 6.5  $\mu$ L thiophenol (.064 mmol, 0.2 equiv.), and 1,2-dichloroethane (3.2 mL) as solvent. Reaction was heterogeneous at initiation. Reaction time was 36 hr. Product was obtained as viscous oil (Average 89 mg, 89% yield over two trials). **<sup>1</sup>H NMR:** (400 MHz, Chloroform-*d*)  $\delta$  7.43 (d, *J* = 7.4 Hz, 2H), 7.35 (t, *J* = 7.4 Hz, 2H), 7.32 - 7.26 (m, 1H), 6.82 (d, *J* = 8.2 Hz, 1H), 6.77 (d, *J* = 2.1 Hz, 1H), 6.68 (dd, *J* = 8.2, 2.1 Hz, 1H), 5.12 (s, 2H), 4.77 - 4.64 (m, 1H), 3.87 (s, 3H), 2.95 (dd, *J* = 14.1, 5.9 Hz, 1H), 2.87 (dd, *J* = 14.2, 5.9 Hz, 1H), 2.50 - 2.36 (m, 1H), 2.36 - 2.28 (m, 1H), 2.26 - 2.17 (m, 1H), 1.99 - 1.84 (m, 1H). **<sup>13</sup>C NMR:** (101 MHz, CDCl<sub>3</sub>)  $\delta$  177.13, 149.49, 147.02, 136.99, 128.84, 128.40, 127.70, 127.15, 121.38, 114.01, 113.05, 80.74, 70.92, 55.90, 40.69, 28.53, 26.81. **MS** (+ESI): Calculated *m/z* for [M+H]<sup>+</sup> = 313.14, Found 313.21. **IR** (Thin Film, cm<sup>-1</sup>): 2937, 1770, 1590, 1513, 1454, 1420. **R<sub>f</sub>** (25% EtOAc / Hexanes) = 0.10.

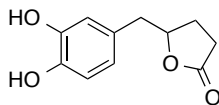


**5-(benzo[*d*][1,3]dioxol-5-ylmethyl)dihydrofuran-2(3*H*)-one (D32):** The title compound was synthesized by a variation of general procedure **E**, with the reaction being run at a more dilute concentration (0.1 M), employing 100 mg (*E*)-5-(benzo[*d*][1,3]dioxol-5-yl)pent-4-enoic acid (0.454 mmol, 1.0 equiv.), 9.1 mg 9-mesityl,10-methylacridinium tetrafluoroborate (.022 mmol, 0.05 equiv.),  $\mu$ L thiophenol (.091 mmol, 0.2 equiv.), and 1,2-dichloroethane (4.5 mL) as solvent. Reaction was heterogeneous at initiation. Reaction time was 36 hr. Product was obtained as viscous oil (Average 89 mg, 89% yield over two trials). Analytical data matches literature values<sup>6</sup>. **<sup>1</sup>H NMR:** (400 MHz, Chloroform-*d*)  $\delta$  6.81 - 6.70 (m, 2H), 6.67 (dd, *J* = 7.8, 1.7 Hz, 1H), 4.73 - 4.62 (m, 1H), 2.97 (dd, *J* = 14.1, 6.2 Hz, 1H), 2.85 (dd, *J* = 14.1, 6.0 Hz, 1H), 2.54 - 2.34 (m, 2H), 2.31 - 2.19 (m, 1H), 2.01 - 1.87 (m, 1H). **<sup>13</sup>C NMR:** (101 MHz, CDCl<sub>3</sub>)  $\delta$  176.95, 147.64, 146.40, 129.42, 122.34, 109.64, 108.23, 100.87, 80.80, 40.82, 28.55, 26.90. **MS** (+ESI): Calculated *m/z* for [M+H]<sup>+</sup> = 221.12, Found 221.11. **IR** (Thin Film, cm<sup>-1</sup>): 2905, 2779, 1772, 1608, 1583, 1503, 1491, 1443. **R<sub>f</sub>** (25% EtOAc / Hexanes) = 0.10.



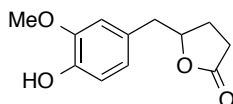
**3-(*sec*-butyl)isochroman-1-one:** The title compound was synthesized by a variation of general procedure **E**, employing 100 mg of a 3.5:1 mixture of E and Z geometric isomers of (0.490 mmol, 1.0 equiv.), 9.6 mg 9-mesityl,10-methylacridinium tetrafluoroborate (0.024 mmol, 0.05 equiv.), 10.0  $\mu$ L thiophenol (.097 mmol, 0.2 equiv.), and 1,2-dichloroethane (1.0  $\mu$ L) as solvent. Additionally, 5.7  $\mu$ L of nitrogen-sparged 2,6-lutidine (.049 mmol) was included in the reaction. Reaction time was 72 hr. Product was obtained as viscous oil (Average 78 mg, 78 % yield as a 1:1 mixture of diastereomers over two trials). Peak enumeration is for a mixture of inseparable diastereomers. **<sup>1</sup>H NMR** (600 MHz, Chloroform-*d*)  $\delta$  7.86 (d, *J* = 7.6 Hz, 2H), 7.65 (t, *J* = 7.5 Hz, 2H), 7.50 (t, *J* = 7.5 Hz, 2H), 7.41 (t, *J* = 7.4 Hz, 2H), 5.51 (m, 2H), 1.93 - 1.75 (m, 3H), 1.75 - 1.63 (m, 2H), 1.58 (m, 2H), 1.43 - 1.32 (m, 1H), 1.26 (m, 2H), 1.05 (d, *J* = 6.6 Hz, 3H), 0.98 (d, *J* = 6.6 Hz, 3H), 0.92 (t, *J* = 7.4 Hz, 3H), 0.87 (t, *J* = 7.4 Hz, 3H). **IR** (Thin Film,  $\text{cm}^{-1}$ ): 3056, 2961, 2875, 1756, 1613, 1600, 1465, 1379. **<sup>13</sup>C NMR** (151 MHz,  $\text{CDCl}_3$ )  $\delta$  170.58, 170.56, 150.68, 150.61, 133.85, 133.82, 128.91, 128.90, 125.83, 125.59, 121.72, 121.59, 80.05, 79.71, 42.18, 42.16, 31.41, 31.25, 30.02, 28.66, 19.62, 18.62, 11.13, 11.00. **MS** (+ESI): Calculated *m/z* for  $[\text{M}+\text{H}]^+ = 205.12$ , Found 205.17. **IR** (Thin Film,  $\text{cm}^{-1}$ ): 3056, 2961, 2875, 1756, 1613, 1600, 1465, 1379. **R<sub>f</sub>** (25% EtOAc / Hexanes) = 0.20.

#### A1.9. Deprotection Conditions for Catechin Metabolite Products.



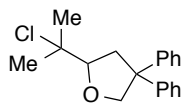
**5-(3,4-dihydroxybenzyl)dihydrofuran-2(3H)-one (D33):** The title compound was prepared by dissolving 5-(3,4-bis((*tert*-butyldimethylsilyl)oxy)benzyl)dihydrofuran-2(3H)-one (48 mg, 0.110 mmol) in 1 mL 3M Methanolic HCl. The reaction was stirred under  $\text{N}_2$  for 15 hours, then concentrated by rotary evaporation. The material was dissolved in dichloromethane, and concentrated directly onto silica gel.

The material was chromatographed with a gradient of 40-75% EtOAc/Hexanes to afford the product as a white solid. (22 mg, .106 mmol, 96%). Characterization matches published data<sup>13</sup>. **<sup>1</sup>H NMR** (600 MHz, Acetonitrile-*d*<sub>3</sub>)  $\delta$  6.49 (d, *J* = 8.0 Hz, 1H), 6.46 (d, *J* = 2.1 Hz, 1H), 6.38 - 6.33 (m, 2H), 6.31 (s, 1H), 4.39 (m, 1H), 2.59 (dd, *J* = 14.1, 6.9 Hz, 1H), 2.52 (dd, *J* = 14.1, 5.9 Hz, 1H), 2.22 - 2.13 (m, 1H), 2.07 (m, 1H), 2.00 - 1.93 (m, 1H), 1.71 - 1.57 (m, 3H). **<sup>13</sup>C NMR** (151 MHz, CD<sub>3</sub>CN)  $\delta$  178.19, 145.32, 144.14, 130.03, 122.07, 117.28, 116.13, 82.06, 41.07, 29.18, 27.74.



**5-(4-hydroxy-3-methoxybenzyl)dihydrofuran-2(3H)-one (D34):** 5-(4-(benzyloxy)-3-methoxybenzyl)dihydrofuran-2(3H)-one (68 mg, 0.22 mmol) was dissolved in 1.0 mL 1M methanolic HCl, and to the solution was added 10 mg 10% Palladium on charcoal (wet). A septum cap was added to the top of the vial, and the reaction was sparged with a balloon of hydrogen for 15 min. The inlet needle was raised above the reaction surface and the vent needle removed, and the reaction was stirred under the atmosphere of hydrogen for 15 hr. The reaction was eluted through a plug of celite, then concentrated. The residue was dissolved in dichloromethane and concentrated directly onto silica gel. The material was chromatographed with a gradient of 20-40% EtOAc/Hexanes, affording the title compound as a white solid. Characterization matches published data<sup>14</sup>. **<sup>1</sup>H NMR** (600 MHz, Chloroform-*d*)  $\delta$  6.85 (d, *J* = 8.0 Hz, 1H), 6.73 (d, *J* = 1.9 Hz, 1H), 6.70 (dd, *J* = 8.0, 2.0 Hz, 1H), 5.60 (s, 1H), 4.78 - 4.66 (m, 1H), 3.87 (s, 3H), 2.95 (dd, *J* = 14.2, 5.8 Hz, 1H), 2.89 (dd, *J* = 14.2, 5.9 Hz, 1H), 2.48 - 2.39 (m, 1H), 2.36 - 2.27 (m, 1H), 2.27 - 2.20 (m, 1H), 1.98 - 1.90 (m, 1H). **<sup>13</sup>C NMR** (151 MHz, CDCl<sub>3</sub>)  $\delta$  177.18, 146.51, 144.61, 127.53, 122.14, 114.37, 111.99, 80.87, 55.93, 40.83, 28.62, 26.80.

#### A1.10. Regioselective Oxy-chlorination of an Alkenol.



**2-(2-chloropropan-2-yl)-4,4-diphenyltetrahydrofuran:** 6-methyl-3,3-diphenylhept-5-en-2-ol (100 mg, 0.3776 mmol, 1.0 equiv.), *p*-toluenesulfonyl chloride (79 mg, 0.414 mmol, 1.1 equiv.), and 9-mesityl,10-methylacridinium tetrafluoroborate (7.5 mg, 0.019 mmol, 0.05 equiv.) were combined in a 1-dram vial, sealed with a septum cap. The reaction was pumped into a glovebox with a nitrogen atmosphere, and 1,2-dichloroethane (0.7 mL) was added to the vial. The vial was sealed, removed from the glovebox, and irradiated for 15 hours with an Ecoxotic PAR38 blue LED floodlamp. The reaction was removed from light, concentrated onto silica gel, and purified by chromatography eluting with 1-2% EtOAc/Hexanes. Product was a slightly yellow oil. Yield: 89 mg (79%). Analytical data for 2-(2-chloropropan-2-yl)-4,4-diphenyltetrahydrofuran: **<sup>1</sup>H NMR** (600 MHz, Chloroform-*d*)  $\delta$  7.38 (d,  $J$  = 7.6 Hz, 2H), 7.33 (t,  $J$  = 7.4 Hz, 4H), 7.28 - 7.21 (m, 4H), 4.81 (d,  $J$  = 8.7 Hz, 1H), 4.14 (d,  $J$  = 8.6 Hz, 1H), 4.00 (dd,  $J$  = 10.0, 5.8 Hz, 1H), 2.76 (dd,  $J$  = 12.2, 10.0 Hz, 1H), 2.62 (dd,  $J$  = 12.1, 5.8 Hz, 1H), 1.64 (s, 3H), 1.57 (s, 3H). **MS** (+ESI): Calculated  $m/z$  for  $[M+H]^+$  = 301.13, Found 301.17. **IR** (Thin Film,  $\text{cm}^{-1}$ ): 3059, 2975, 2931, 2869, 1599, 1495, 1446, 1385.

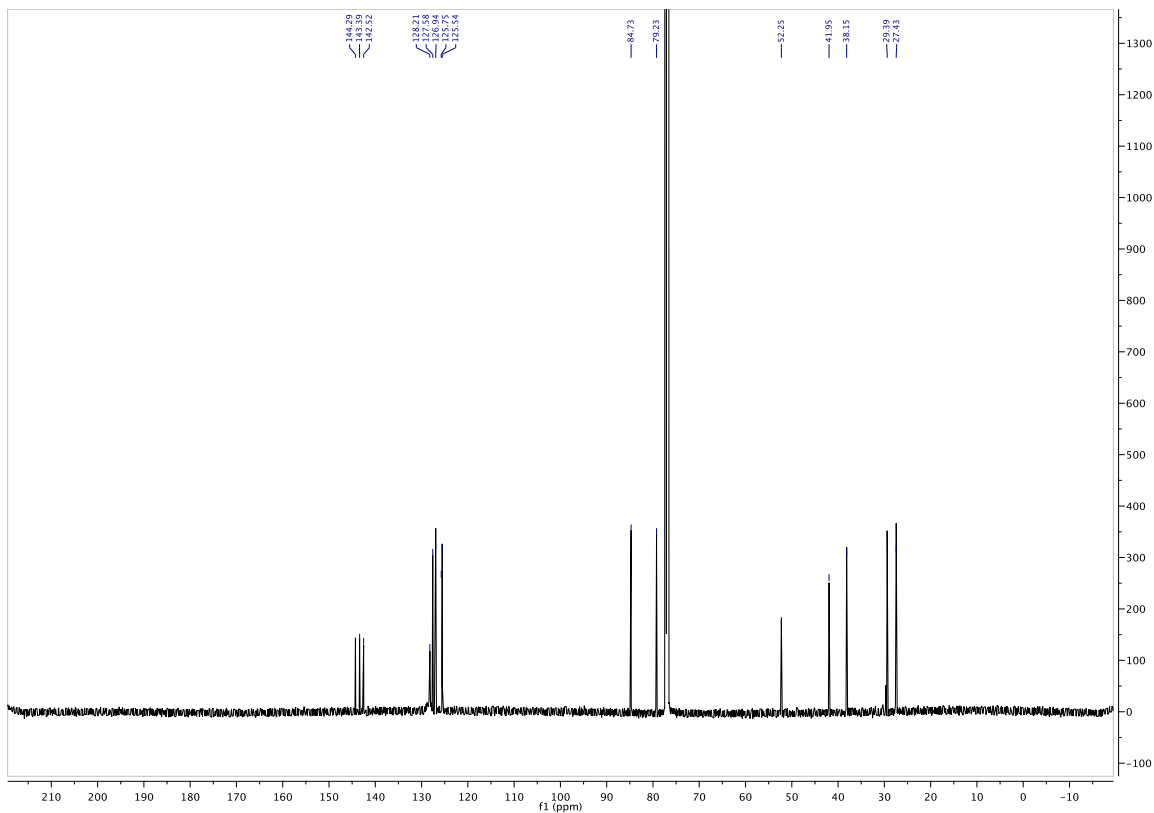
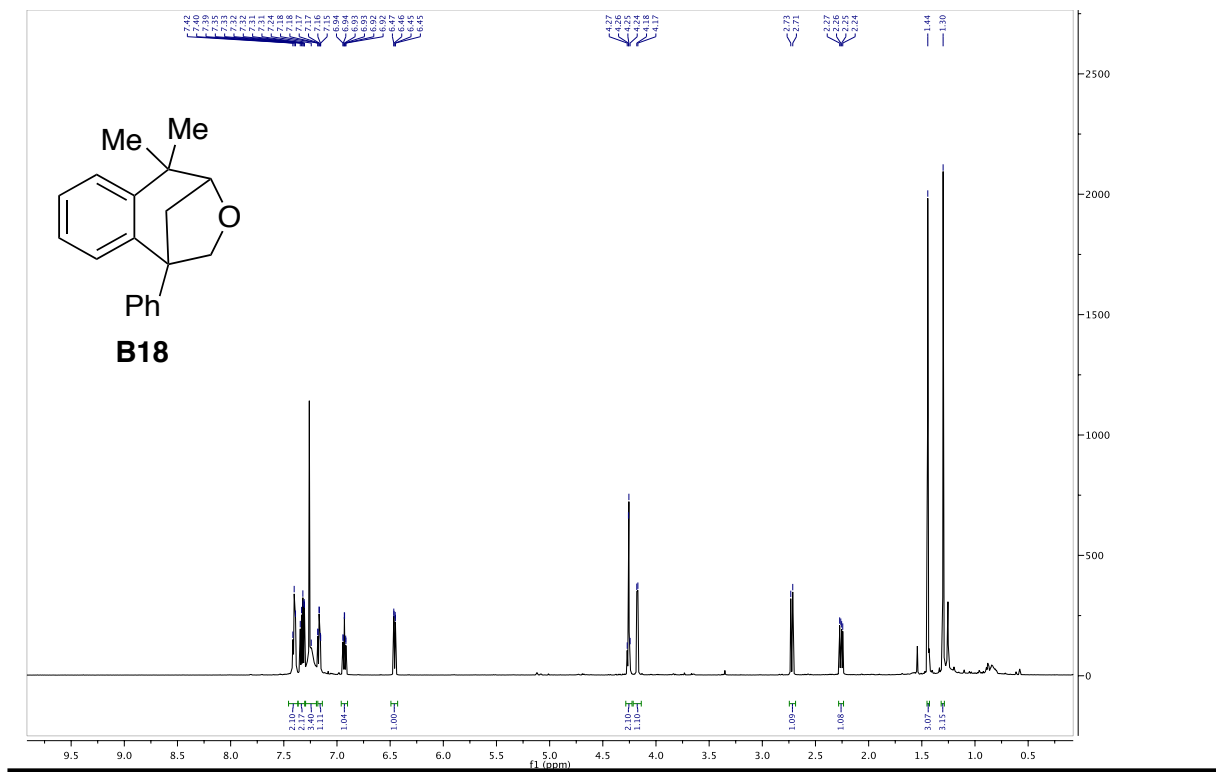
## REFERENCES

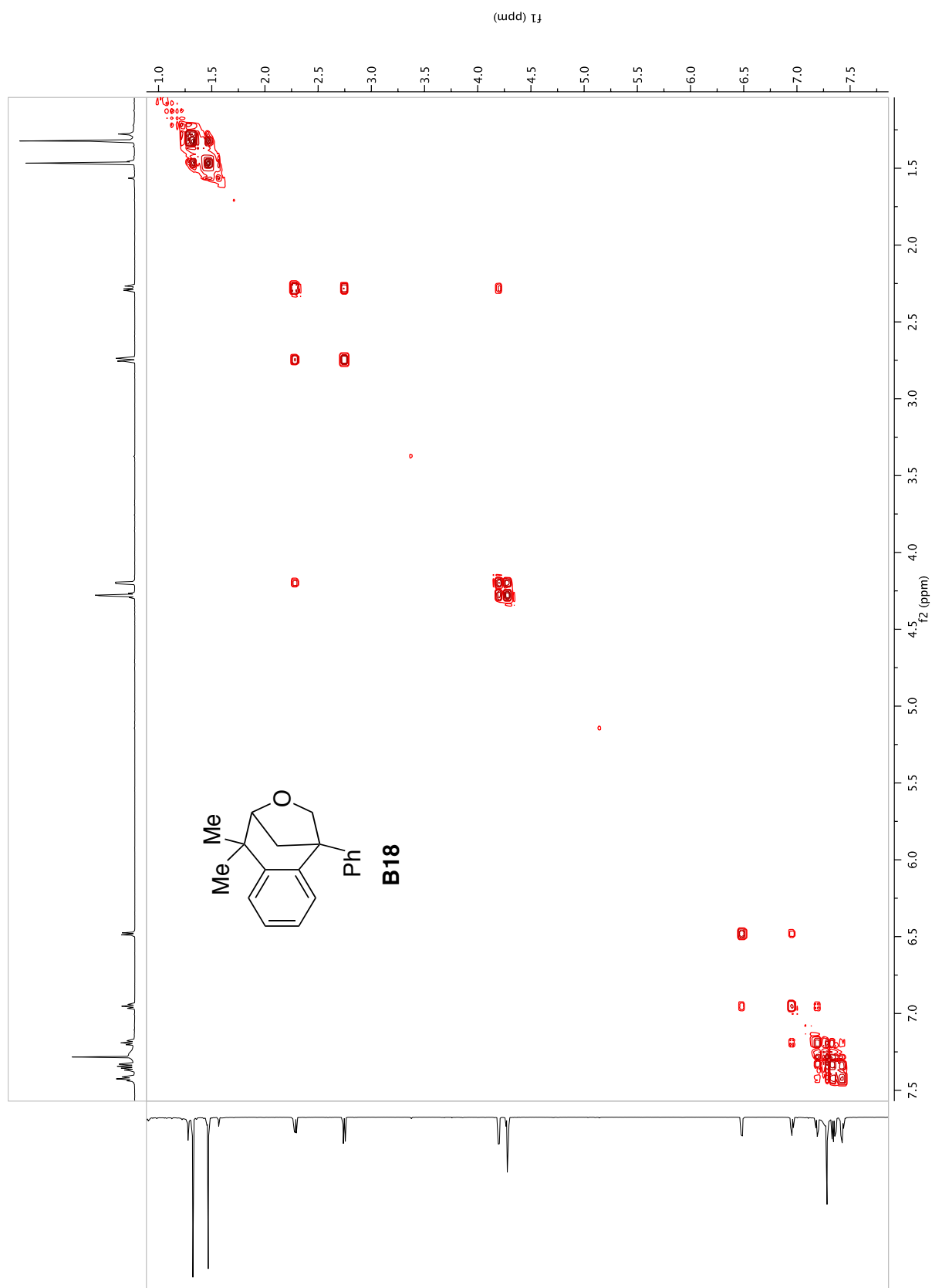
- (1) Hamilton, D. S.; Nicewicz, D. A. Direct Catalytic Anti-Markovnikov Hydroetherification of Alkenols. *J. Am. Chem. Soc.* **2012**, *134*, 18577–18580.
- (2) Jarboe, S. G.; Beak, P. Mechanism of Oxygen Transfer in the Epoxidation of an Olefin by Molecular Oxygen in the Presence of an Aldehyde. *Org. Lett.* **2000**, *2*, 357–360.
- (3) Jeong, Y.; Kim, D.-Y.; Choi, Y.; Ryu, J.-S. Intramolecular Hydroalkoxylation in Brønsted Acidic Ionic Liquids and Its Application to the Synthesis of (±)-Centrolobine. *Org. Biomol. Chem.* **2010**, *9*, 374–378.
- (4) Reynolds, N. T.; Rovis, T. The Effect of Pre-Existing Stereocenters in the Intramolecular Asymmetric Stetter Reaction. *Tetrahedron* **2005**, *61*, 6368–6378.
- (5) Protti, S.; Dondi, D.; Fagnoni, M.; Albini, A. Photochemical Arylation of Alkenols: Role of Intermediates and Synthetic Significance. *Eur. J. Org. Chem.* **2008**, *2008*, 2240–2247.
- (6) Protti, S.; Fagnoni, M.; Albini, A. Benzyl (Phenyl)  $\Gamma$ - and  $\Delta$ -Lactones via Photoinduced Tandem Ar–C, C–O Bond Formation. *J. Am. Chem. Soc.* **2006**, *128*, 10670–10671.
- (7) Abul Hashem, M.; Weyerstahl, P. Reactivity of 1-Cyclopropene-1-Lactones Dependent on the Substitution Degree. *Tetrahedron* **1984**, *40*, 2003–2009.
- (8) Takemiya, A.; Hartwig, J. F. Rhodium-Catalyzed Intramolecular, Anti-Markovnikov Hydroamination. Synthesis of 3-Arylpiperidines. *J. Am. Chem. Soc.* **2006**, *128*, 6042–6043.
- (9) Constant-Urban, C.; Charif, M.; Goffin, E.; Van Heugen, J.-C.; Elmoualij, B.; Chiap, P.; Mouithys-Mickalad, A.; Serteyn, D.; Lebrun, P.; Pirotte, B.; De Tullio, P. Triphenylphosphonium Salts of 1,2,4-Benzothiadiazine 1,1-Dioxides Related to Diazoxide Targeting Mitochondrial ATP-Sensitive Potassium Channels. *Bioorg. Med. Chem. Lett.* **2013**, *23*, 5878–5881.
- (10) Uchiyama, M.; Ozawa, H.; Takuma, K.; Matsumoto, Y.; Yonehara, M.; Hiroya, K.; Sakamoto, T. Regiocontrolled Intramolecular Cyclizations of Carboxylic Acids to Carbon–Carbon Triple Bonds Promoted by Acid or Base Catalyst. *Org. Lett.* **2006**, *8*, 5517–5520.
- (11) Brenzovich, W. E.; Brazeau, J.-F.; Toste, F. D. Gold-Catalyzed Oxidative Coupling Reactions with Aryltrimethylsilanes. *Org. Lett.* **2010**, *12*, 4728–4731.
- (12) Zhang, G.; Cui, L.; Wang, Y.; Zhang, L. Homogeneous Gold-Catalyzed Oxidative Carboheterofunctionalization of Alkenes. *J. Am. Chem. Soc.* **2010**, *132*, 1474–1475.
- (13) Lambert, J. D.; Rice, J. E.; Hong, J.; Hou, Z.; Yang, C. S. Synthesis and Biological Activity of the Tea Catechin Metabolites, M4 and M6 and Their Methoxy-Derivatives. *Bioorg. Med. Chem. Lett.* **2005**, *15*, 873–876.

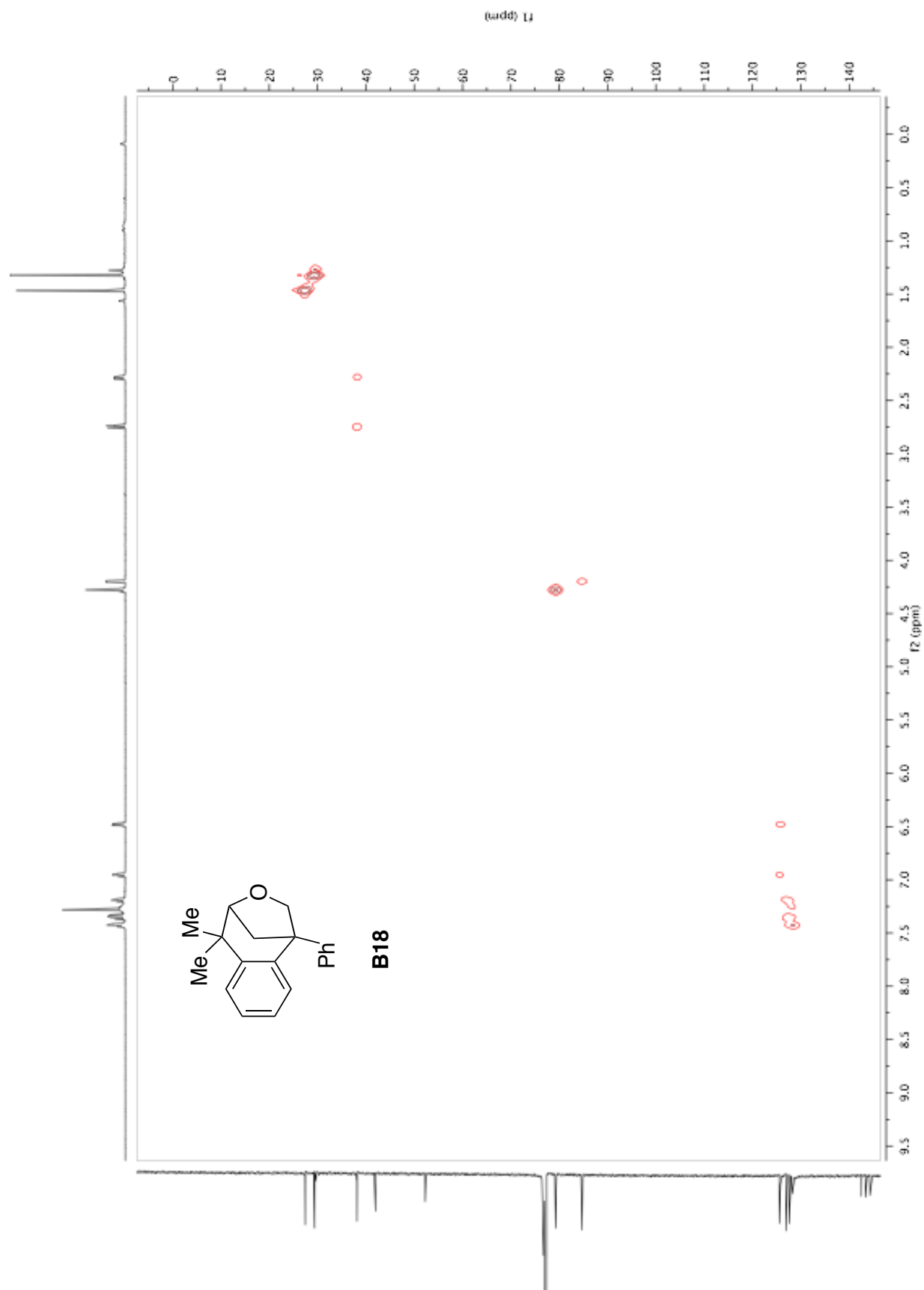


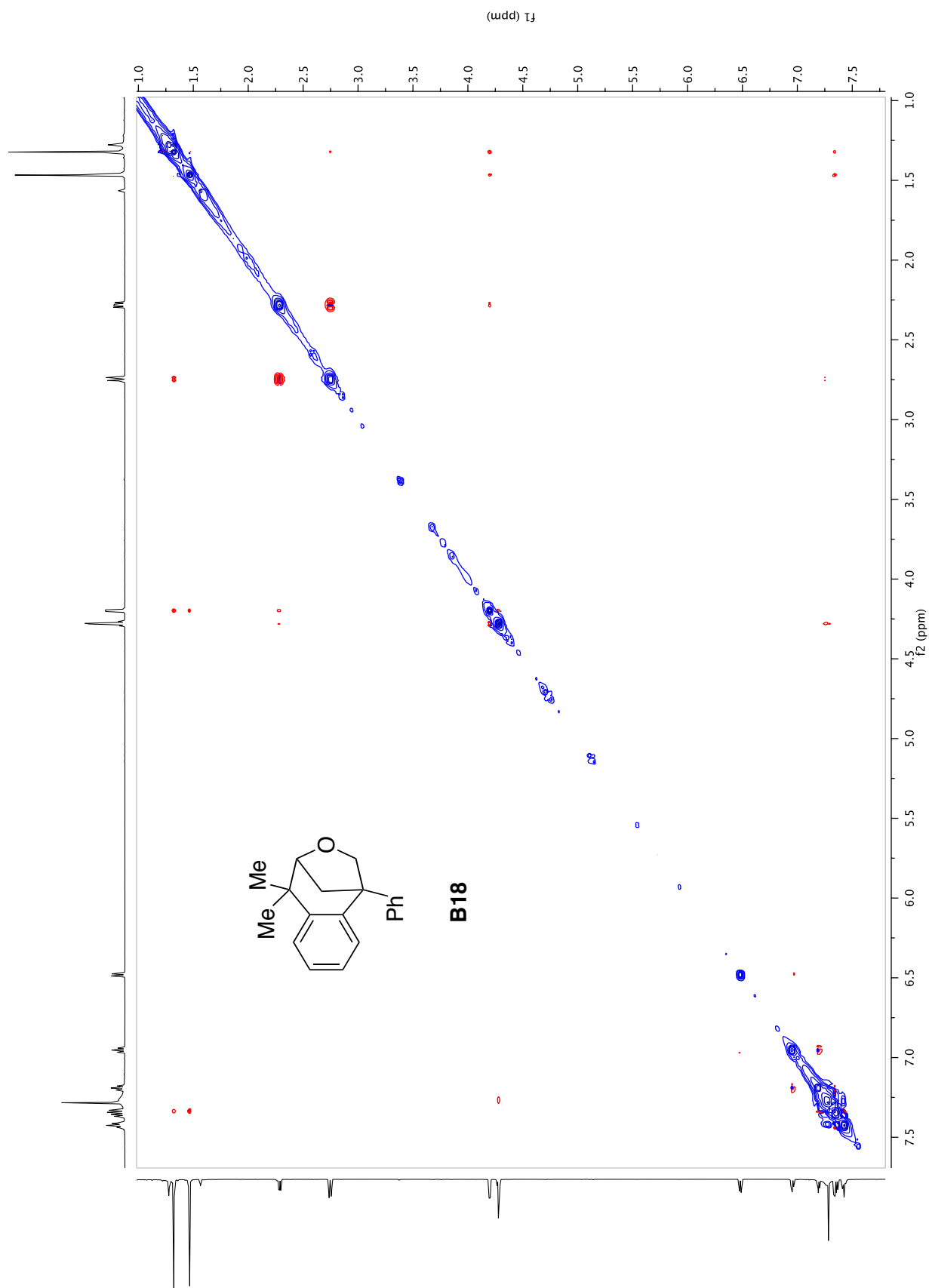
- (14) Chang, X.; Peng, W.; Yao, Y.-F.; Koek, J. Concise Synthesis of Ring-Fission Metabolites of Epicatechin: 5-(3,4-Dihydroxybenzyl)dihydrofuran-2(3H)-One M6. *Synth. Commun.* **2010**, *40*, 3346–3352.

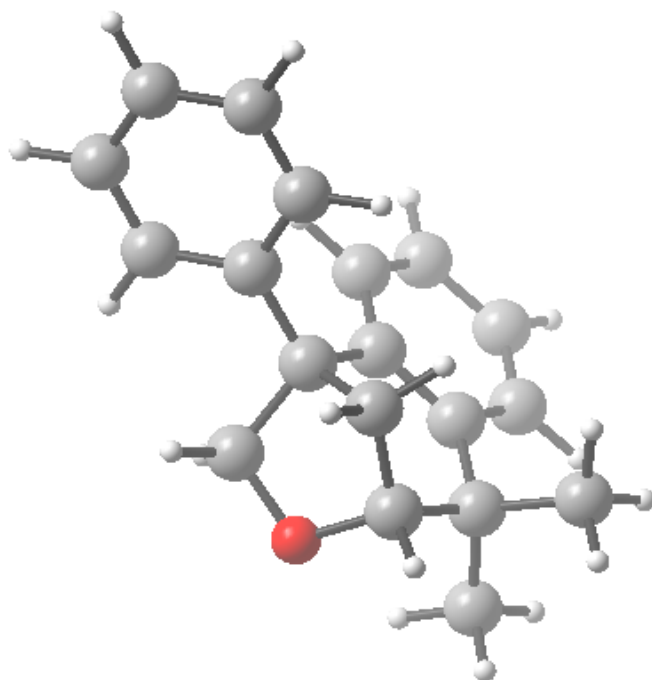
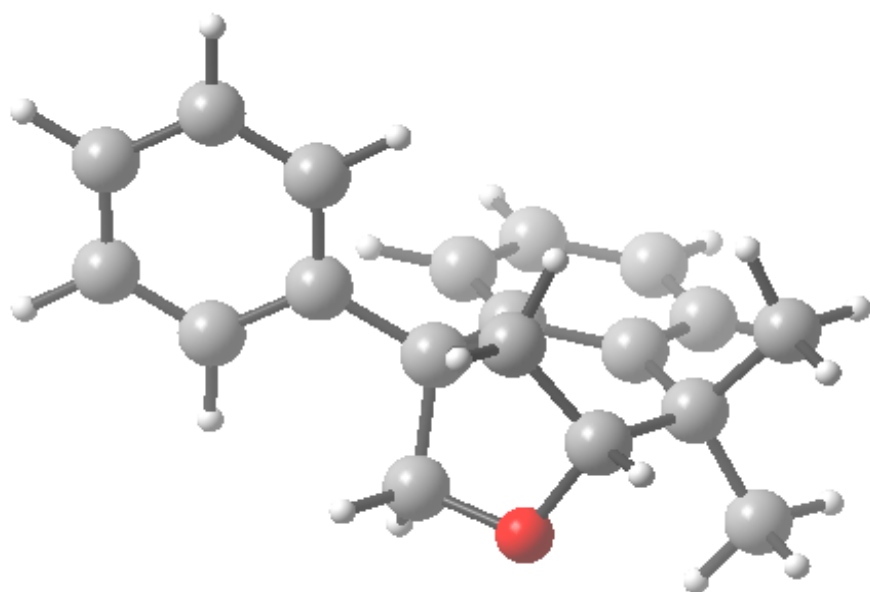
## APPENDIX 2: SELECTED SPECTRA AND VOLTAMMOGRAMS

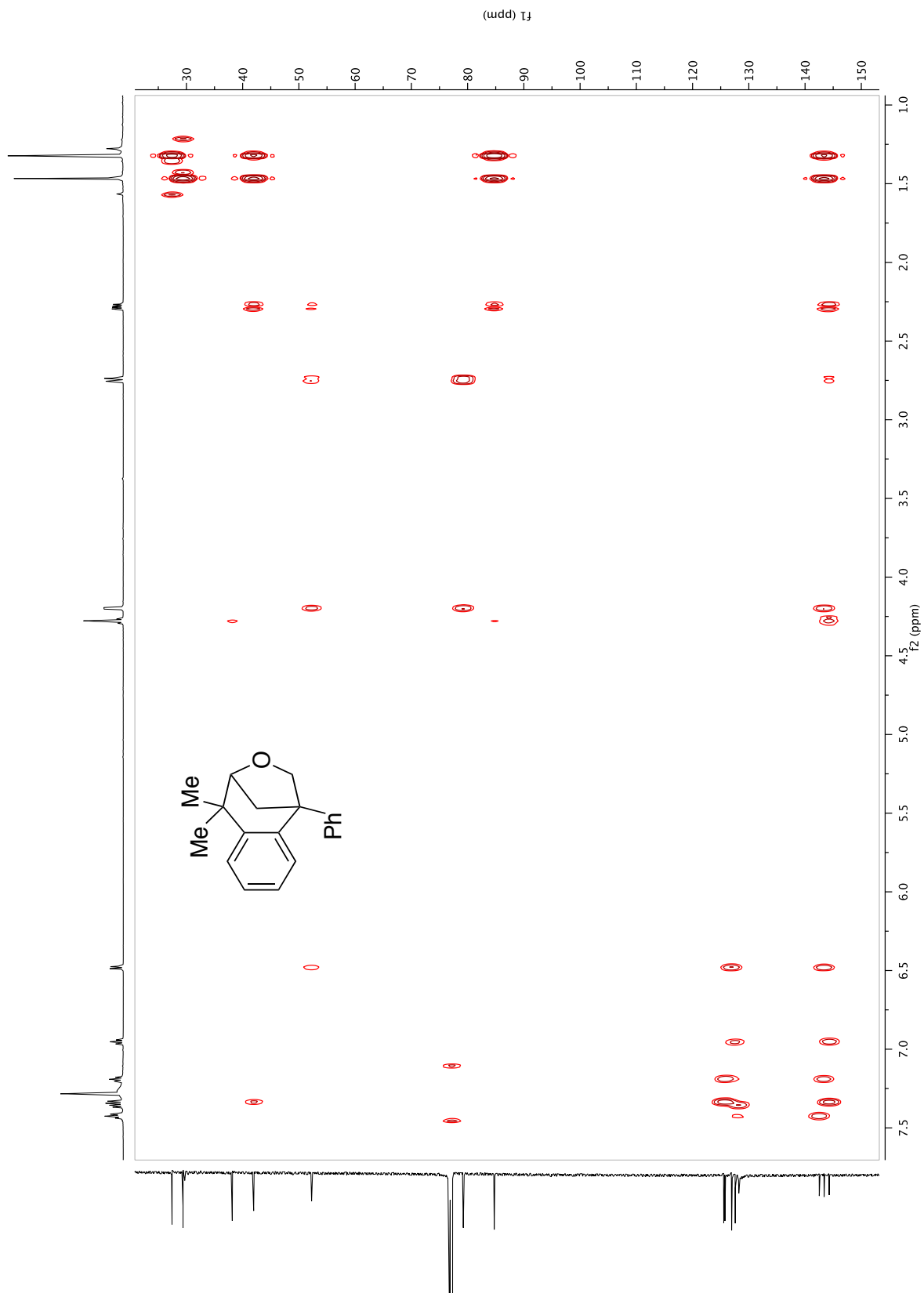


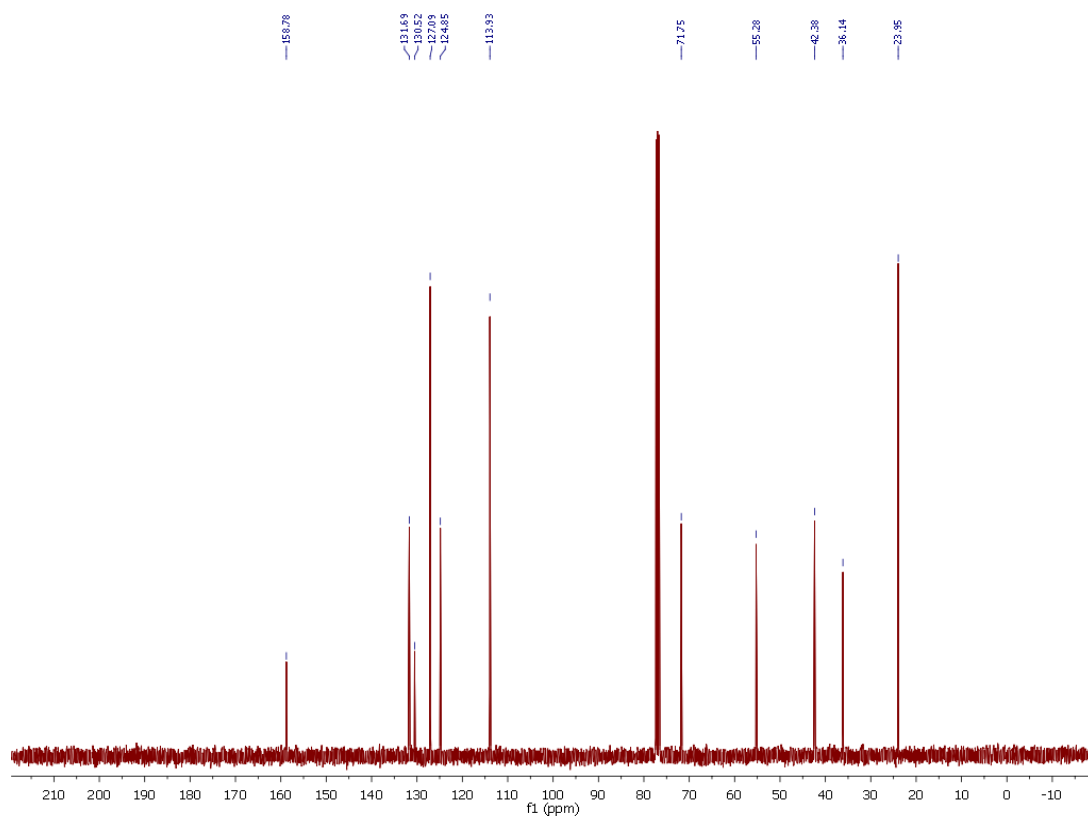
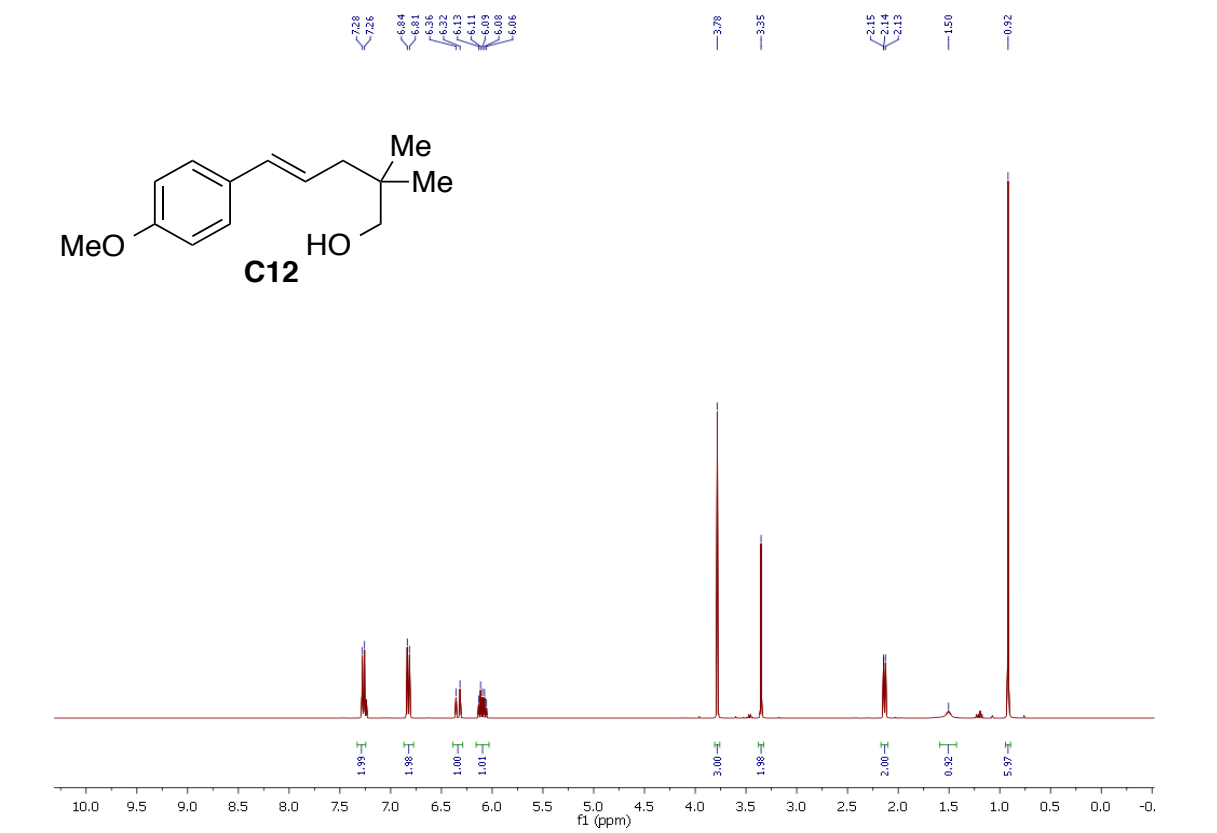




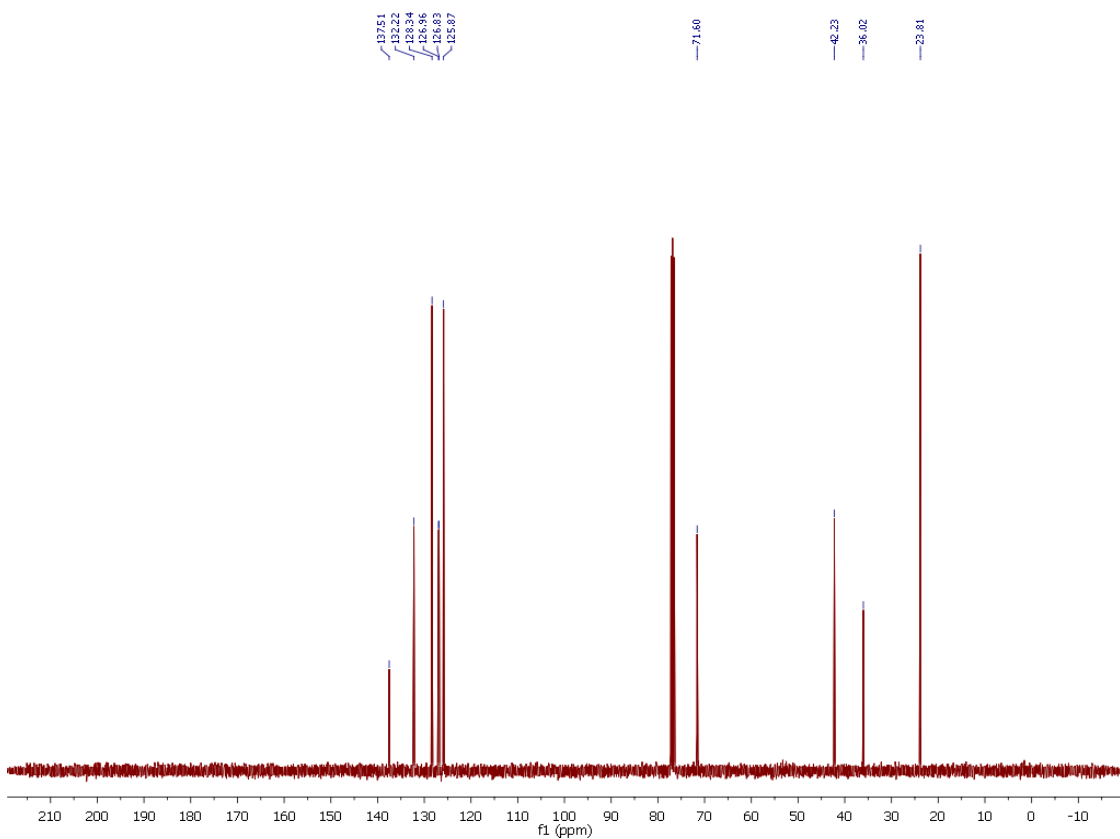
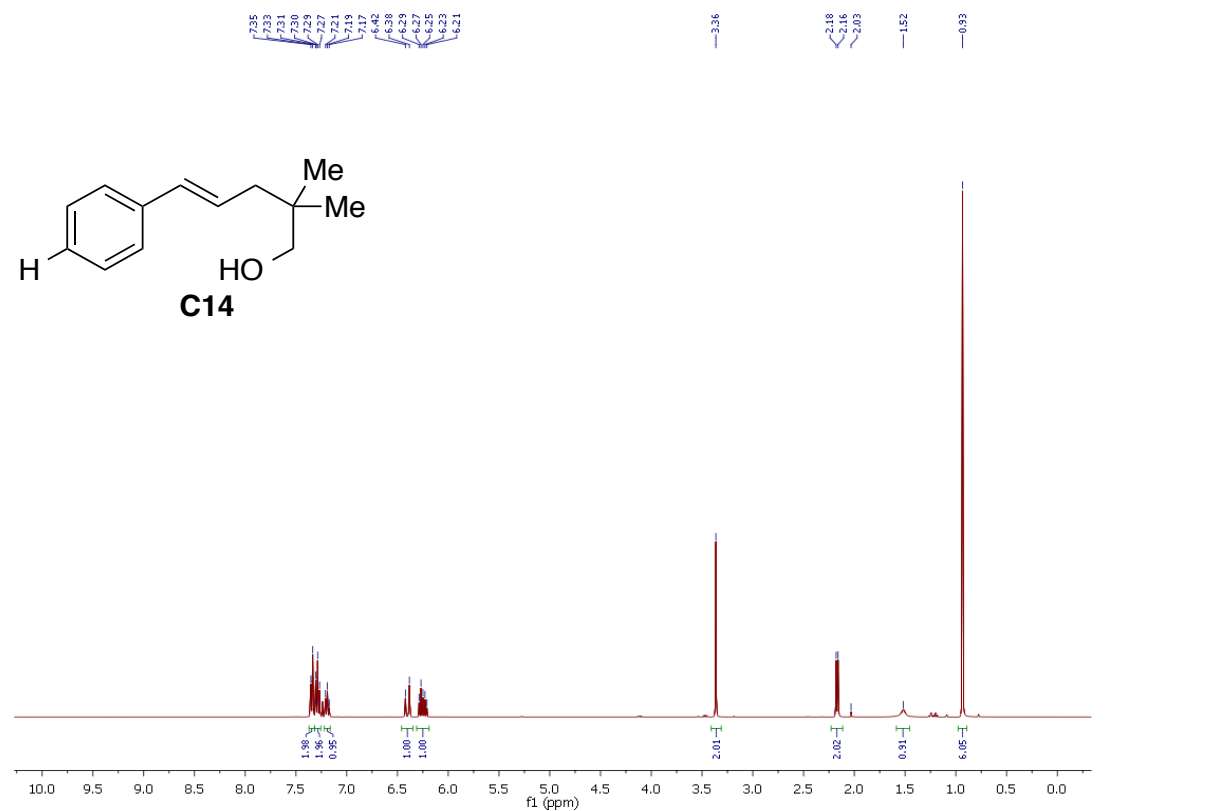


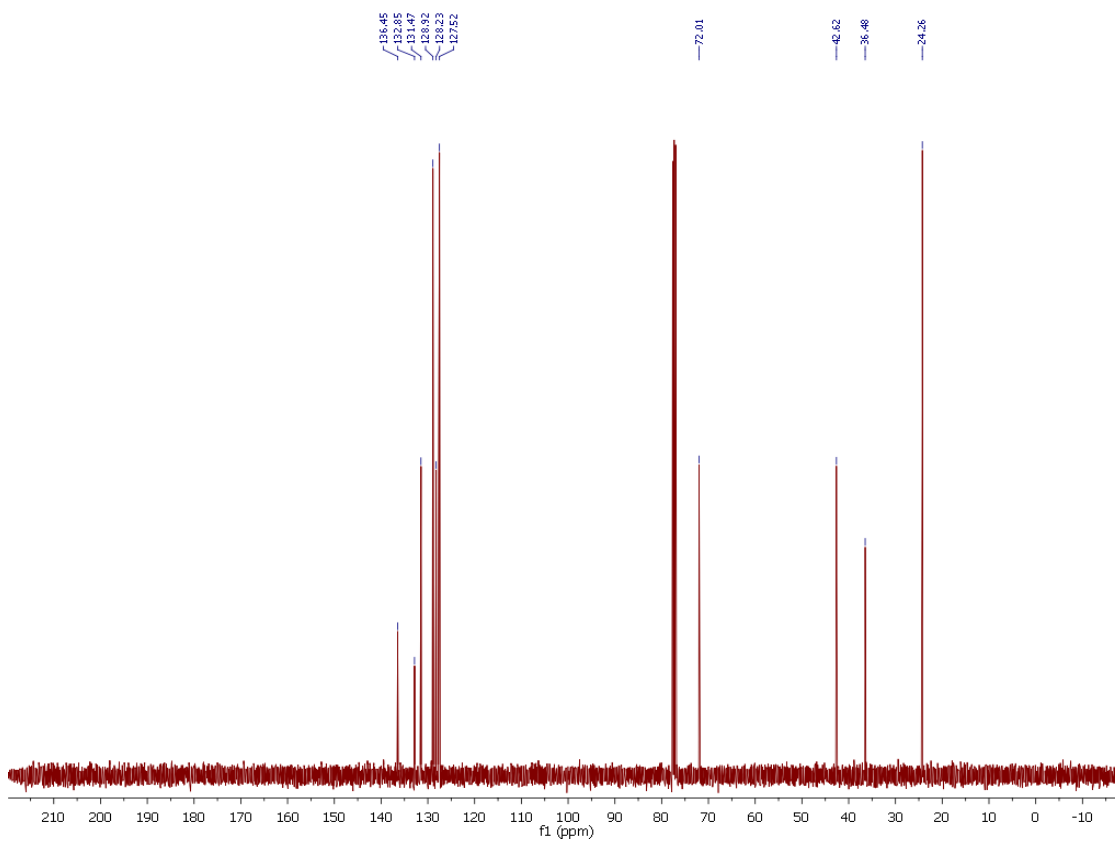
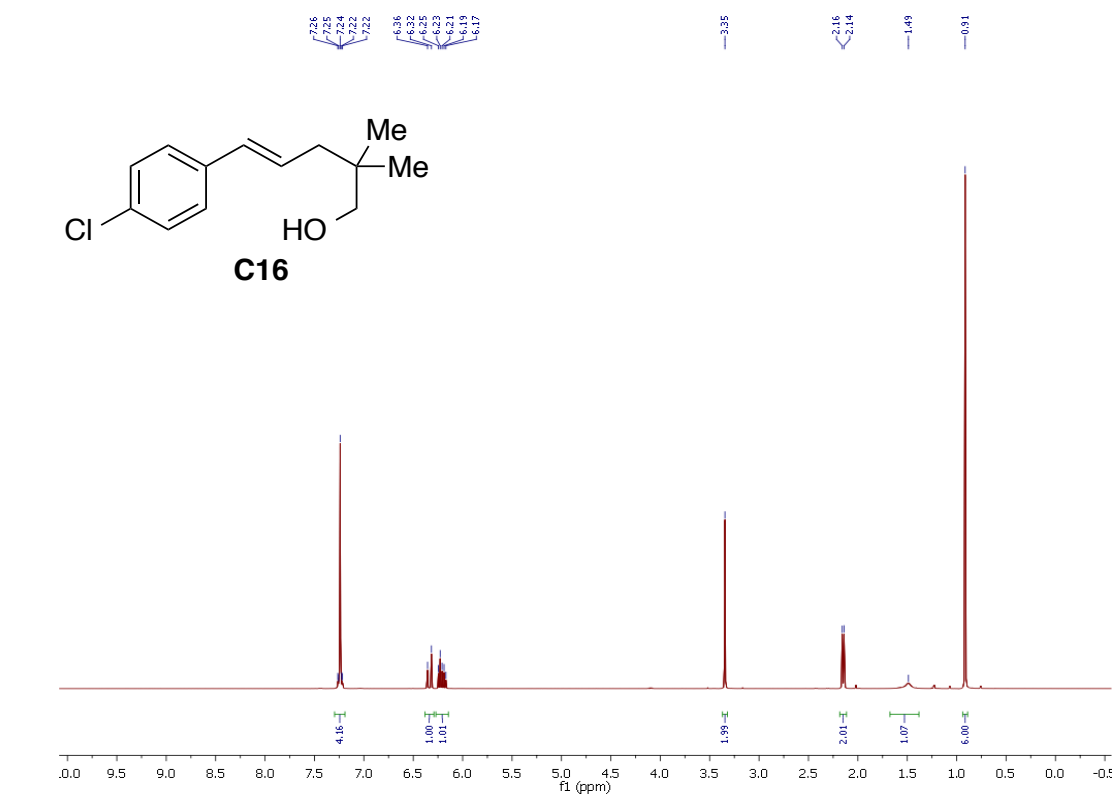


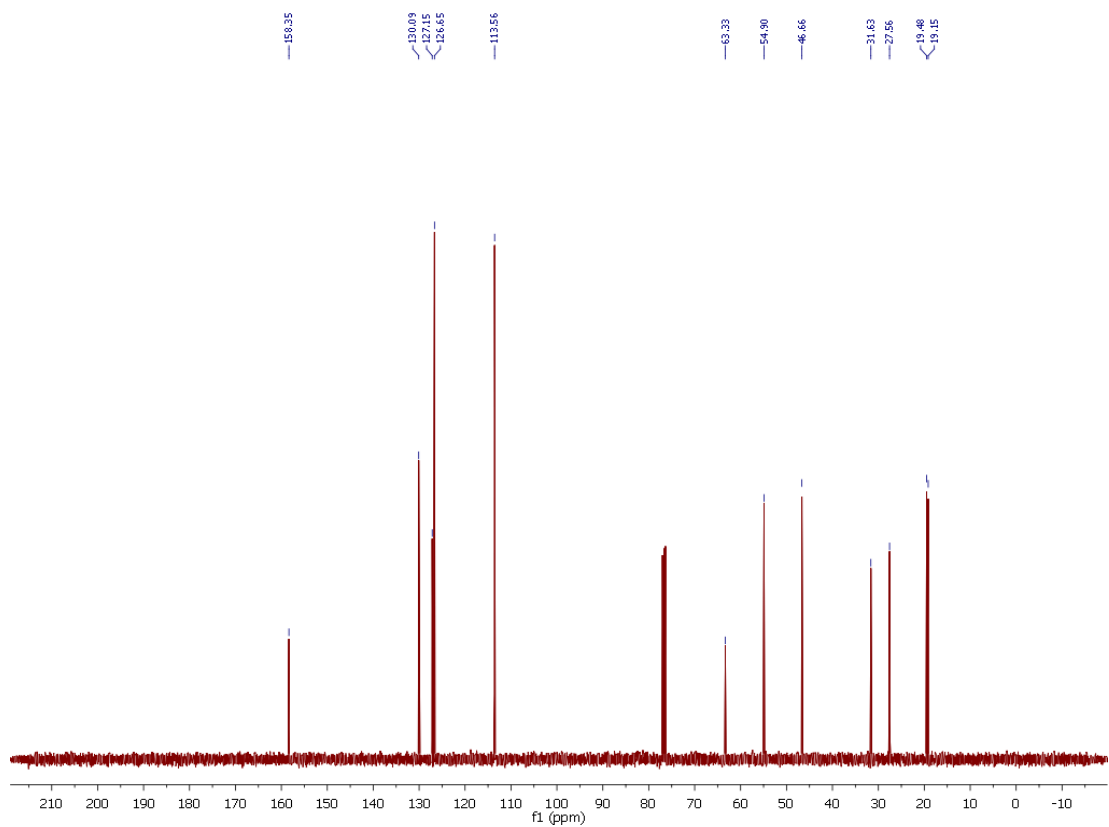
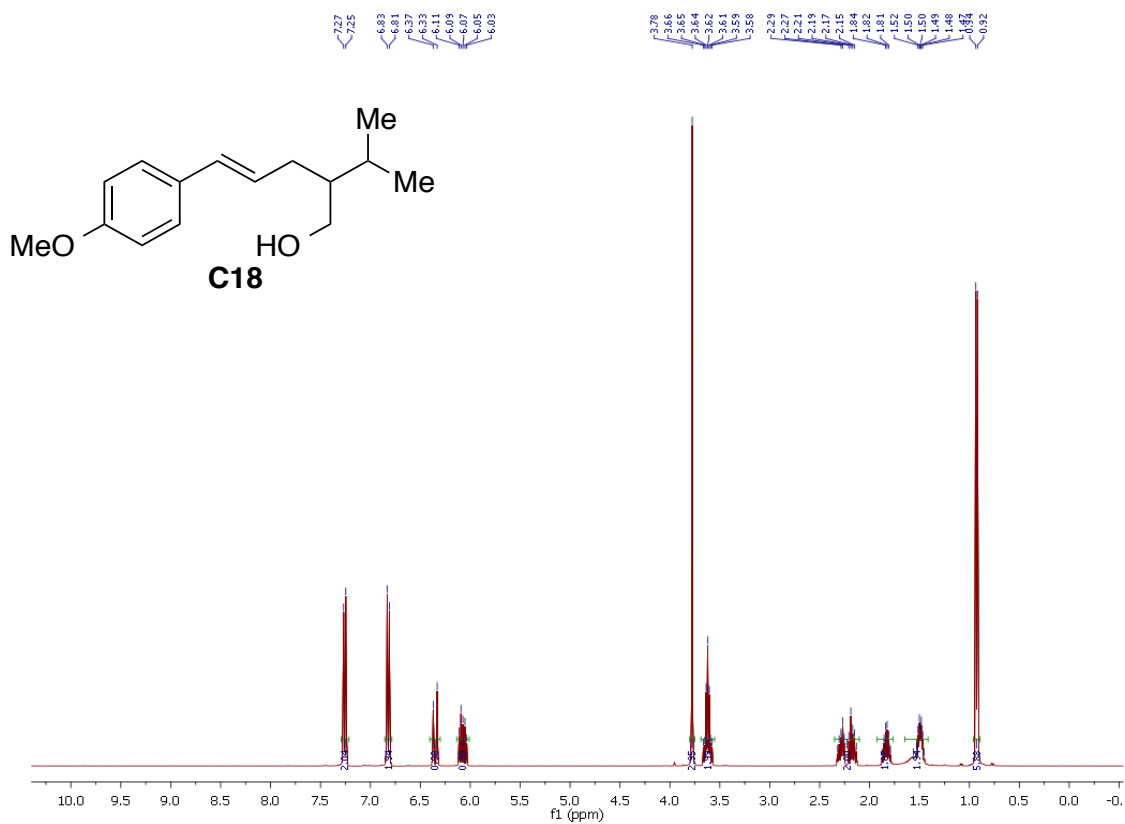


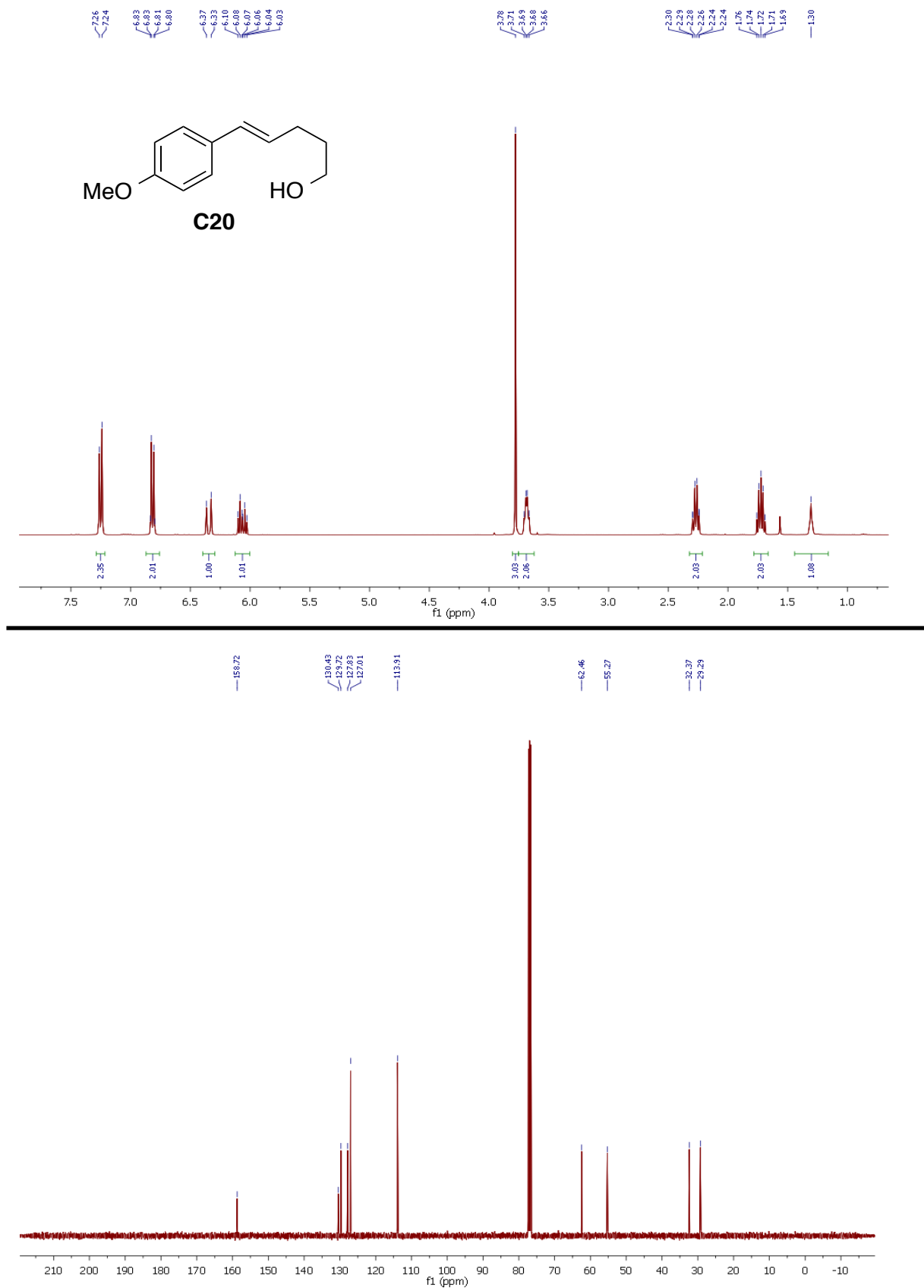


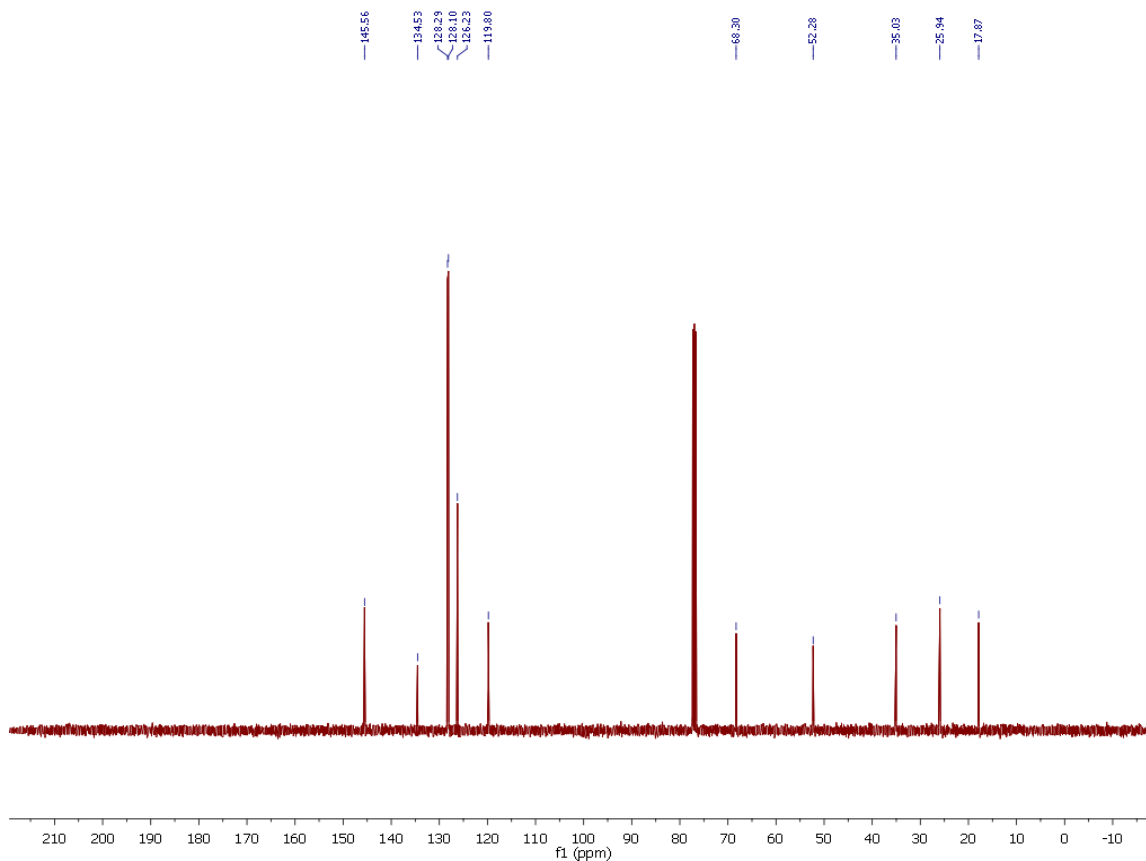
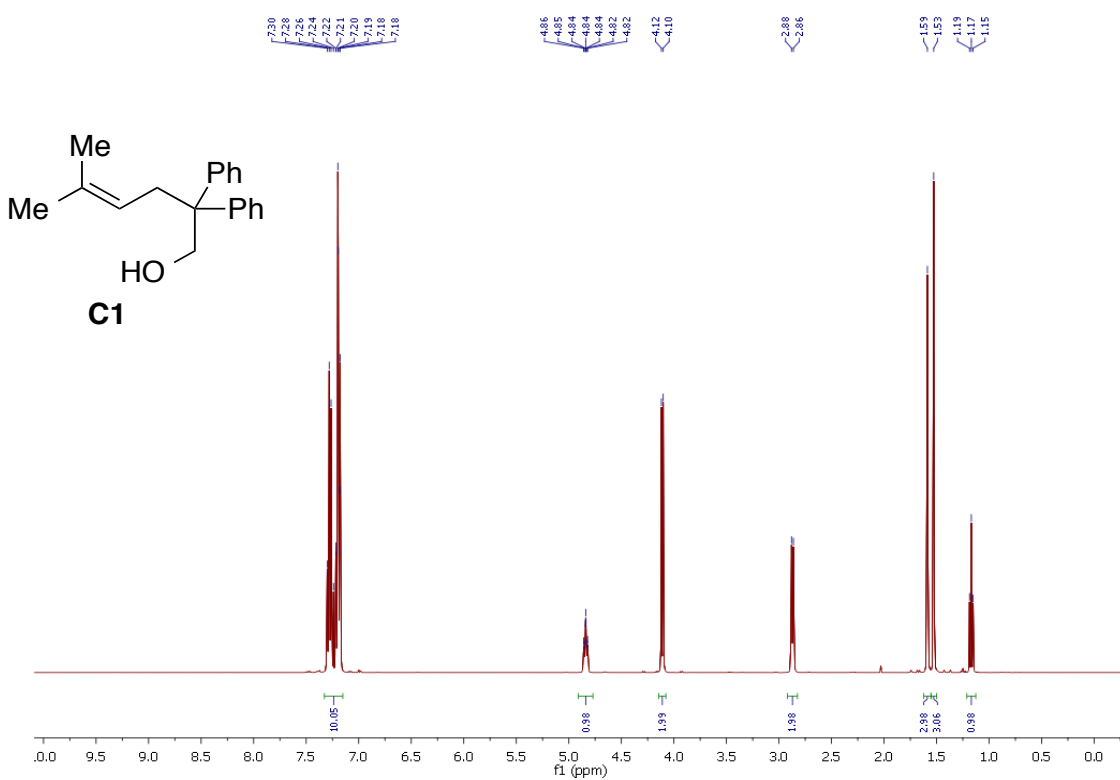


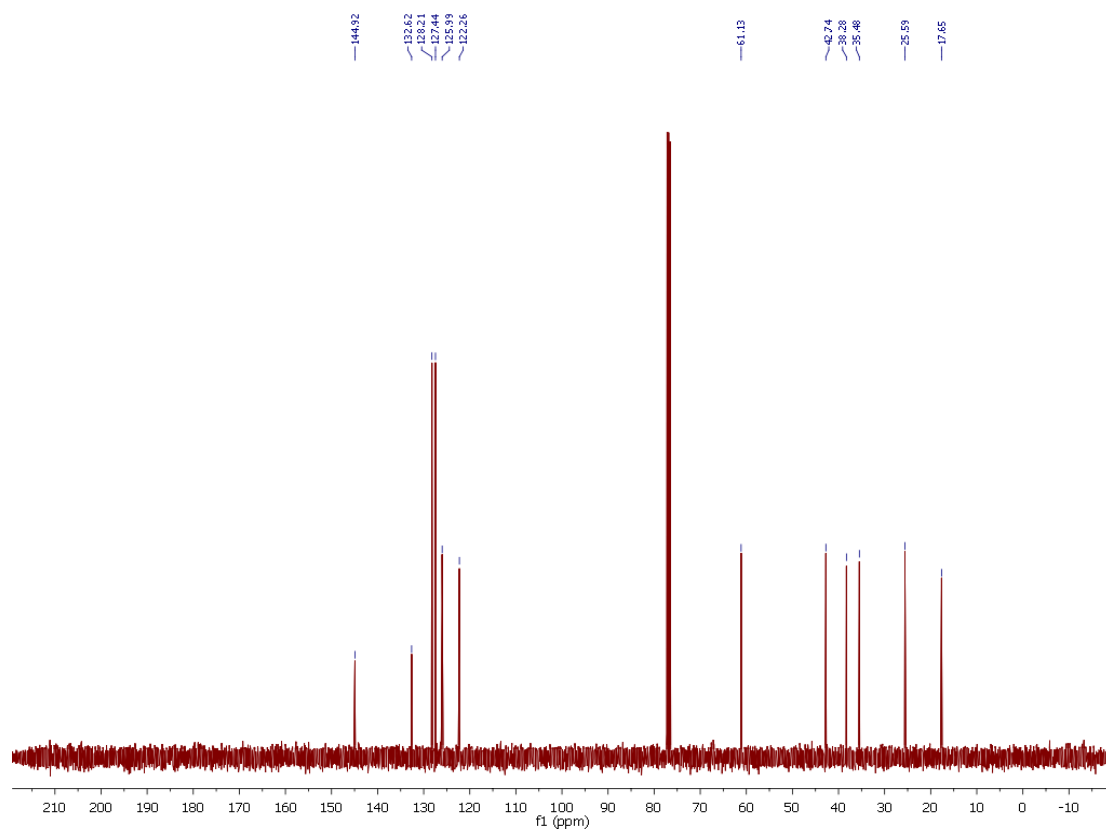
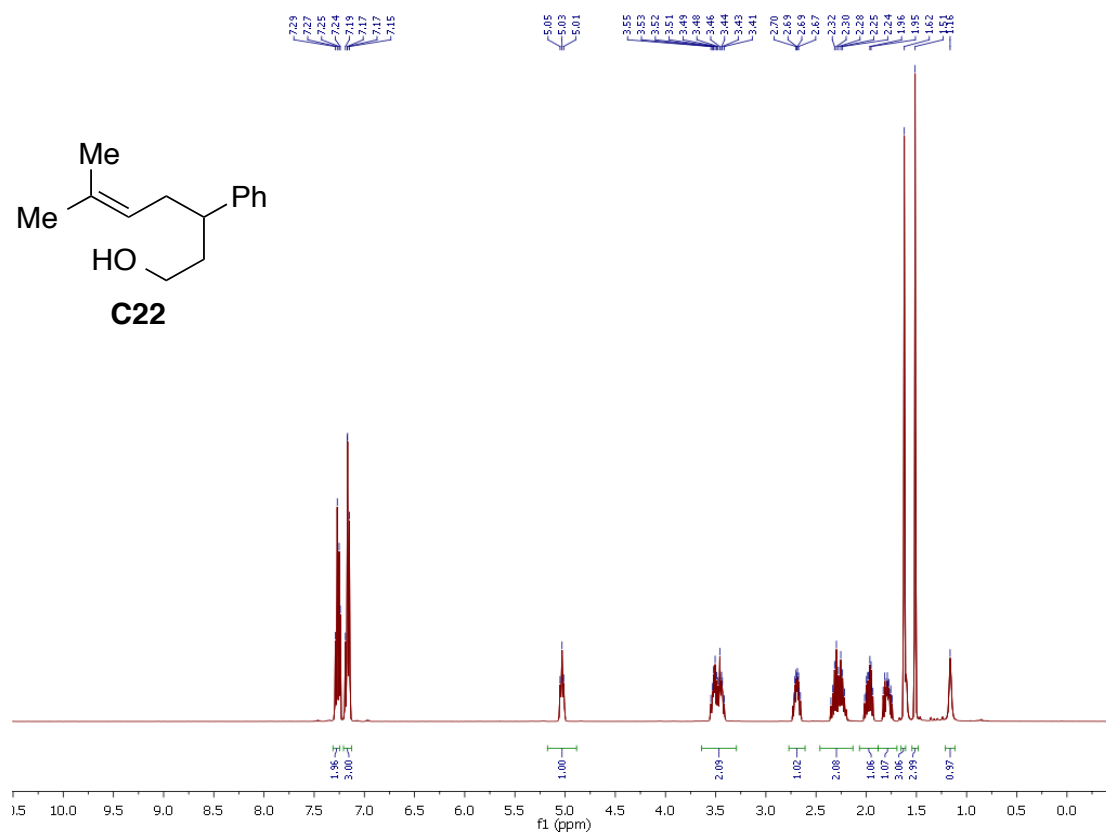
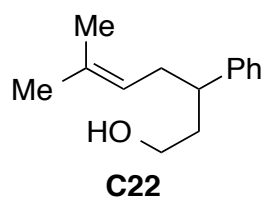


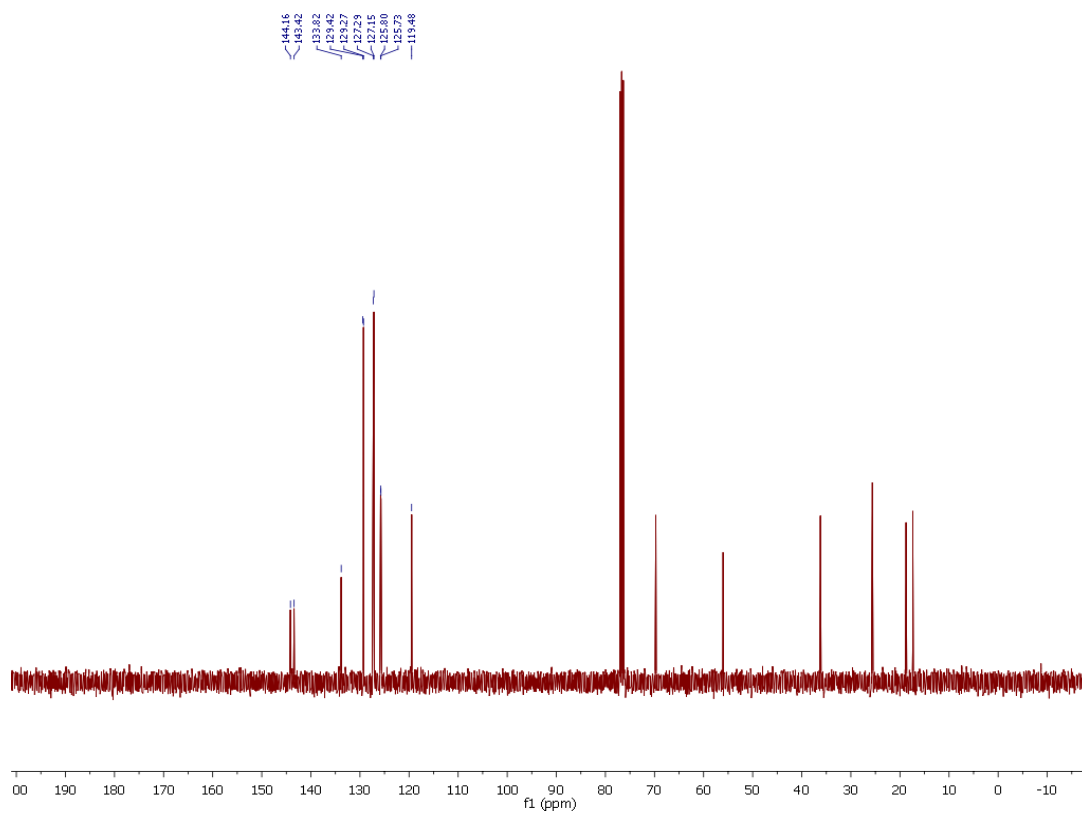
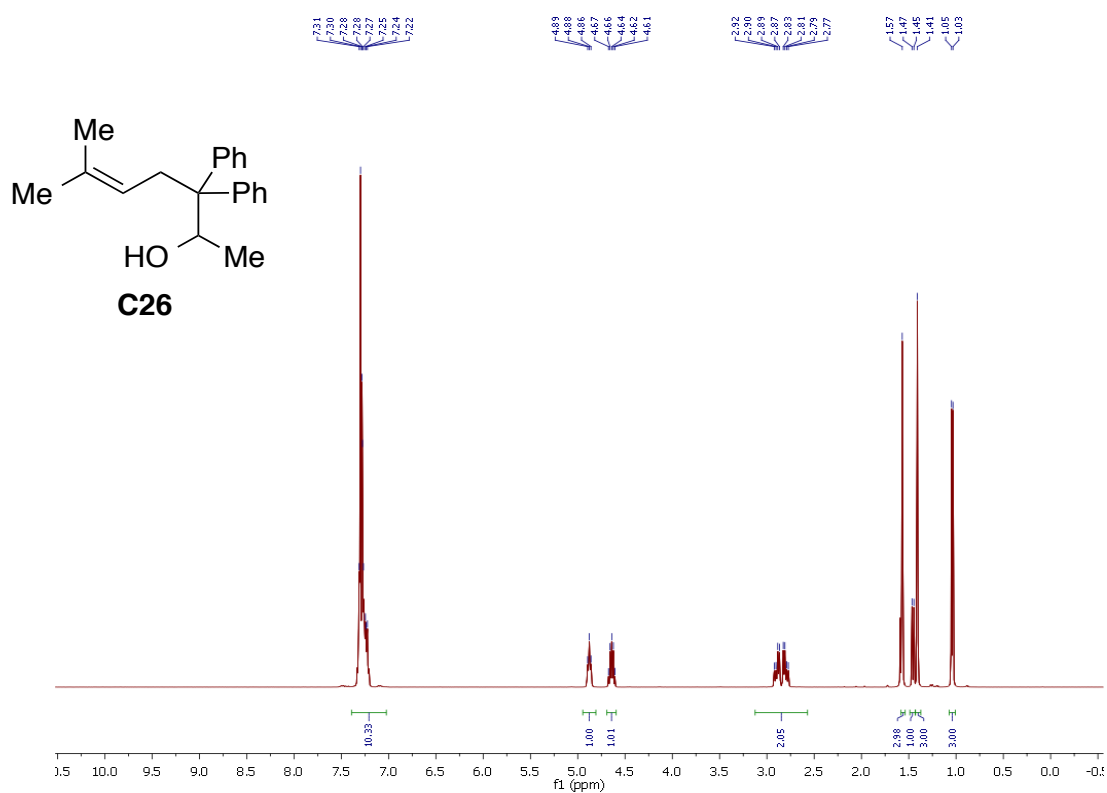


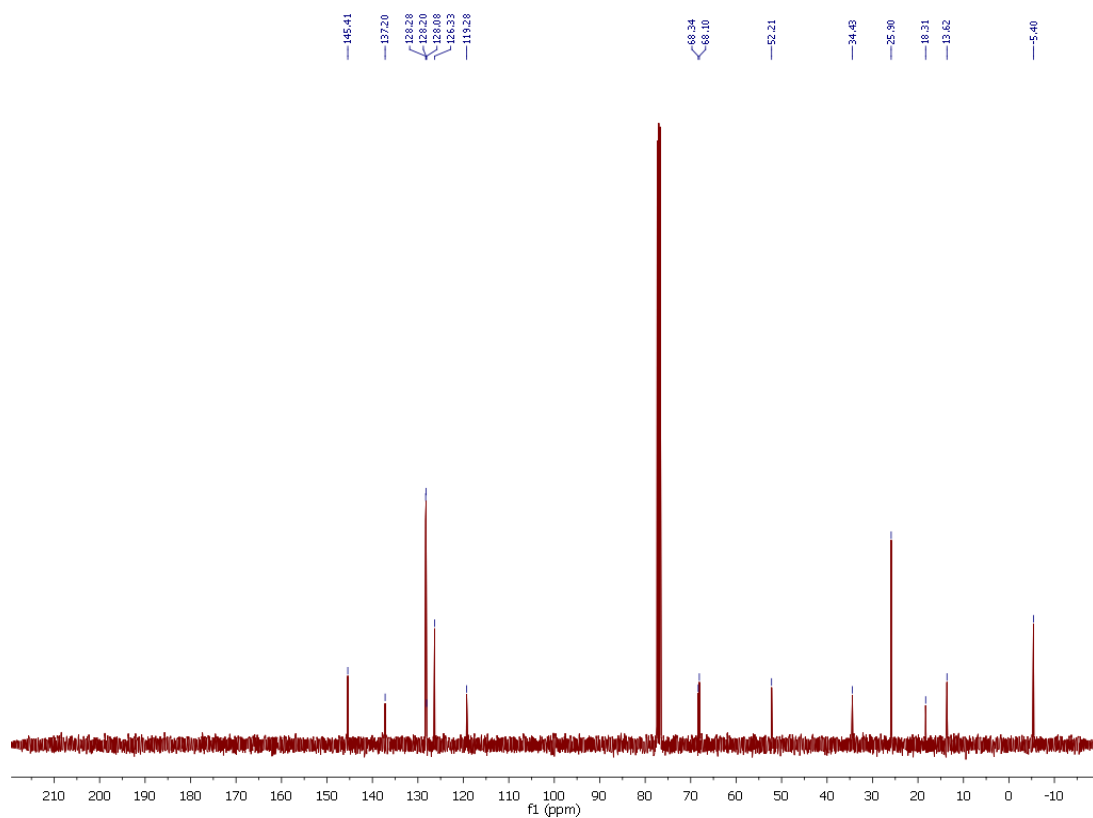
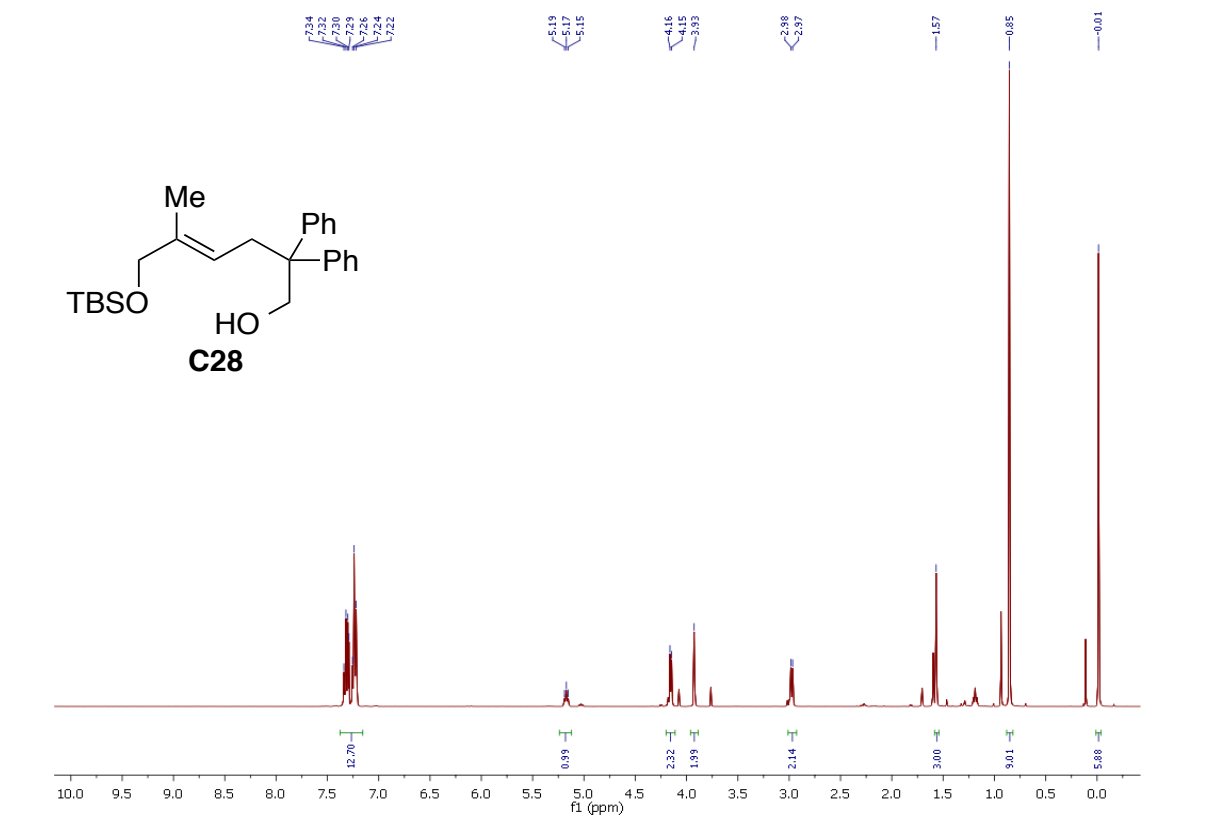




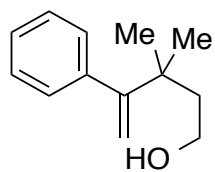




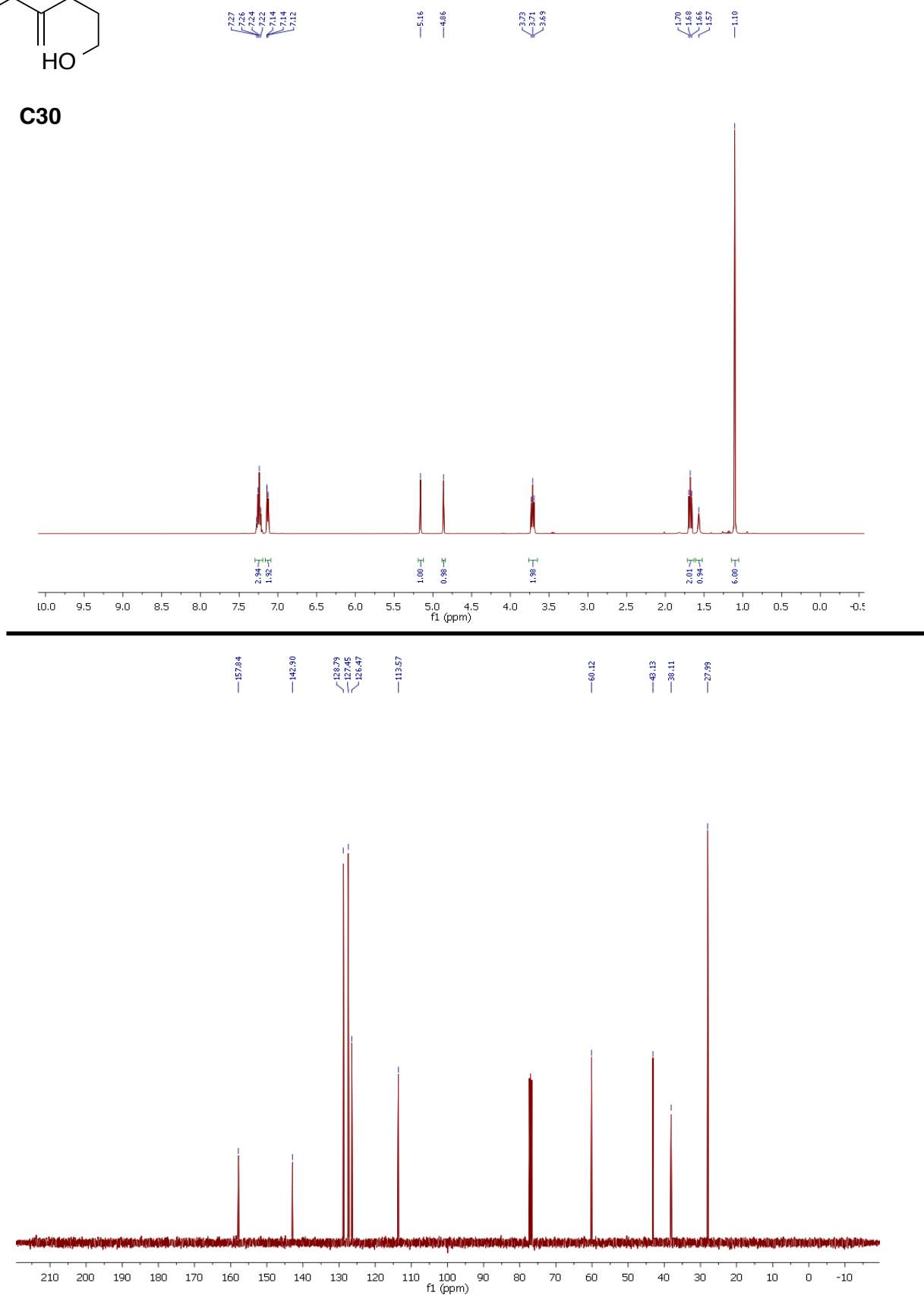


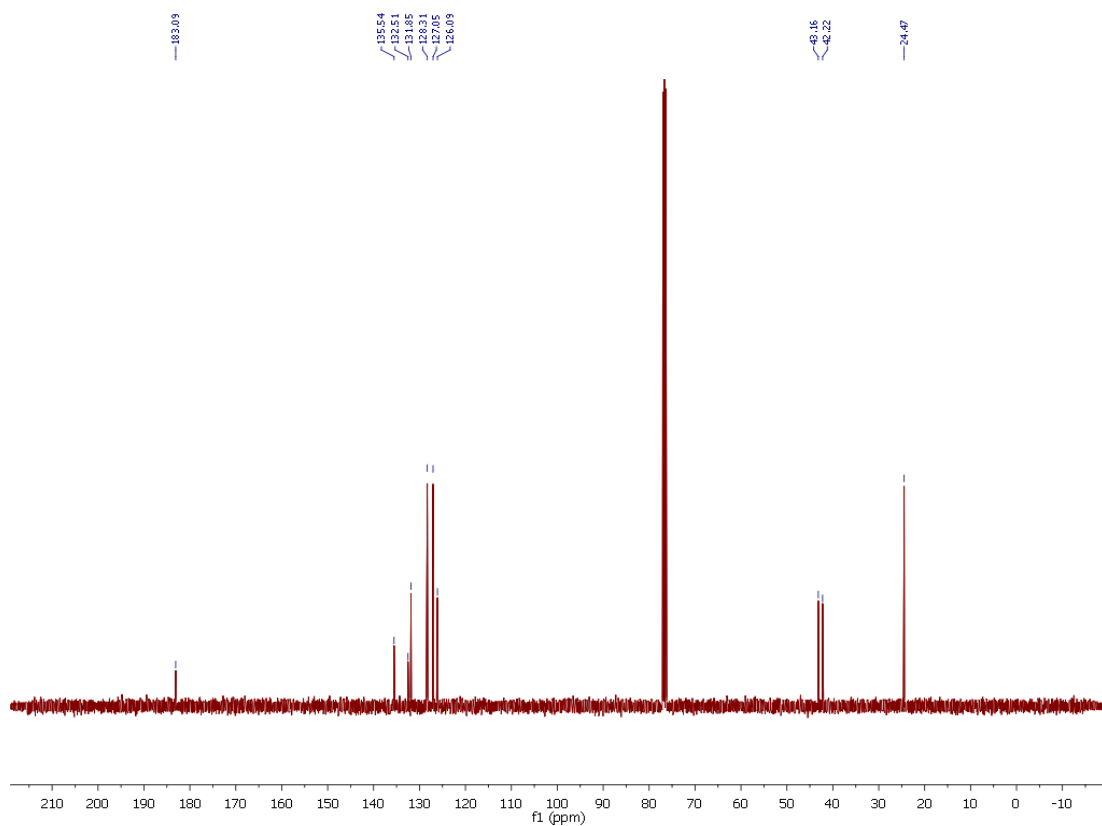
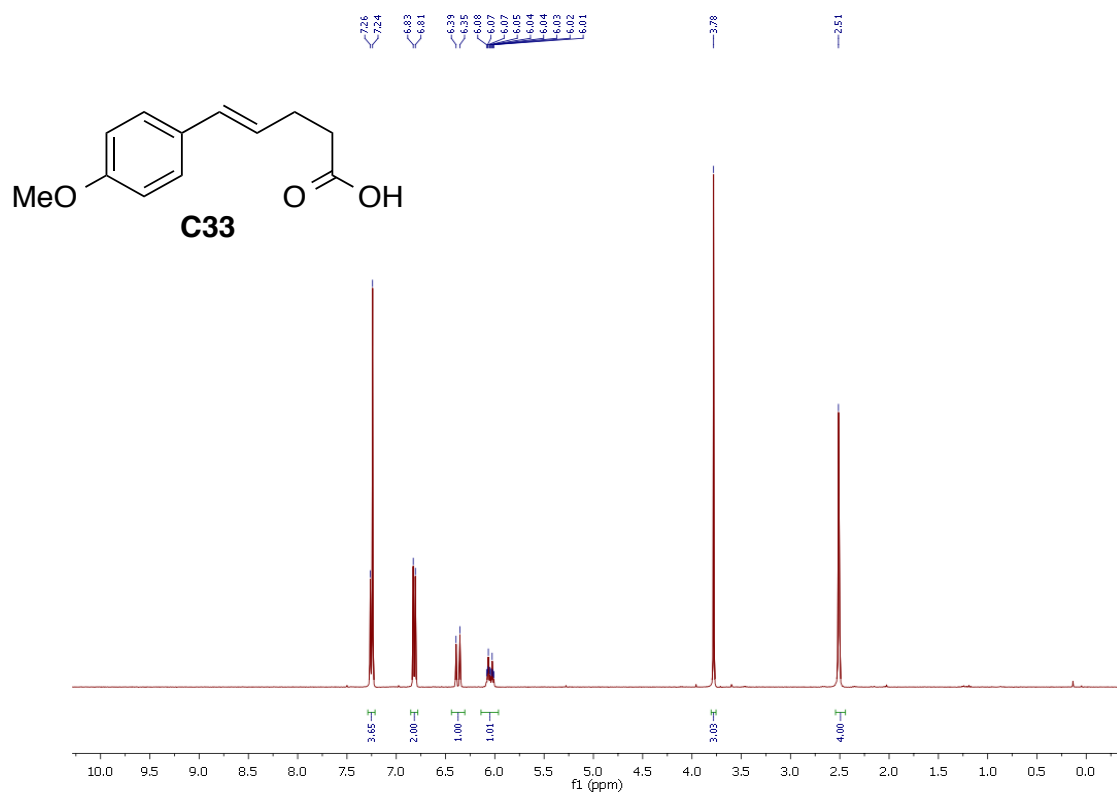


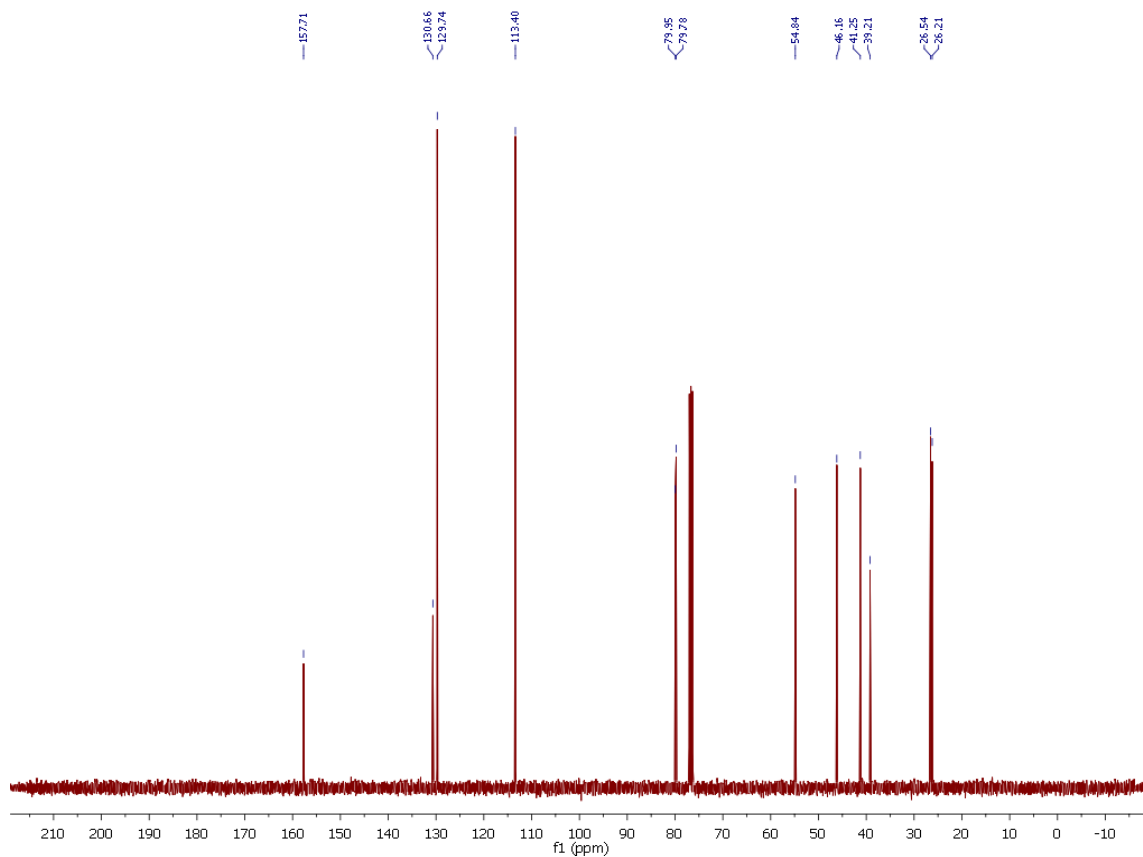
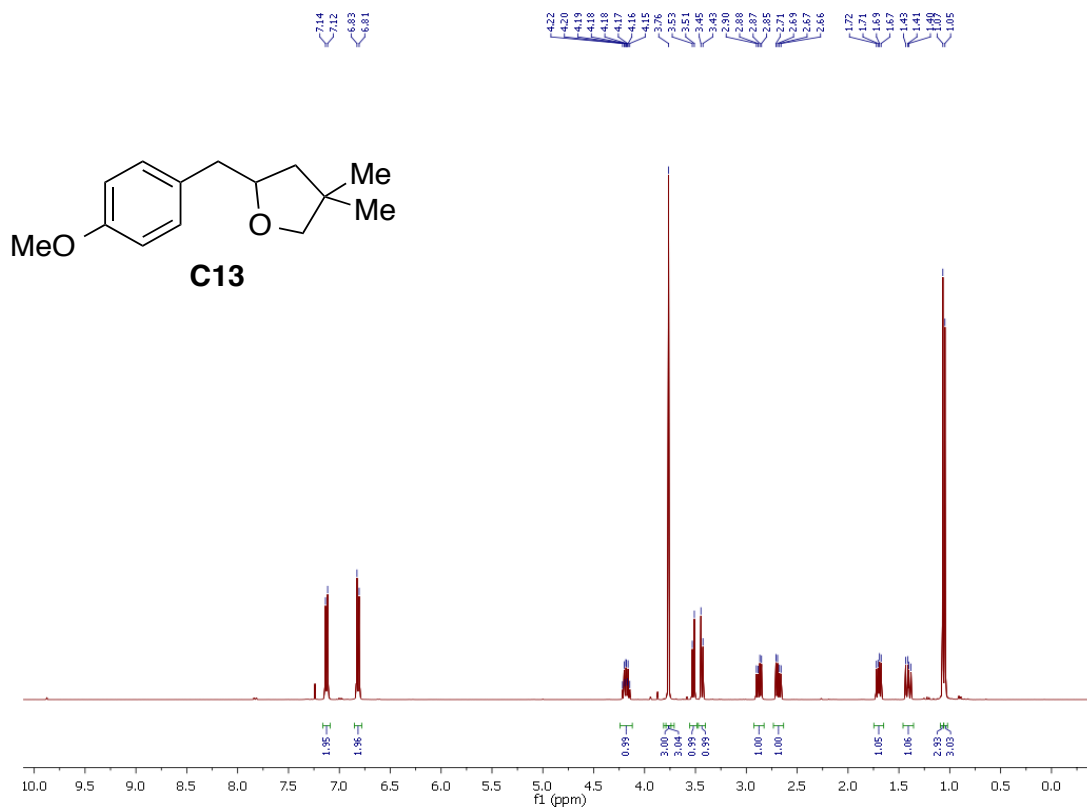


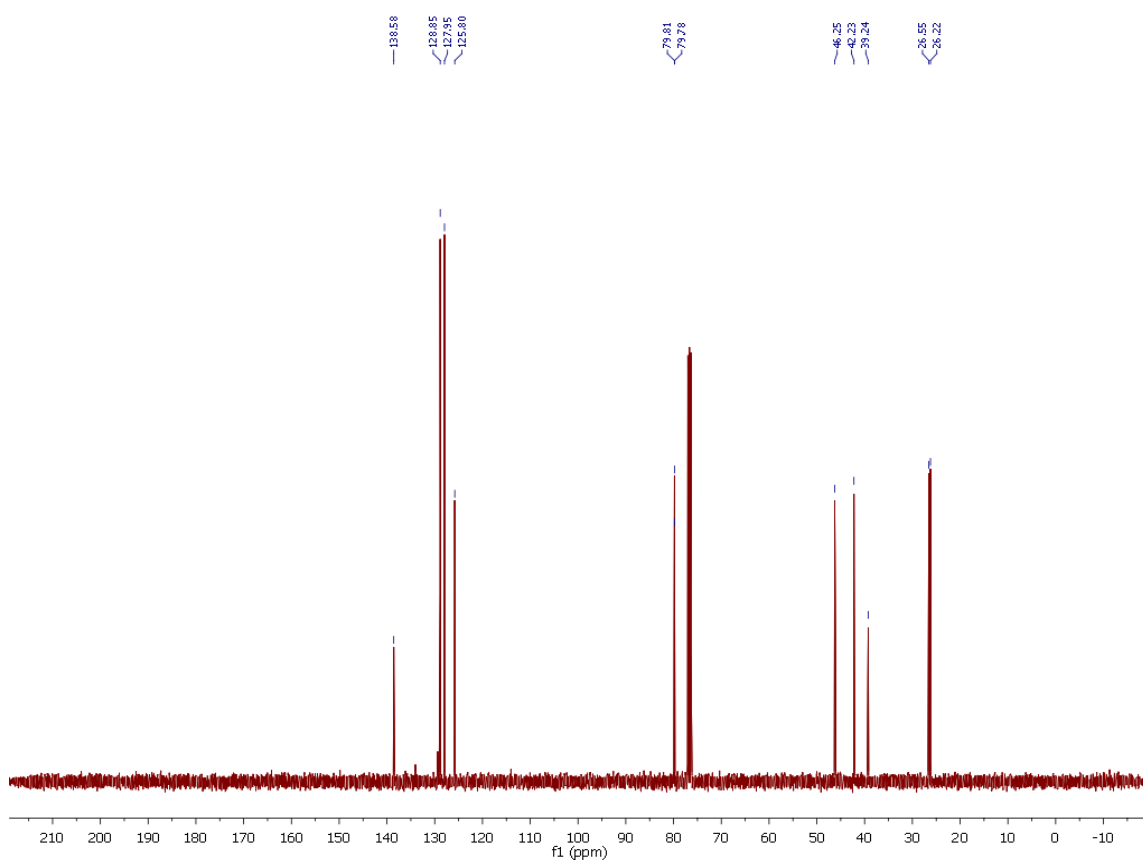
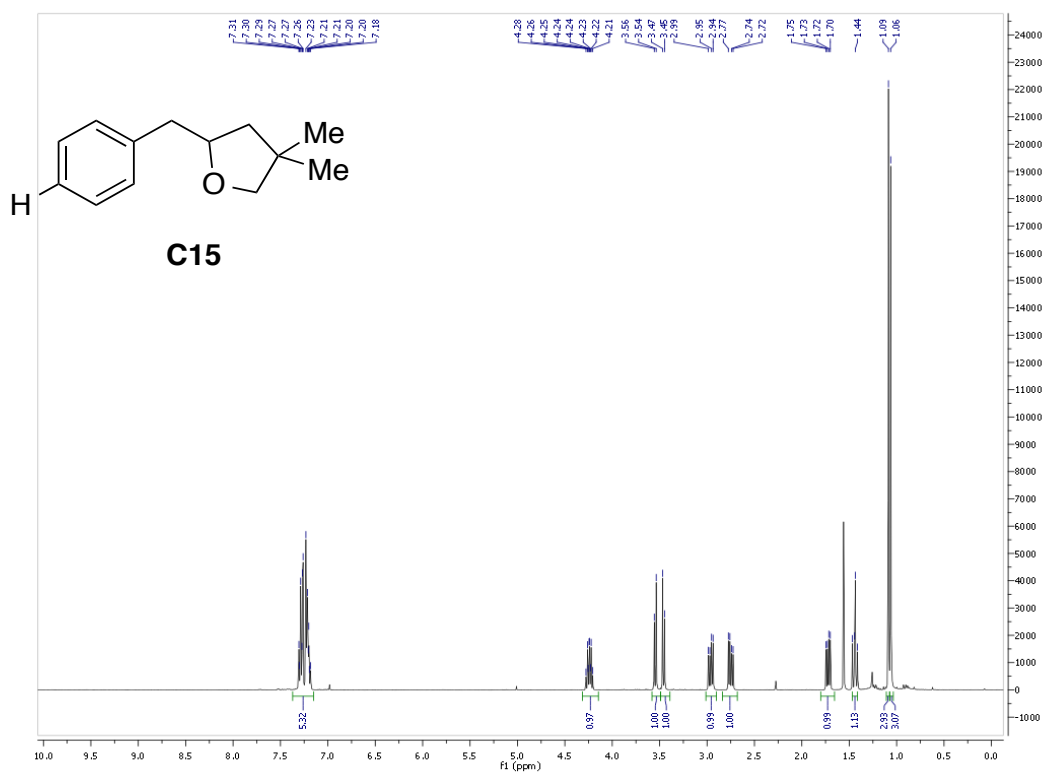


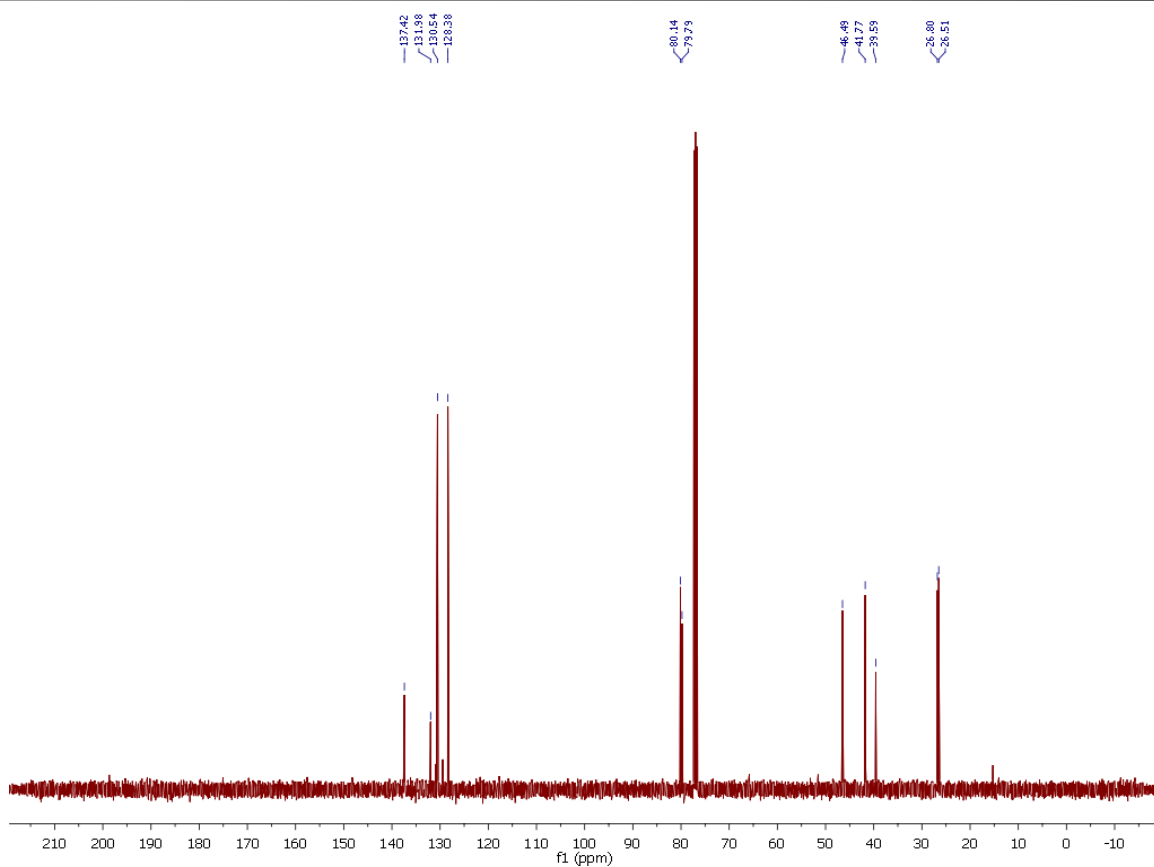
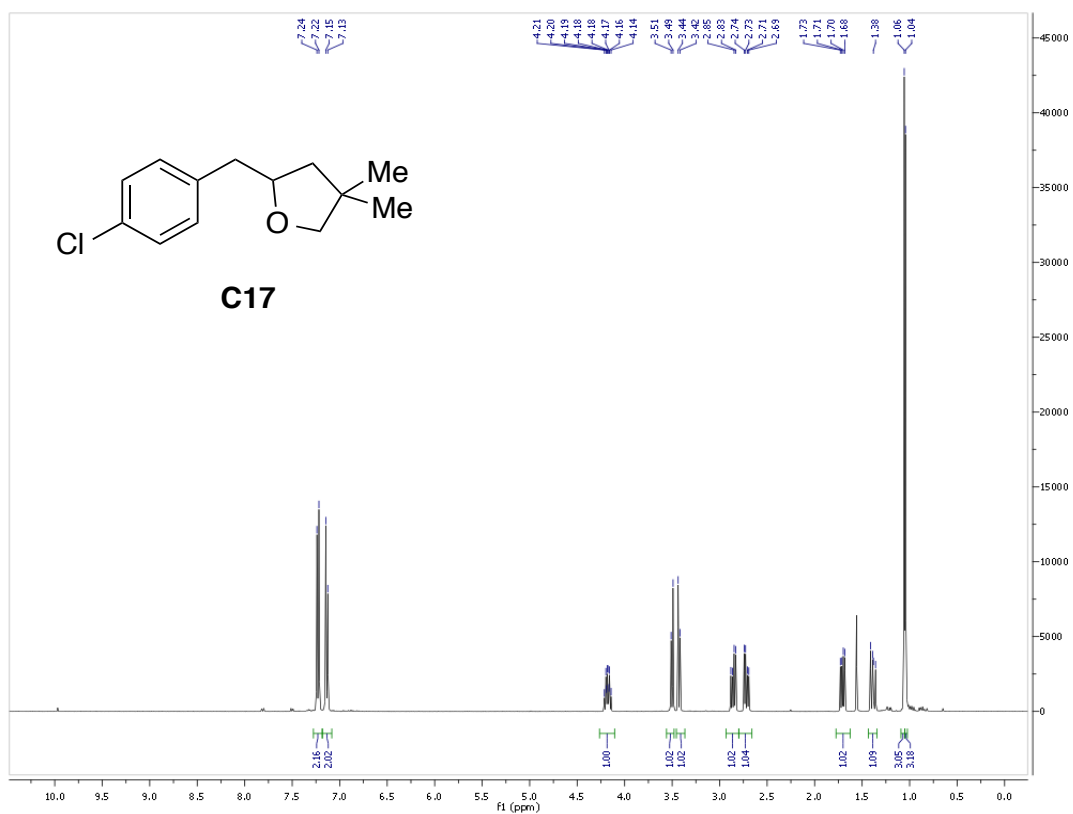
**C30**

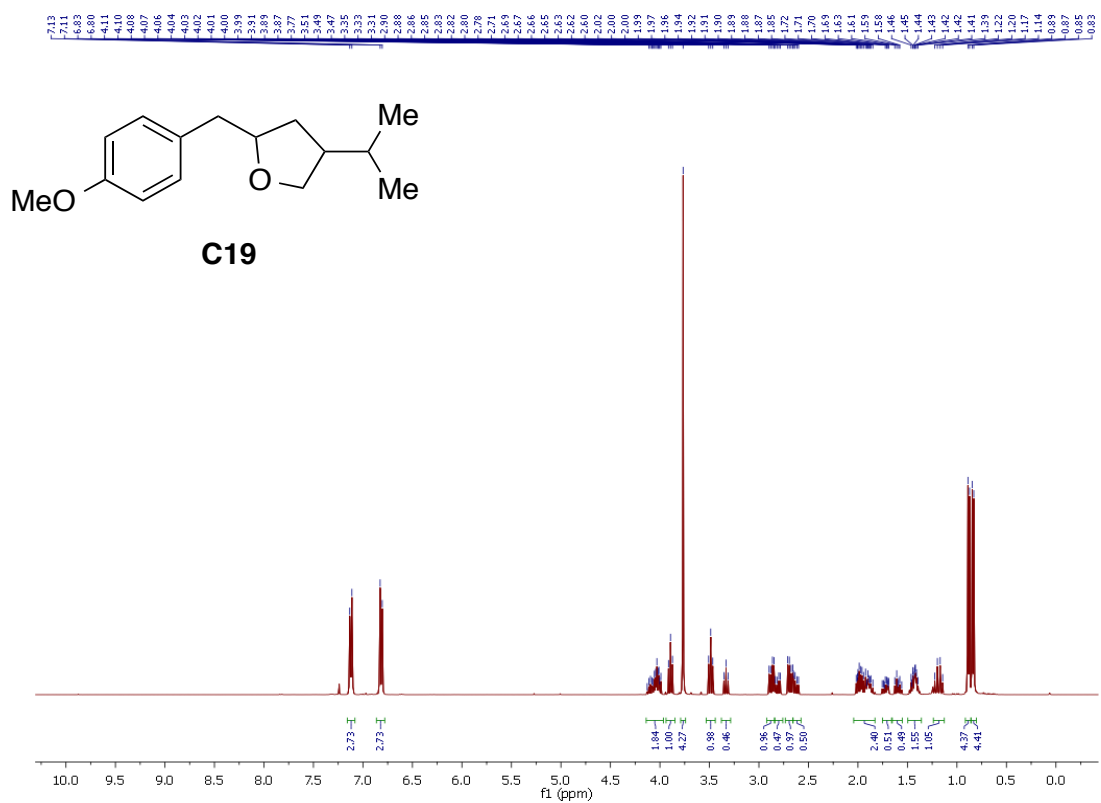


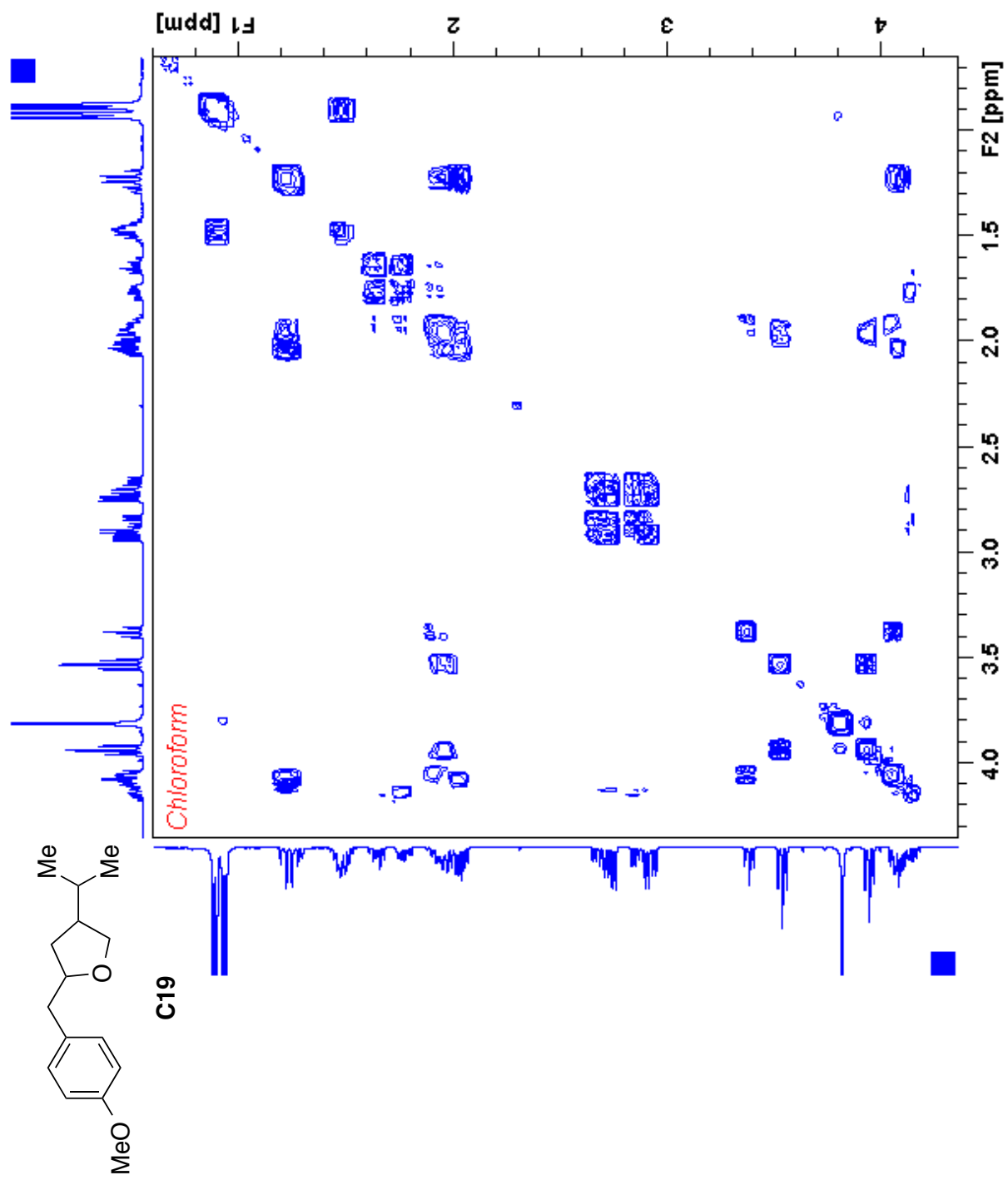


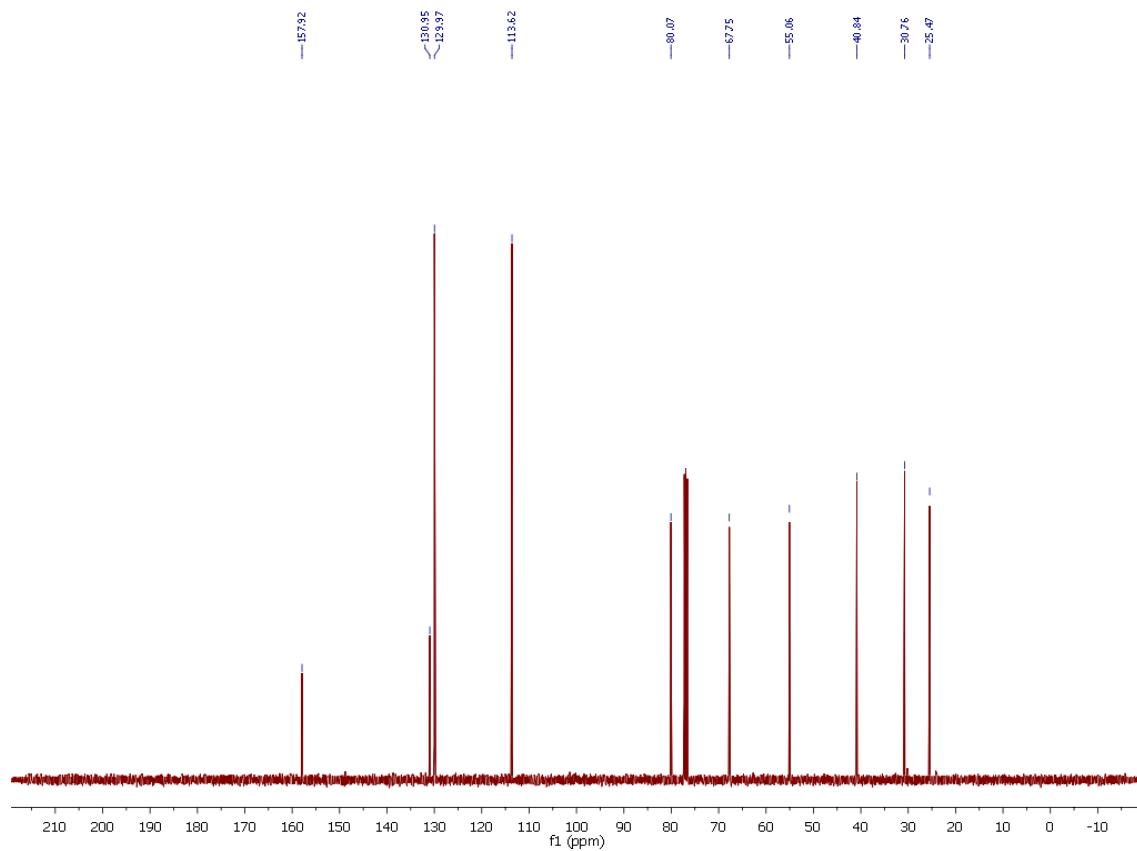
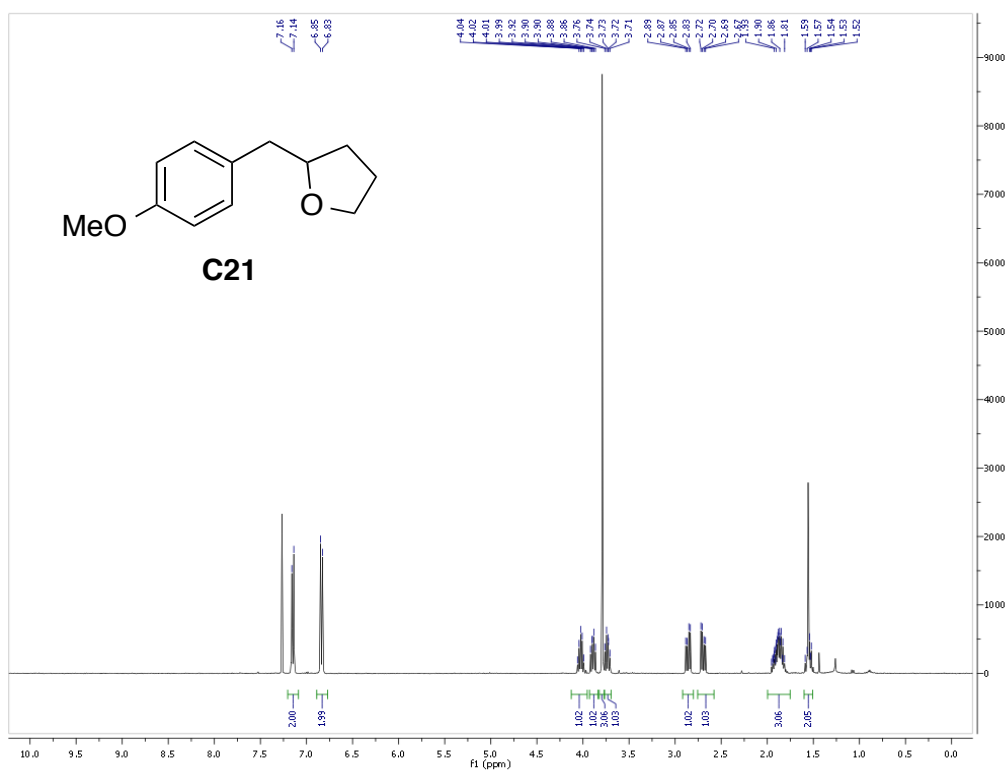




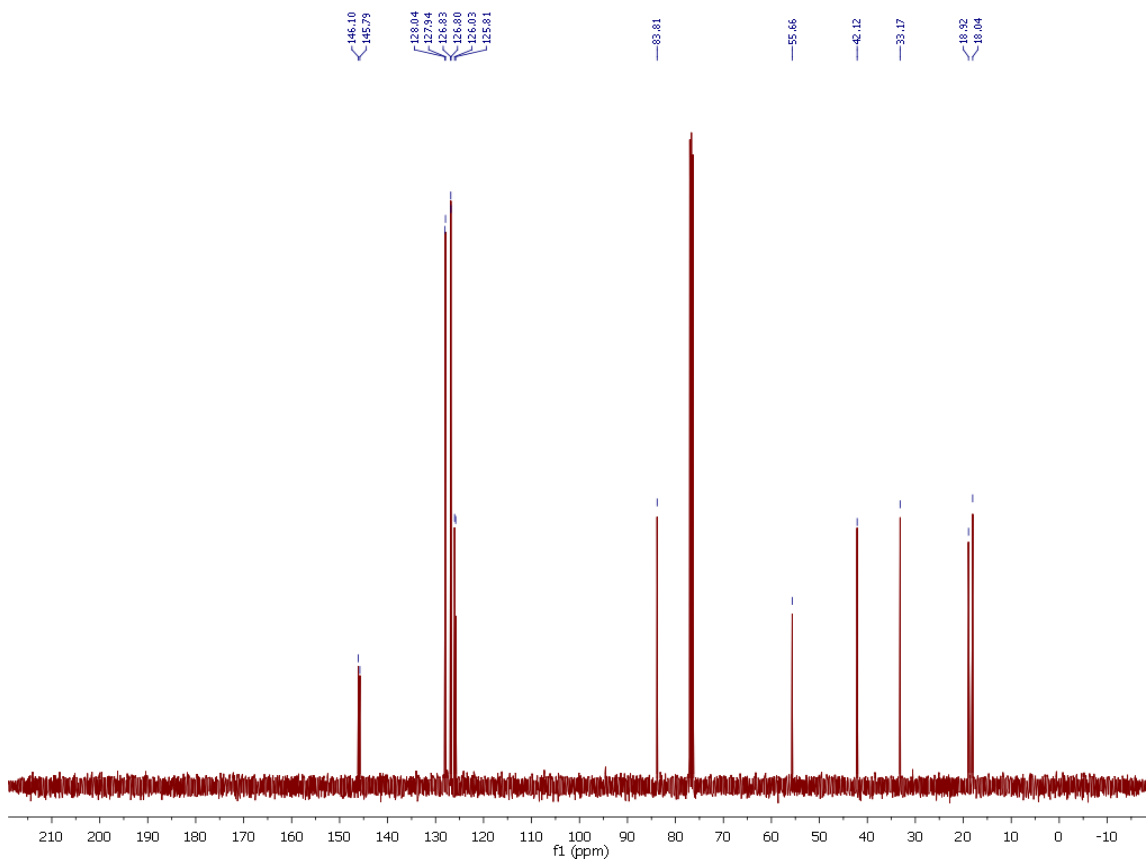
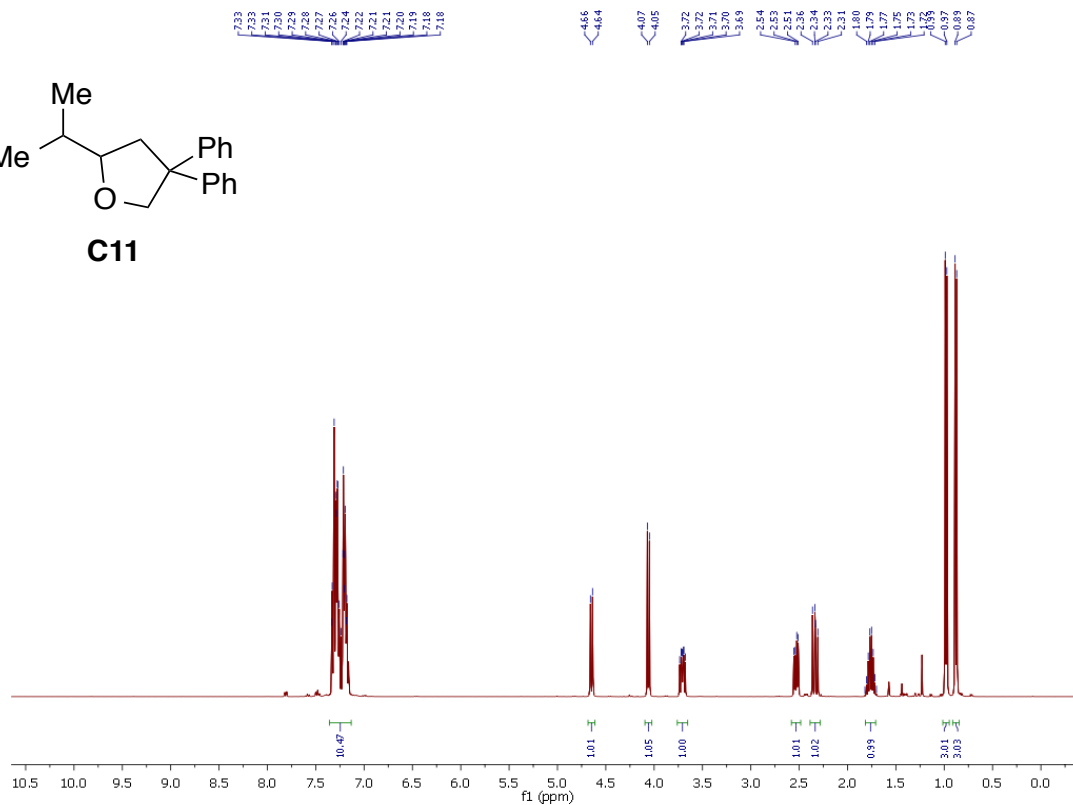
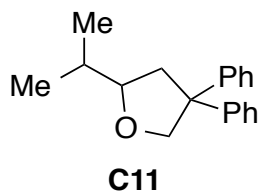


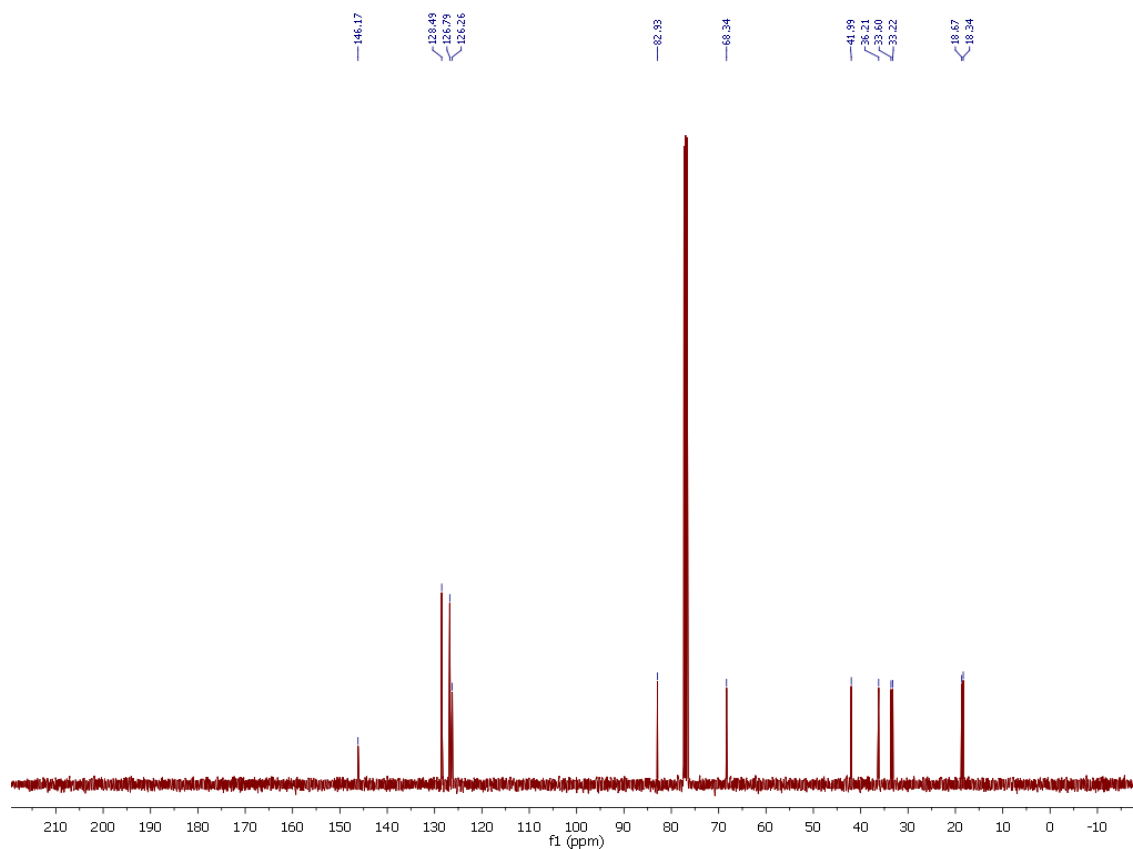
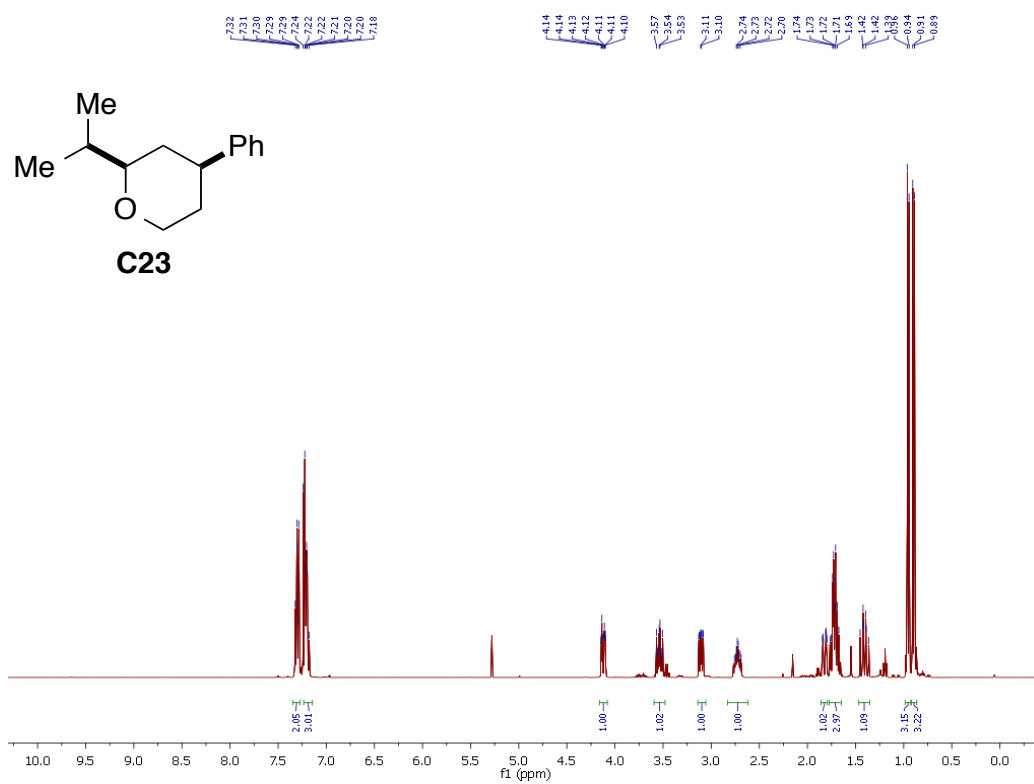


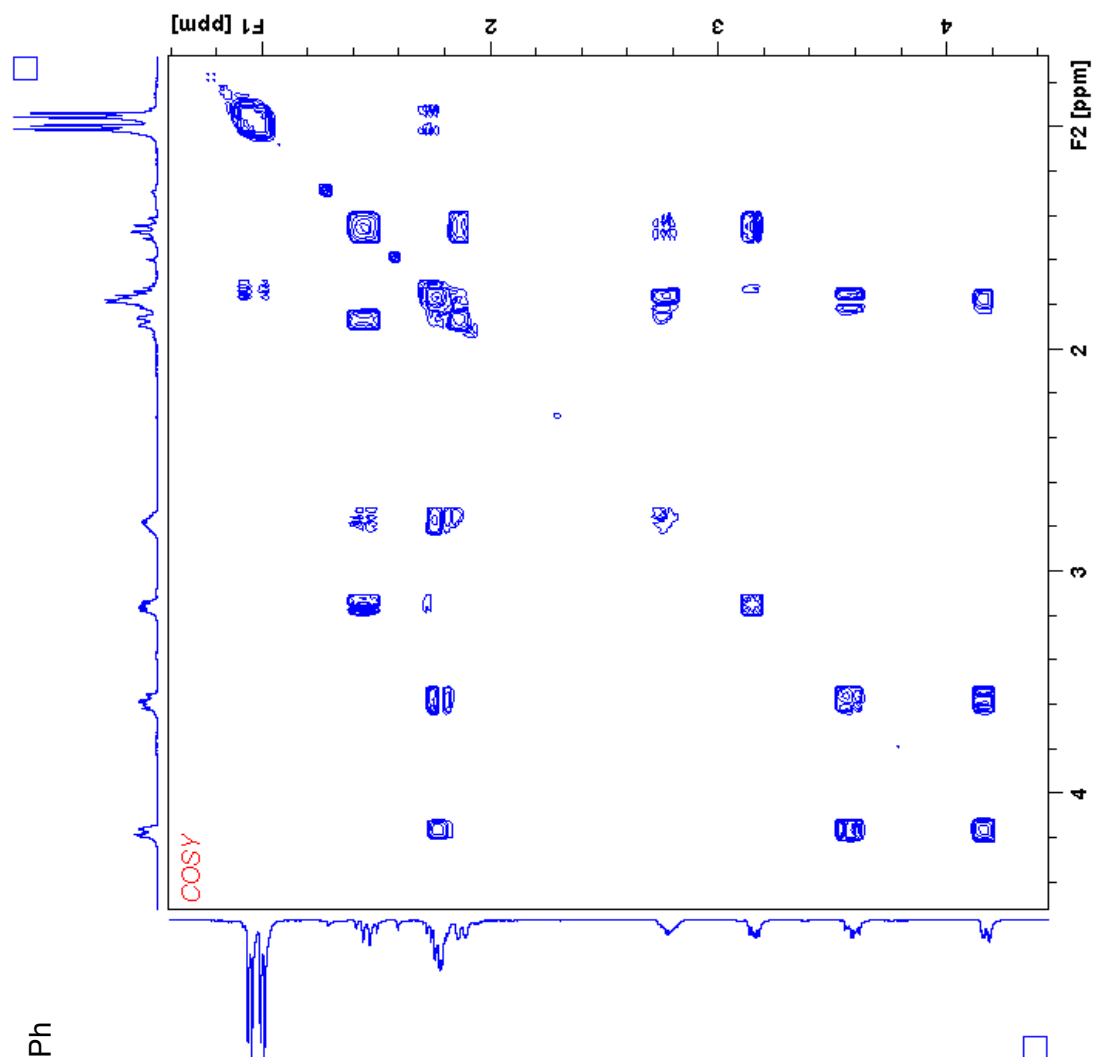
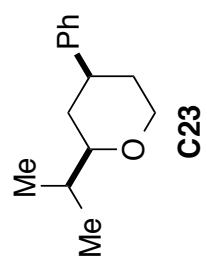


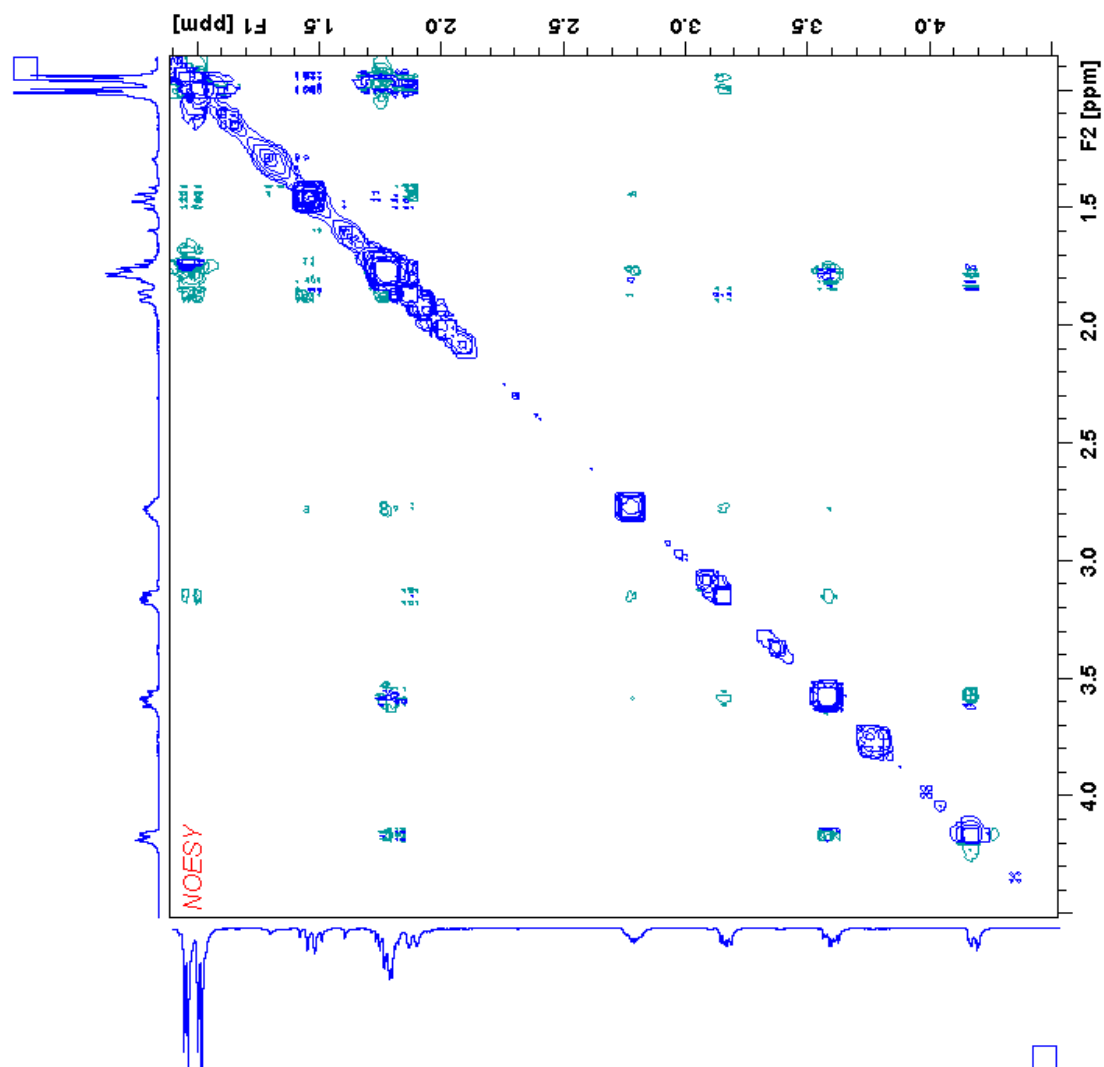
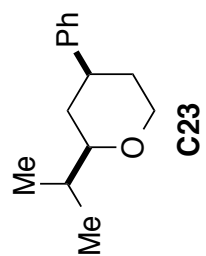


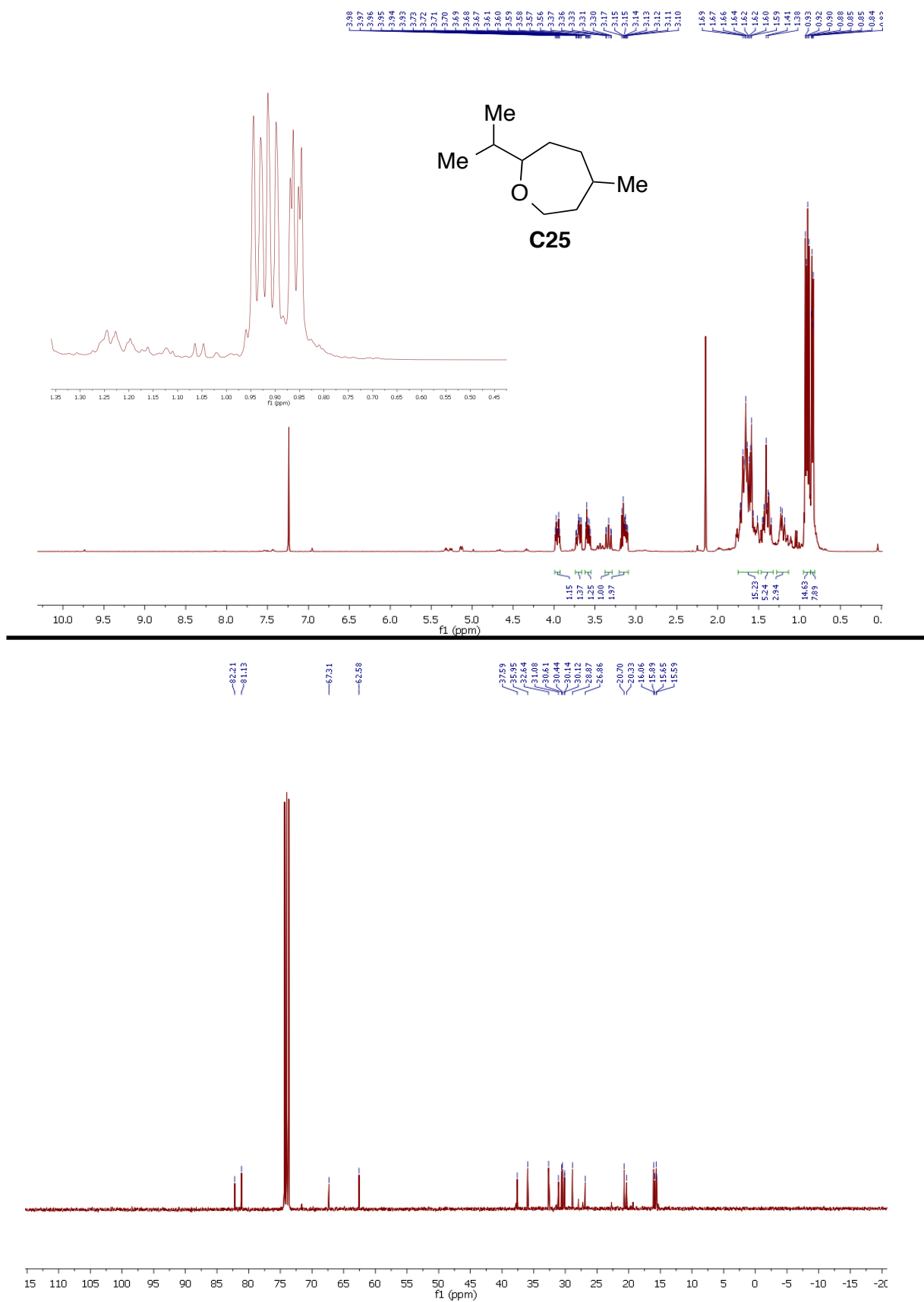




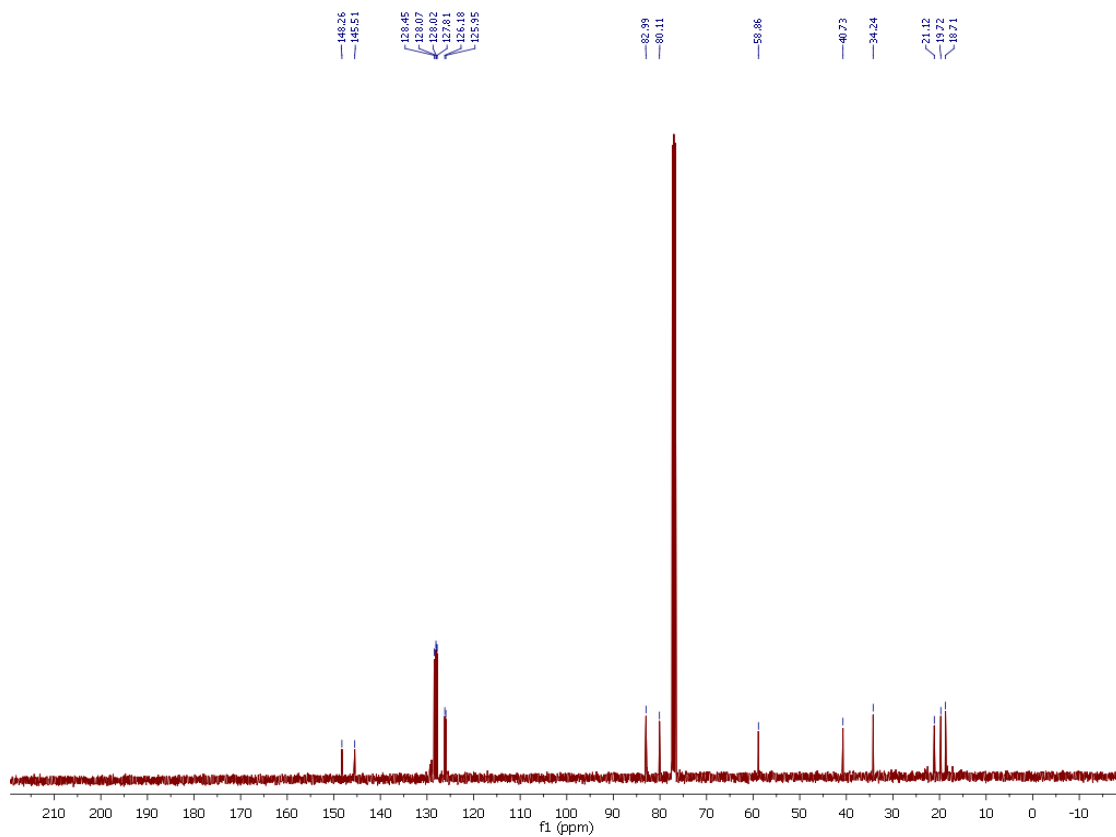
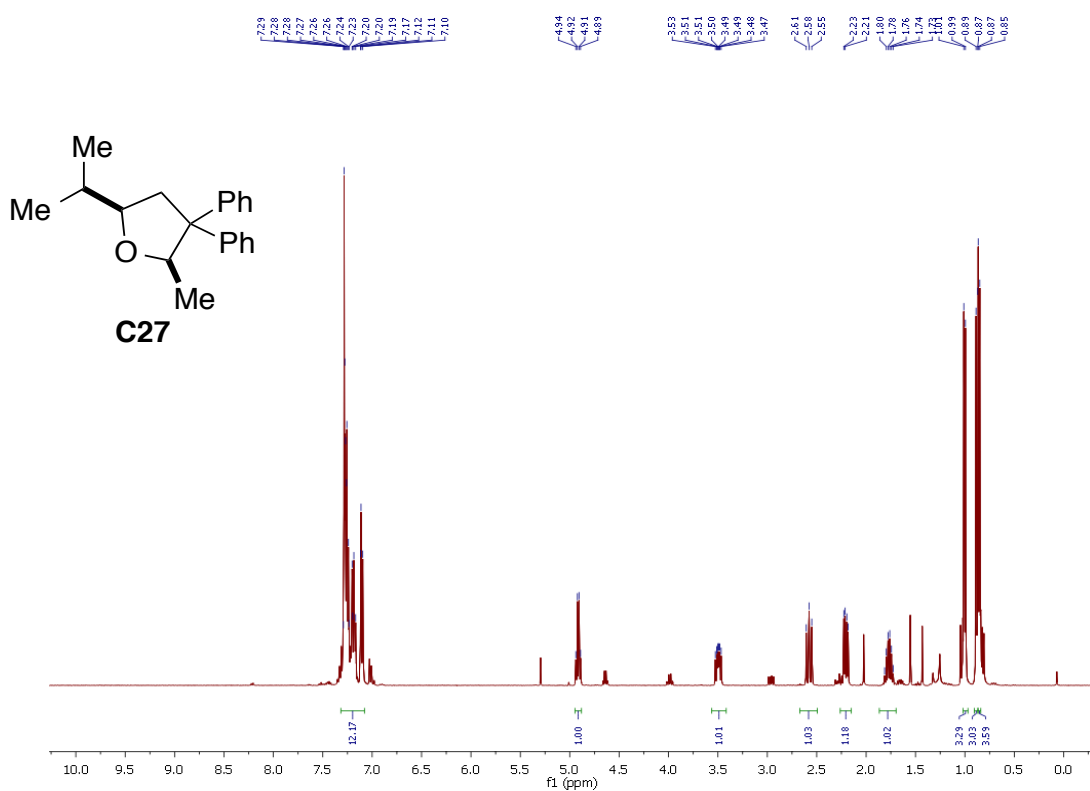


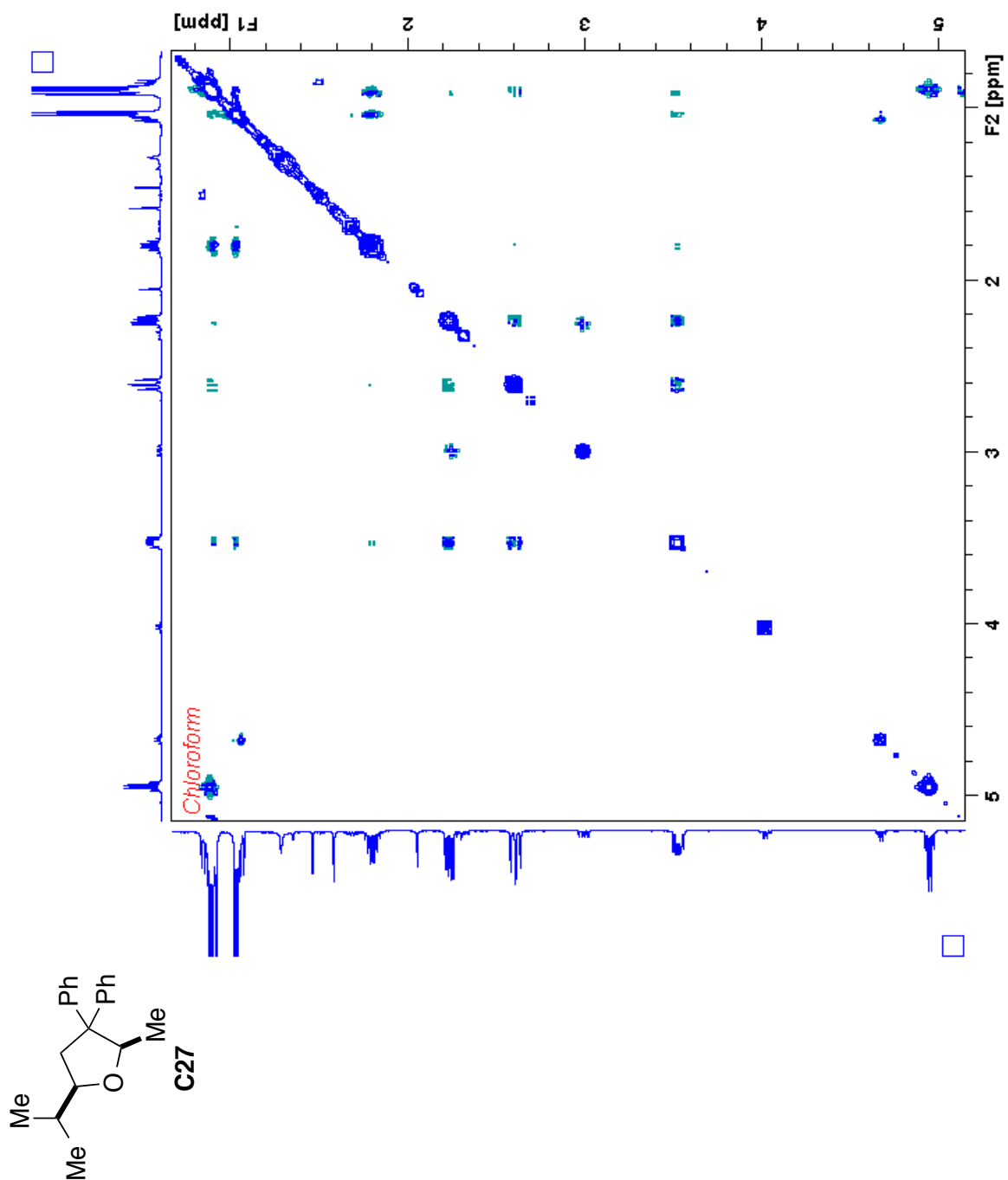




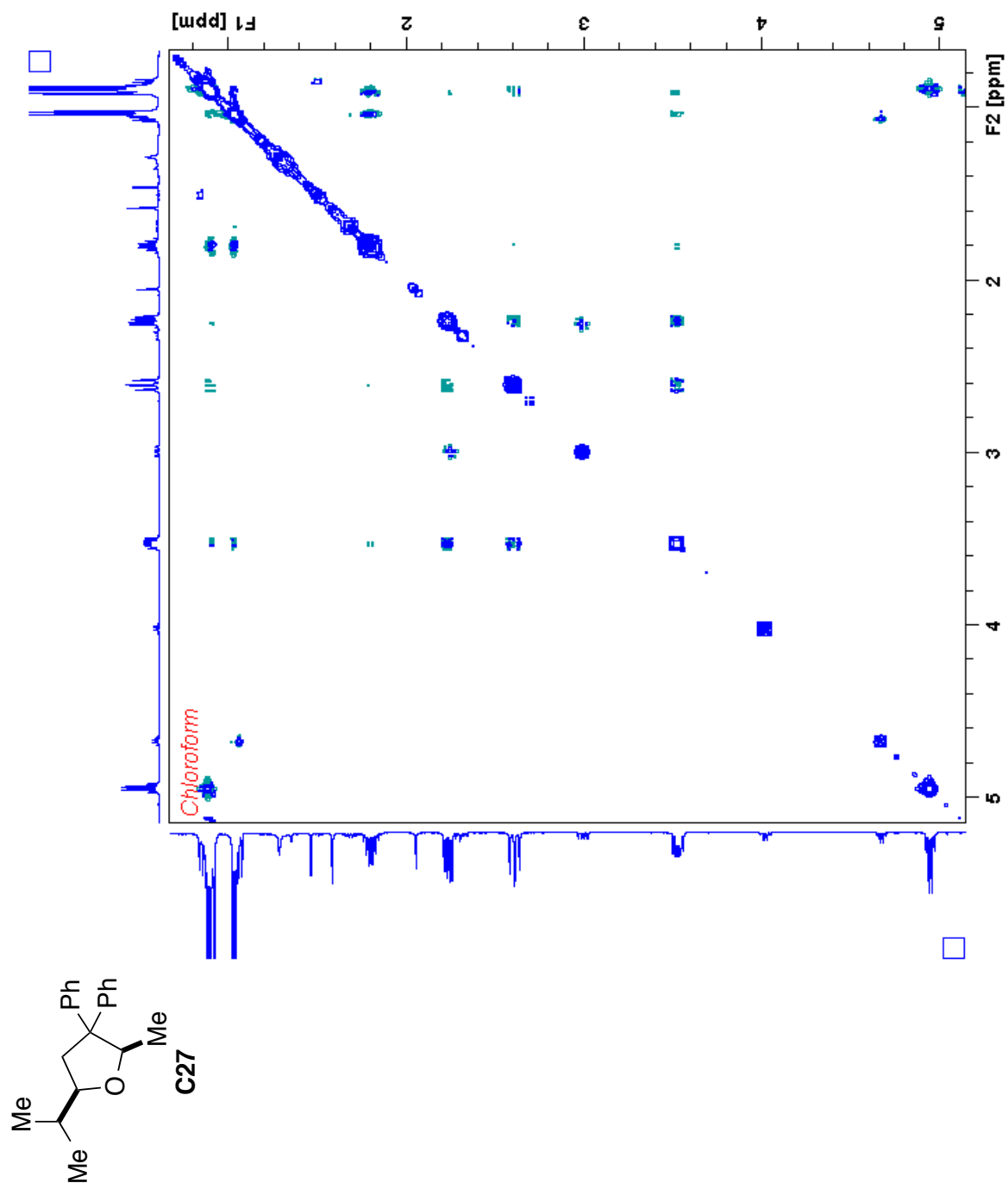


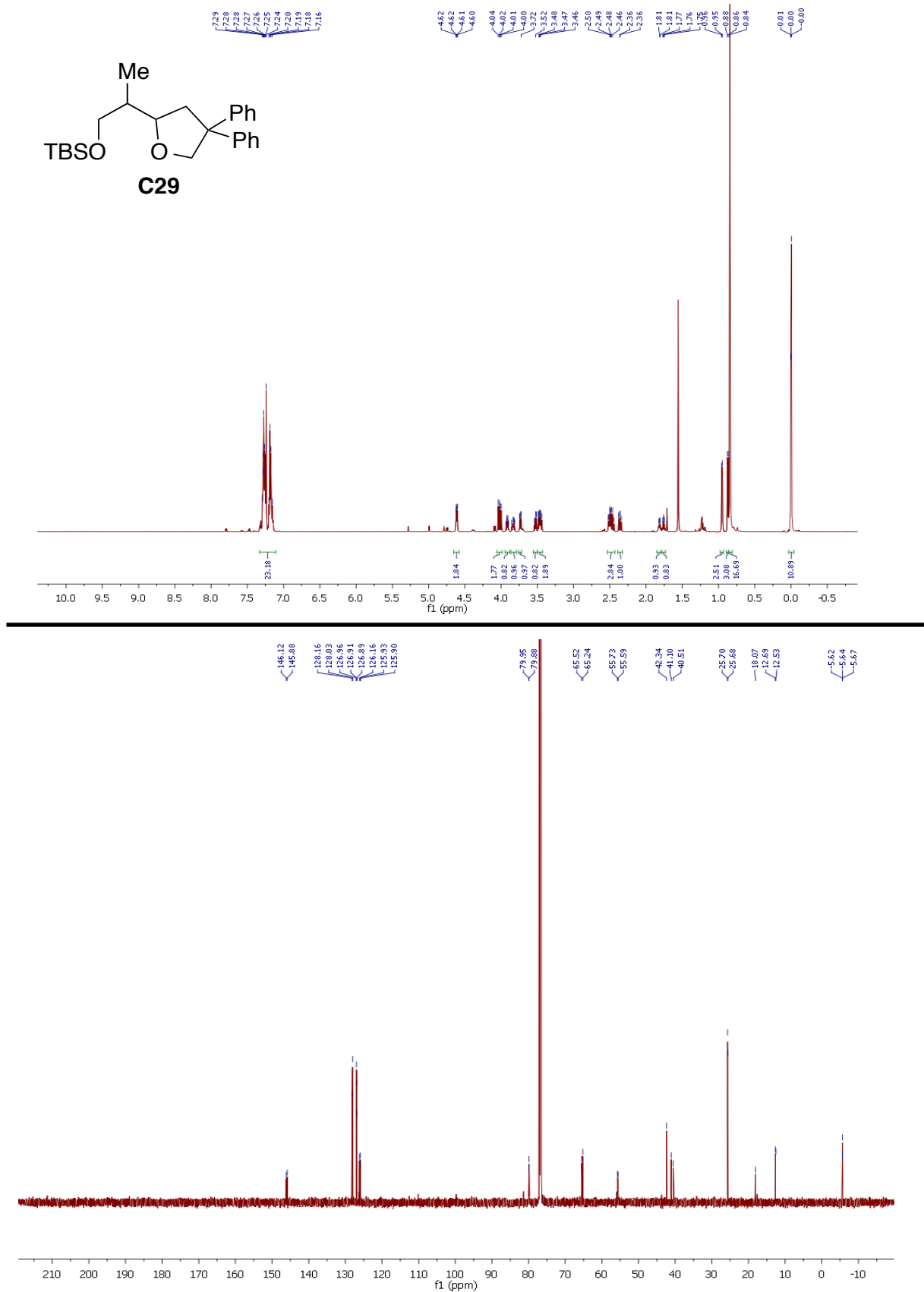


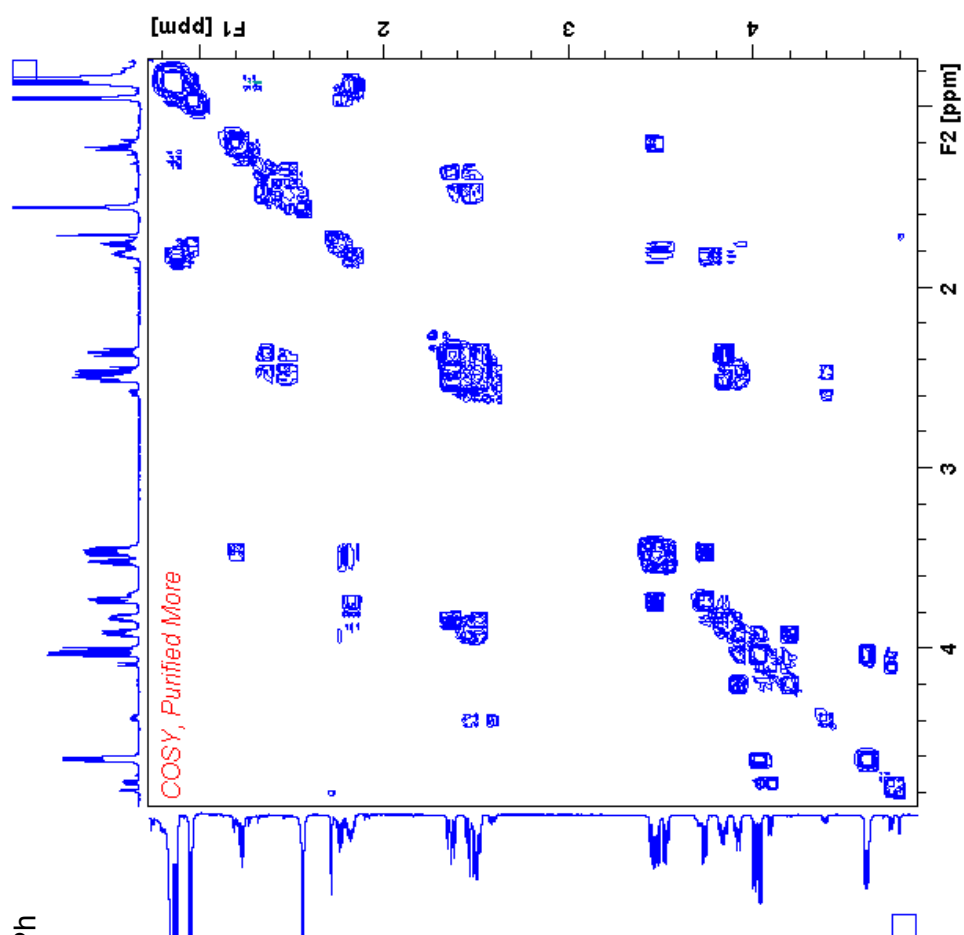
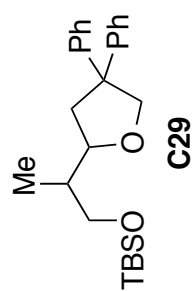


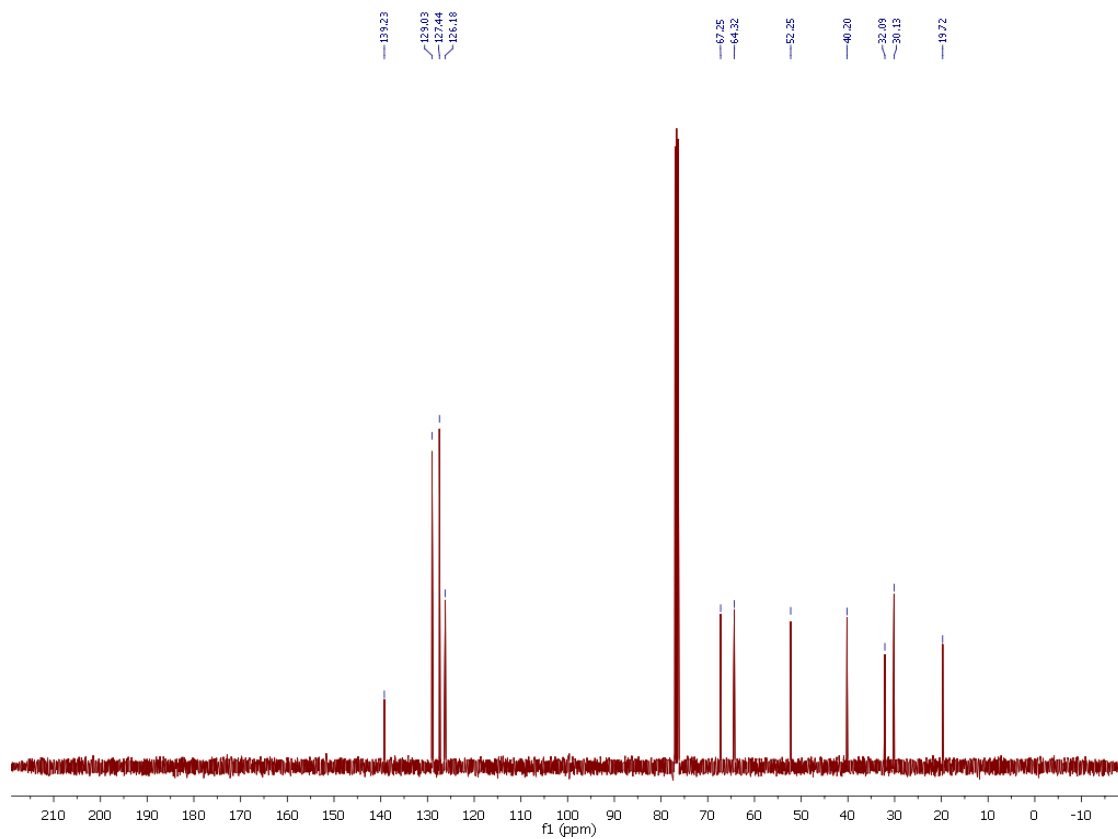
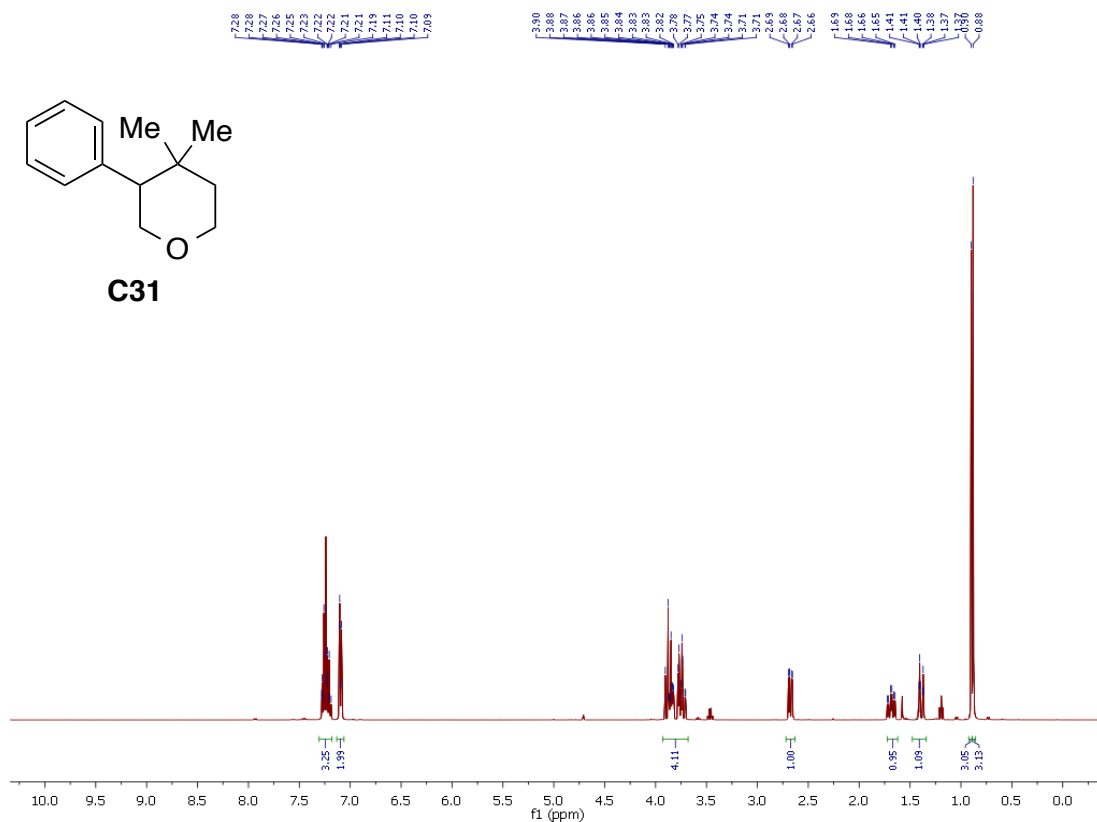
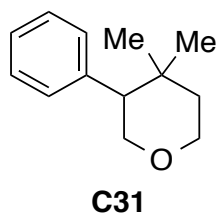


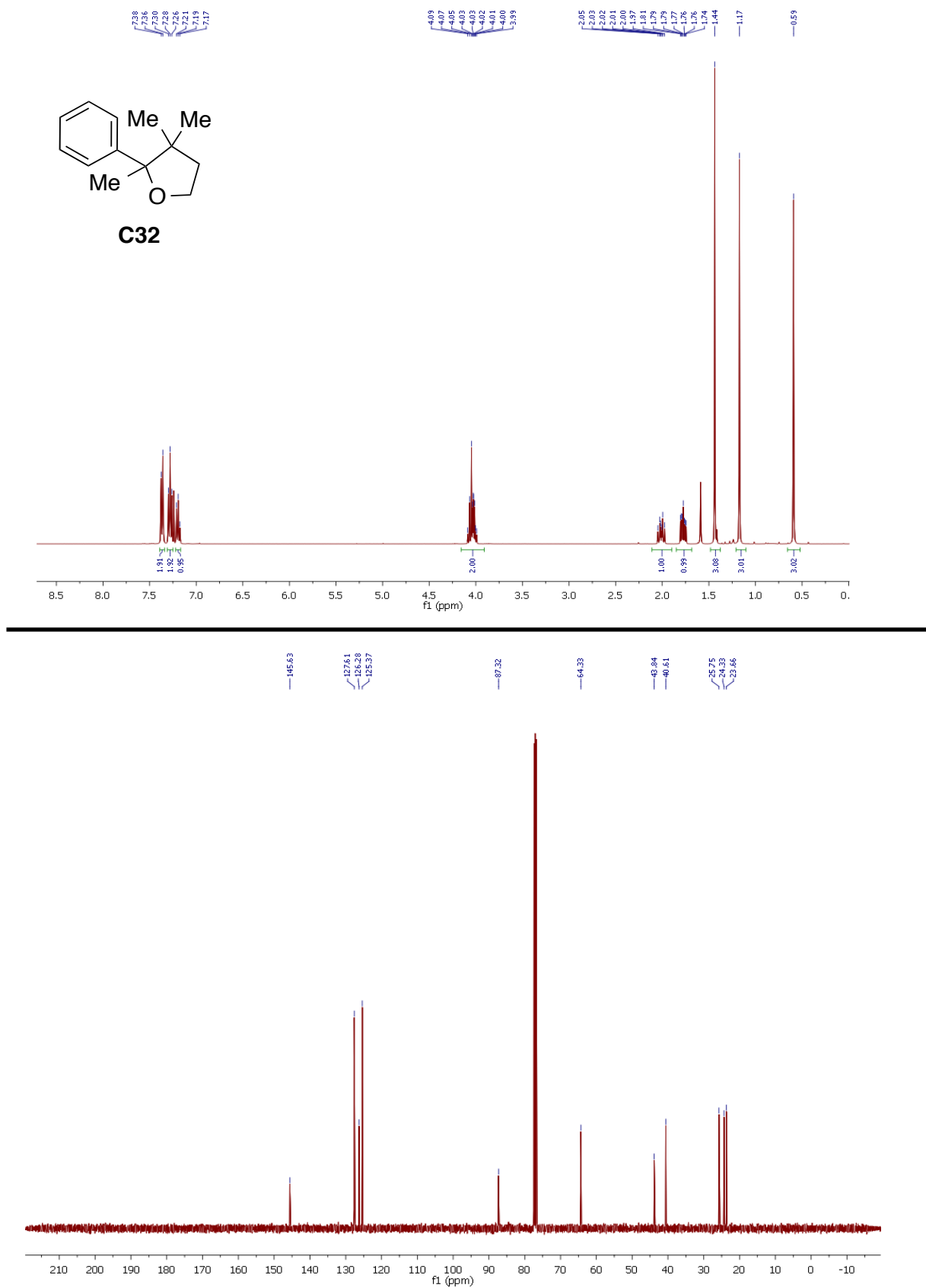


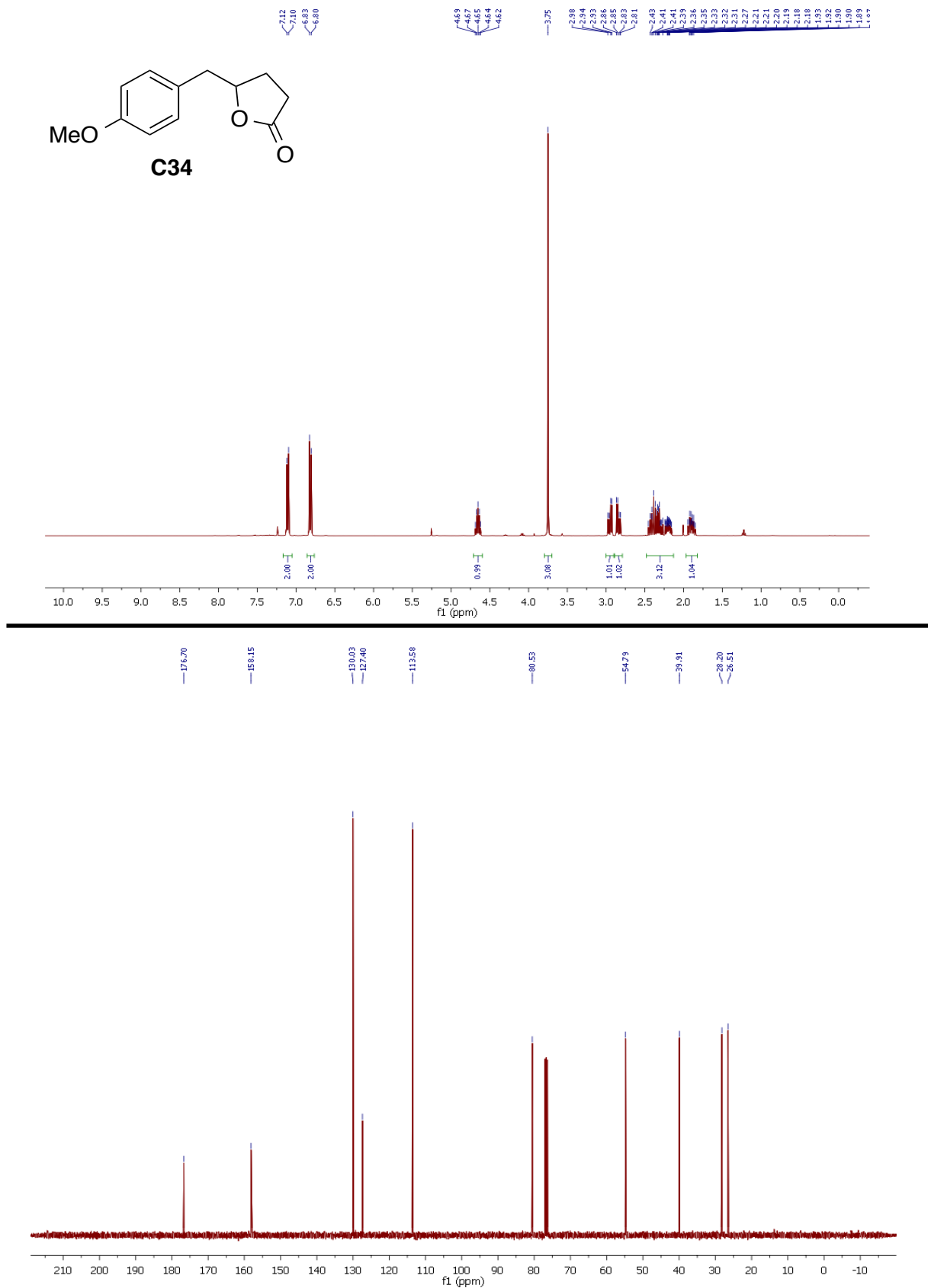


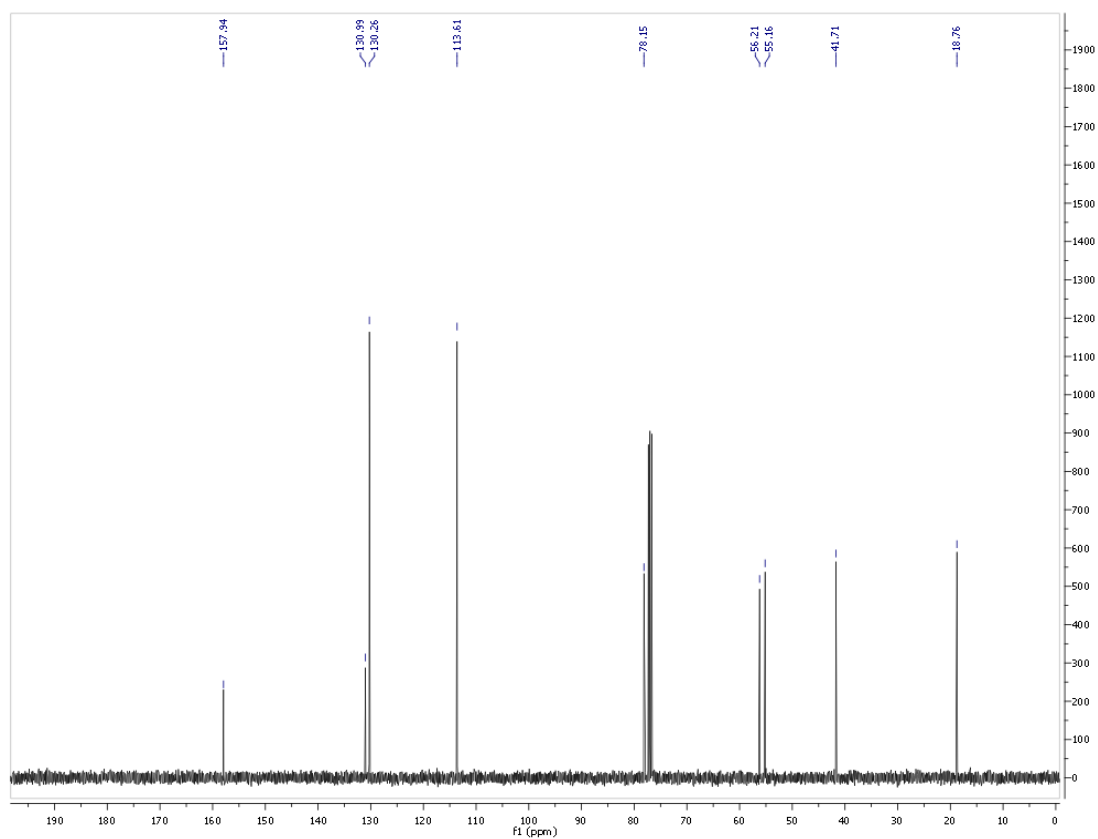
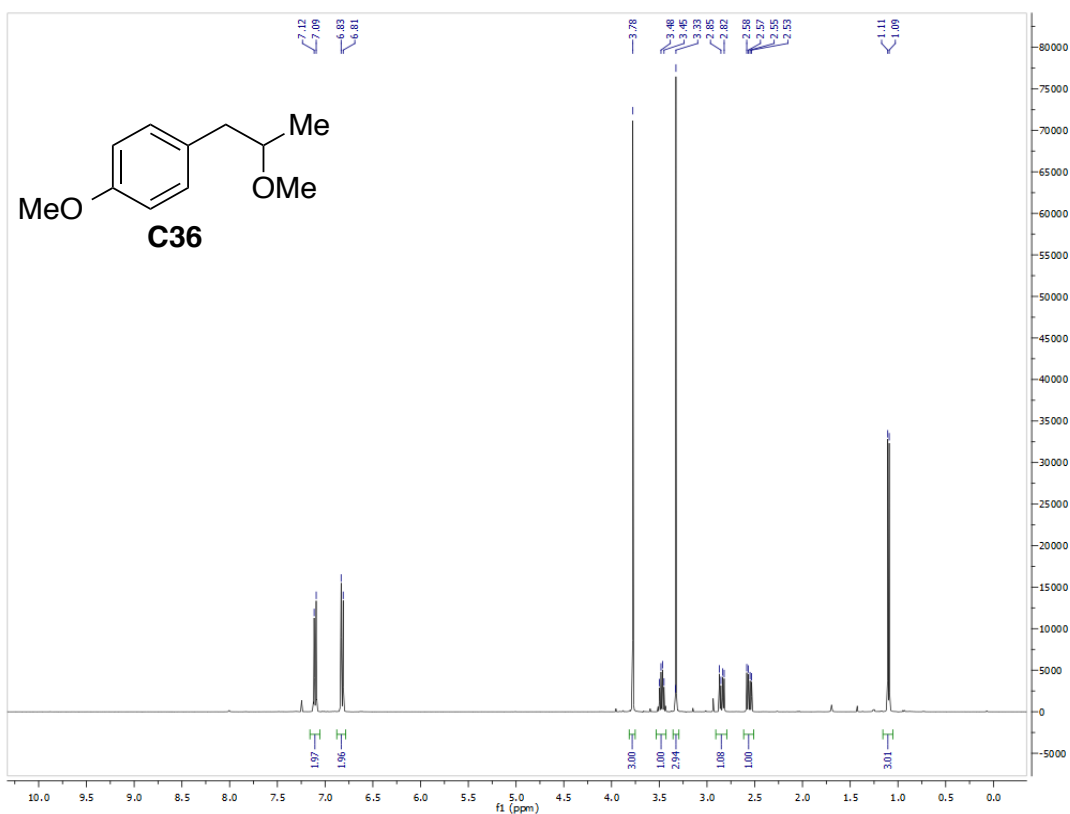






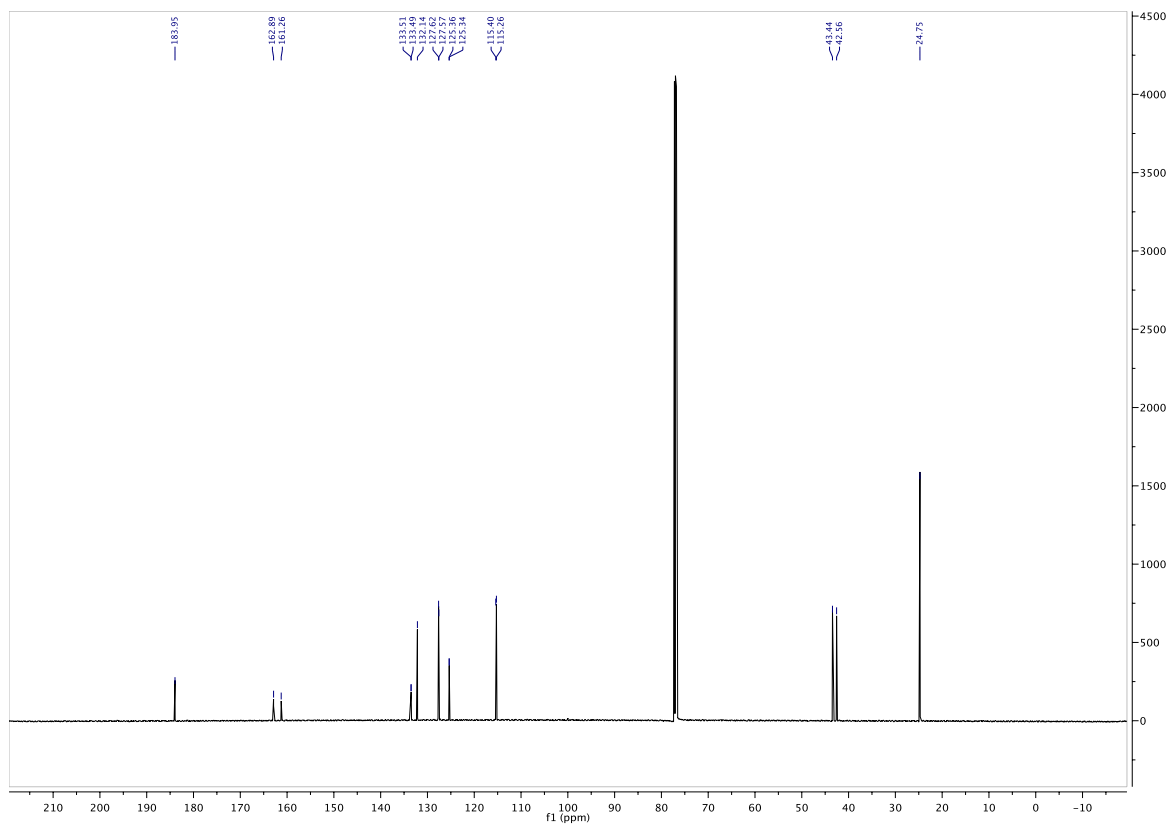
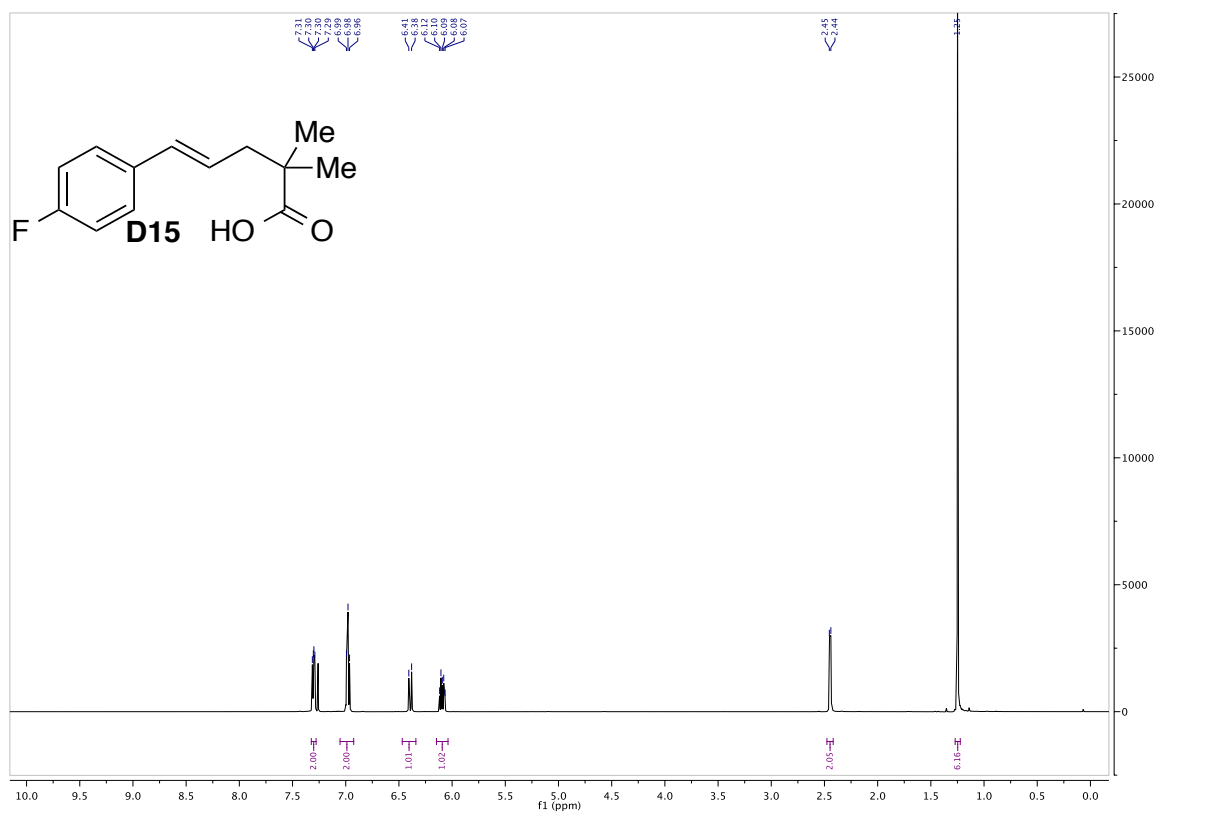


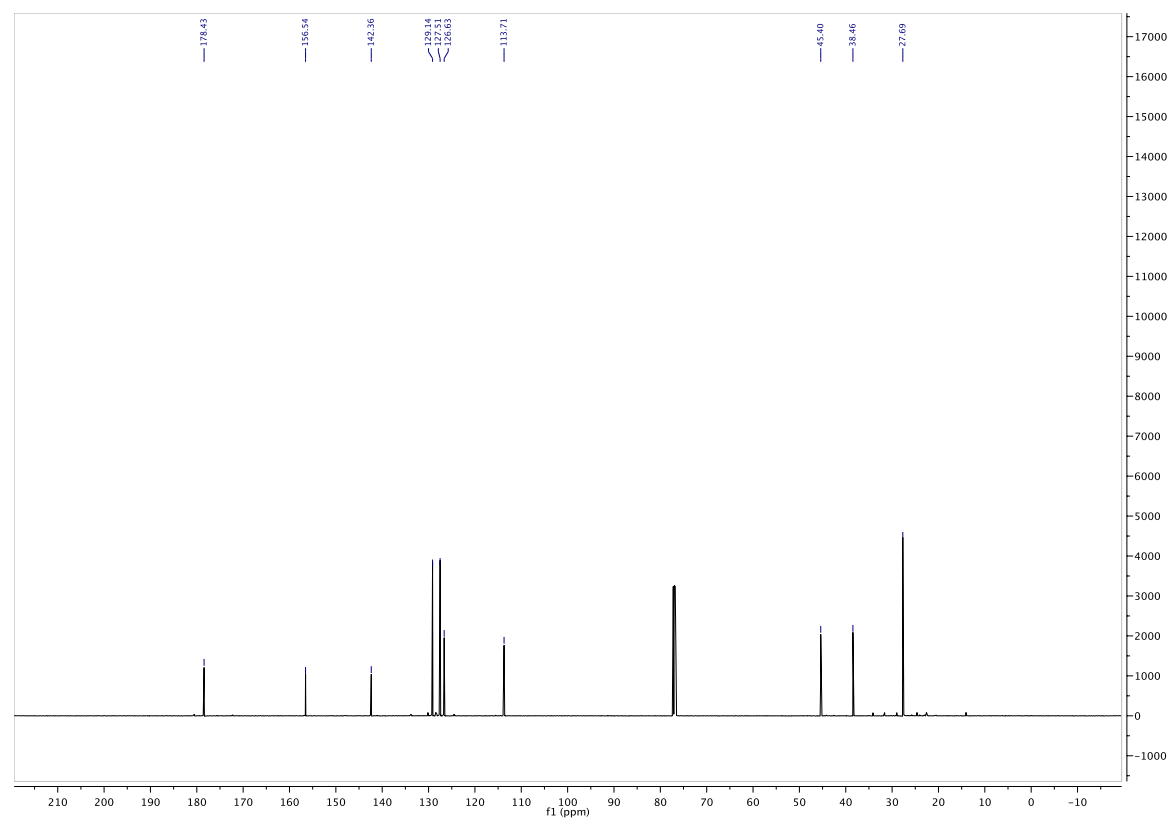
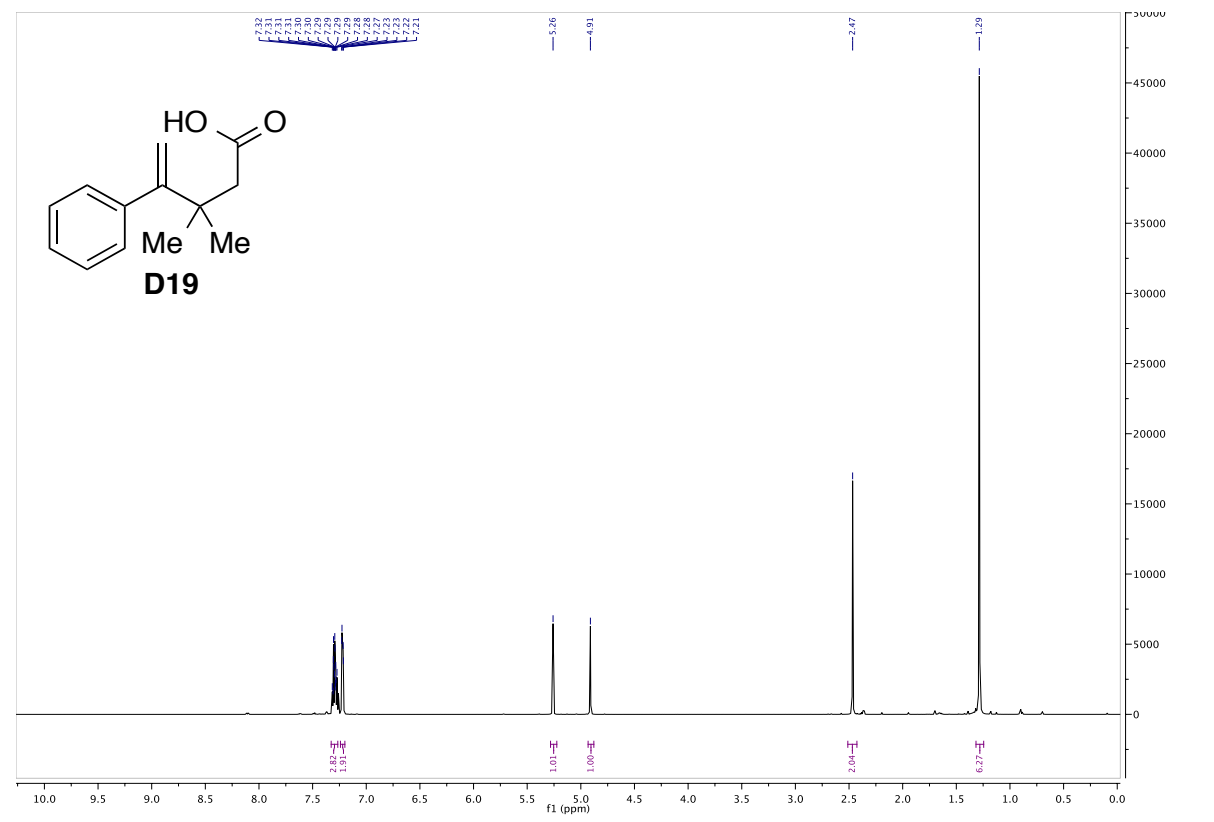






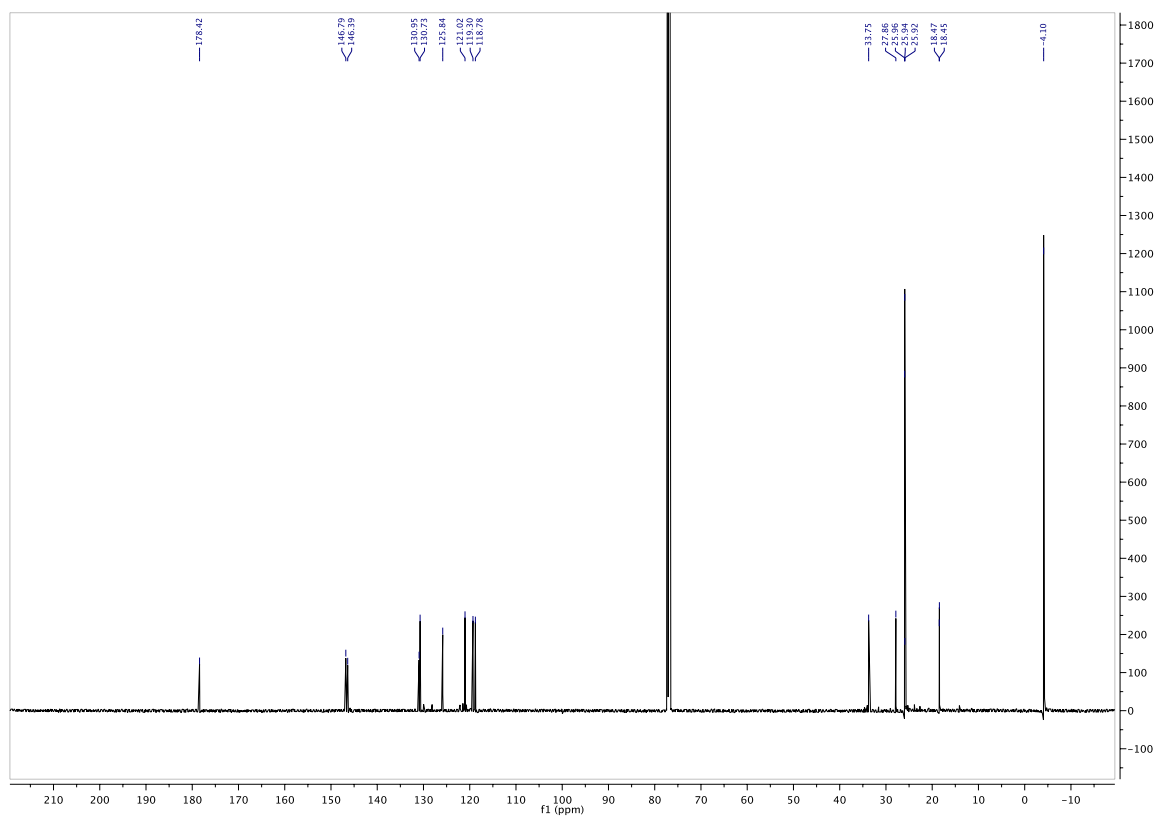
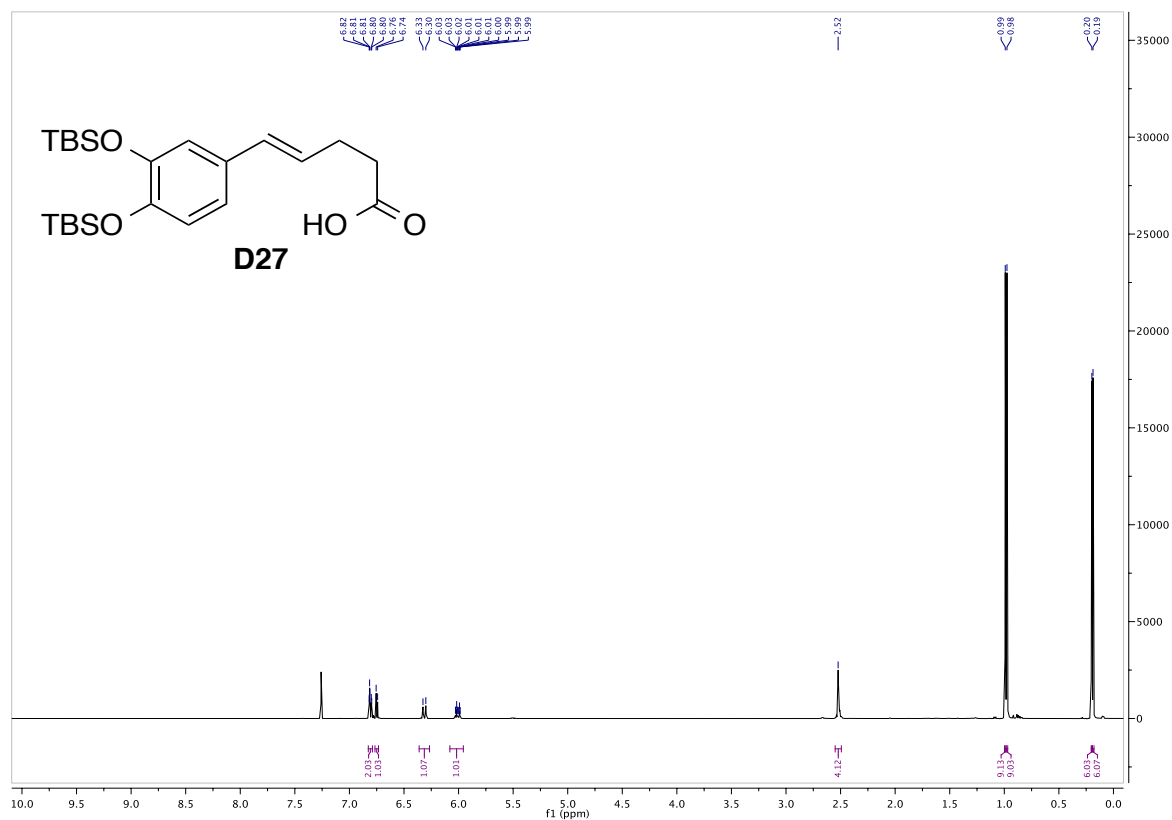


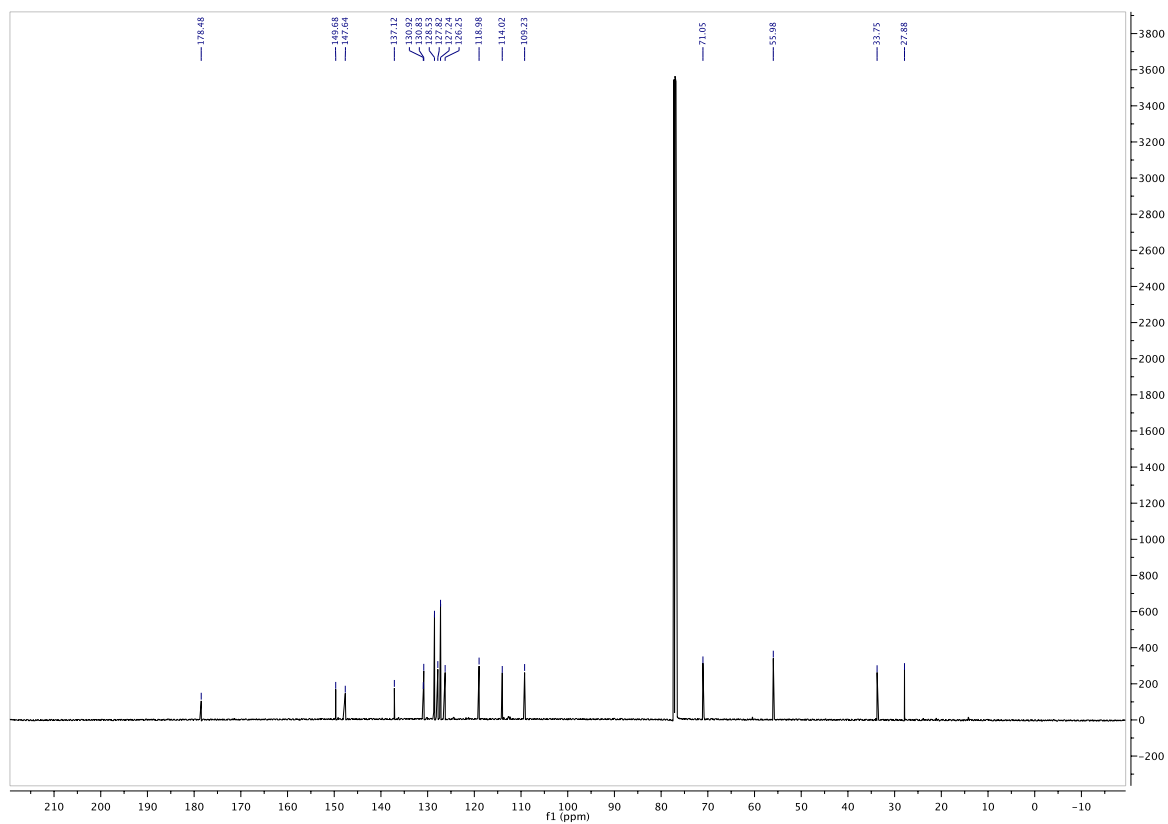
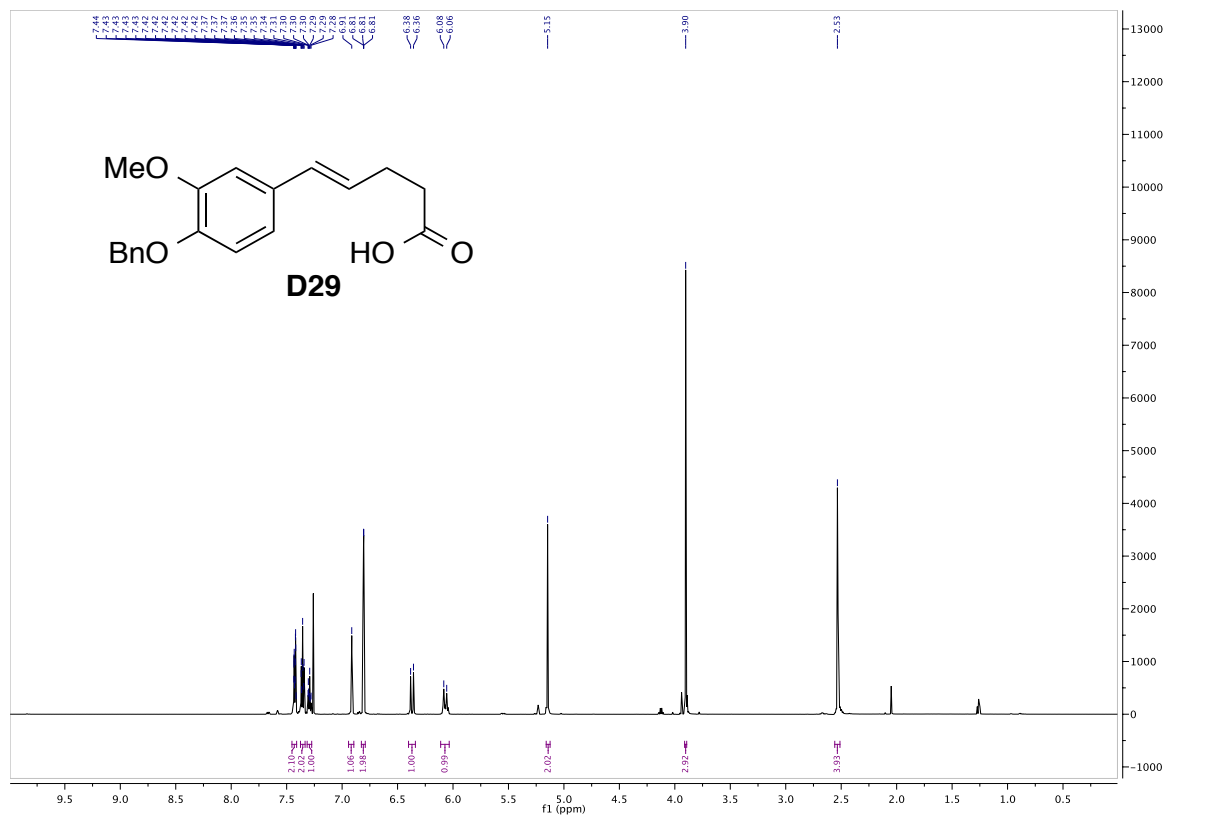


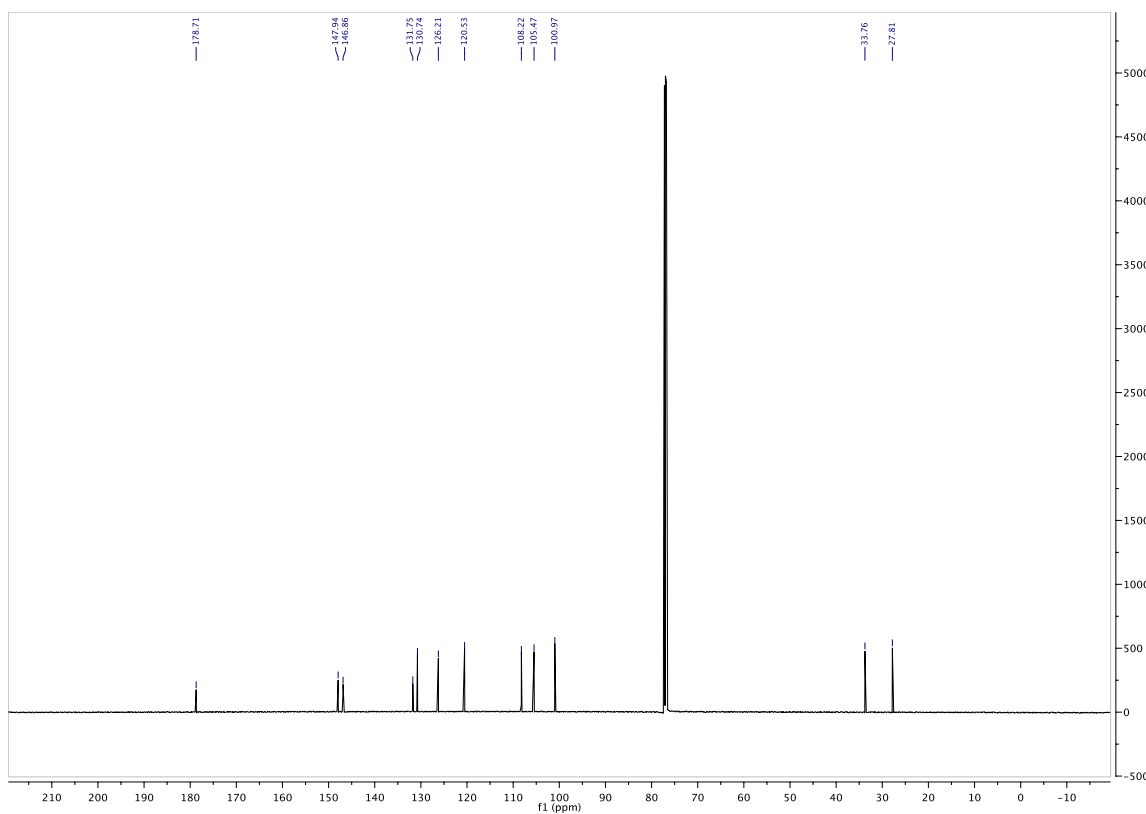
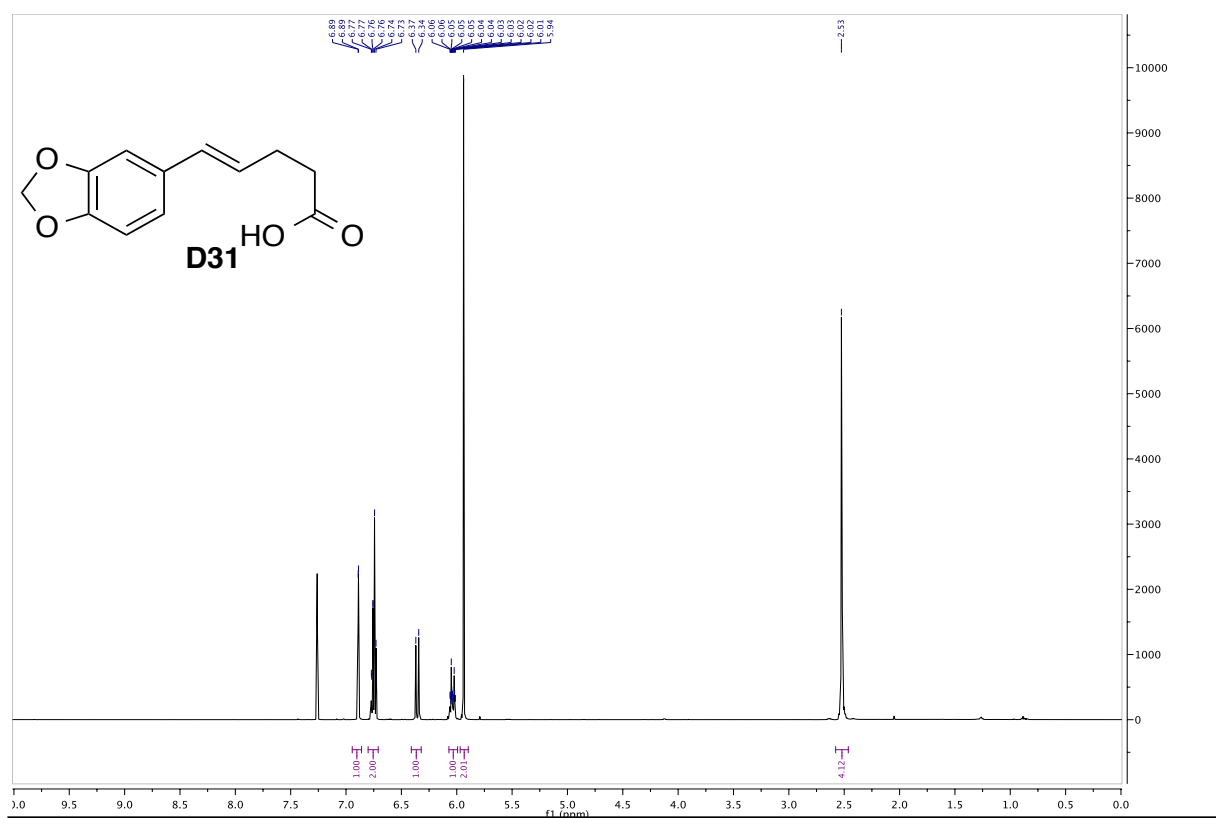


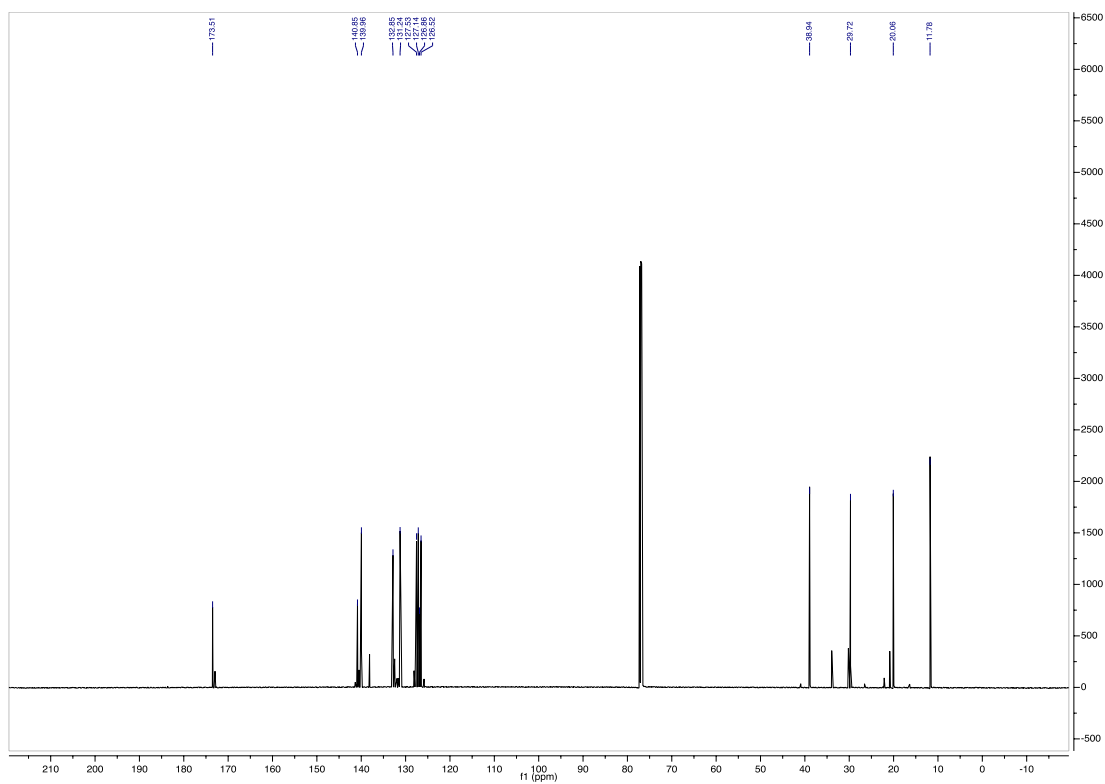
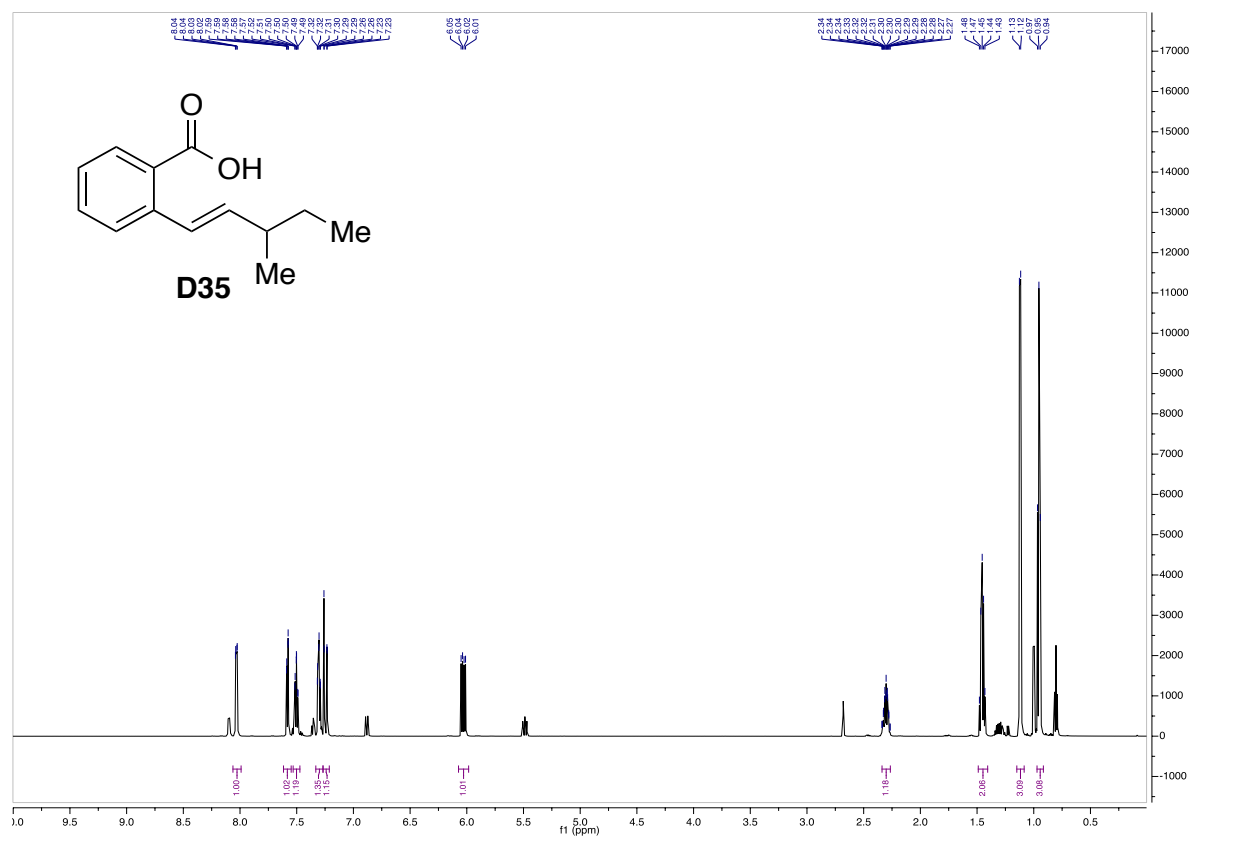




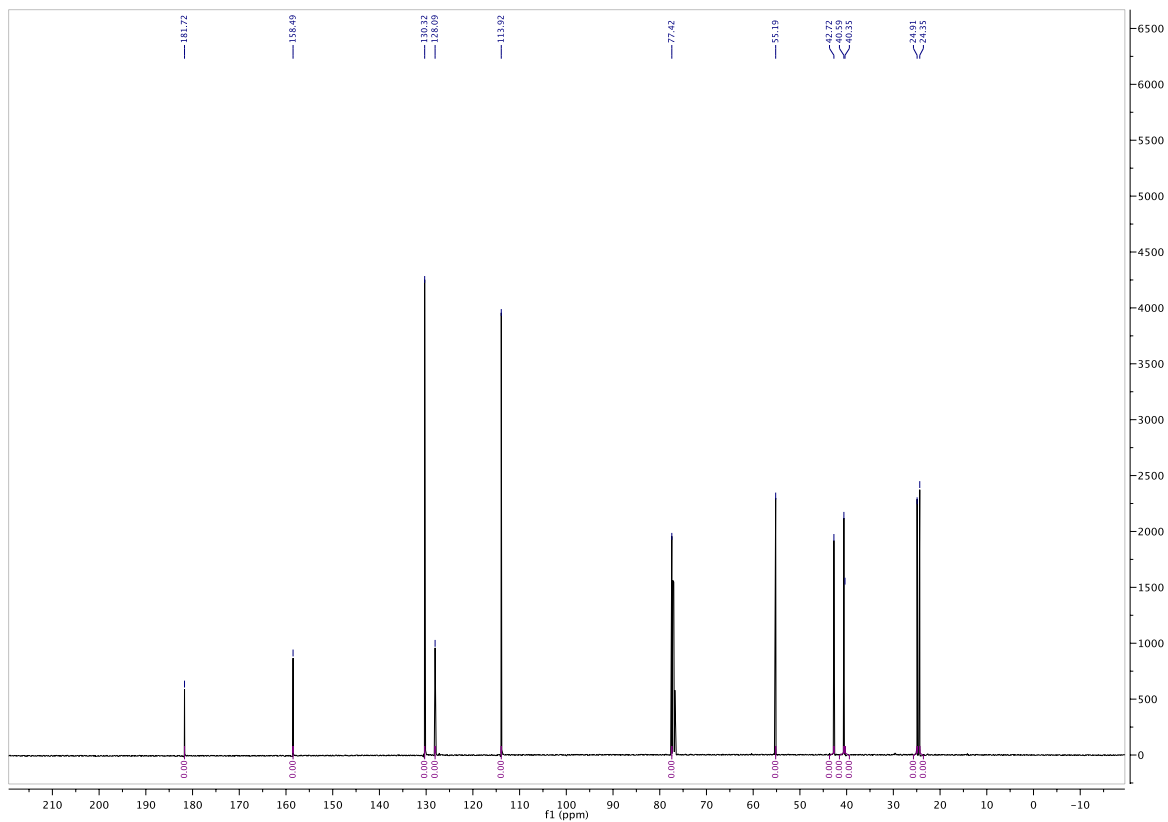
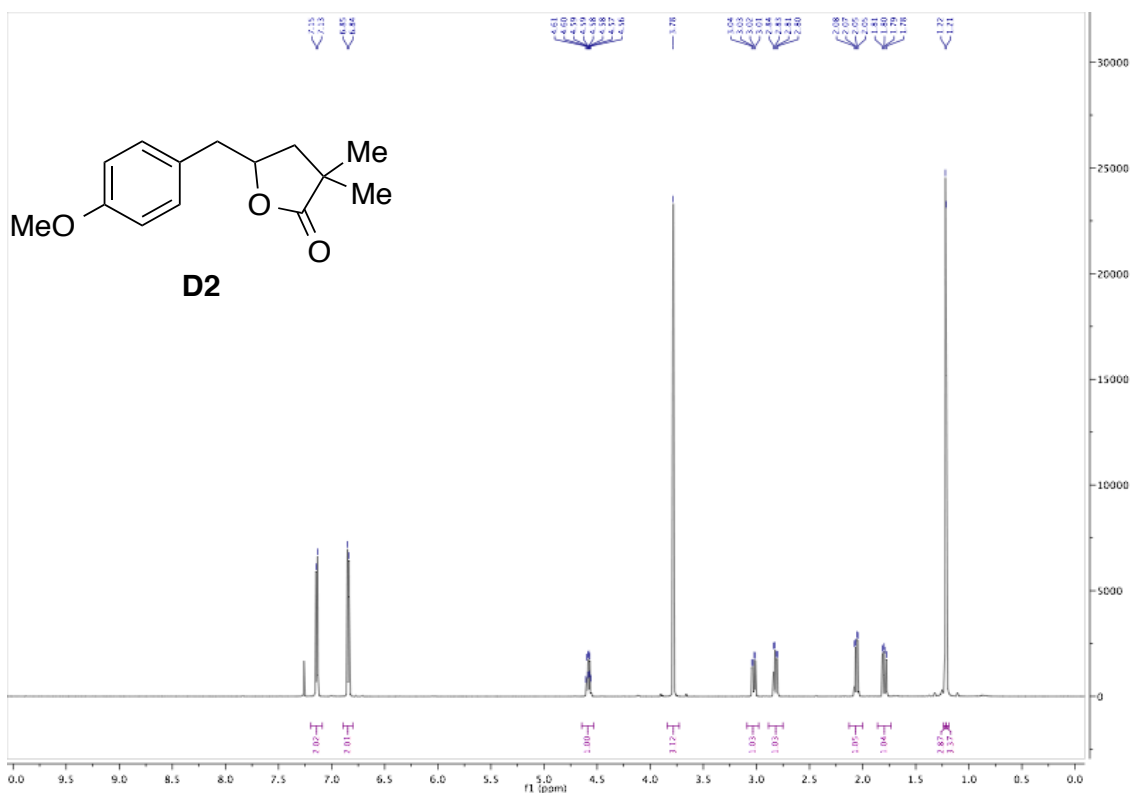




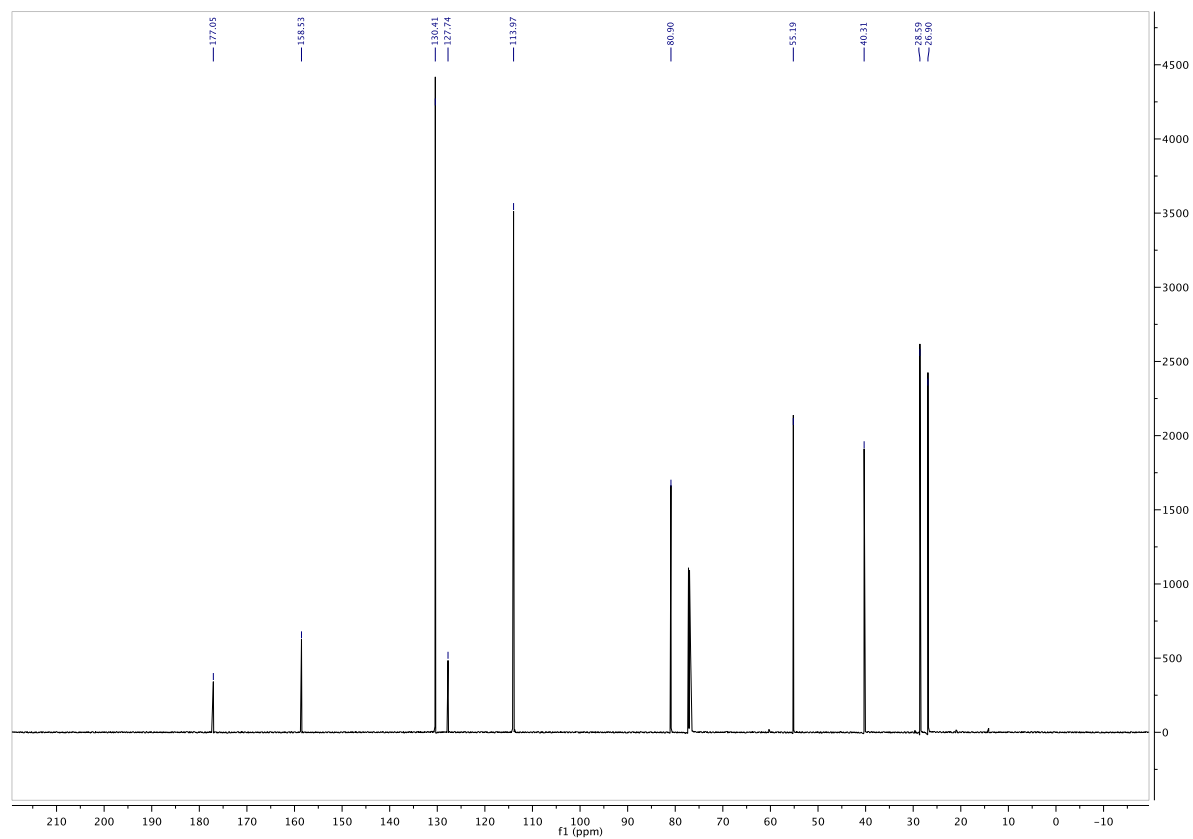
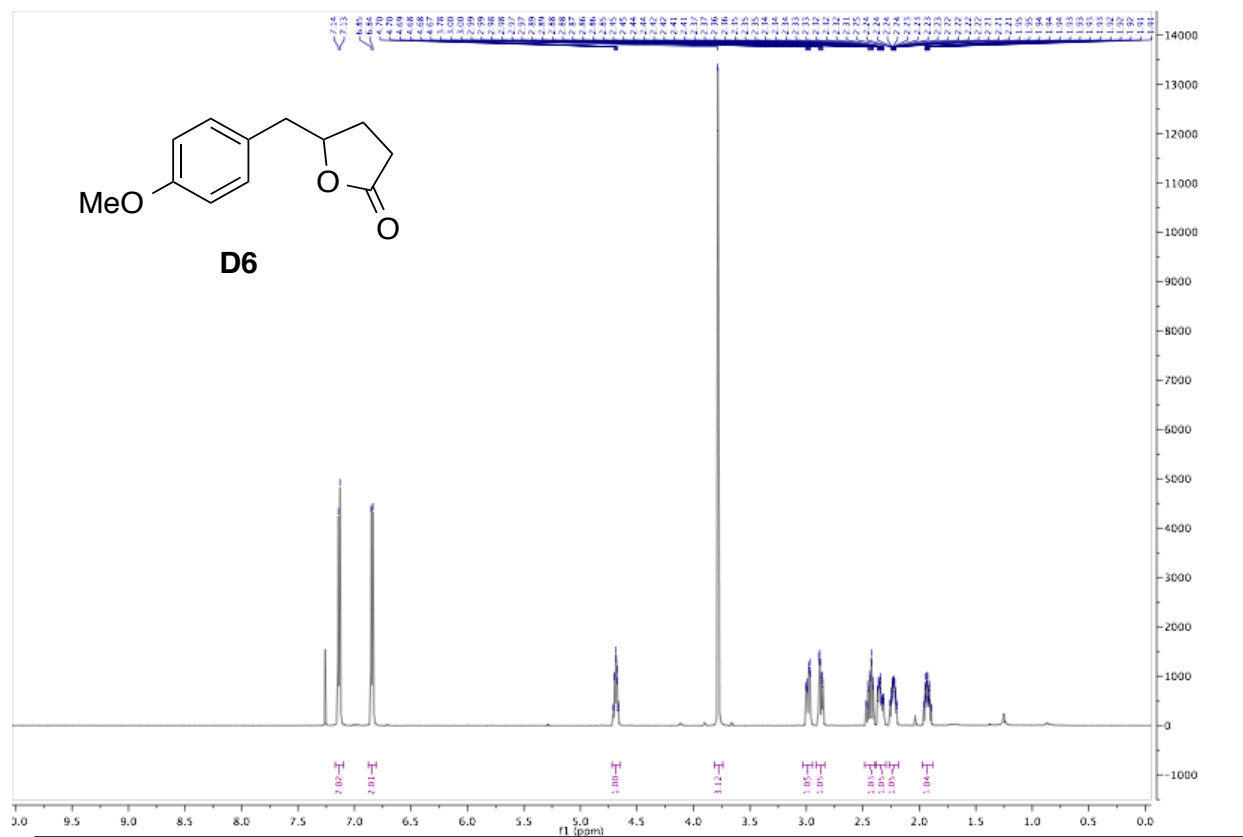


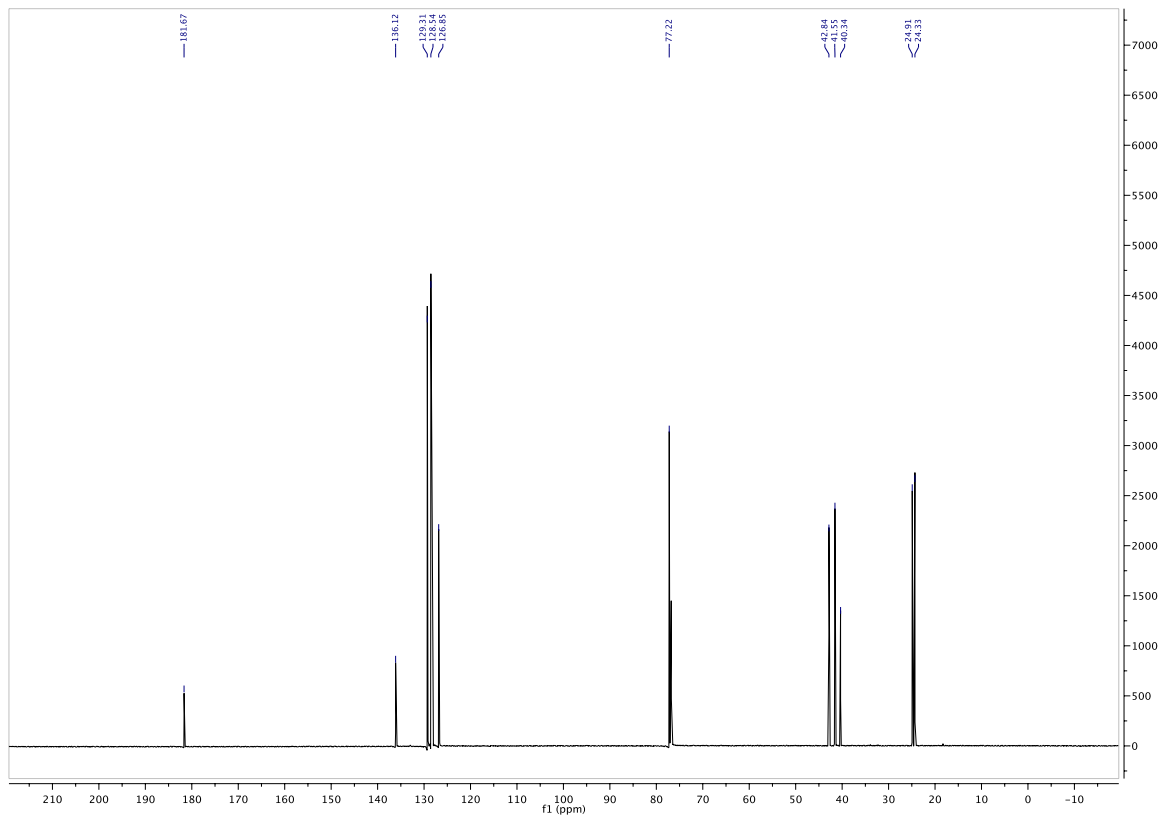
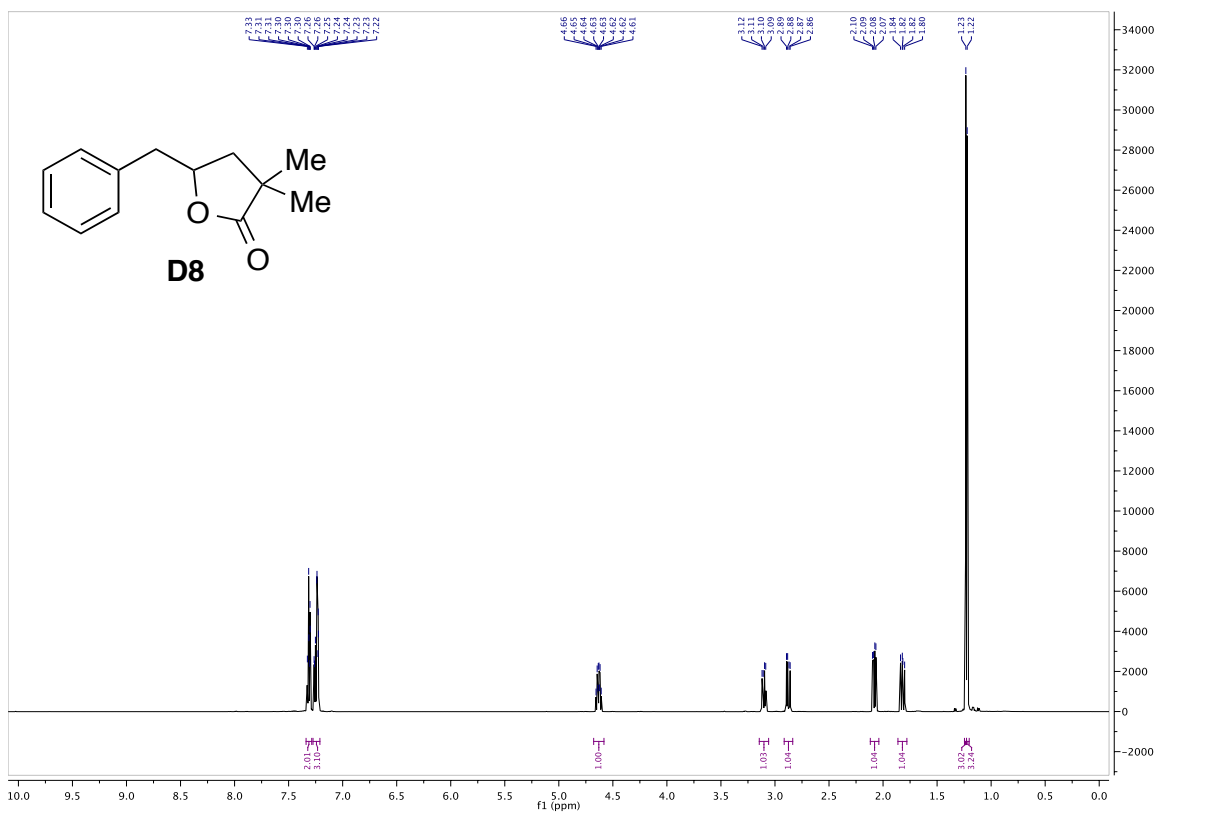


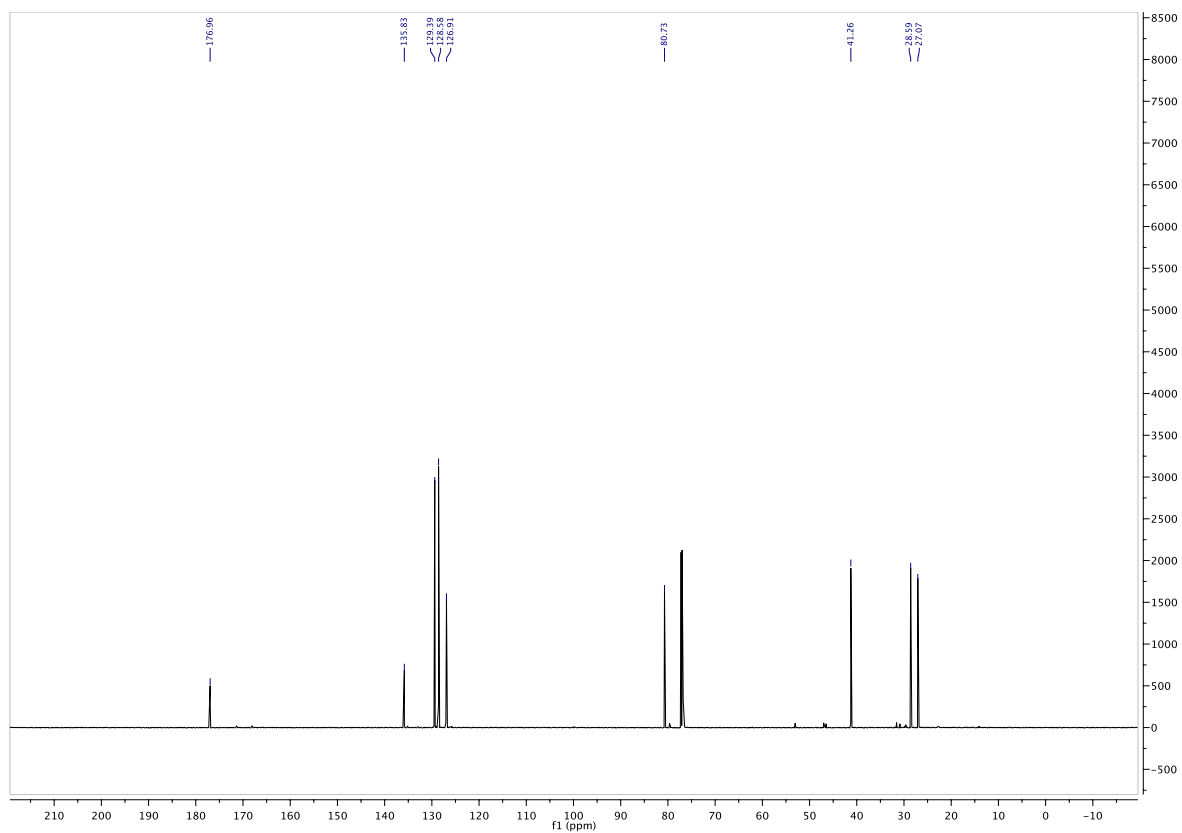
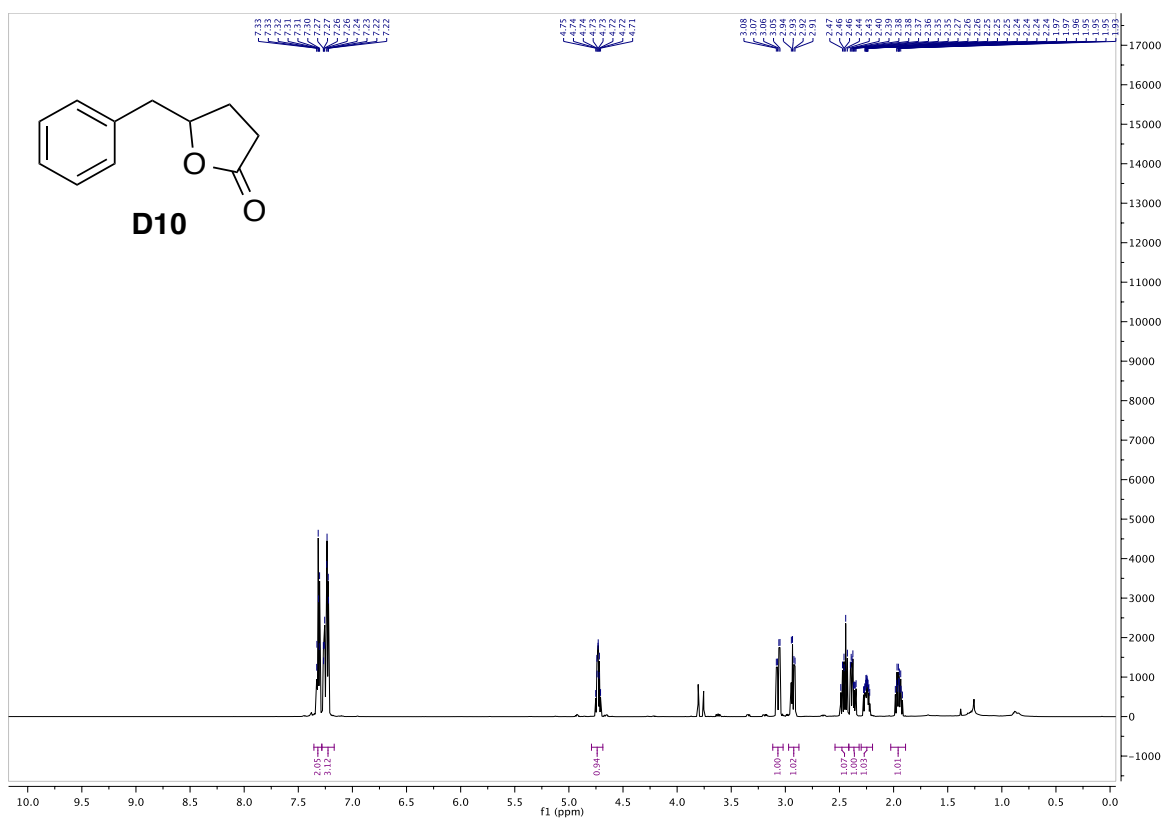


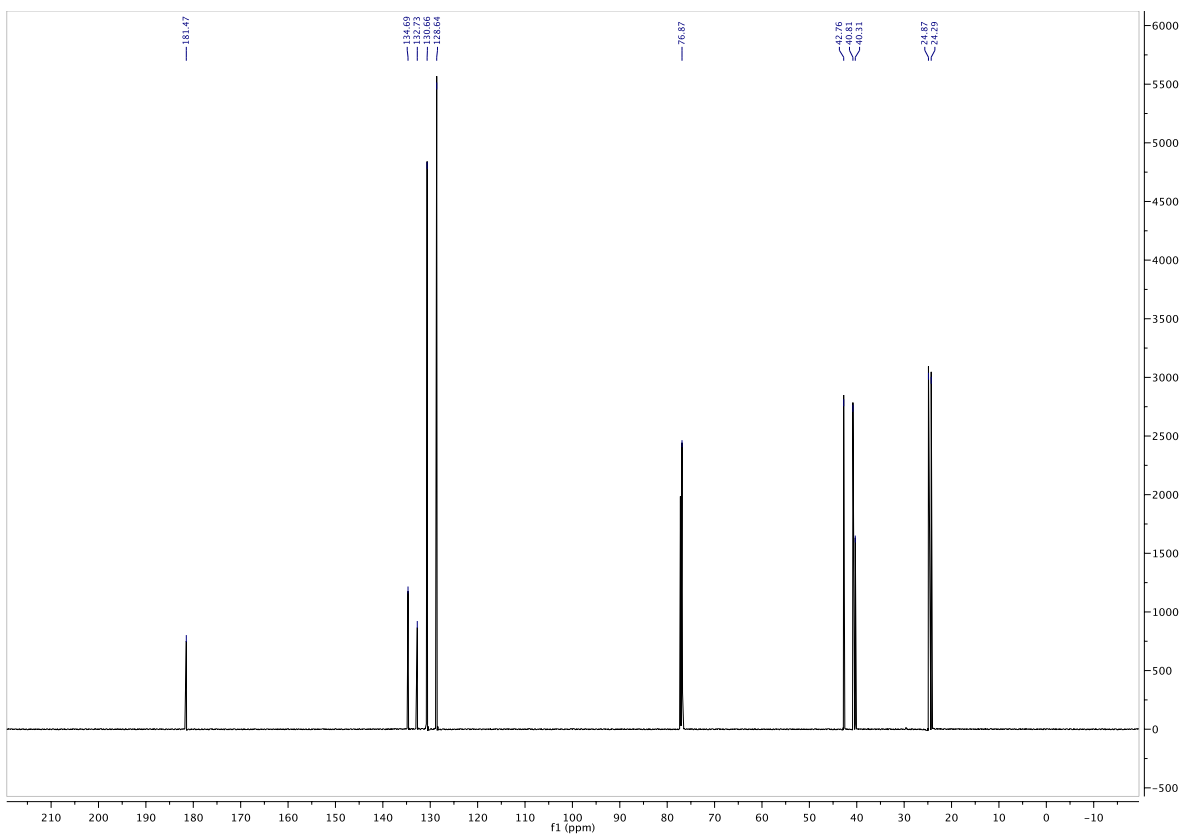
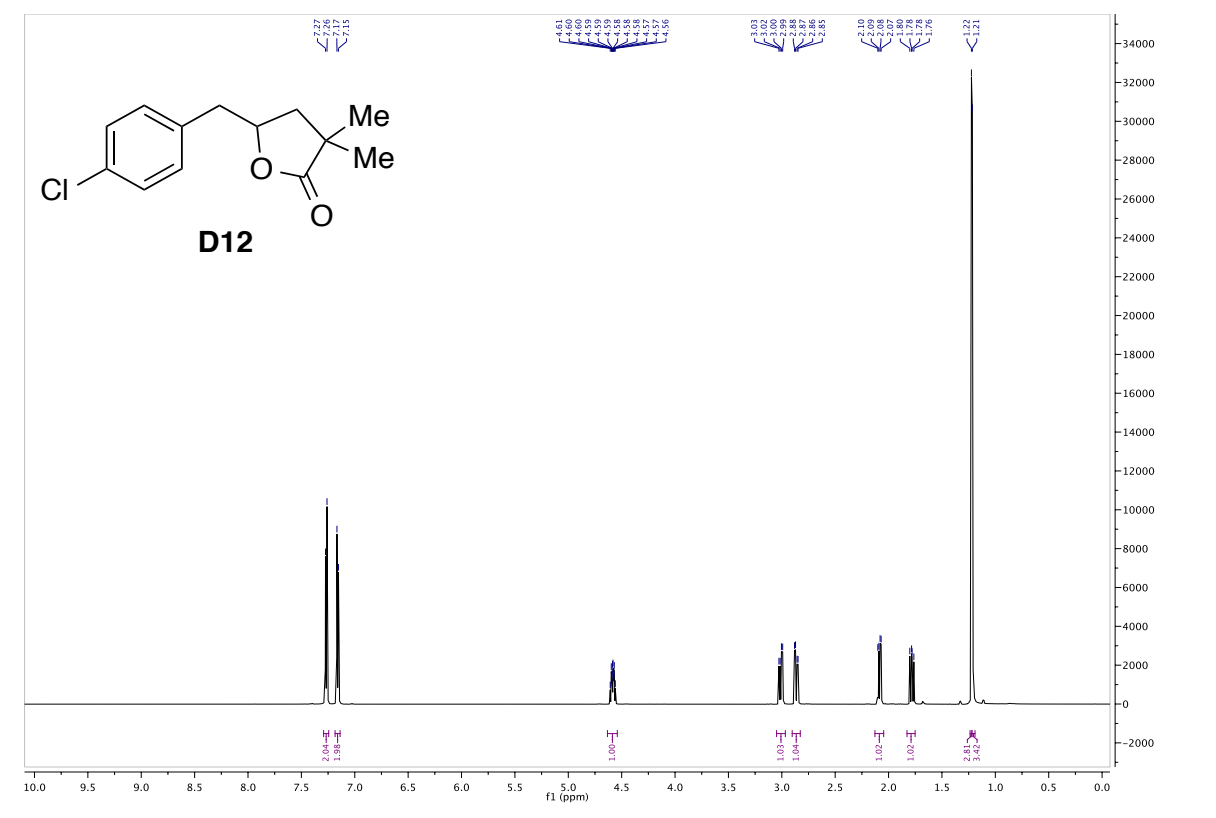


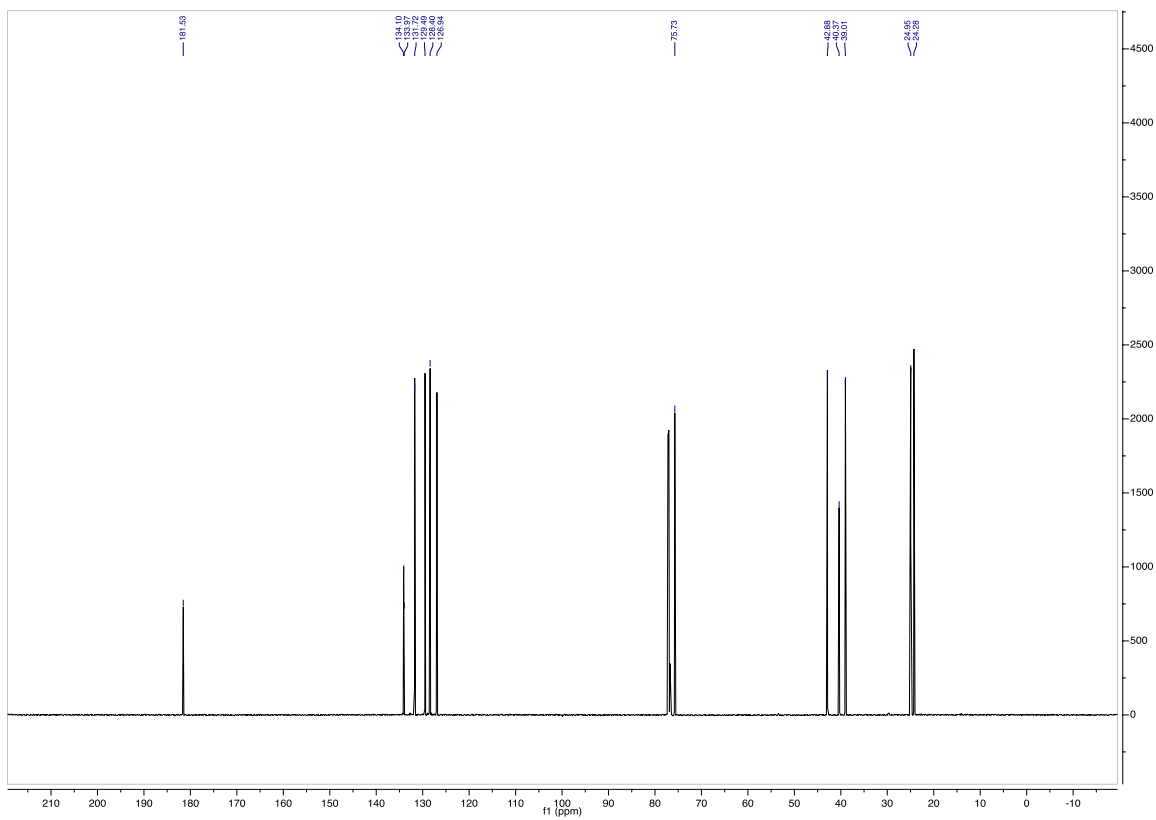
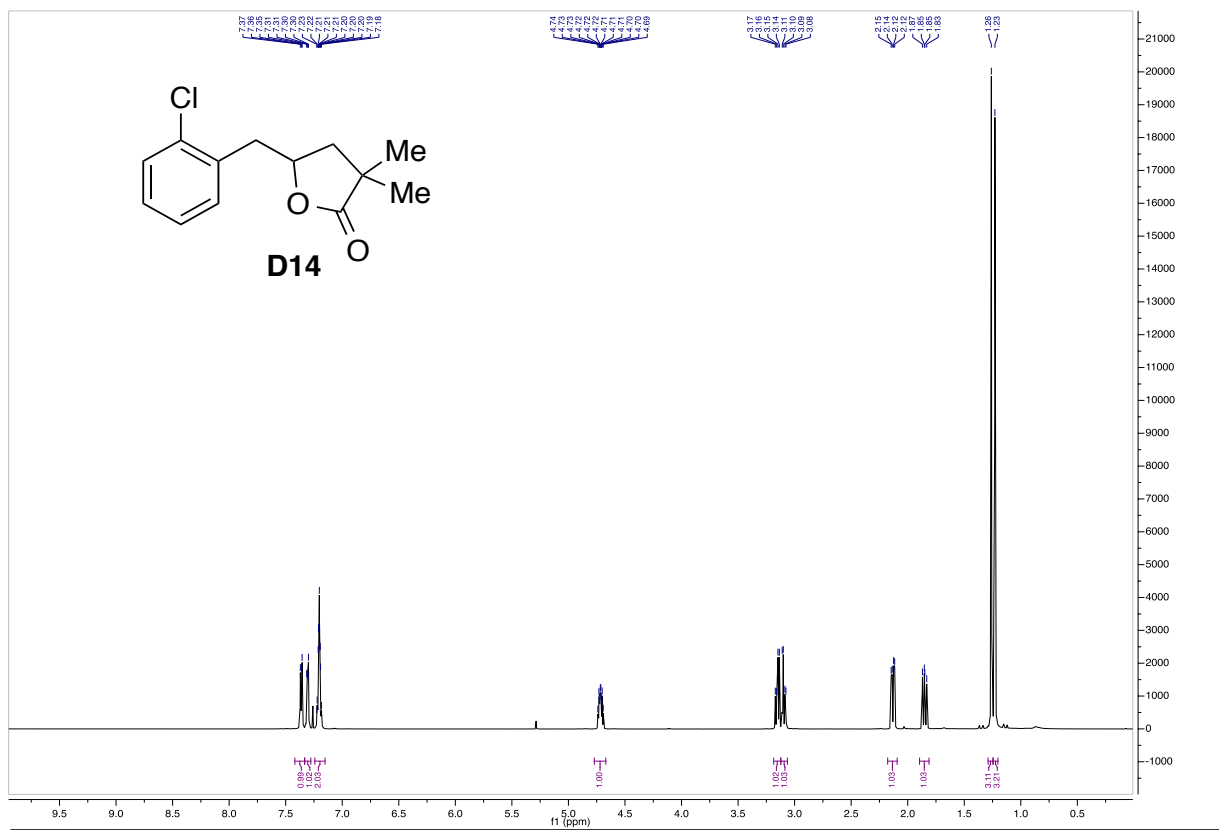


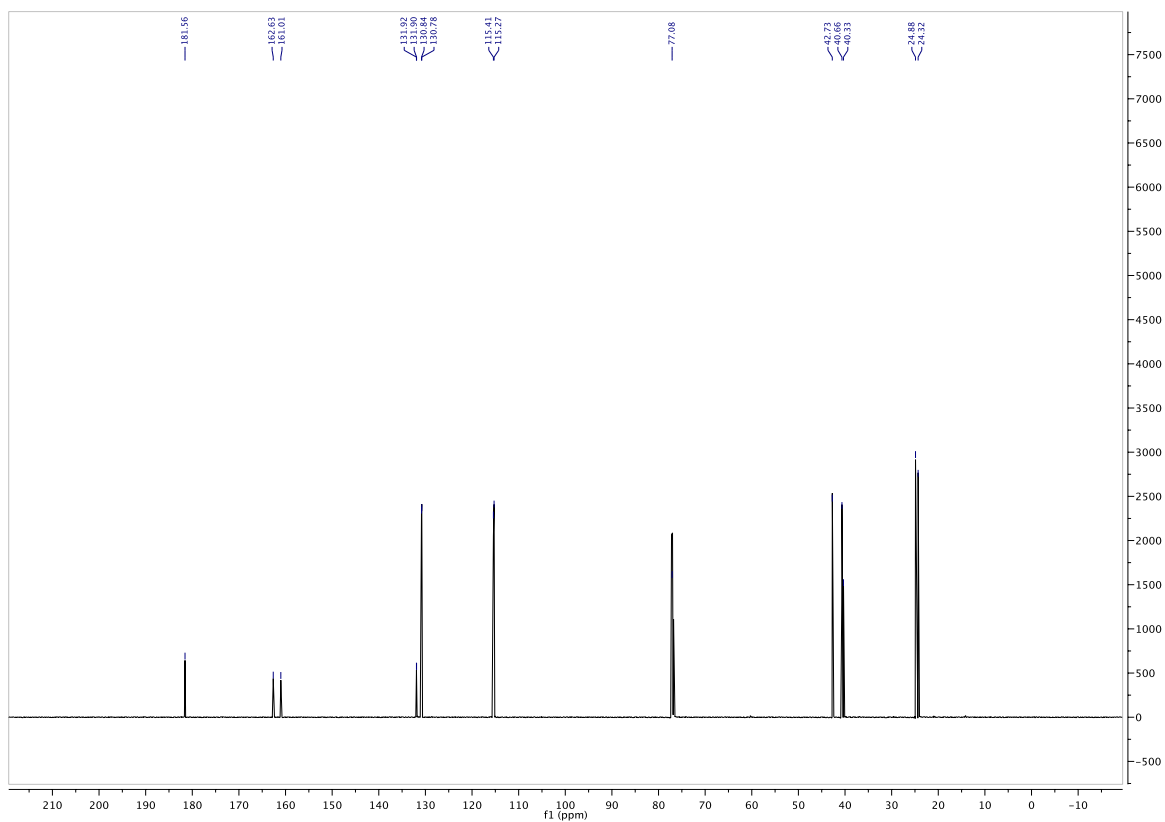
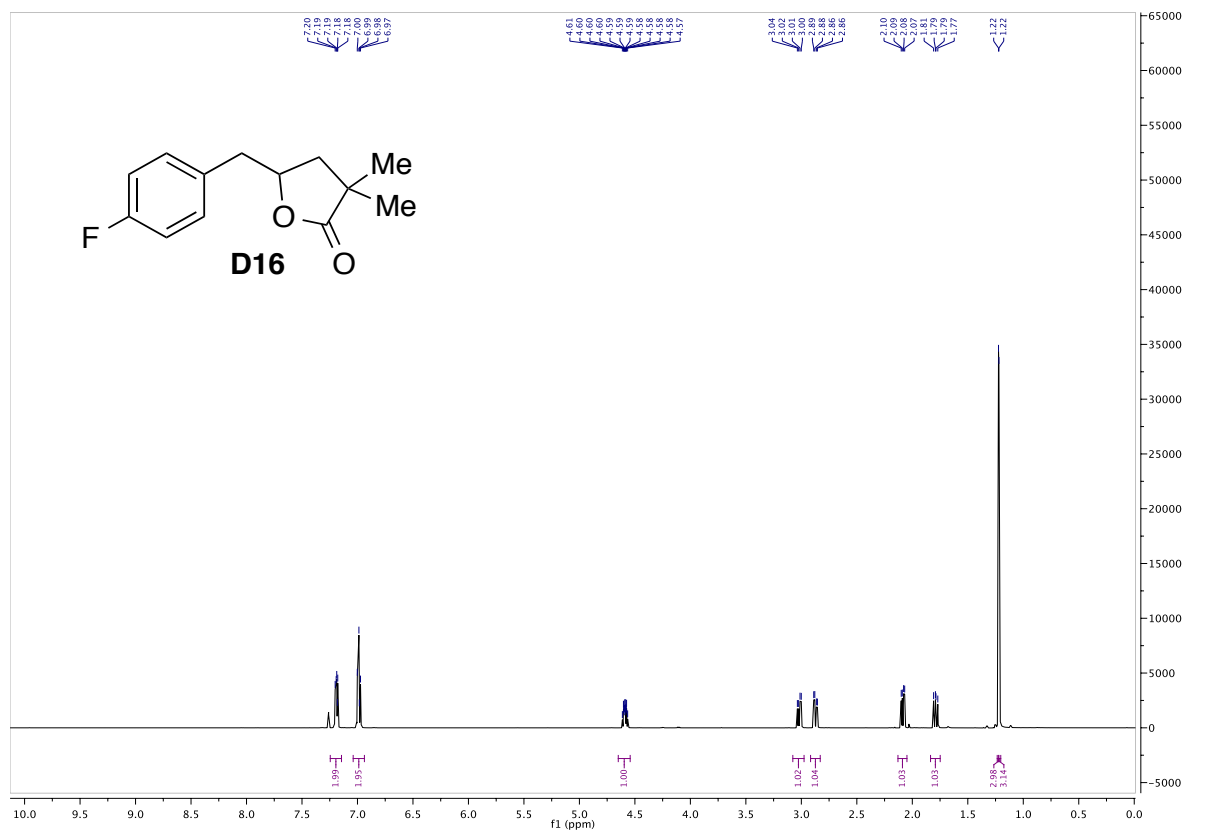




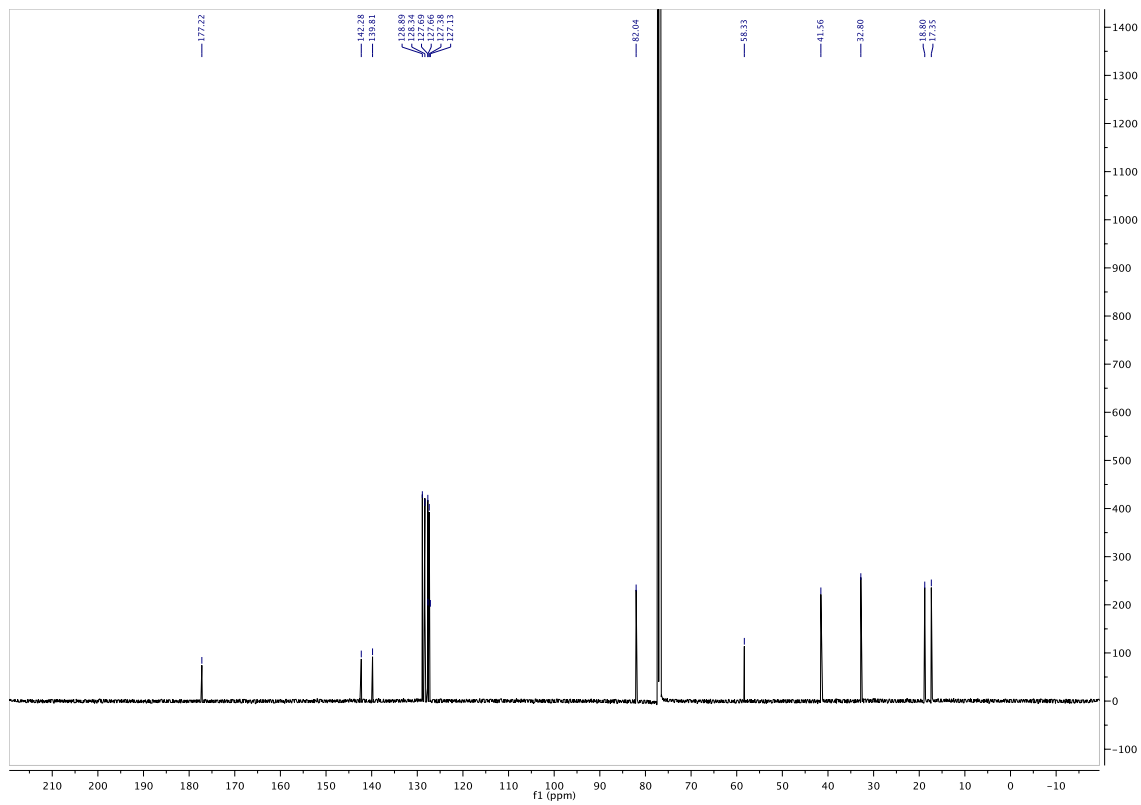
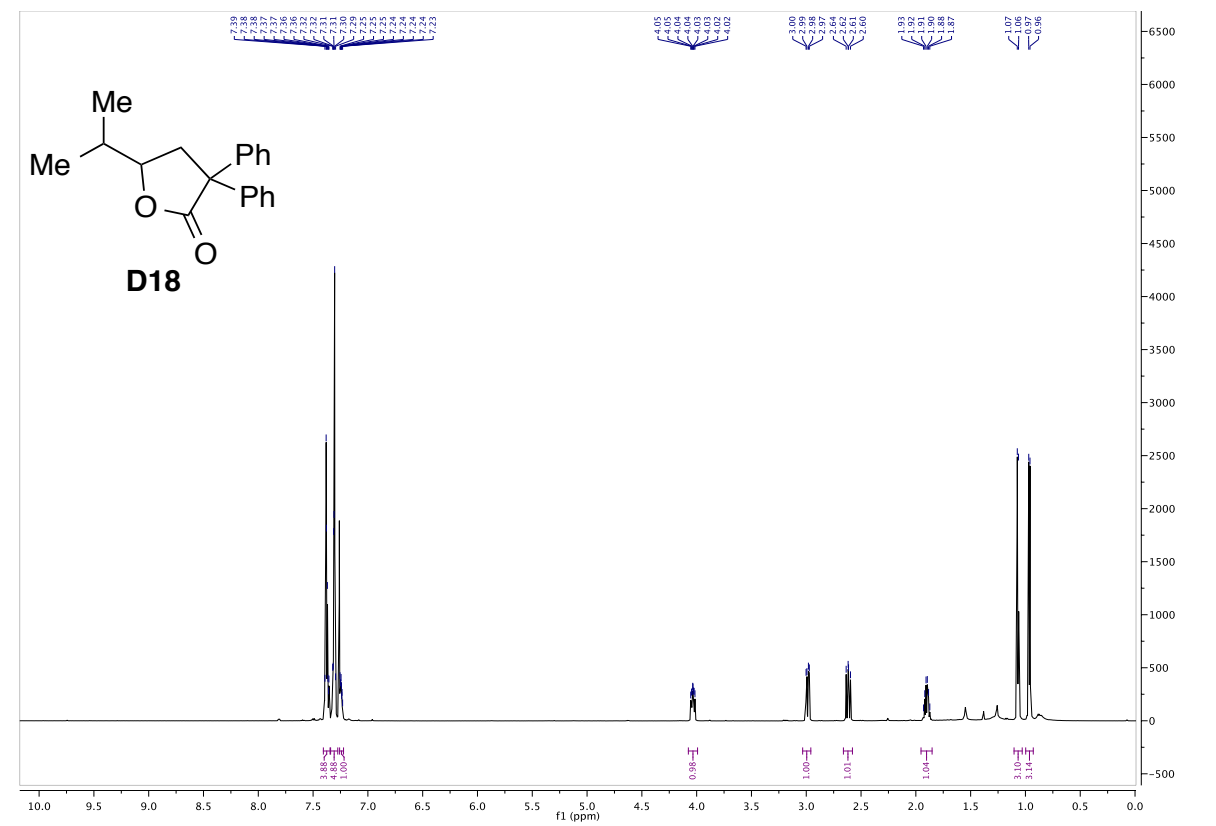


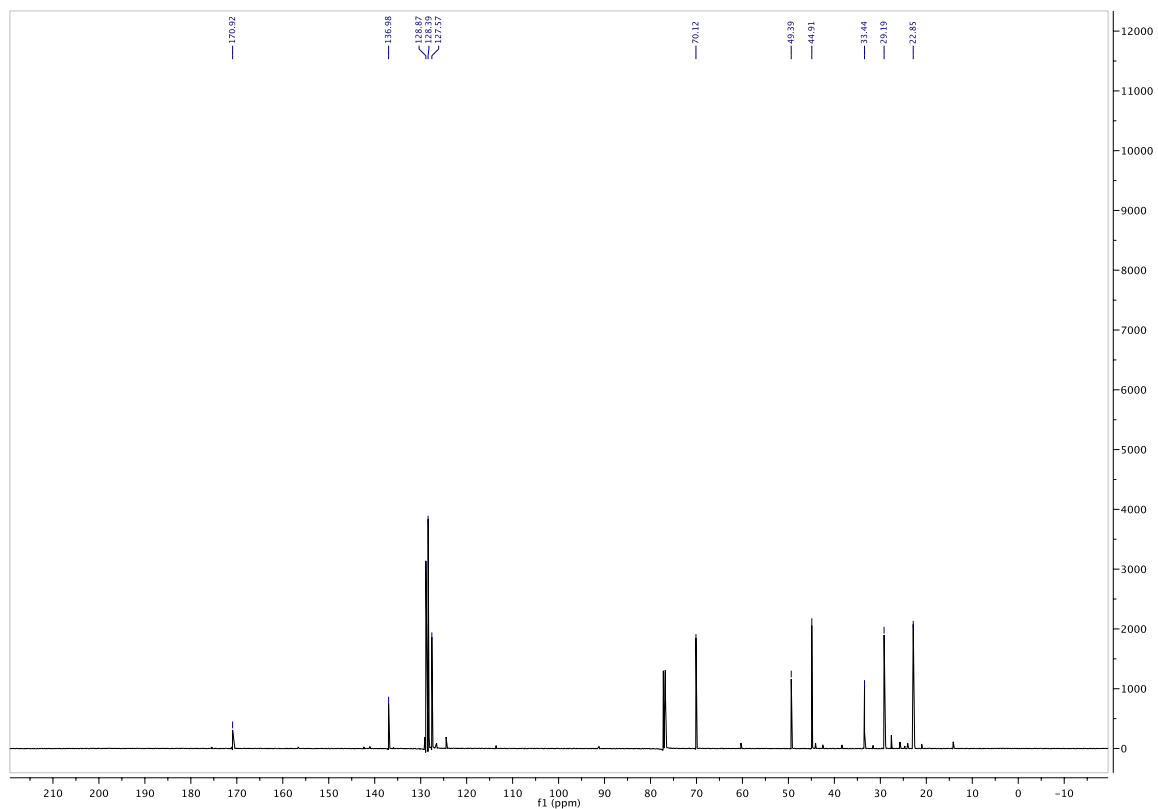
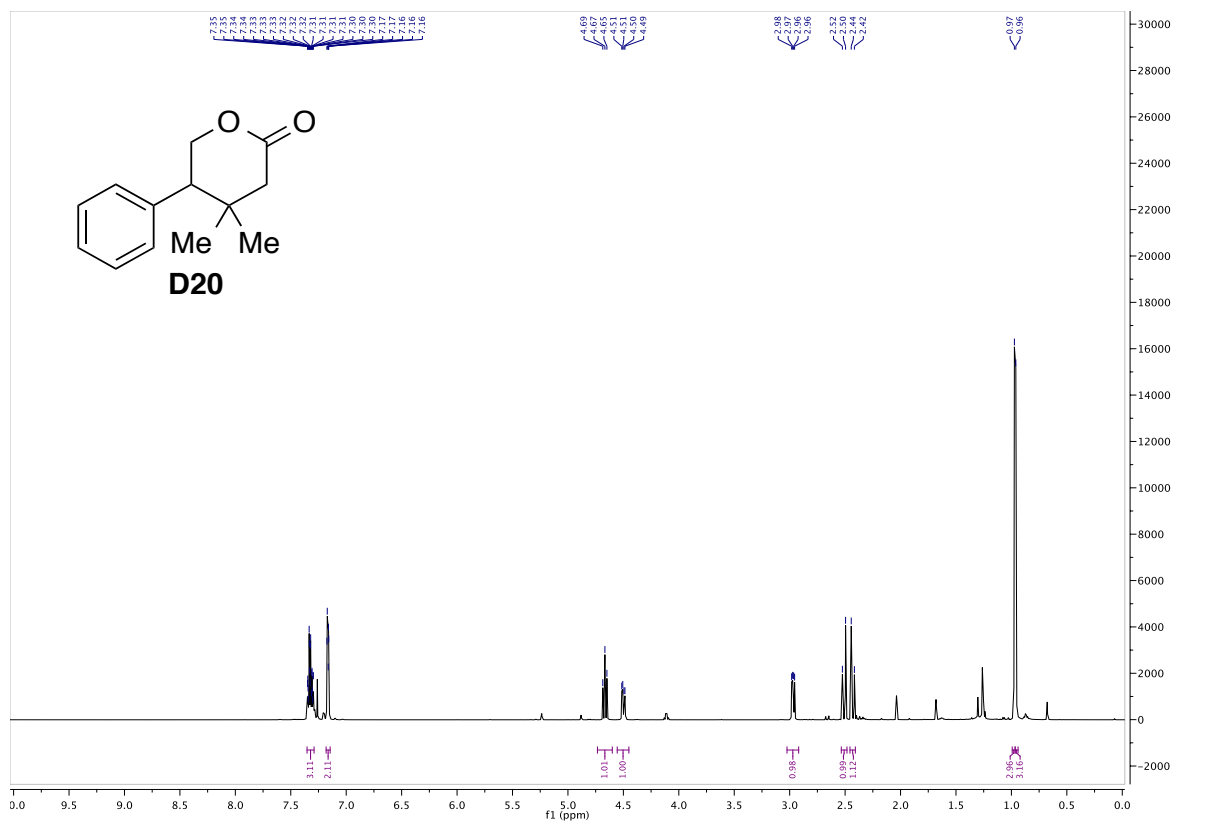


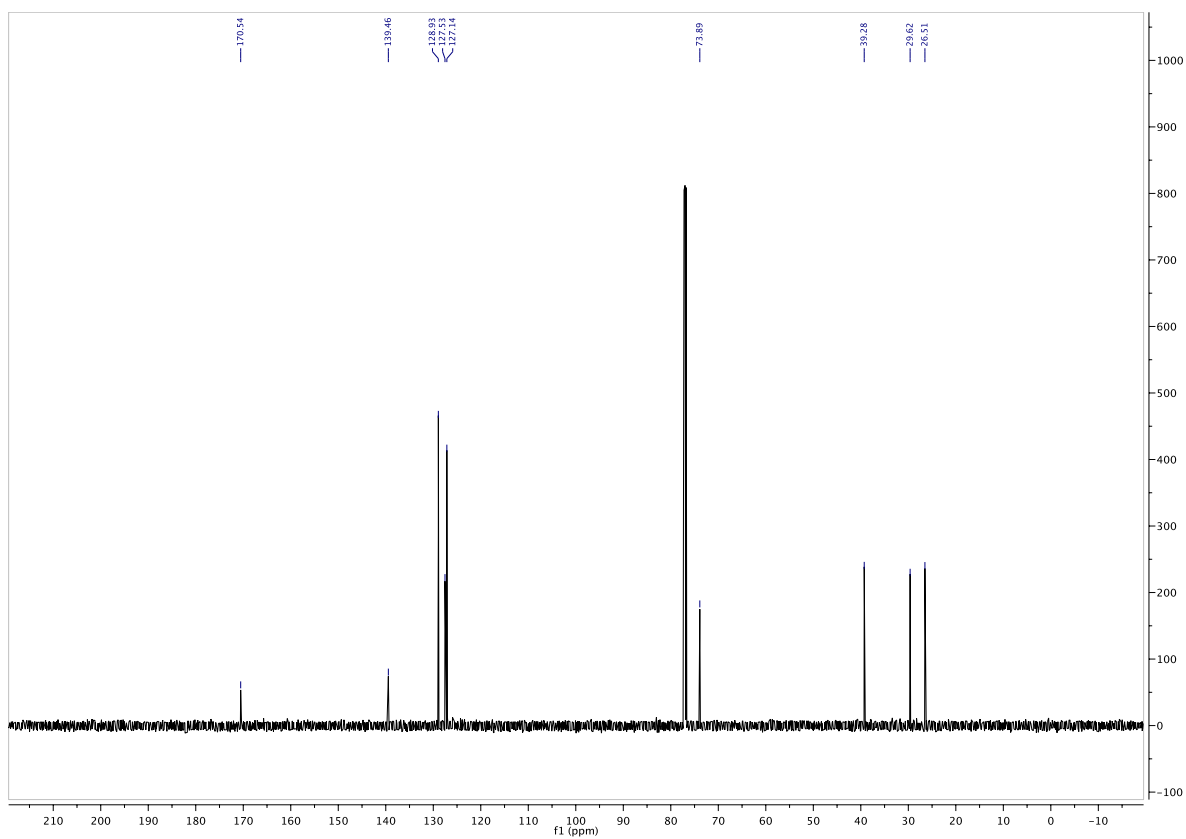
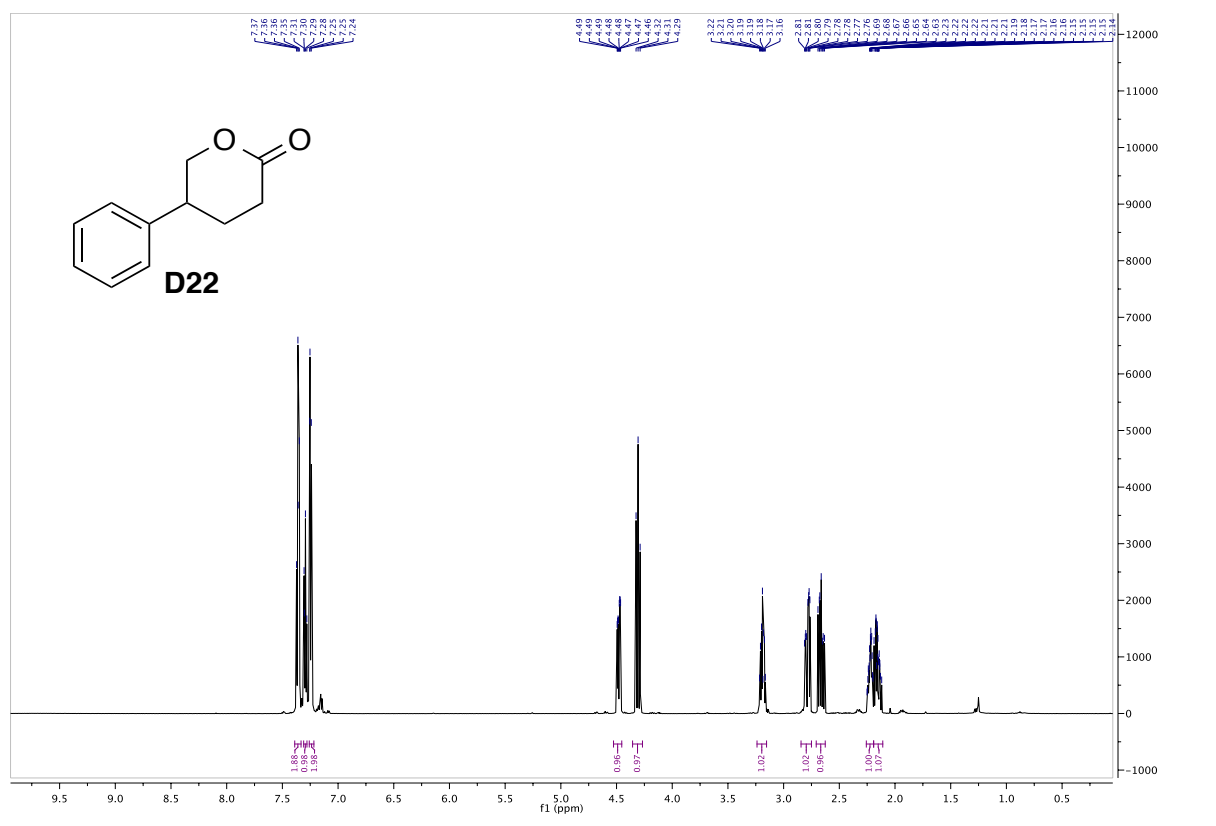


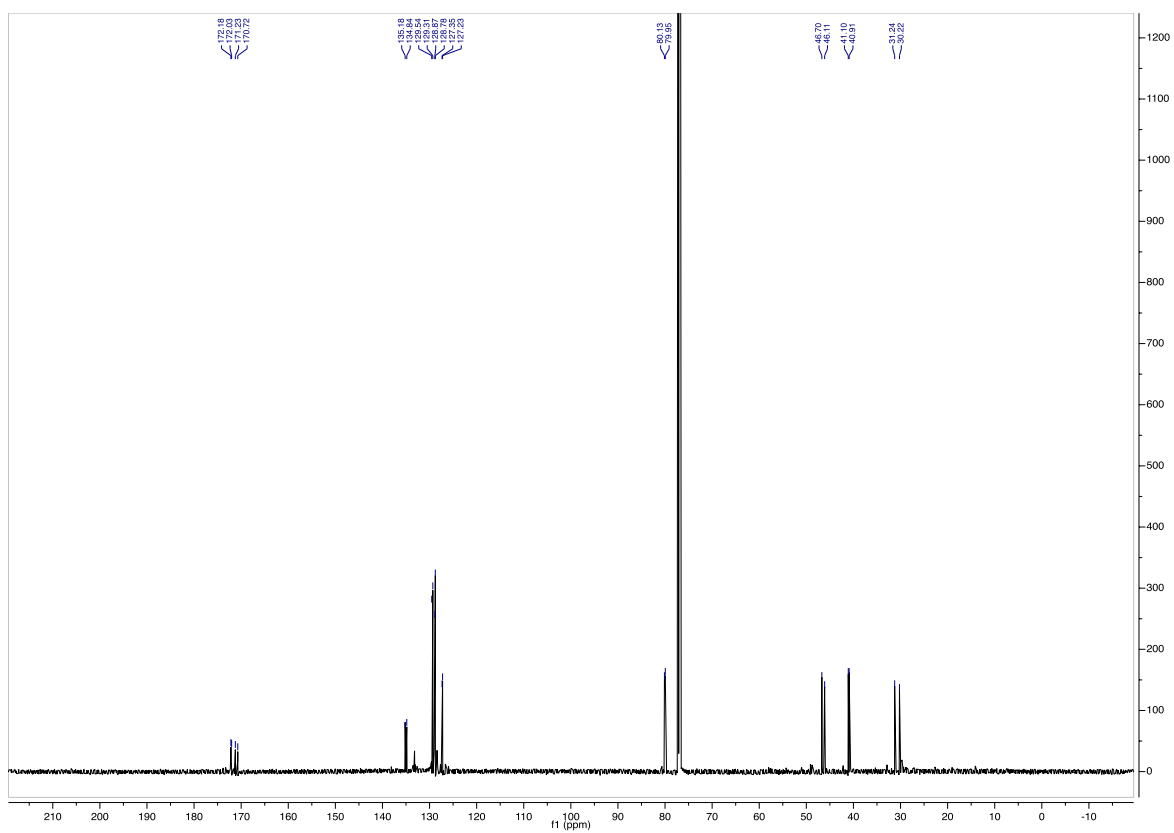
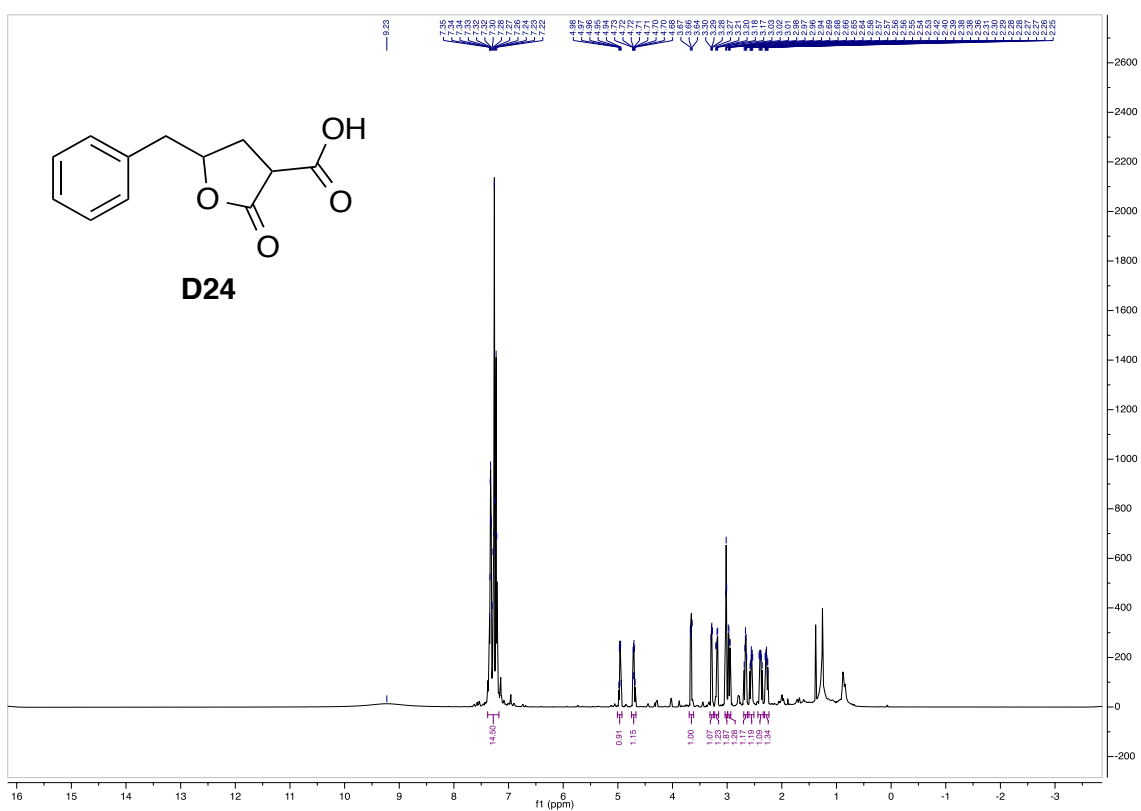




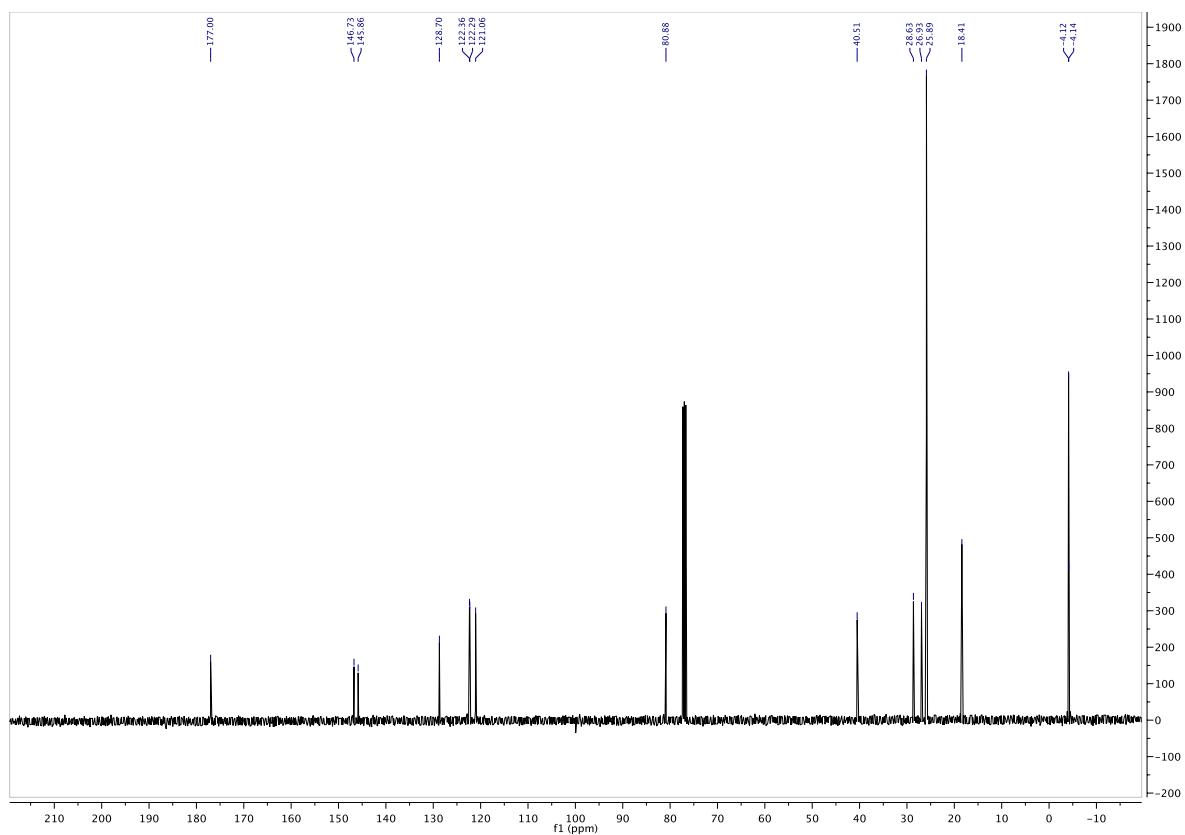
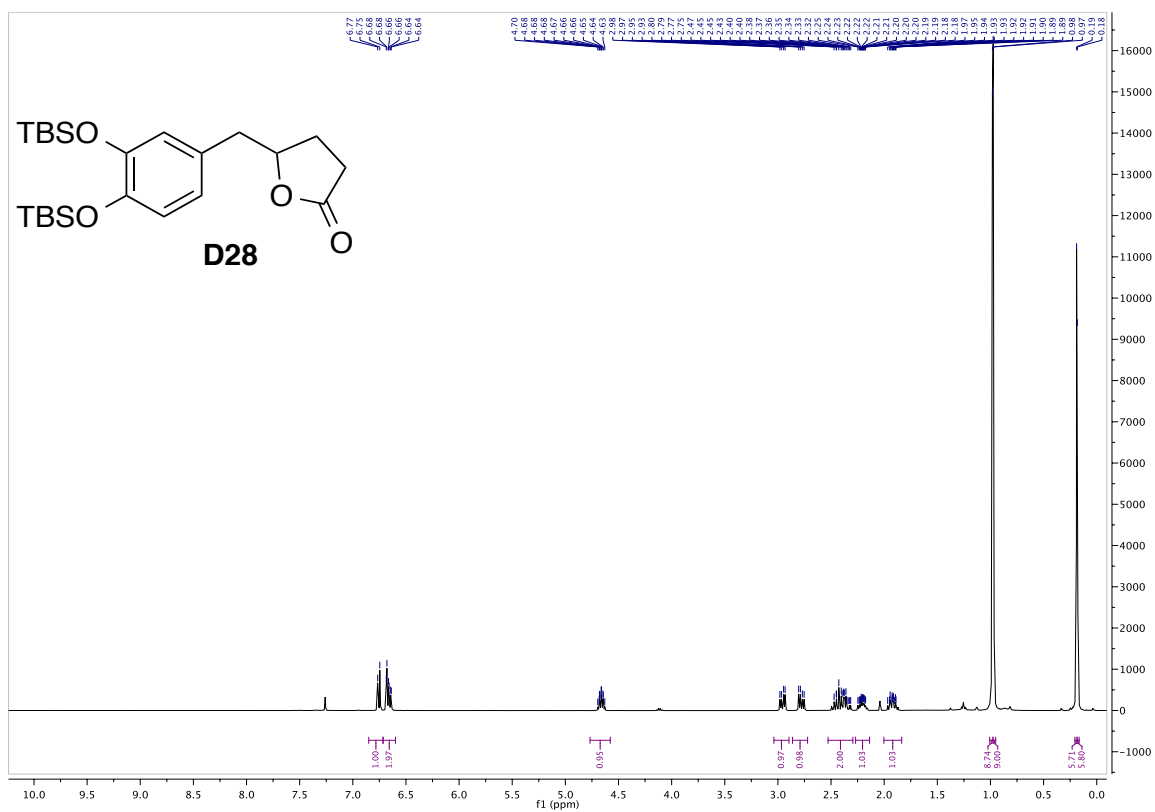


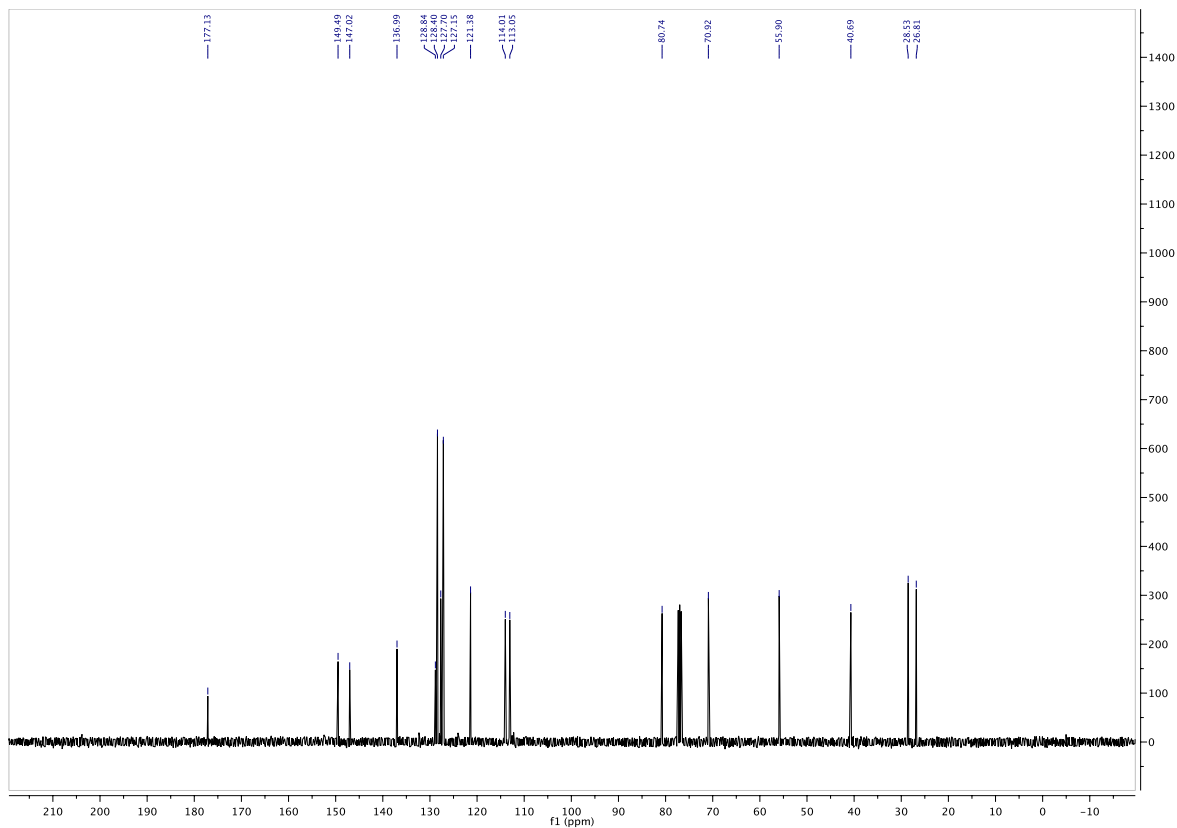
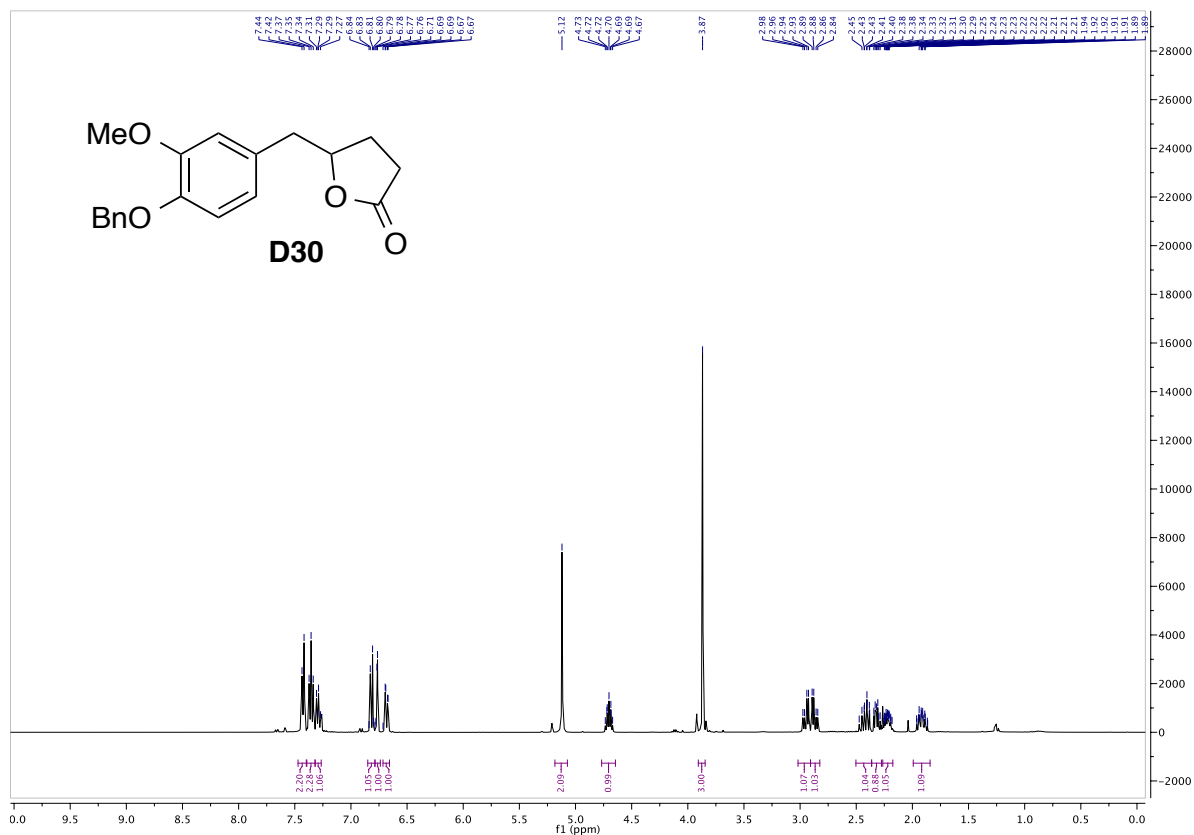


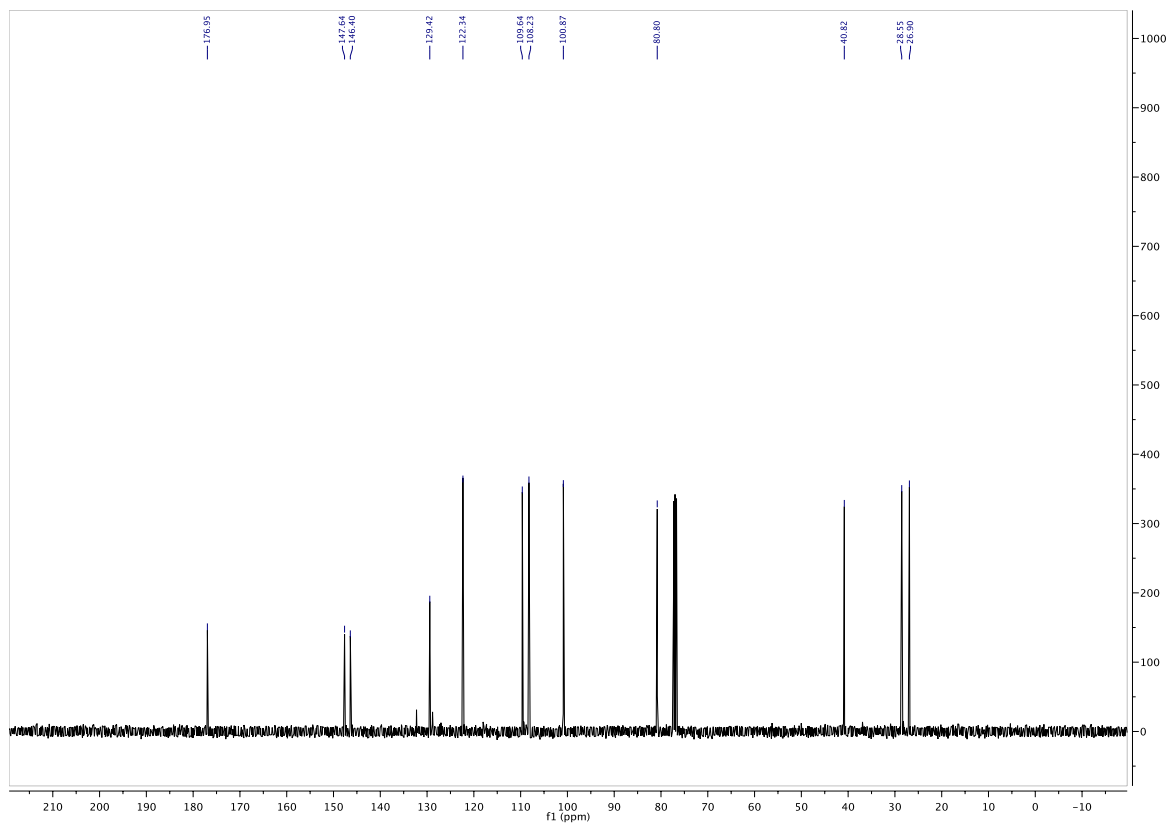
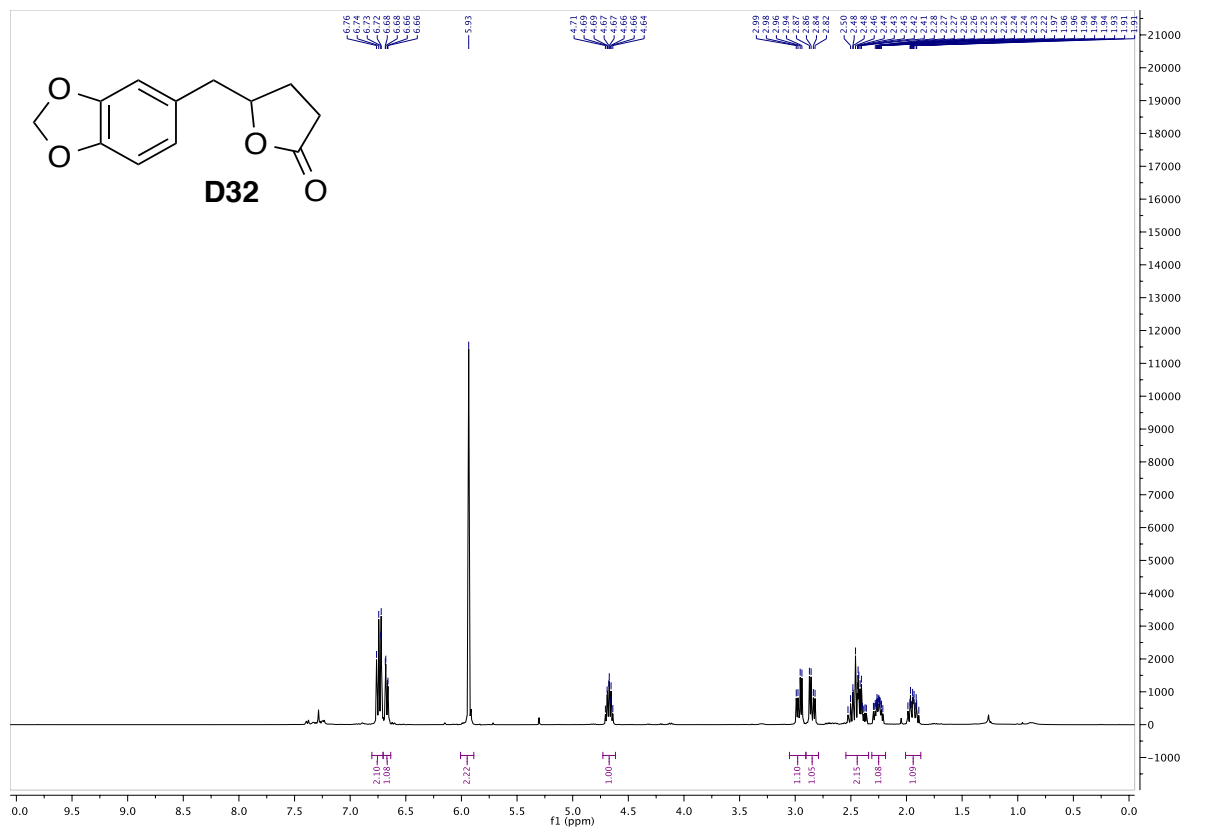






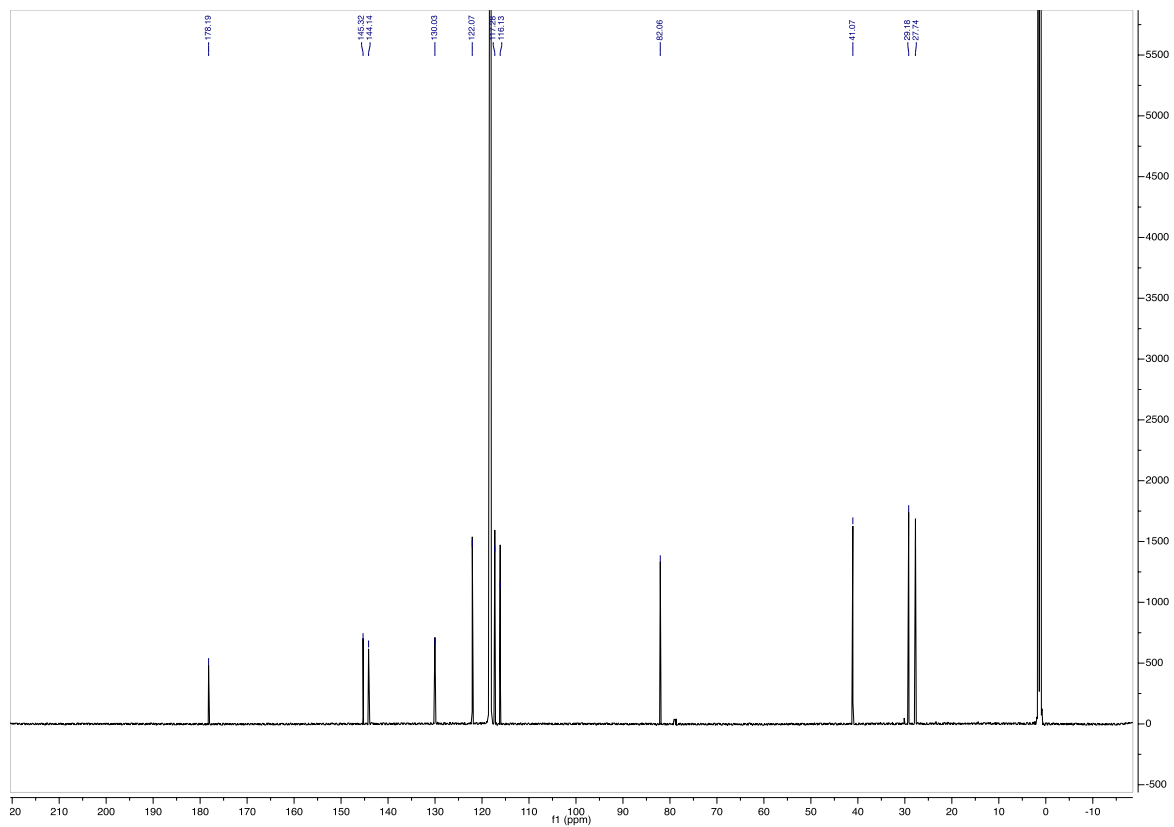
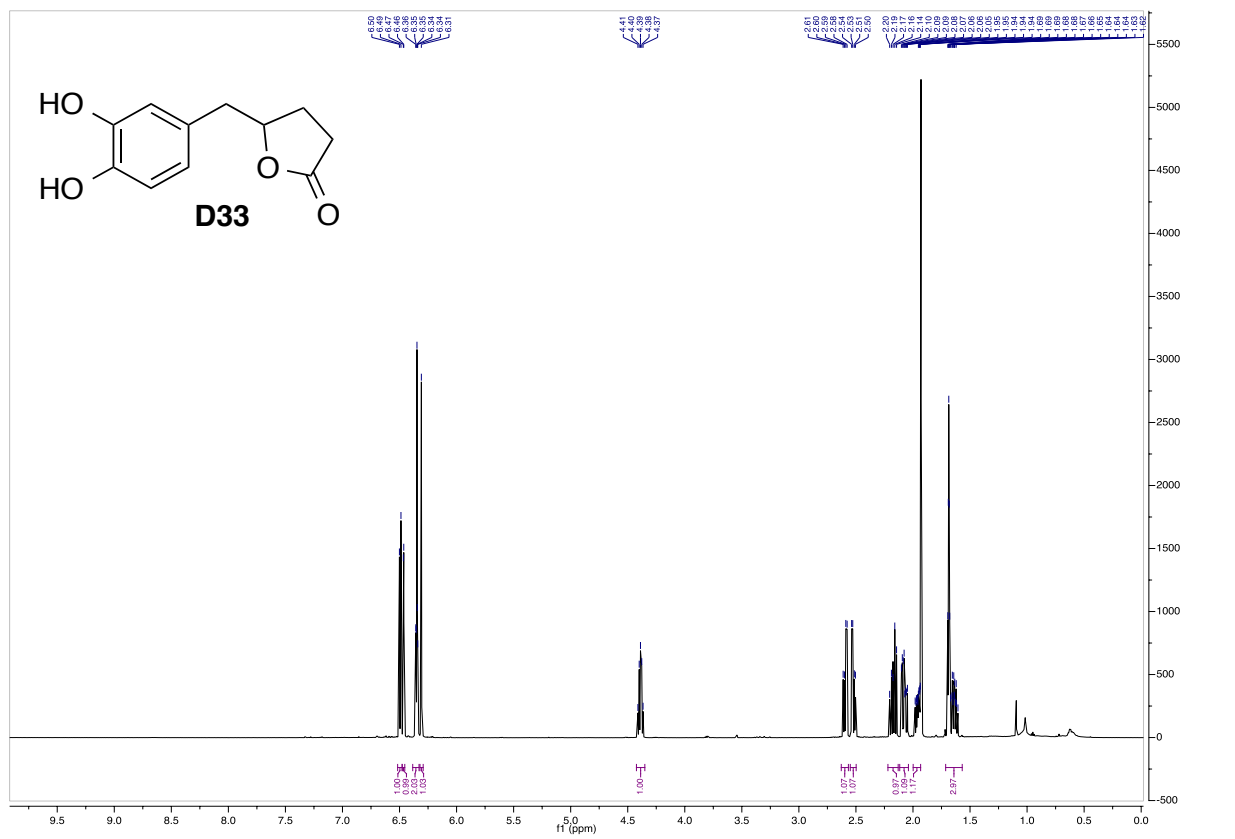


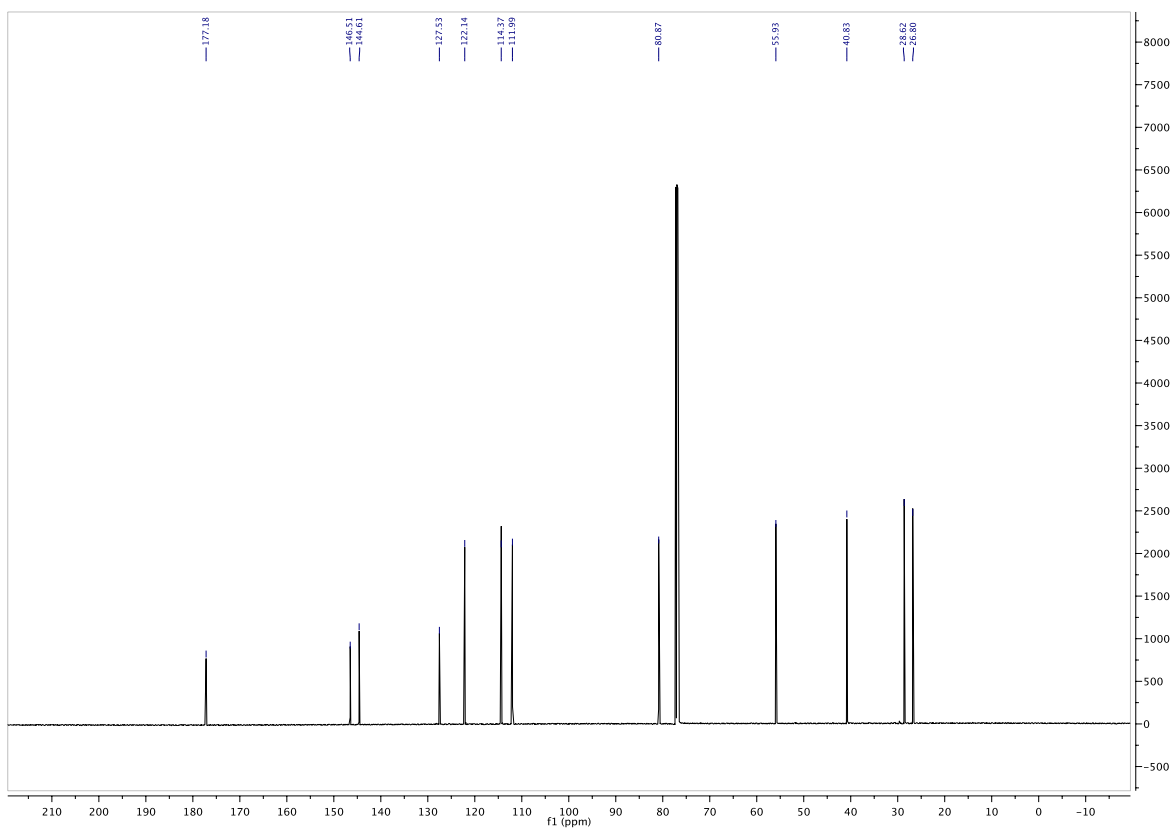
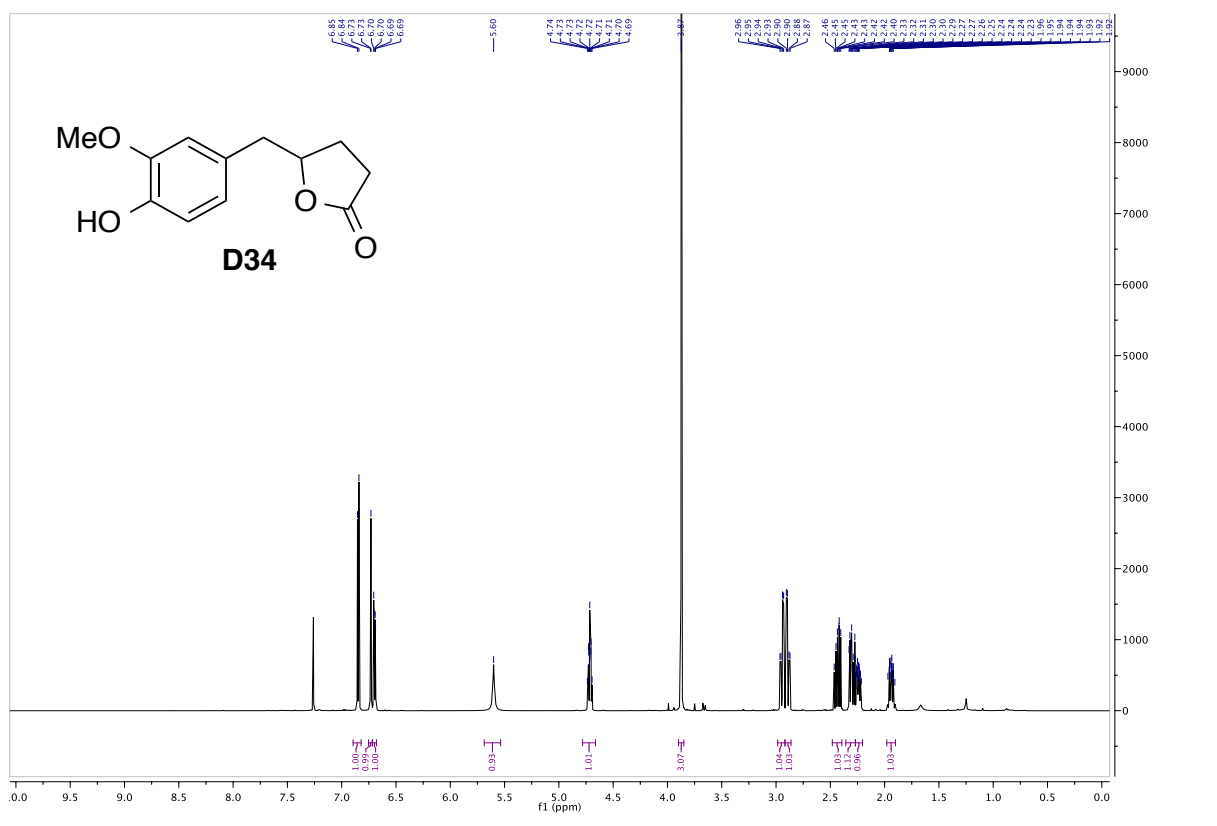


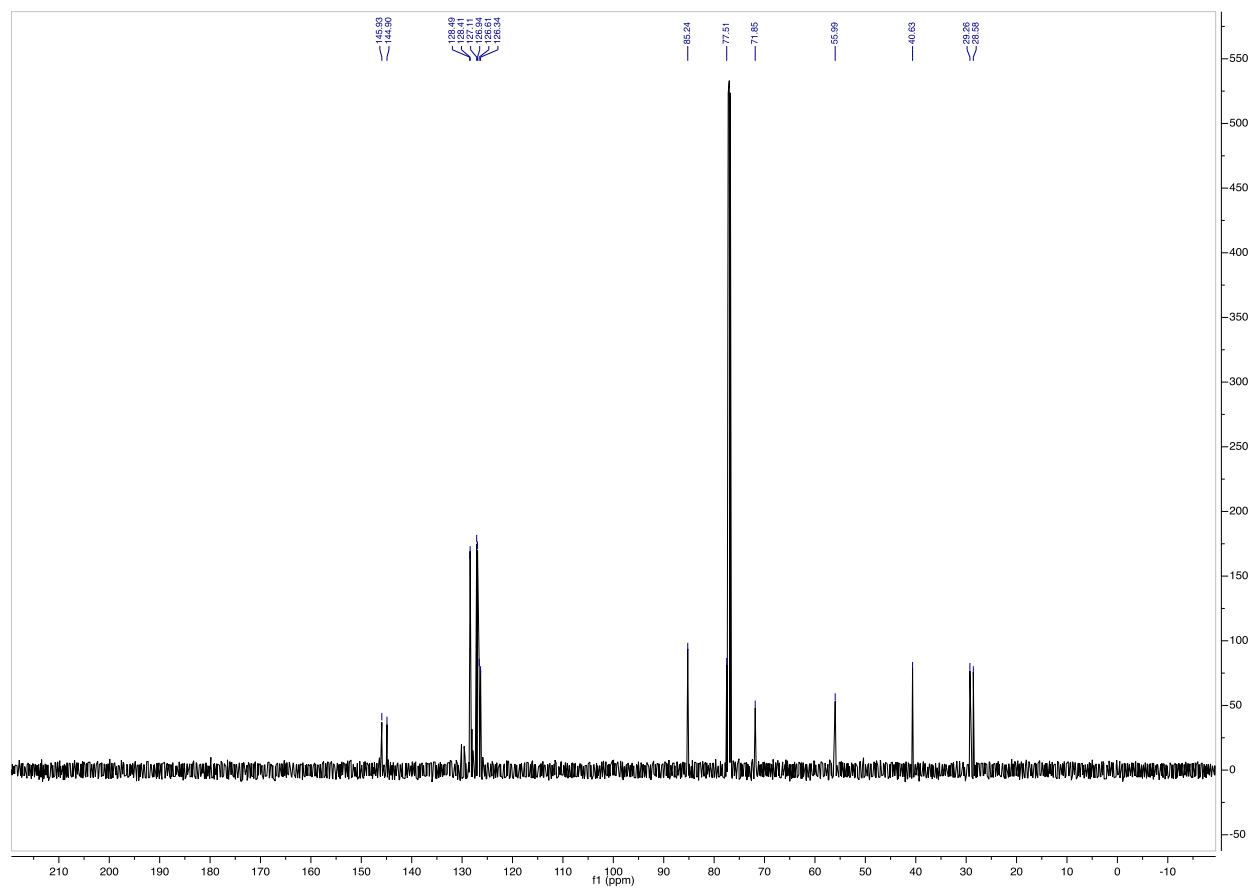
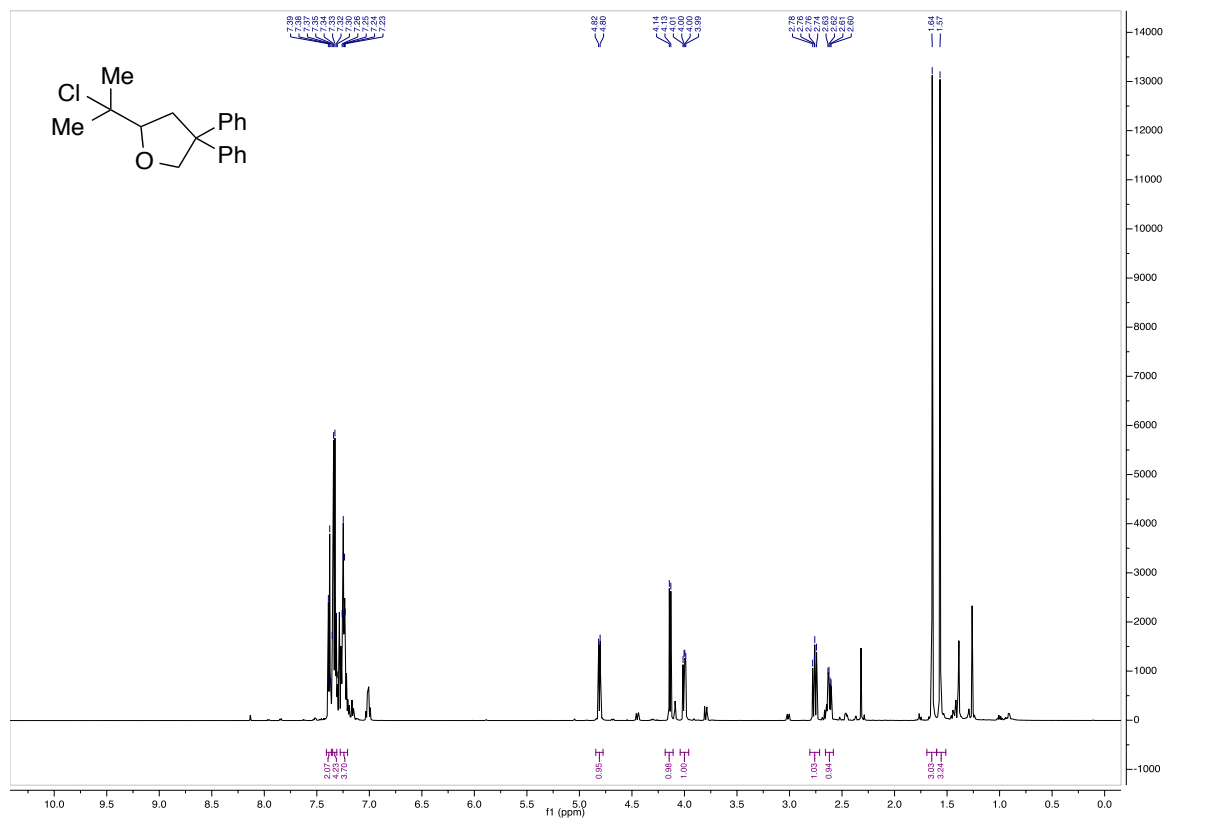


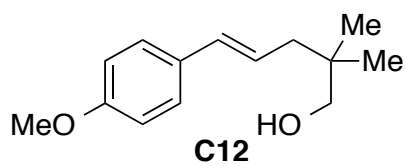








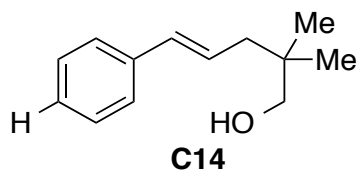
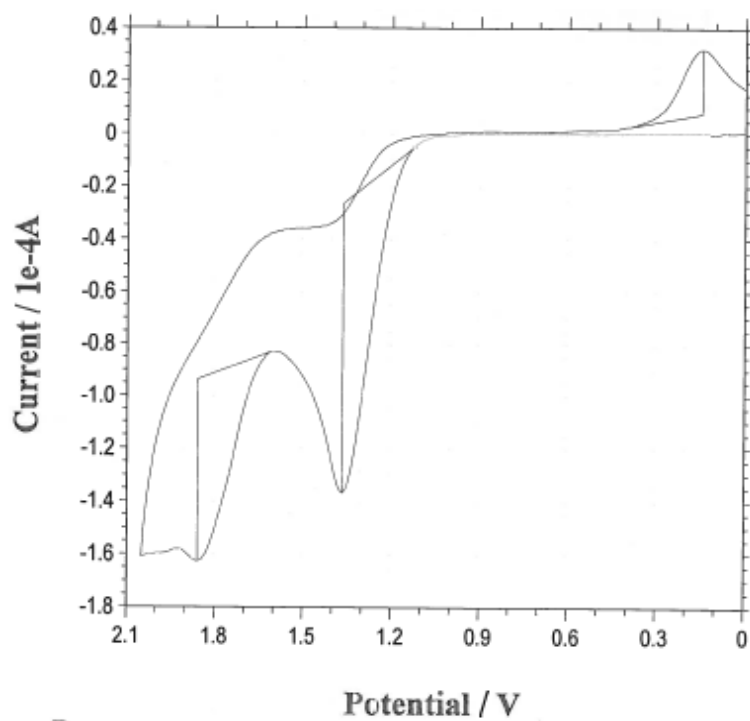




Scan Rate: 0.1 V/s

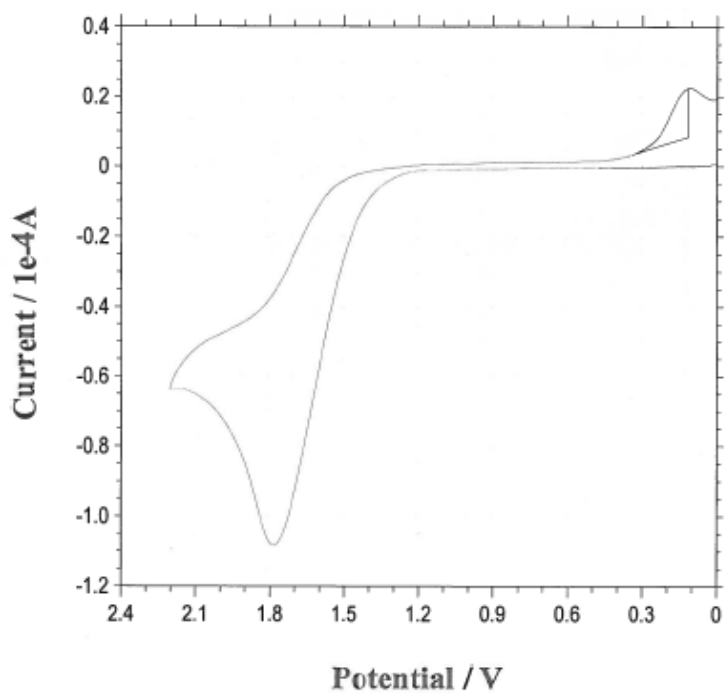
$E_{p/2} = +1.26$  V

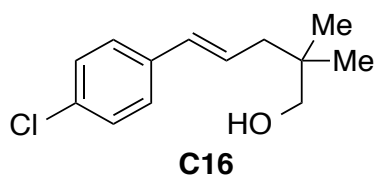
vs. Ag/AgCl



Scan Rate: 0.1 V/s

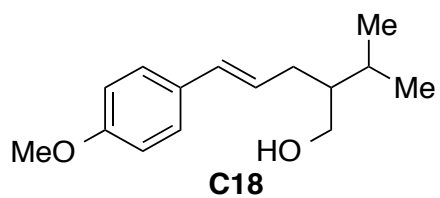
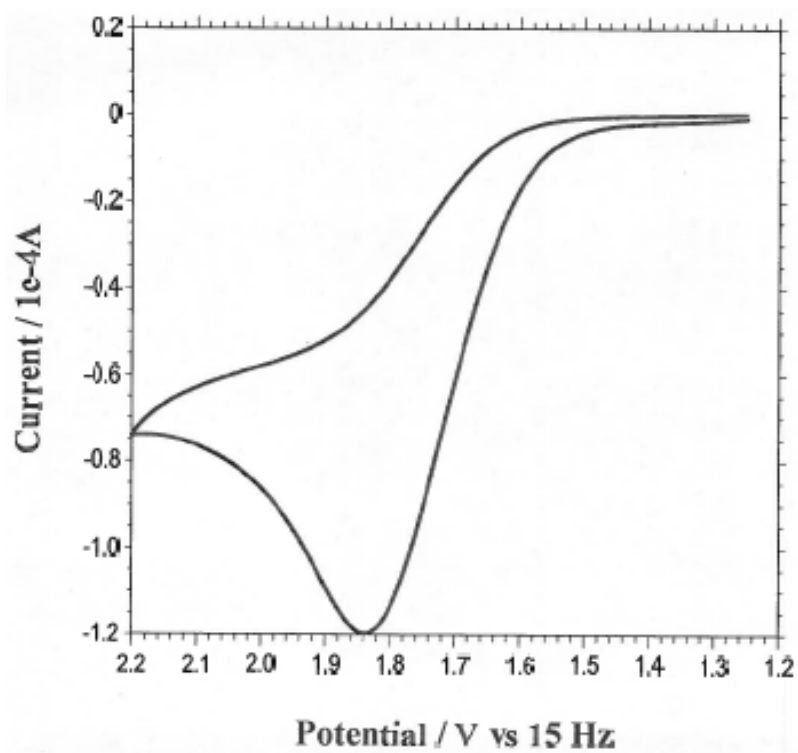
$E_{p/2} = +1.62$  V





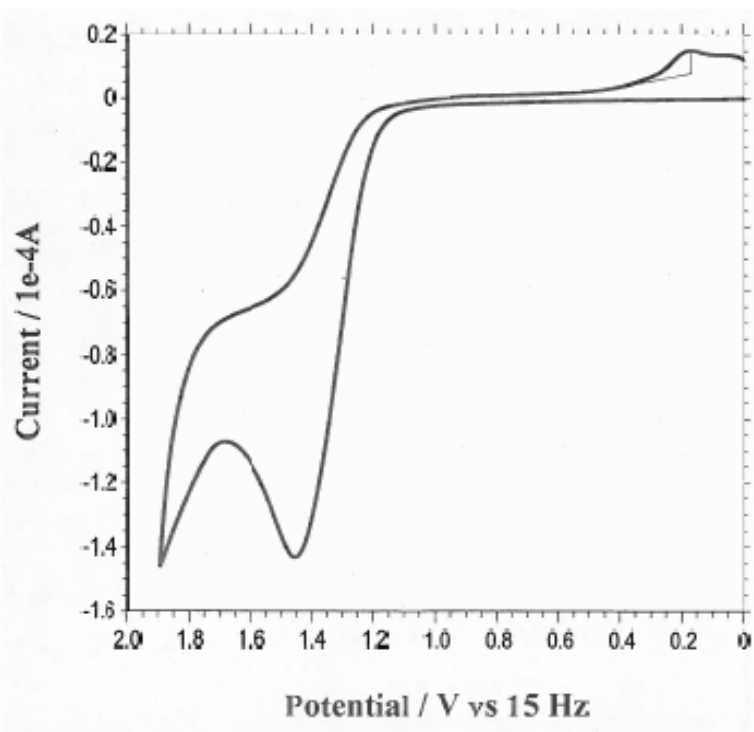
Scan Rate: 0.1 V/s

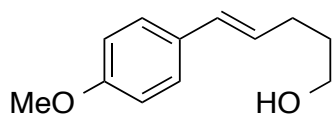
$E_{p/2} = +1.69$  V  
vs. Ag/AgCl



Scan Rate: 0.2 V/s

$E_{p/2} = +1.30$  V  
vs. Ag/AgCl



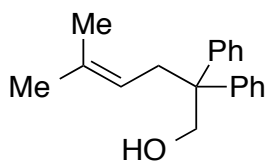
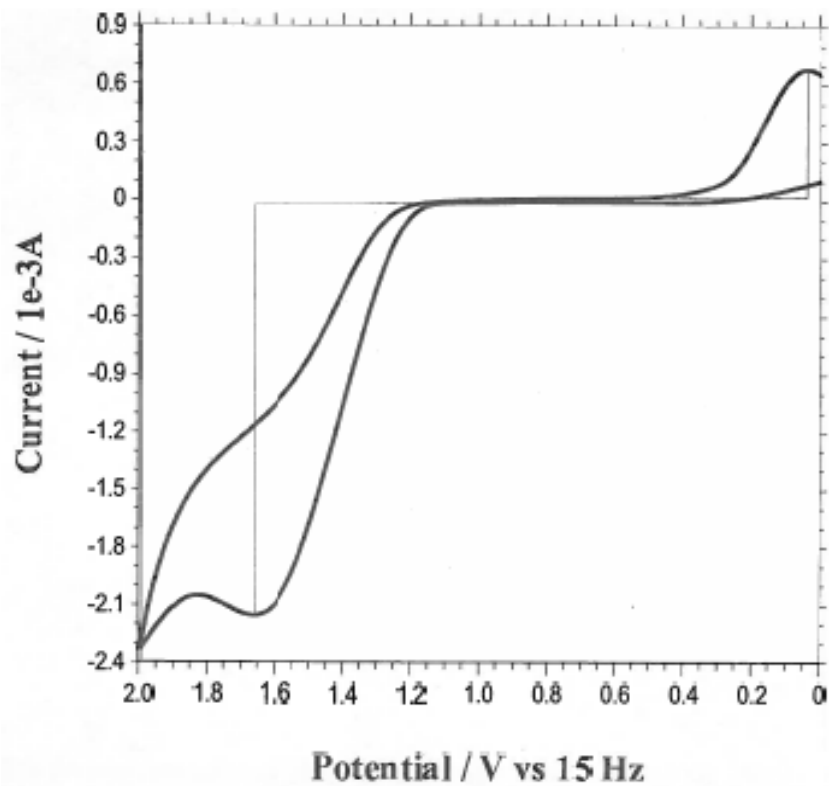


**C20**

Scan Rate: 0.1 V/s

$E_{p/2} = +1.41$  V

vs. Ag/AgCl

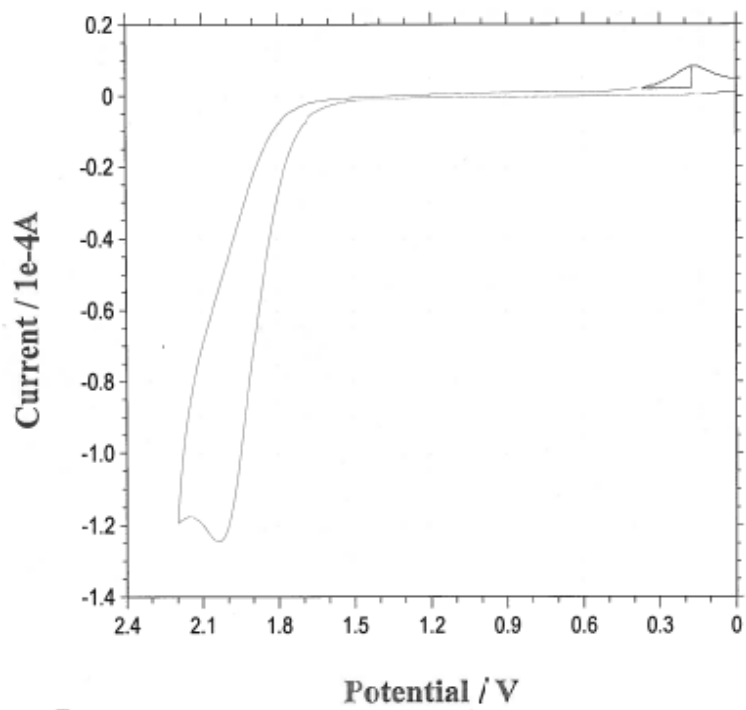


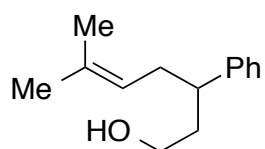
**C1**

Scan Rate: 0.1 V/s

$E_{p/2} = +1.95$  V

vs. Ag/AgCl

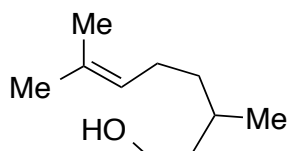
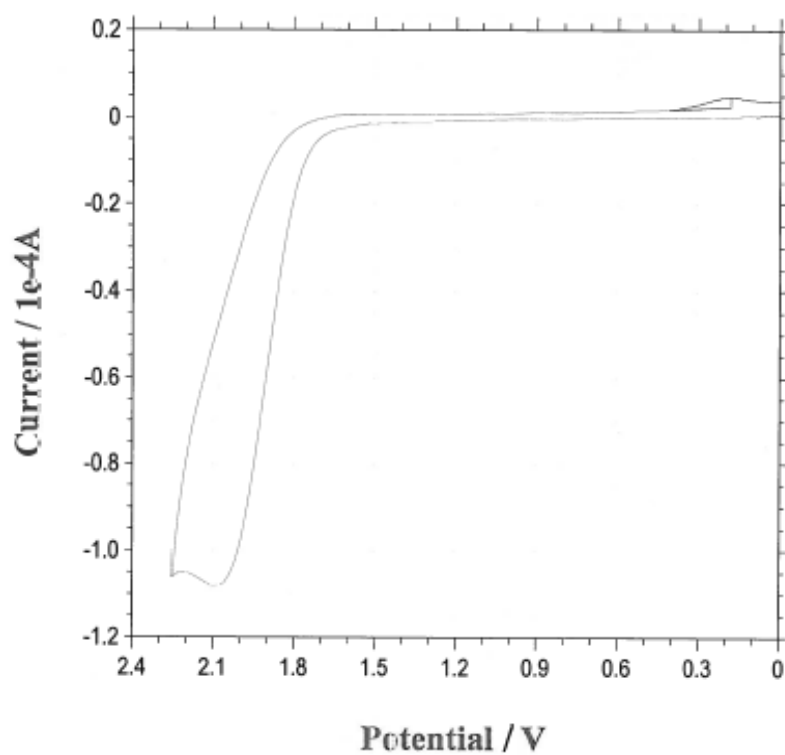




**C22**

Scan Rate: 0.1 V/s

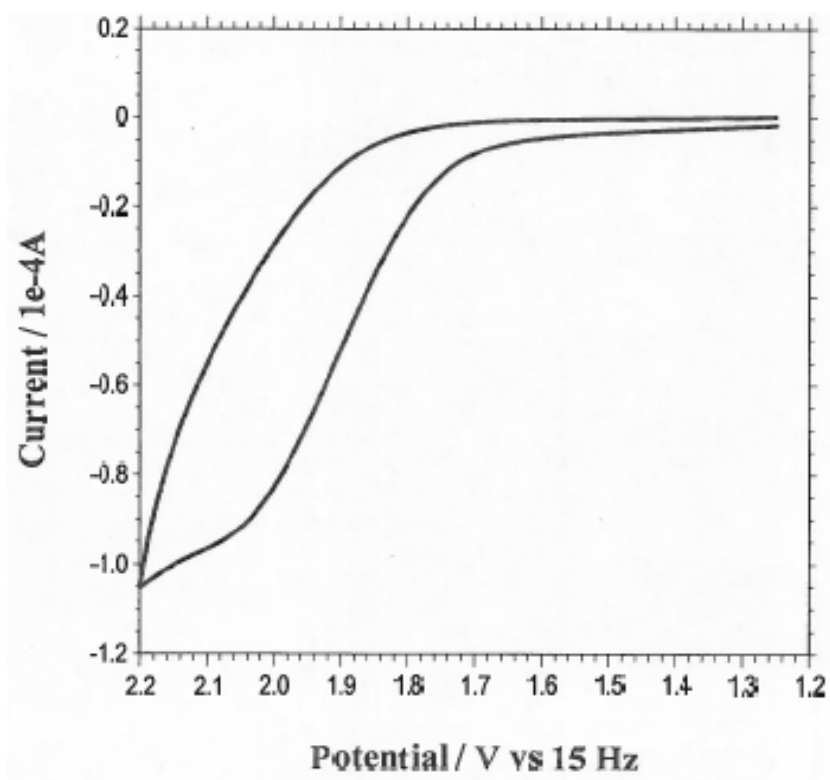
$E_{p/2} = +1.88$  V  
vs. Ag/AgCl



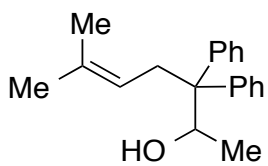
**C24**

Scan Rate: 0.1 V/s

$E_{p/2} = +1.92$  V  
vs. Ag/AgCl





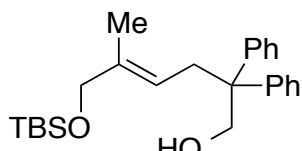
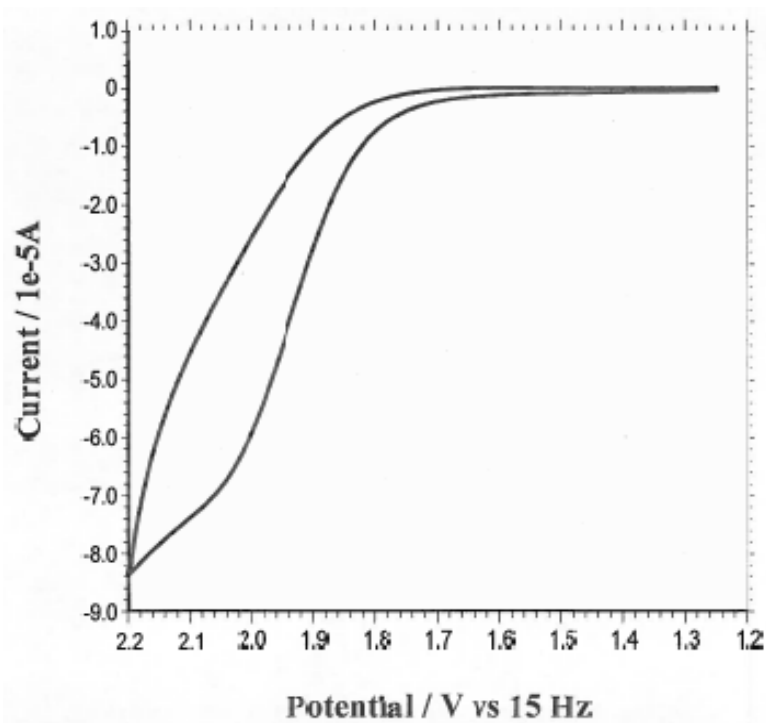


**C26**

Scan Rate: 0.05 V/s

$E_{p/2} = +1.98$  V

vs. Ag/AgCl

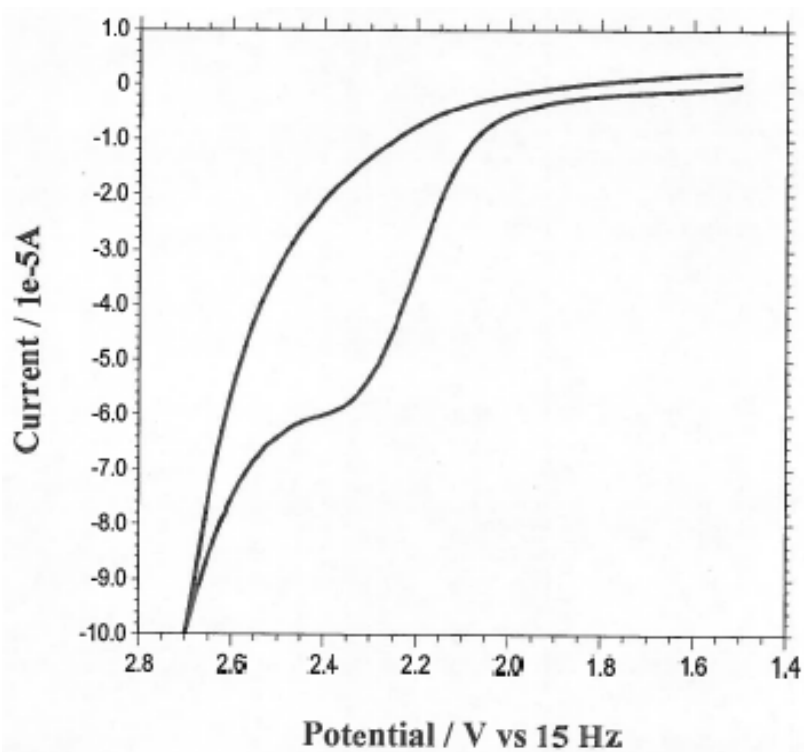


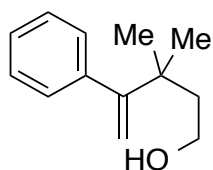
**C28**

Scan Rate: 0.1 V/s

$E_{p/2} = +2.10$  V

vs. Ag/AgCl



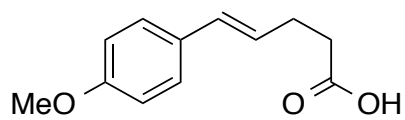
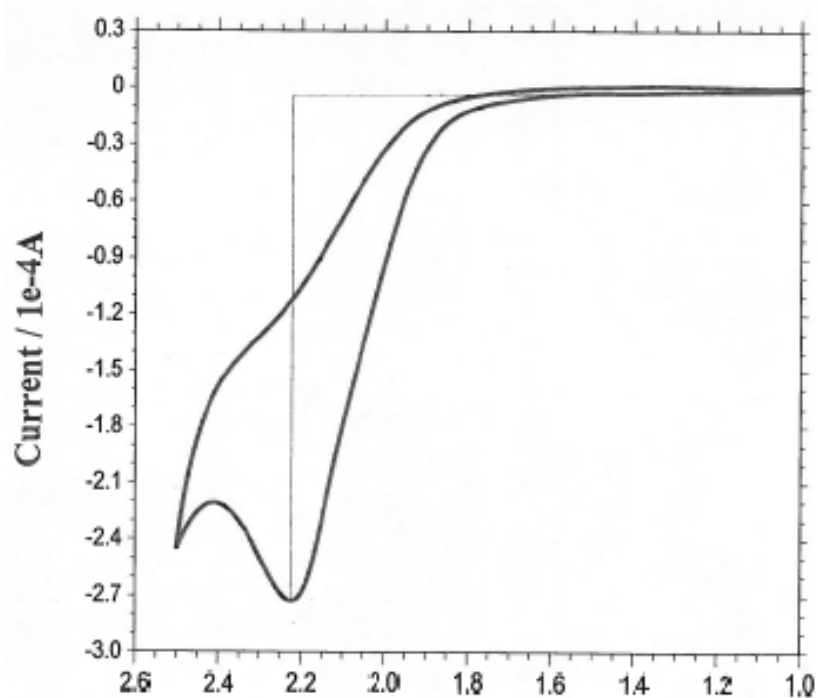


**C30**

Scan Rate: 0.1 V/s

$E_{p/2} = +2.05$  V

vs. Ag/AgCl

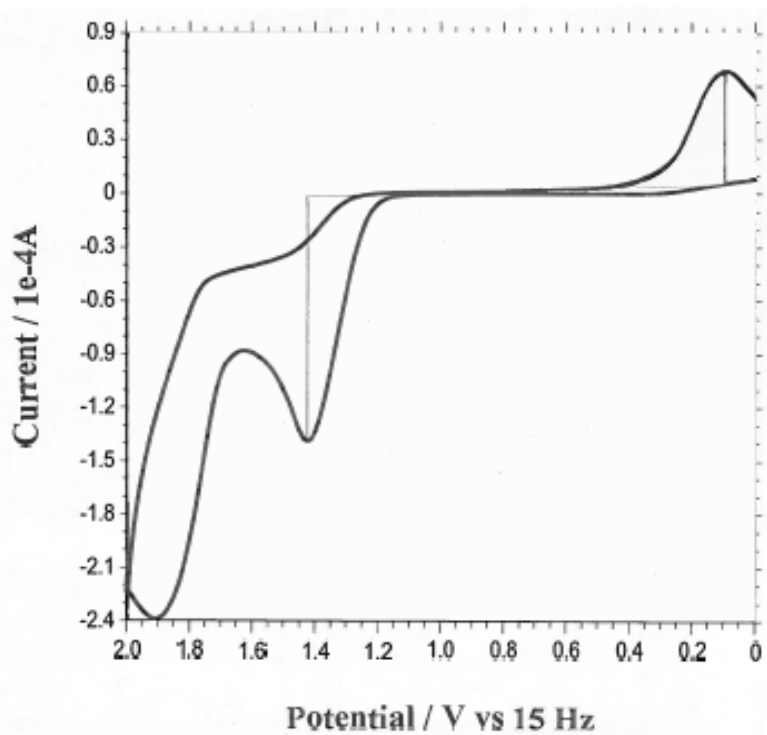


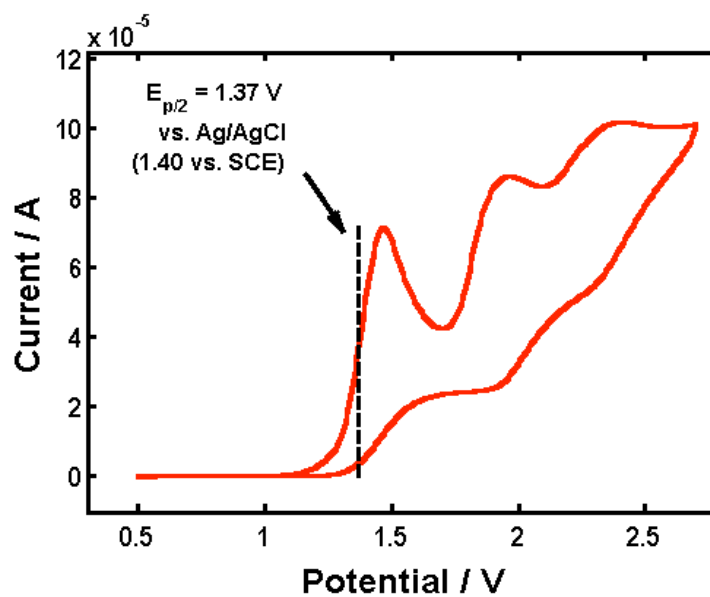
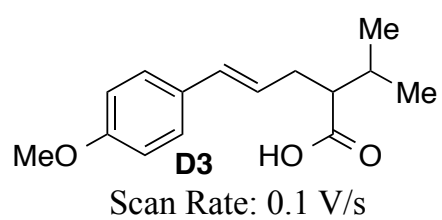
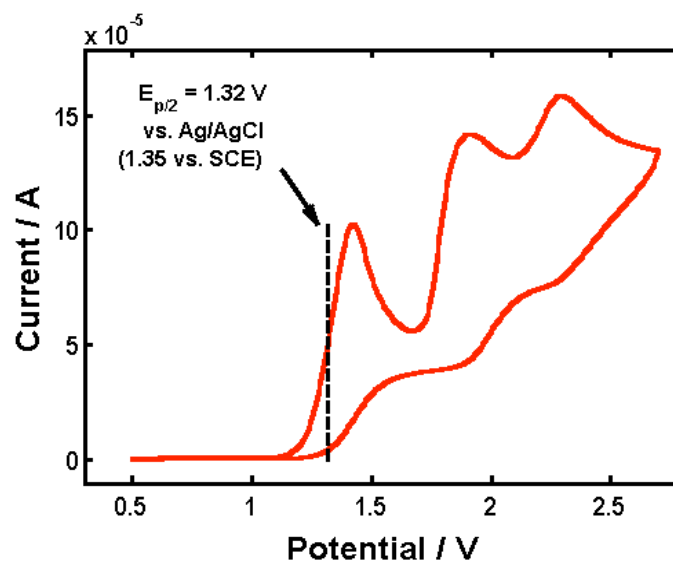
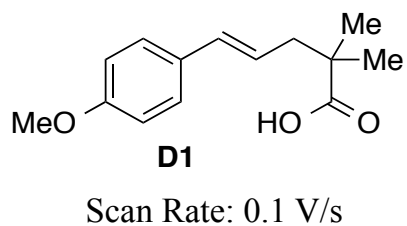
**C33**

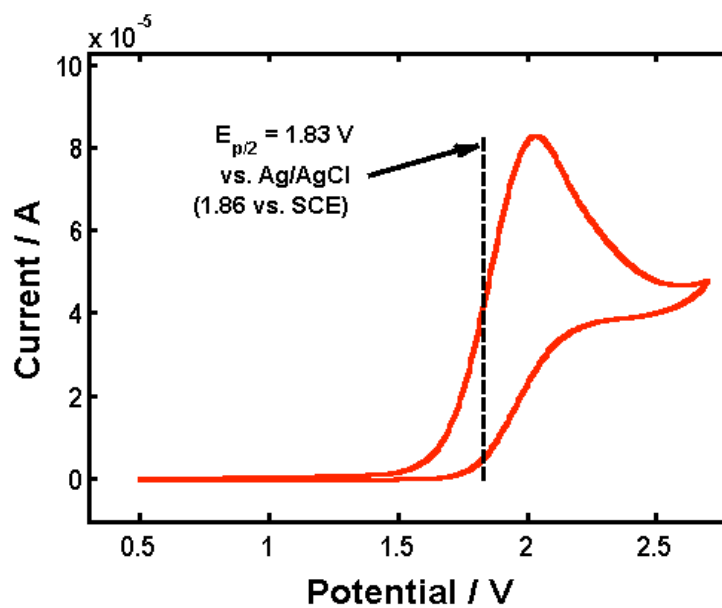
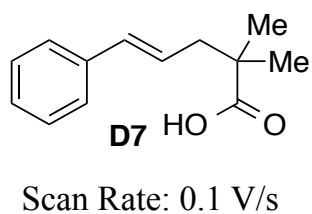
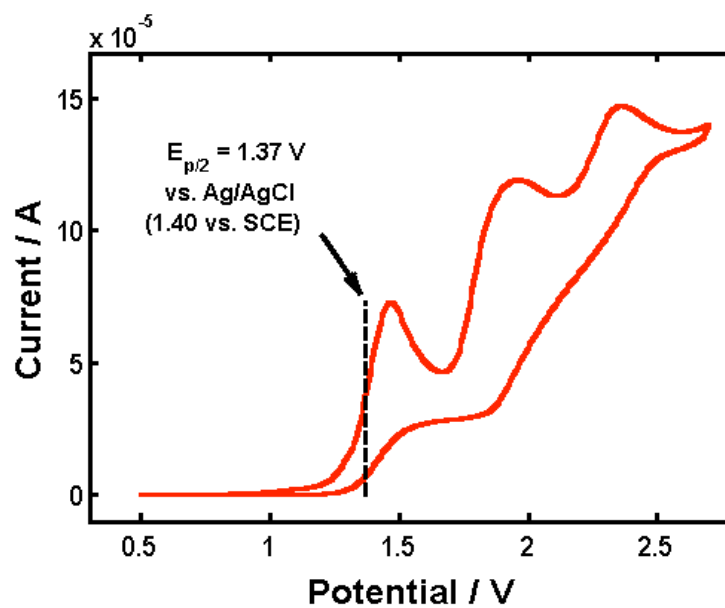
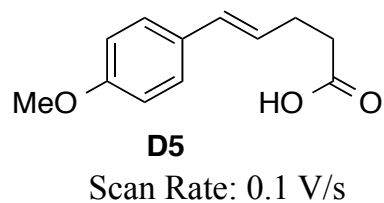
Scan Rate: 0.2 V/s

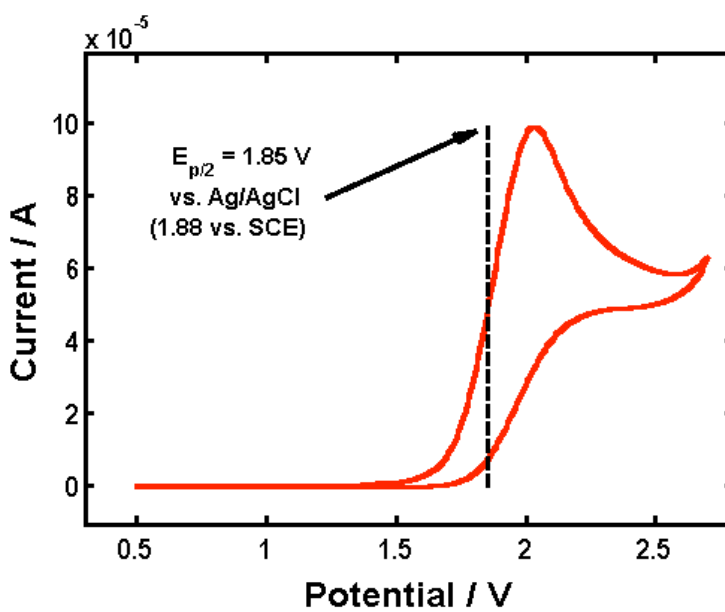
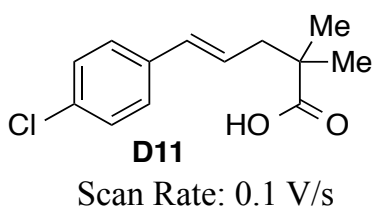
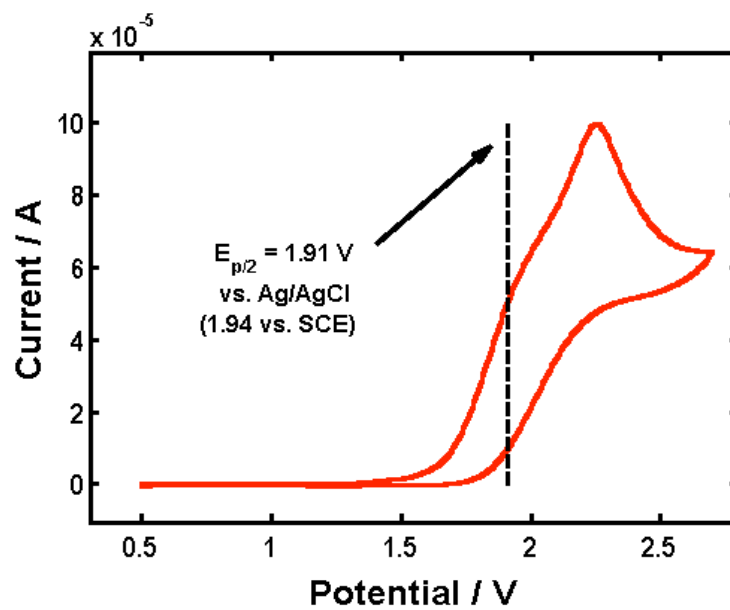
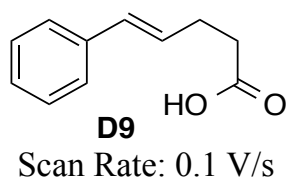
$E_{p/2} = +2.05$  V

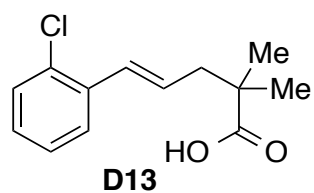
vs. Ag/AgCl



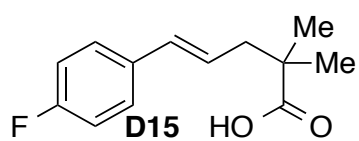
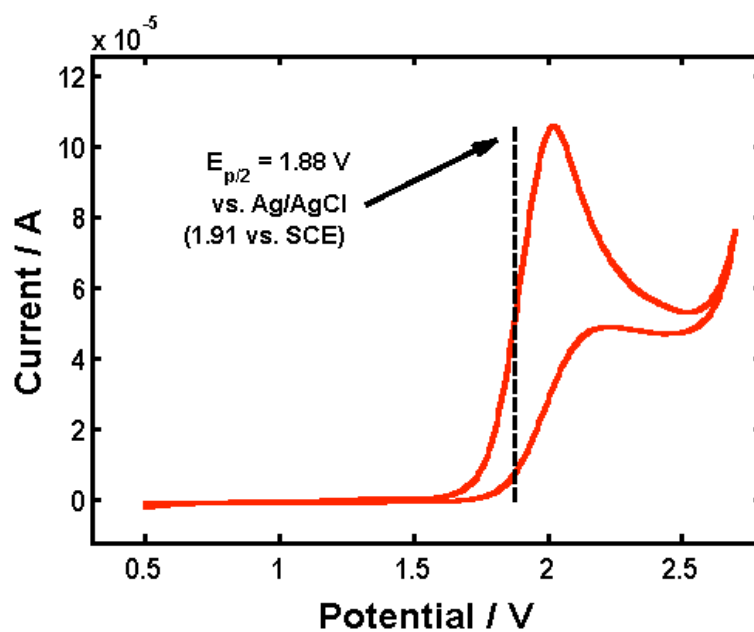




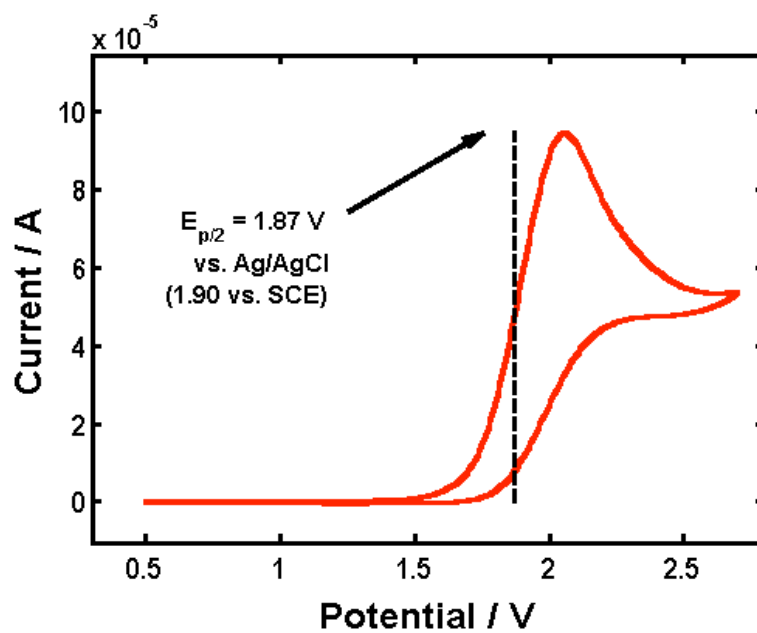


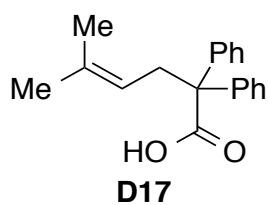


Scan Rate: 0.1 V/s

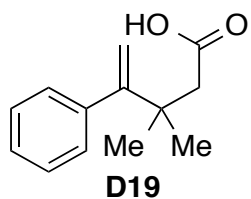
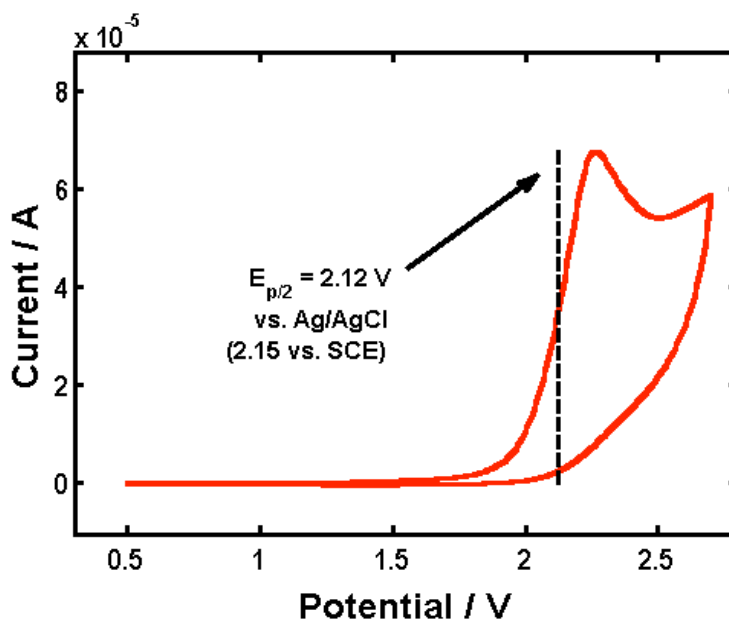


Scan Rate: 0.1 V/s

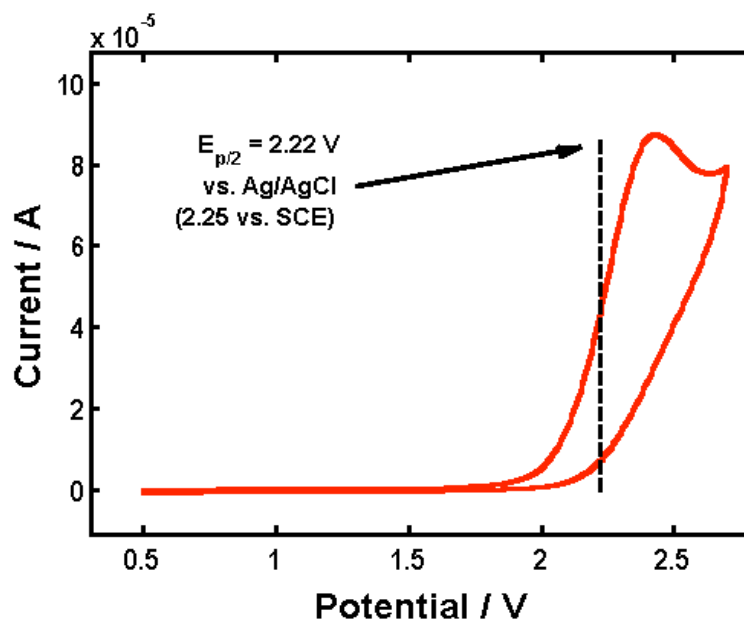




Scan Rate: 0.1 V/s

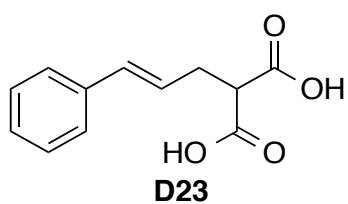
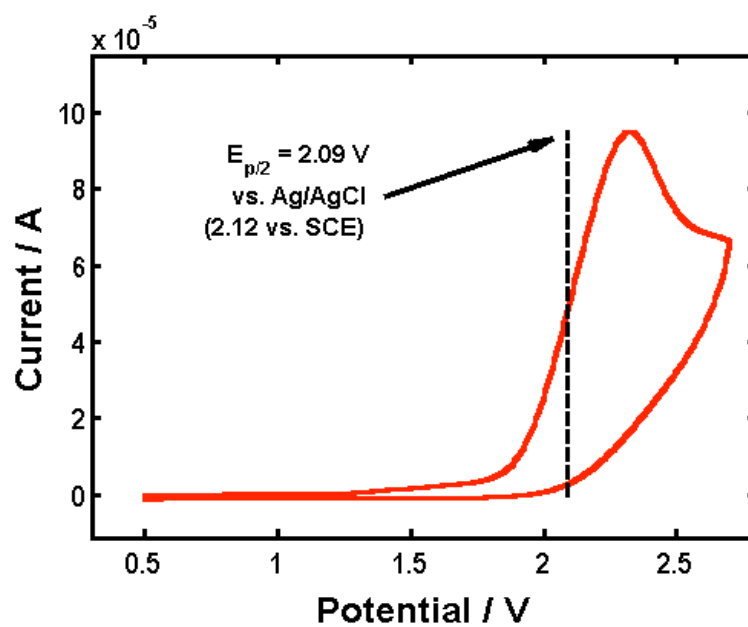


Scan Rate: 0.1 V/s





Scan Rate: 0.1 V/s



Scan Rate: 0.1 V/s

